Structures and Dynamics of Formamides, Acetamides, and Propionamides

Von der Fakultät für Mathematik, Informatik und Naturwissenschaften der RWTH Aachen University zur Erlangung des akademischen Grades einer Doktorin der Naturwissenschaften genehmigte Dissertation

vorgelegt von

Raphaela Kannengießer M. Sc.
aus Freren-Thuine

Berichter: Univ.-Prof. Dr. rer. nat. Wolfgang Stahl

Univ.-Prof. Dr. rer. nat. Arne Lüchow

Tag der mündlichen Prüfung: 25.04.2017

meinen Eltern

Author:
Raphaela Kannengiesser
Mauerstr. 96
52064 Aachen
raphaela.kannengiesser@rwth-aachen.de

Diese Dissertation wurde im Zeitraum von September 2013 bis Dezember 2016 am Lehr- und Forschungsgebiet Molekülspektroskopie, Institut für Physikalische Chemie der RWTH Aachen University angefertigt. Die Arbeit wurde durch die Graduiertenförderung der RWTH Aachen finanziell unterstützt.

Parts of this dissertation were already published in scientific journals as well as presented on international conferences as talks or posters and were done in cooperation with international researchers.

Publications

1. **R. Kannengießer**, W. Stahl, H.V.L. Nguyen, Two Conformers of N,N-Diethylpropionamide As Observed by Microwave Spectroscopy and Quantum Chemistry *J. Phys. Chem. A*, 2016, *120*, 5979-5984.
2. **R. Kannengießer**, W. Stahl, H.V.L. Nguyen, I. Kleiner, ^{14}N Nuclear Quadrupole Coupling and Methyl Internal Rotation in N-*tert*-Butylacetamide As Observed by Microwave Spectroscopy *J. Phys. Chem. A*, 2016, *120*, 3992-3997.
3. **R. Kannengießer**, W. Stahl, H.V.L. Nguyen, W.C. Bailey, ^{14}N Quadrupole Coupling in the Microwave Spectra of N-Vinylformamide, *J. Mol. Spectrosc.*, **2015**, *317*, 50-53.
4. **R. Kannengießer**, M. Lach, W. Stahl, H.V.L. Nguyen, Acetyl Methyl Torsion in N-Ethylacetamide: A Challenge for Microwave Spectroscopy and Quantum Chemistry, *ChemPhysChem*, **2015**, *16*, 1906-1911.
5. **R. Kannengießer**, S. Klahm, H.V.L. Nguyen, A. Lüchow, W. Stahl, The Effects of Methyl Internal Rotation and ^{14}N Quadrupole Coupling in the Microwave Spectra of two Conformers of N,N-Diethylacetamide, *J. Chem. Phys.*, **2014**, *141*, 204308.

Conference Papers

20. - 24.07.2016	71^{th} International Symposium on Molecular Spectroscopy in Urbana, USA **R. Kannengießer**, W. Stahl, H.V.L. Nguyen, W.C. Bailey Talk: *^{14}N quadrupole coupling in the microwave spectra on N-vinylformamide*
15. - 16.10.2015	GDRI HiResMIR Meeting in Creteil, France **R. Kannengießer**, K. Eibl, L. Ferres, W. Stahl, H.V.L. Nguyen, I. Kleiner Poster: *Microwave spectroscopy as a tool to determine very low torsional barriers*
24. - 28.08.2015	24^{th} Colloquium on High Resolution Molecular Spectroscopy in Dijon, France **R. Kannengießer**, M. Lach, W. Stahl, H.V.L. Nguyen Poster: *The acetyl methyl torsion and ^{14}N quadrupole coupling in N-ethylacetamide and N-ethylacetamide-water-complexes* K. Eibl, **R. Kannengießer**, H.V.L. Nguyen, W. Stahl Poster: *Internal rotation and quadrupole coupling in N-methyldiacetamide*
22. - 26.06.2015	70^{th} International Symposium on Molecular Spectroscopy in Urbana, USA **R. Kannengießer**, K. Eibl, W. Stahl, H.V.L. Nguyen Talk: *The effects of internal rotation and ^{14}N quadrupole coupling in N-methyldiacetamide*
27.11.2014	5^{th} Scientific Day of Meetings Aachen-Namur in Namur, Belgium **R. Kannengießer**, M. Lach, W. Stahl, H.V.L. Nguyen Talk: *The effects of internal rotation and ^{14}N quadrupole coupling in N-ethylacetamide*
07. - 13.09.2014	French-German Summer School SPECMO-2014 in Bastia, France **R. Kannengießer**, H.V.L. Nguyen, W. Stahl Invited talk: *Internal rotation and ^{14}N quadrupole coupling in acetamides*

02. - 06.09.2014	23^{rd} International conference on High Resolution Molecular Spectroscopy in Bologna, Italy **R. Kannengießer**, S. Klahm, H.V.L. Nguyen, A. Lüchow, W. Stahl Talk: *The effects of internal rotation and ^{14}N quadrupole coupling in N,N-diethylacetamide*

Also research projects and a bachelor thesis were supervised in the scope of this dissertation. I would like to thank the students for their participation in this work.

Students Reseach Projects and Bachelor Thesis

Bastian Fenger	Research Project: *Microwave spectroscopic studies of N-tert-butylformamide*
Marcel Joseph Lach	Bachelor Thesis: *Microwave spectroscopic and quantum chemical studies on N-ethylacetamide and N-ethylacetamide-water-complexes*
Konrad Eibl	Research Project: *Internal rotation and quadrupole coupling in N-methyldiacetamide*

Danksagung

Zuallererst möchte ich mich bei meinem Doktorvater **Prof. Dr. Wolfgang Stahl** bedanken, für die tolle Forschung die wir zusammen betrieben haben und die wunderbare Zeit, die ich dabei in seiner Arbeitsgruppe verbringen durfte. Ich danke ihm für die stets produktiven Gespräche und Fachdiskussionen und seine jederzeit offene Tür, die dies ermöglicht hat. Ich möchte mich außerdem bei Ihm dafür bedanken, dass er immer Vertrauen in mich und meine wissenschaftlichen Fähigkeiten hatte und mich in meiner Arbeit und meinem Lebensweg mit allen Ihm möglichen Mitteln unterstützt hat.

Meiner Betreuerin **Dr. Ha Vinh Lam Nguyen** möchte ich ebenfalls besonders danken, da Sie mich seit meiner Bachelorarbeit steht außerordentlich gut betreut hat und immer mit neuen Ideen und Projekten gefordert und gefördert hat. Ihrer Unterstützung verdanke ich ein paar wissenschaftliche Veröffentlichungen, auf die ich besonders stolz bin, sowie einige Erfahrungen, die ich nicht missen möchte.

Dr. Isabelle Kleiner danke ich besonders für die tolle Kooperation, die sich mit Beginn meines Forschungsaufenthalts im Jahr 2012 sehr produktiv entwickelt hat. Bei Prof. Dr. Arne Lüchow bedanke ich mich, für die gute Zusammenarbeit beim N,N-Diethylacetamide, sowie seine Hilfe bei quantenchemischen Fragestellungen. Prof. Dr. Marcel Liauw möchte ich dafür danken, dass er mich seit dem ersten Semester als Mentor begleitet und mich als Gutachter für die Graduiertenförderung so gut unterstützt hat.

Ein besonders großer Dank geht an meine Kollegen: Dr. Halima Mouhib, Dr. Theo Attig, Vinh Van, Konrad Eibl, Lynn Ferres, Dr. Lilian Sutikdja, Dr. Yueyue Zhao, Dr. Layla Tulimat und Daniela Lucht für die angenehme Arbeitsatmosphäre und die Unterstützung und Hilfe über die Jahre. Besonders möchte ich Dr. Halima Mouhib danken, für ihr große Hilfsbereitschaft und Kollegialität. Dr. Theo Attig danke ich für seine interessanten Projekte, an denen er mich hat teilhaben lassen und die sich aus der Zusammenarbeit entwickelte Freundschaft. Vinh Van danke ich dafür, dass er mir oft geholfen hat und über die Jahre ein sehr guter Büropartner war.

Zum Schluss möchte ich mich bei meinen Freunden und meiner Familie, besonders bei meinen Eltern, **Monika und Andreas Kannengießer**, dafür bedanken, dass Sie mich immer unterstützt haben und alle Höhen und Tiefen des Studiums und der Dissertation mit mir durchlebt und mir immer den nötigen Rückhalt gegeben haben.

Vielen Dank.

Summary

In this dissertation the structures and dynamics of two formamides, five acetamides and two propionamides were investigated, whereat the focus was set on the effects of internal rotation and quadrupole coupling. The investigation was carried out using a combination of molecular beam Fourier transform microwave spectroscopy and quantum chemical calculations.

The investigated formamides are N-vinyl- and N-*tert*-butylformamide. Both have been measured before with low resolution spectroscopy at room temperature. Thus, they were remeasured with high resolution in this thesis, in order to analyze the quadrupole hyperfine splittings. In the scope of these investigations a new calibration method was developed, which is suitable for unsaturated, π-conjugated systems like N-vinylformamide.
Furthermore the three secondary acetamides, N-ethyl-, N-*tert*-butyl-, and N-vinylacetamide were measured and assigned. These molecules showed internal rotation as well as quadrupole coupling, which could be fully analyzed and assigned. The barriers to internal rotation were obtained to be 73.4 cm^{-1} and 65.6 cm^{-1} for N-ethyl- and N-*tert*-butylacetamide, respectively. Both molecules were fitted with the programs XIAM and BELGI-C_1-hyperfine. The BELGI-C_1-hyperfine program was developed for this purpose in the scope of this thesis.
In the case of N-vinylacetamide a spectrum with a remarkably small amount of lines was observed, which enabled only an assignment of the A-species, whereas the assignment of the E-species did not succeed.
For the two tertiary propionamides, N,N-diethylpropionamide and N,N-dimethylpropionamide, and the tertiary acetamides N,N-diethylacetamide and N-methyldiacetamide very complex spectra were observed.
For N,N-diethylpropionamide ten different minima were calculated, whereat two of them could be found in the measured spectrum. In these conformers the propionyl ethyl group lies in the same plane as the amide bond.
In the case of N,N-dimethylpropionamide splittings due to the two nitrogen methyl rotors were found. The barriers are 137.8 and 226.3 cm^{-1}. Moreover, some transitions showed very small additional splittings in the order of a few kHz, which are probably due to the internal rotation of the propionyl methyl group.
Both tertiary acetamides showed internal rotation due to the acetyl methyl group, with very high barriers. In the case of N,N-diethylacetamide the two assigned conformers gave surprisingly different barrier heights of 517 cm^{-1} and 619.5 cm^{-1} for

conformer I and II, respectively. For N-methyldiacetamide one of the two acetyl methyl rotors could be assigned to a barrier of 679.6 cm^{-1}, whereat the second acetyl methyl rotor could not be resolved. Thus we assume a barrier which is probably greater than 800 cm^{-1}. The nitrogen methyl rotation for this molecule was obtained with a barrier to internal rotation of 147.2 cm^{-1}.

In general the barriers to internal rotation of all investigated amides were greatly influenced by the substituents at the nitrogen atom, which change the electronic structure of the molecules. Tertiary amides have barriers, which are increased by one order of magnitude compared to the secondary amides. Moreover, effects like π-conjugation and inductive effects also influence the barrier height.
The quadrupole coupling is also influenced by the change in the electronic structures of the molecules. Especially in the case of π-conjugated systems exceptionally small values for the z-component of the coupling tensor in the principal axis system were observed.

Zusammenfassung

In dieser Doktorarbeit wurden die Strukturen und die Dynamik von zwei Formamiden, fünf Acetamiden und zwei Propionamiden untersucht, wobei der Fokus auf die Effekte der internen Rotation und der Quadrupolkopplung gelegt wurde. Die Untersuchungen wurden mit einer Kombination aus Molekularstrahl-Fouriertransform-Mikrowellenspektroskopie und quantenchemischen Rechnungen durchgeführt.

Die untersuchten Formamide sind N-Vinyl- und N-*tert*-Butylformamid. Beide wurden bereits mit niedrig auflösender Spektroskopie bei Raumtemperatur gemessen. Daher wurden sie im Rahmen dieser Arbeit mit hoher Auflösung nachgemessen, um die Quadrupol-Hyperfein-Aufspaltung zu analysieren. Im Rahmen dieser Untersuchungen wurde eine neue Kalibriermethode entwickelt, welche für ungesättigte, π-konjugierte Systeme wie N-Vinylformamid geeignet ist.
Des Weiteren wurden die drei sekundären Acetamide, N-Ethyl-, N-*tert*-Butyl- und N-Vinylacetamid gemessen und zugeordnet. Diese Moleküle zeigten sowohl interne Rotation als auch Quadrupolkopplung, welche vollständig analysiert und zugeordnet werden konnten. Die erhaltenen Barrieren der internen Rotation sind 73.4 cm^{-1} und 65.6 cm^{-1} für N-Ethyl- und N-*tert*-Butylacetamid. Beide Moleküle wurden mit den Programmen XIAM und BELGI-C_1-hyperfine gefittet. Das Programm BELGI-C_1-hyperfine wurde zu diesem Zweck ihm Rahmen dieser Arbeit entwickelt.
Im Fall des N-Vinylacetamids wurde ein Spektrum mit einer ausgesprochen geringen Anzahl an Linien erhalten, welches nur die Zuordnung der A-Spezies ermöglichte. Die Zuordnung der E-Spezies hingegen war nicht erfolgreich.
Für die beiden tertiären Propionamide, N,N-Diethyl- und N,N-Dimethylpropionamid und die beiden tertiären Acetamide, N,N-Diethylacetamid und N-Methyldiacetamid wurden sehr komplexe Spektren erhalten.
Für N,N-Diethylpropionamid wurden zehn unterschiedliche Minima berechnet, von denen zwei in dem gemessenen Spektrum gefunden werden konnten. In diesen Konformeren liegt die Propionyl-Ethylgruppe in derselben Ebene wie die Amidbindung.
Im Fall des N,N-Dimethylpropionamids wurden Aufspaltungen durch die beiden am Stickstoff befindlichen Methylgruppen gefunden. Die Barrieren sind 137.8 und 226.3 cm^{-1}. Zusätzlich zeigten einige wenige Übergänge sehr kleine Aufspaltungen, welche vermutlich durch die interne Rotation der Propionyl-Methylgruppe verursacht werden.

Bei den tertiären Acetamiden zeigten beide Verbindungen interne Rotation der Acetyl-Methylgruppe mit sehr großen Barrieren. Dabei hatten die beiden zugeordneten Konformere von N,N-Diethylacetamid überraschend unterschiedliche Barrierenhöhen von 517 cm^{-1} für Konformer I und 619.5 cm^{-1} für Konformer II. Für N-Methyldiacetamid konnte einer der beiden Acetyl-Methylrotoren mit einer Barriere von 679.6 cm^{-1} zugeordnet werden, wohingegen der zweite Acetyl-Methylrotor nicht aufgelöst werden konnte. Daher wird vermutet, dass die Barriere der internen Rotation entsprechend größer als 800 cm^{-1} ist. Für die Stickstoff-Methylgruppe wurde eine interne Rotationsbarriere von 147.2 cm^{-1} erhalten.

Im Allgemeinen werden die internen Rotationsbarrieren der untersuchten Amide stark durch die Art der Substituenten am Stickstoffatom beeinflusst, welche die elektronische Struktur der Moleküle verändern. Die Barrieren der tertiären Amide sind um eine Größenordnung größer als die der sekundären Amide. Des Weiteren beeinflussen Effekte wie π-Konjugation oder induktive Effekte die Barriere zusätzlich.
Die Quadrupolkopplung wird ebenfalls durch den Austausch der Substituenten und somit die veränderte elektronische Struktur beeinflusst. Besonders im Fall von π-konjugierten Systemen wurden außergewöhnlich kleine Werte für die z-Komponenten des Kopplungstensors im Hauptachsensystem erhalten.

Contents

Chapter 1

Introduction

Investigation of geometrical and dynamical properties of molecules are crucial to explain the origin of their macroscopic properties and characteristics. These investigations can be performed in a very careful and highly precise way by the use of microwave spectroscopy in combination with quantum chemical calculations.
This dissertation concentrates on the conformational arrangements, internal rotation dynamics, and electric quadrupole coupling in amides.

Amides are a very important molecular class and often show interesting chemical properties, due to the inclusion of the amide bond as a basic structure element.
The amide bond is of inevitable importance in the description of proteins, their reactions, their structural preferences, and many other characteristics. It remains, however, surprisingly unexplored in biology, chemistry, and spectroscopy. While amide bonds are found in virtually all metabolites, enzymes, and hormones as well as being important in drug design and medical applications, still very little quantitative information on their impact in metabolic processes is available. Chemically, amides participate in many classical reactions, such as Hofmann rearrangement [1] and amide reduction [2]. Described by two limiting mesomeric structures, they exhibit a complicated electronic configuration due to a conjugation between the carbonyl π electrons and the lone electron pair of the nitrogen, which forces the C$-$(C=O)$-$N subunit to planarity. Consequently, the motif of the amide bond is the origin of a characteristic behavior in chemical reactions as well as biological processes.

Several formamides such as formamide [3], N-methylformamide [4], N-ethylformamide [5] and a few more have been investigated so far. In the class of the amides and especially the acetamides only a few molecules were investigated. Detailed information on some of these molecules and their dynamical structures are given in the review

article of Kawashima et al. [6]. However, in order to answer questions concerning the electronic structure in the amid bond and its environment further investigations on this molecules are essential.

In this dissertation two different formamides, N-vinylformamide (chapter 6) and N-*tert*-butylformamide (chapter 7), were investigated. These molecules show ^{14}N quadrupole coupling in the microwave investigations, but no additional dynamics like internal rotation. Thus, these sections concentrate on the quadrupole coupling and different methods of calculation for quadrupole coupling constants of nitrogen containing molecules, especially π-conjugated systems.
The secondary amides N-ethylacetamide (chapter 9), N-*tert*-butylacetamide (chapter 10), and N-vinylacetamide (chapter 11) show in addition to the quadrupole coupling of the ^{14}N nucleus, splittings due to internal rotation of the acetyl methyl group. This dynamic is also present in the more complex tertiary amides N,N-diethylacetamide (chapter 15) and N-methyldiacetamide (chapter 16), where the latter contains two acetyl methyl groups, which rotate internally. In these sections I concentrate on the differences in the internal rotation barriers of secondary and tertiary amides, and the influence of the nitrogen substituents and multiple internal rotors on the barrier to internal rotation.
In N,N-diethylpropionamide (chapter 13) the propionyl group does not show internal rotation as the barrier is to high. Here the complexity of the spectrum due to multiple conformers was investigated. In N,N-dimethylpropionamide (chapter 14) the internal rotation of the two methyl groups at the nitrogen were analyzed.

Chapter 2

Theory

2.1 Internal Rotation

Internal rotation is a form of large amplitude motion, where a molecular group called the internal rotor, rotates against the rest of the molecule, which is often denoted as the frame. The internal rotor can be symmetrical or asymmetrical.

Best known examples of internal rotors are methyl groups, as they are groups with a small moment of inertia and frequently occur in organic compounds. In our model, we assume that methyl internal rotors have C_{3v} symmetry and a threefold potential [7]:

$$V(\alpha) = \frac{V_3}{2}(1 - cos(3\alpha)) \tag{2.1}$$

with the rotational angle of the methyl rotation α and the barrier to internal rotation V_3.

Several molecules with methyl internal rotors have been investigated by microwave spectroscopy. Acetaldehyde is one of the smallest molecules containing a methyl internal rotor. The barrier to internal rotation of acetaldehyde CH_3CHO was obtained for the first time by Kilb and Lin to be 406.4 cm^{-1} [1] . Acetic acid CH_3COOH has a barrier of 168.01(05) cm^{-1} [9].
Especially interesting are acetic acid esters, also called acetates CH_3COO-R. They contain the CH_3COO group as a construction element, where the internal methyl

[1] Calculated from the published value of 1162(30) cal [8]

rotor is separated from the rest R by the ester group[2]. For the n-alkyl acetates the barrier to internal rotation is almost always in the order of 100 cm^{-1}. Examples are methylacetate with a barrier of 99.56(8) cm^{-1} [10], ethylacetate with 99.57(11) cm^{-1} [11], and butylacetate with 94.8219(80) cm^{-1} [12]. Is a triple bond inserted between the methyl rotor and the rest of the molecule an almost free rotation of the methyl group is observed as the triple bond works as a spacer. Examples for this are the newly investigated alkynoles, 3-propyn-1-ol ($CH_3-C\equiv C-C_2H_4OH$) [13] and 4-hexyn-3-ol ($CH_3-C\equiv C-CH(OH)C_2H_5$) [14] with barriers to internal rotation of 9.4548(94) cm^{-1} and 15.7 cm^{-1}, respectively or 2-butynoic acid ($CH_3-C\equiv C-COOH$) with an even lower barrier of 1.00900(42) cm^{-1} [15].

In a water complex, the water molecule can also rotate internally against the monomer attached to it. In 1993 trimethylamine-water was investigated by M. J. Tubergen and R. L. Kuczkowski [16]. Even though water has C_{2v} symmetry and should therefore give asymmetric rotor spectra, in the case of trimethylamine-water symmetric rotor spectra where obtained, due to a free internal rotation of the water molecule. Free rotation of water was often found in several constellations with different monomer molecules as for example ethers [17, 18], amines [16, 19], amides [20, 21] or aminoacids [22].
In the case of isoflourane-water, investigated by Q. Gou et. al. in 2014, an almost but not totally free rotation of water was observed for the heavy water isotopologue D_2O [23].

In order to treat molecular data of molecules with internal rotation several fitting routines were developed over the years. Most of these programs are available on the PROSPE website [24].

XIAM is a well-known internal rotation fitting program capable of fitting up to three internal rotors [25]. It works with an e**X**tended **I**nternal **A**xis **M**ethod, as it sets up the Hamiltonian in the principal axis system of the molecular frame. The operators of the internal rotation are set up in their own rho axis system. XIAM shows advantages especially in its use for assignment purposes, as it is fast and convenient to use.

Another internal rotation program is the BELGI code, which was developed by I. Kleiner. It exists in three versions: BELGI-C_s is designed for one C_{3v} internal rotor attached to a C_s framework [26], BELGI-C_1 is an extended version of BELGI-C_s

[2]We define the ester group as COO.

allowing also asymmetrical frames with C_1 symmetry [27]. Both, BELGI-C_s and BELGI-C_1 can only treat one internal rotor. To apply data from a molecule with two internal rotors BELGI-C_1-twotops has to be used [28].

Another program based on the same method as BELGI is the program RAM36 [29]. It is designed to treat a threefold rotation with a C_{3v} internal rotor attached to a C_s frame or a six-fold rotation of a C_{3v} internal rotor on a C_{2v} frame. RAM36 has the advantage that it is also capable of treating weak quadrupole coupling for C_s molecules.

For internal rotors of a different then the C_{3v} symmetry of methyl groups the program ERHAM can be used [30, 31]. It can treat molecules of C_{2v}, C_2 or C_s symmetry with two equivalent rotors, C_1 and C_s- molecules with non-equivalent rotors or single top molecules of C_1 and C_s-symmetry. ERHAM works with an **E**ffective **R**otational **HAM**iltonian.

2.2 Quadrupole Coupling

Quadrupole coupling is an electronic effect, which occurs with nuclei of a nuclear spin $I > \frac{1}{2}$. These nuclei posses an electric quadrupole moment, which interacts with the electric field gradient (EFG), a non-spherical distribution of all other charges in the molecule at the site of the nucleus. A force due to the EFG promotes the alignment of the nuclear spin along the direction of the EFG. This interaction is denoted as quadrupole coupling. In quantum mechanics it is basically a coupling of the rotational angular momentum with the nuclear spin.
Since the EFG due to a charge at a distance r from the nucleus is proportional to $1/r^3$, only electrons associated with the nucleus have major contributions to the EFG. Indeed, the work of Townes and Dailey [32] argues that only valence p electrons need be considered, thereby establishing a link between chemical bonding and nuclear quadrupole coupling. Thus, analysis of the quadrupole hyperfine structure yields information not only on the EFG at the site of the nitrogen nucleus, but also on the nature of the chemical bond.

Nitrogen containing molecules show all quadrupole coupling as the most abundant isotope, the ^{14}N, has a nuclear spin of $I = 1$. The ^{15}N isotope possesses a nuclear spin of $I = \frac{1}{2}$ and shows therefore no quadrupole interaction.

From the quadrupole hyperfine structure the nuclear quadrupole coupling constants (NQCCs) can be obtained. They are defined as:

$$\chi_{ij} = eQq_{ij} \tag{2.2}$$

with $i, j = a, b, c$

The most simple nitrogen containing molecules are diatomic molecules: The nitrogen molecule N_2, phosphorus nitride PN, the cyanide anion CN^- and the nitric oxide cation NO^+. Their NQCCs are given in Table 2.1.

Table 2.1: Experimental and calculated NQCCs χ_{zz} of nitrogen containing diatomic molecules in MHz.

	formula	calc.[a]	exp.	ref.[b]
nitrogen	N_2	−5.312	−5.3(1)	[33]
phosphorus nitride	PN	−5.194	−5.1718(5)	[34]
cyanide anion	CN^-	−4.236	−4.238(32)	[35]
nitric oxide cation	NO^+	−6.778	−6.76(10)	[36]

[a] Calculated NQCCs in MHz by W. C. Bailey [37]. [b] References of experimental NQCCs.

With these only very small changes in the electric environment of the nitrogen nucleus one sees a variation in the NQCCs in the order of MHz. Especially in the cases of the ions, very low values are obtained for the cyanide anion and high values for the nitric oxide cation.

Some more examples of quadrupole coupling in different molecular classes are given in Table 2.2. All χ_{zz} values are usually in the range of −3.5 to −5 MHz. In the cases of methyl cyanide and ammonia the $\chi_{zz} = \chi_{aa}$ due to symmetry reasons. Therefore χ_{zz} can be directly obtained from the measurements. The calculated values of methyl cyanide and ammonia are, as well as for the diatomic molecules in Table 2.1, very close to the experimental values.
In the case of formamide, which is the smallest possible amide the χ_{zz} value is remarkably low with a value of −3.921 MHz. This is a first hint that the molecular class of amides with the characteristic peptide bond contains a special electronic environment at the side of the nucleus.

In order to fit spectra with quadrupole coupling, commonly known and often used is the SPFIT/SPCAT package of H. M. Pickett [38]. This is a program package with a wide range of use for different types of symmetric and asymmetric tops optional with different types of splittings due to quadrupole coupling, Coriolis coupling, etc. Unfortunately Pickett's program is not straightforward usable for internal rotation problems. On the other hand quadrupole coupling of even more than one nucleus is possible.

Table 2.2: Experimental and calculated NQCCs χ_{zz} of small nitrogen containing molecules.

	formula	calc. [a]	exp.	ref. [b]
methyl cyanide	CH_3CN	−4.208	−4.22324(108)	[39]
ammonia	NH_3	−4.080[c]	−4.08984(70)	[40]
methylamine	CH_3NH_2	−4.781	-	
formyl cyanide	H(C=O)CN	−4.792	-	
formamide	H_2N(C=O)H	−3.921	-	

[a] Calculated NQCCs by W. C. Bailey [37]. [b] References of experimental NQCCs. [c] Calculated NQCC by Demaison et. al. [41].

To treat quadrupole coupling in combination with internal rotation up to now only the two programs XIAM and RAM36 are available, where RAM36 can only be used for C_s molecules.

Throughout this work, the programs XIAM and BELGI were used. As all examined molecules contain a nitrogen atom, weak quadrupole coupling occurs, which can be easily treated with XIAM. With BELGI, a treatment of quadrupole coupling was initially not available and therefore developed in the context of this work. The respective theory and the development of the code is described in subsection 3.2.1.

Chapter 3

Fit Routines

The program XIAM is based on the theory given in the references [25] and [42]. In BELGI the Hamiltonian is constructed in the rho axis system based on the work of Kirtman [43], Lees and Baker [44], and Herbst et. al. [45]. Basics to internal rotation are discussed in detail in the article from C. C. Lin and J. D. Swalen [46]. Relevant parts for this dissertation are taken from these references and summarized in the following.

3.1 XIAM

The program XIAM, as already mentioned in section 2.1, is an internal rotor program, but has also a rigid rotor mode for the treatment of molecules without internal rotation. Additionally, it can treat weak hyperfine splittings, such as those that appear by ^{14}N nuclei. It is very comfortable to use and fast in operation, which makes it a very powerful tool, especially in the assignment process of microwave spectra. It was therefore used throughout this work for all measured molecules.

In XIAM a rigid rotor Hamiltonian is programmed in the principal axis system. In this axis system the moment of inertia tensor is diagonal:

$$\mathbf{I} = \begin{pmatrix} I_a & 0 & 0 \\ 0 & I_b & 0 \\ 0 & 0 & I_c \end{pmatrix} \tag{3.1}$$

with

$$I_a = \sum_{i=1}^{N} m_i(b_i^2 + c_i^2); \quad I_b = \sum_{i=1}^{N} m_i(a_i^2 + c_i^2); \quad I_c = \sum_{i=1}^{N} m_i(a_i^2 + b_i^2) \tag{3.2}$$

N is the number of atoms, m_i the mass of the atom i, and a_i, b_i, c_i are the nuclear coordinates of the atom i.

The kinetic energy T can be written in a very simple way using the angular velocity $\overrightarrow{\omega}$:

$$T = \frac{1}{2}\overrightarrow{\omega}^{+} I \overrightarrow{\omega} \tag{3.3}$$

with

$$\overrightarrow{\omega}^{+} = \begin{pmatrix} \omega_a & \omega_b & \omega_c \end{pmatrix}, \overrightarrow{\omega} = \begin{pmatrix} \omega_a \\ \omega_b \\ \omega_c \end{pmatrix} \tag{3.4}$$

From Equation 3.1 and Equation 3.3 follows:

$$T = \frac{1}{2}I_a\omega_a^2 + \frac{1}{2}I_b\omega_b^2 + \frac{1}{2}I_c\omega_c^2 \tag{3.5}$$

With the use of the angular momenta P_g with $g = a, b, c$ one obtains:

$$P_a = I_a\omega_a; \quad P_b = I_b\omega_b; \quad P_c = I_c\omega_c \tag{3.6}$$

$$T = \frac{1}{2I_a}P_a^2 + \frac{1}{2I_b}P_b^2 + \frac{1}{2I_c}P_c^2 \tag{3.7}$$

The internal rotation in XIAM is treated by internal rotation operators in the rho axis system of one rotor. They form the torsional Hamiltonian H_t, which is set up as a combination of a kinetic and a potential energy part taking the 3-fold nature of methyl rotors into account:

$$H_t = F(p_\alpha - \rho P_z)^2 + \frac{1}{2}V_3(1 - cos3\alpha) + \frac{1}{2}V_6(1 - cos6\alpha) + \ldots \tag{3.8}$$

F is the reduced rotational constant of the internal rotor, p_α the angular momentum of the internal rotor, α the torsional angle and $\rho = \sqrt{\rho_x^2 + \rho_y^2 + \rho_z^2}$ with $\rho_g = \lambda_{i,g}\frac{I_\alpha}{I_g}$; $\lambda_{i,g} = cos(\measuredangle i, g)$; $g = x, y, z$.

The use of the rho axis system has the advantage that the rotation-torsion coupling is much easier to describe as the coupling terms $p_\alpha P_x$ and $p_\alpha P_y$ vanish. Using the torsional Hamiltonian an internal rotation matrix is then set up and diagonalized in a first diagonalization step. The obtained eigenfunctions[1] are used as torsional eigenfunctions for a second diagonalization step. In this step the internal rotation, overall rotation, and the rotation-torsion coupling is taken into account and a second matrix is set up and diagonalized in the principal axis system.

3.2 BELGI

The Hamiltonian programmed in BELGI can we written as follows [26, 27]:

$$H = H_r + H_t + H_{rt} \tag{3.9}$$

with H_t describing the torsional Hamiltonian, which is basically the same as the one given in Equation 3.8. H_r is the rotational and H_{rt} the rotational-torsional-coupling Hamiltonian.

The rotational Hamiltonian H_r in its simplest form, which is valid for C_s molecules, is the following[2]:

$$H_r = AP_a^2 + \frac{B+C}{2}(P_b^2 + P_c^2) + \frac{B-C}{2}(P_b^2 - P_c^2) + D_{ab}(P_aP_b + P_bP_a) \tag{3.10}$$

In the case of C_1 molecules further terms for example $D_{bci}(P_bP_c + P_cP_b)$ and $D_{aci}(P_aP_c + P_cP_a)$ have to be added.

[1] The eigenfunctions are linear combinations of the planar rotor $\psi(\varphi) = \sqrt{\frac{1}{2\pi}}e^{im\varphi}$.

[2] In BELGI the I^r representation is used: $z = a, x = b, y = c$; $P_z = P_a, P_x = P_b, P_y = P_c$, etc.

The part which makes BELGI quite powerful in some cases, is the implementation of a high number of rotation-torsion-coupling parameters, which are used as effective parameters. A few important ones are indicated in the following:

$$\begin{aligned} H_{rt} &= P^2 && [F_V(1-cos3\alpha) && + G_V(p_\alpha - \rho P_a)^2 && + L_V P_a(p_\alpha - \rho P_a) && + \dots] \\ &+ P_a^2 && [k_5(1-cos3\alpha) && + k_2(p_\alpha - \rho P_a)^2 && + k_1 P_a(p_\alpha - \rho P_a) && + \dots] \\ &+ (P_b^2 - P_c^2) && [c_2(1-cos3\alpha) && + c_1(p_\alpha - \rho P_a)^2 && + c_4 P_a(p_\alpha - \rho P_a) && + \dots] \\ &+ (P_aP_b + P_bP_a)\,[\dots] + (P_aP_c + P_cP_a)\,[\dots] + (P_bP_c + P_cP_b)\,[\dots] \\ &+ \dots \end{aligned} \tag{3.11}$$

In BELGI also a two steps diagonalization process is used, where first only the torsional part is diagonalized, followed by a global diagonalization. The global diagonalization is in contrast to XIAM also carried out in the rho axis system.

3.2.1 BELGI-C_1-hyperfine

In the scope of this investigation on amides, the program BELGI-C_1 was extended in order to treat spectra with internal rotation and weak quadrupole coupling. The extended program-version is called **BELGI-C_1-hyperfine**. In the following the basics are given, which have been published in reference [47].

To deal with the hyperfine structure, we used a perturbation approach similar to the one used for acetamide, a C_s molecule with one methyl internal rotor (see Eq. 1 of Ref. [48]), but we extended it by including terms allowed under C_1 symmetry. The procedure is the following: We first obtained the rotation-torsion eigenvalues and eigenvectors from the usual two-step diagonalization of the Hamiltonian $\widehat{H}$ in the rho axis system. The global fitting program was modified to output expectation values of $\langle P_a^2\rangle, \langle P_b^2\rangle, \langle P_c^2\rangle, \langle P_aP_b+P_bP_a\rangle, \langle P_aP_c+P_cP_a\rangle, \langle P_bP_c+P_cP_b\rangle$ in the rho axis system. We then used in a second step numerical values for these quantities in the standard hyperfine energy expression [7]:

$$\begin{aligned} E_{hf}(I,J,F) = [&\chi_{aa}\langle P_a^2\rangle + \chi_{bb}\langle P_b^2\rangle - (\chi_{aa}+\chi_{bb})\langle P_c^2\rangle + \chi_{ab}\langle P_aP_b + P_bP_a\rangle \\ &+\chi_{ac}\langle P_aP_c + P_cP_a\rangle + \chi_{bc}\langle P_bP_c + P_cP_b\rangle]\ 2\ \frac{f(I,J,F)}{J(J+1)} \end{aligned} \tag{3.12}$$

where χ_{ij} with $i, j = a, b, c$ are the quadrupole coupling constants (see Equation 2.2) and $f(I, J, F)$ is the Casimir function [7]:

$$f(I, J, F) = \frac{\frac{3}{4}C(C+1) - I(I+1)J(J+1)}{2(2J-1)(2J+3)I(2I-1)} \tag{3.13}$$

with

$$C = F(F+1) - I(I+1) - J(J+1) \tag{3.14}$$

For a ^{14}N nucleus with a nuclear spin $I = 1$ follows:

$$f(1, J, F) = \frac{\frac{3}{4}C(C+1) - \mathbf{2}J(J+1)}{2(2J-1)(2J+3)\mathbf{1}} \tag{3.15}$$

$$C = F(F+1) - \mathbf{2} - J(J+1) \tag{3.16}$$

With Equation 3.12 the shifts for each rotation-torsion energy level due to the quadrupole coupling can be calculated, and therefore the shift ΔE_{Qshift} of hyperfine components for each rotation-torsional transition:

$$\Delta E_{Qshift} = E'_{hf}(I', J', F') - E''_{hf}(I'', J'', F'') \tag{3.17}$$

To calculate the shifts one needs the J and F quantum numbers of the transitions. These were obtained by taking into account the selection rules:

$$\Delta F = 0, \pm 1; \quad \Delta J = 0, \pm 1 \tag{3.18}$$

Afterwards, the quadrupole shift was added to the calculated energy for the rotation-torsion energy levels, which are calculated in BELGI in the already mentioned two-step diagonalization of the rotation-torsion Hamiltonian.

In the code the quadrupole coupling constants χ_{aa}, χ_{bb}, χ_{cc}, χ_{ab}, χ_{ac}, χ_{bc} were included as XAA, XBB, XCC, XAB, XAC, XBC. The shift-calculation was programmed as follows, where the Casimir function in the code was directly extended by the factor $\frac{1}{J(J+1)}$ (see Equation 3.12) for programming purposes:

```
1  ...
2  c      ---------- calculation of the hyperfine shift ----------
3         chiu=XAA*PPA2(2)+XBB*PPB2(2)-(XAA+XBB)*PPC2(2)
4        &+XAB*PPAB(2)+XAC*PPAC(2)+XBC*PPBC(2)
5         chil=XAA*PPA2(1)+XBB*PPB2(1)-(XAA+XBB)*PPC2(1)
6        &+XAB*PPAB(1)+XAC*PPAC(1)+XBC*PPBC(1)
7
8         calcfreq(k)=ejuan
9        & + chiu*casimir(1.d0,nobs(2,k),ifobs(2,k))
10       & - chil*casimir(1.d0,nobs(1,k),ifobs(1,k))
11
12        qshift(k)= chiu*casimir(1.d0,nobs(2,k),ifobs(2,k))
13       & - chil*casimir(1.d0,nobs(1,k),ifobs(1,k))
14
15        euphyp=eupper+chiu*casimir(1.d0,nobs(2,k),ifobs(2,k))
16        elowhyp=elower+chil*casimir(1.d0,nobs(1,k),ifobs(1,k))
17
18 ...
19
20 c      ---------- definition of the casimir funktion ----------
21        function casimir(ei,j,f)
22
23        implicit double precision (a-h,o-z)
24        integer f
25        if(j.eq.0) go to 100
26        c=f*(f+1.d0)-1.d0*2.d0-j*(j+1.d0)
27        casimir=(0.75d0*c*(c+1.d0)-1.d0*2.d0*j*(j+1.d0))/
28       & (2.d0*1.d0*j*(j+1.d0)*(2.d0*j-1.d0)*(2.d0*j+3.d0))
29        return
30   100  casimir = 1.d0
31        return
32        end
33 ...
```

The most complex part of the programming was the implementation of this shift calculation in the already existing diagonalization and least square-fit routines implemented in BELGI. For the least-square fit the so called **V**-matrix is set up:

$$\mathbf{V_{kl}} = \begin{pmatrix} V_{1,1} & \dots & V_{1,l} \\ \vdots & \ddots & \vdots \\ V_{k,1} & \dots & V_{k,l} \end{pmatrix} \tag{3.19}$$

$$l = parameters(A, B, C, \Delta_J, \dots, V_3, \rho, D_{ab}, D_{bci}, \dots, \chi_{aa}, \chi_{bb}, \dots)$$

$$k = transitions$$

The matrix elements of the **V**-matrix are the derivatives of the frequencies ν_k with respect to the parameter x_l:

$$V_{kl} = \frac{d\nu_k}{dx_l} \tag{3.20}$$

In BELGI-C_1-hyperfine the derivatives of the quadrupole coupling constants had to be calculated and added to the V-matrix. As an example the **V**-matrix elements of the χ_{aa} and χ_{ab} parameters are given:

$$V_{k\chi_{aa}} = \frac{d\nu_k}{d\chi_{aa}} = \left(\langle P_a^2\rangle' - \langle P_a^2\rangle''\right)\ 2\ \frac{f(I,J,F)}{J(J+1)} \tag{3.21}$$

$$V_{k\chi_{ab}} = \frac{d\nu_k}{d\chi_{ab}} = \left(\langle P_aP_b + P_bP_a\rangle' - \langle P_aP_b + P_bP_a\rangle''\right)\ 2\ \frac{f(I,J,F)}{J(J+1)} \tag{3.22}$$

Using BELGI-C_1-hyperfine, all hyperfine patterns can be fitted, floating the nuclear quadrupole coupling constants together with the rotational parameters such as the rotational constants A, B, C and the centrifugal distortion constants Δ_J, Δ_{JK}, Δ_K, δ_J, δ_K, and rotation-torsion parameters. In BELGI a great number of rotation-torsion parameters are included. The most important are V_3, ρ, D_{ab}, D_{bci}, D_{aci}.

The BELGI-C_1-hyperfine code was first tested with the C_1 molecule N-ethylacetamide. The results are revisited in section 9.4. Additionally, the code can be used to treat molecules with C_s symmetry like N-*tert*-butylacetamide by fixing all out of plane C_1 terms to zero. The results for this molecule are given in section 10.4.

To do a fit with BELGI-C_1-hyperfine, first the lines from the XIAM output have to be converted into the format used in BELGI. For this purpose the program *convertXIAMtoBELGI* can be used. It automatically gives all fitted data in the correct format, which is shown in Figure 3.1.

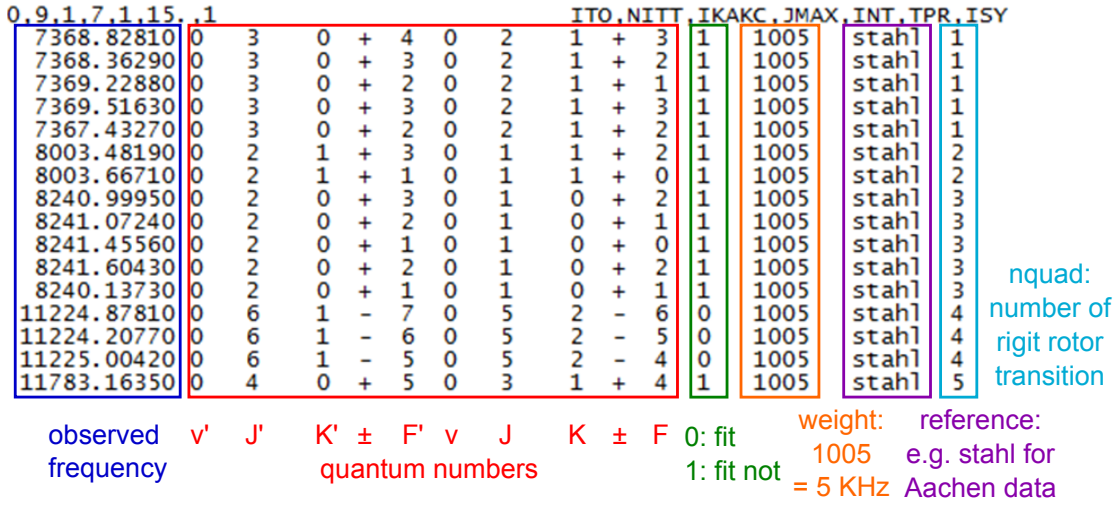

Figure 3.1: The format of the microwave data in the BELGI-C_1-hyperfine input.

After a fit with BELGI, one often wants to compare the results to values in the principal axis system. For this purpose W. Stahl developed the program RAM2PAM. It was also extended for the purpose of converting the RAM-quadrupole coupling constants into the PAM system.
In RAM2PAM first the matrix **D** is diagonalized with the Jacobi-algorithm:

$$\mathbf{D}_{RAM} = \begin{pmatrix} A & D_{ab} & D_{ac} \\ D_{ab} & B & D_{bc} \\ D_{ac} & D_{bc} & C \end{pmatrix}^{RAM} \xrightarrow{Jacobi} \mathbf{D}_{PAM} = \begin{pmatrix} A & 0 & 0 \\ 0 & B & 0 \\ 0 & 0 & C \end{pmatrix}^{PAM} \tag{3.23}$$

This algorithm delivers the eigenvalues, which are the rotational constants A, B, C in the principal axis system and the eigenvectors, which form the rotation matrix **R**.

With this rotation matrix $\mathbf{R}$ and its transposed matrix $\mathbf{R^T}$ the quadrupole coupling tensor $\mathbf{X_{RAM}}$ can be transformed in the principal axis system.

$$\mathbf{X_{PAM}} = \mathbf{R^T} \cdot \mathbf{X_{RAM}} \cdot \mathbf{R} \tag{3.24}$$

with

$$\mathbf{X} = \begin{pmatrix} \chi_{aa} & \chi_{ab} & \chi_{ac} \\ \chi_{ab} & \chi_{bb} & \chi_{bc} \\ \chi_{ac} & \chi_{bc} & \chi_{cc} \end{pmatrix} \tag{3.25}$$

Chapter 4

Experimental

4.1 Microwave Spectroscopy

All spectra throughout this work were measured using two molecular beam Fourier transform microwave (MB-FTMW) spectrometers operating in the frequency ranges from 2 - 26.5 GHz [49] and from 26.5 - 40 GHz [50]. The spectrometers are shown in Figure 4.1

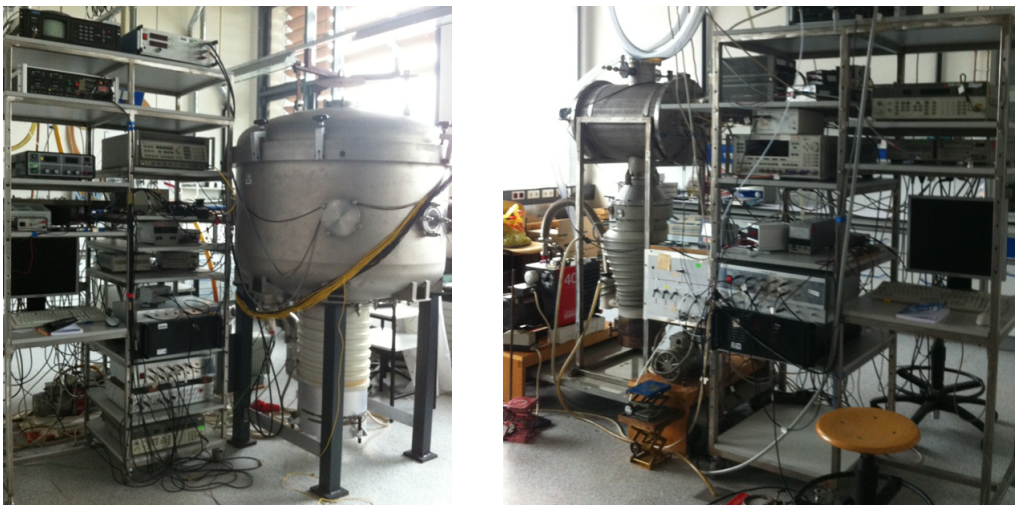

Figure 4.1: Two molecular beam Fourier transform microwave spectrometers with Fabry-Pérot cavities and electronics for the signal processing.

Both spectrometers have two operation modes, a scan mode of lower resolution and a high resolution mode, which enables spectral data with a resolution of about 2 kHz for isolated lines [51].

In the scan mode of the spectrometer single measurements are recorded in steps of 0.25 MHz and automatically summarized to a broadband scan. With this mode a broad frequency range can be obtained in a relatively short time in order to indicate rough frequencies of the rotational transitions. As an example Figure 4.2 shows a typical part of a broadband scan. It gives various lines with different intensities, given in a logarithmic scale with arbitrary units. Some lines are broadened due to the quadrupole coupling of the nitrogen nucleus. The hyperfine structure of nitrogen usually gives overall splittings up to 10 MHz, where splittings between individual lines are often in the order of a few hundreds of kHz.

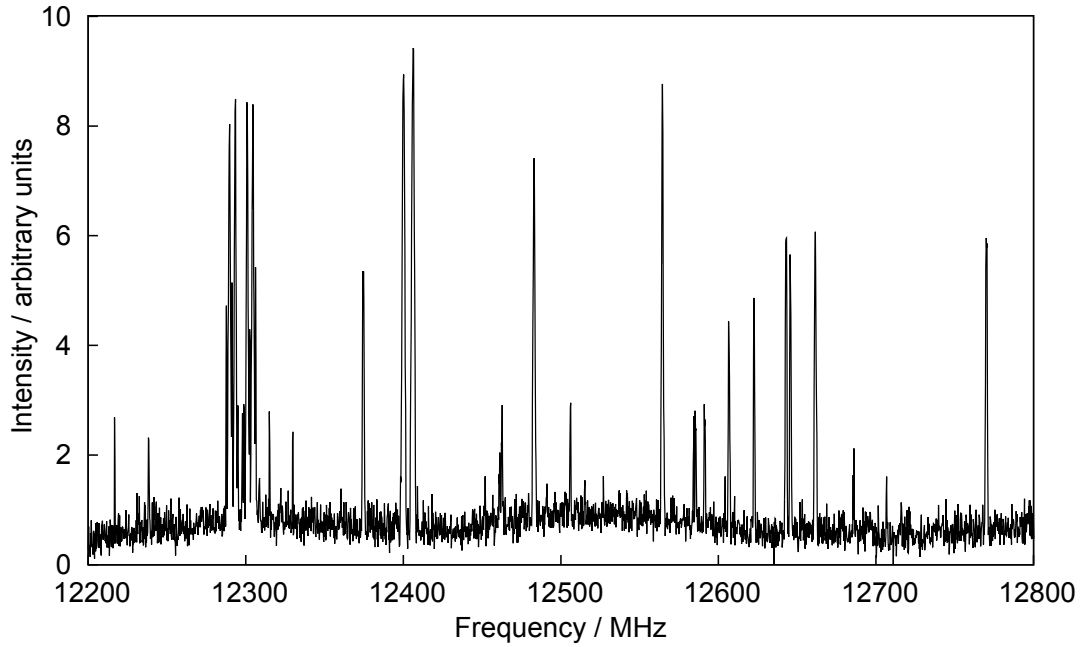

Figure 4.2: Typical part of a broadband scan observed with a Fourier transform microwave spectrometer.

Lines identified with the use of the scan mode are afterwards remeasured in the high resolution mode to provide highly resolved data, where also very small splittings, which occur e.g. for molecules with highly hindered internal rotors or quadrupole coupling, can be resolved. An example of a high resolution measurement is given in Figure 4.3. It shows splittings due to internal rotation ($\Delta\nu_{IR}$) and quadrupole coupling ($\Delta\nu_{12}$, $\Delta\nu_{23}$, $\Delta\nu_{34}$). Additionally, all lines are further split into two Doppler components ($\Delta\nu_D$). This Doppler splitting is caused by the expansion of the molecular beam along the resonator-axis. The Full Width at Half Maximum (FWHM) of the lines is about 2 kHz.

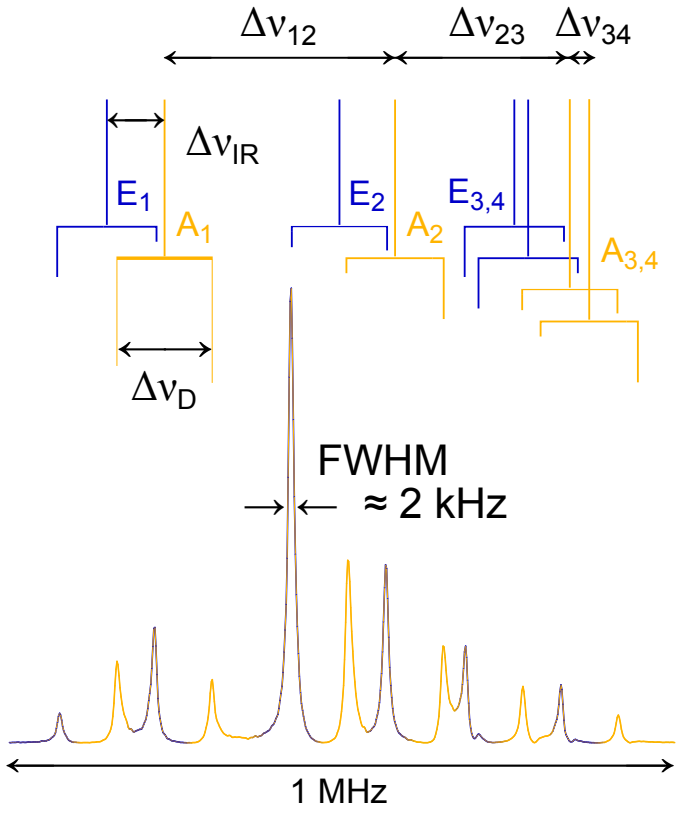

Figure 4.3: Typical high resolution measurement observed with a Fourier transform microwave spectrometer for a nitrogen containing molecule including highly hindered internal rotation (here: DEAA chapter 15). The Doppler splitting is indicated by $\Delta\nu_D$, the internal rotation splitting by $\Delta\nu_{IR}$ and the hyperfine splitting by $\Delta\nu_{12}$, $\Delta\nu_{23}$, and $\Delta\nu_{34}$. The Full Width at Half Maximum FWHM $\approx$ 2 kHz.

For the injection of the substances, two different methods were applied for liquid substances (Method A) and solid substances (Method B):

Method A: A pipe cleaner, which is used as a carrier material, is soaked with the liquid substance and inserted in a stainless steel tube in front of the nozzle. In the case of very low vapor pressures, the steel tube was additionally heated, to support the evaporation of the substance. Helium was flown over the pipe cleaner at a pressure of 150 to 200 kPa to pick up the evaporated substance.

Method B: Solid substances are filled directly into the stainless steel tube and placed in front of the nozzle. To prevent the solid from moving and plugging the nozzle, the tube is capped with small pieces of pipe cleaner at both ends (0.5 cm). Due to lower permeability of solid substances a higher pressure of 200 to 250 kPa of the helium carrier gas is necessary.

All measured substances are listed in Table 4.1 giving also the company, which provided the substance, the stated purity, and the calculated vapor pressure at 25°C. All substances were used without further purification. For substances that are solid at room-temperature the melting point is also given in Table 4.1.

Table 4.1: Molecular formula, provider, purity, and vapor pressure of the measured substances.

substance	**formula**	**provider**	**purity**	$\mathbf{p_{vap}}$ [a]/torr
N-Vinyl-formamide	$H(C{=}O)NHC_2H_3$	TCI Deutschland GmbH, Eschborn, Germany.	>98%	0.470
N-*tert*-Butyl-formamide	$H(C{=}O)NHC_4H_9$	TCI Europe, Zwijndrecht, Belgium	>97%	0.299
N-Ethyl-acetamide	$CH_3(C{=}O)NHC_2H_5$	Alfa Aesar GmbH & Co KG, Karlsruhe, Germany	99%	0.256
N-*tert*-Butyl-acetamide	$CH_3(C{=}O)NHC_4H_9$	Alfa Aesar GmbH & Co KG, Karlsruhe, Germany	98%	0.345 T_m=95-99°C
N-Vinyl-acetamide	$CH_3(C{=}O)NHC_2H_3$	TCI Europe, Zwijndrecht, Belgium	>98%	0.222 T_m=53°C
N,N-Diethyl-propionamide	$C_2H_5(C{=}O)N(C_2H_5)_2$	TCI Europe, Zwijndrecht, Belgium	>98%	0.444
N,N-Dimethyl-propionamide	$C_2H_5(C{=}O)N(CH_3)_2$	TCI Europe, Zwijndrecht, Belgium	>98%	1.12
N,N-Diethyl-acetamide	$CH_3(C{=}O)N(C_2H_5)_2$	Merck Schuchardt OHG, Hohenbrunn, Germany	98%	0.695
N-Methyl-diacetamide	$(CH_3(C{=}O))_2NCH_3$	Alfa Aesar GmbH & Co KG, Karlsruhe, Germany	90%	1.070

[a] The vapor pressure p_{vap} is calculated by scifinder [52] at a temperature of 25°C.

4.2 Quantum Chemical Calculations

For the quantum chemical calculations the GAUSSIAN09 suite of programs was used [53]. Different methods such as MP2, DFT, and HF as well as different basis sets were chosen.

4.2.1 Conformational Analysis

For the conformational analysis usually the calculations were carried out at the MP2/6-311G(d,p) level of theory. The nature of the stationary points was afterwards confirmed by frequency calculations. Additionally the assigned conformers were often recalculated at different level of theory.

4.2.2 ^{14}N Nuclear Quadrupole Coupling

As all investigated molecules contain a nitrogen nucleus the quadrupole coupling constants had to be calculated in order to assign the hyperfine structure. This was done using a calculation method of W. C. Bailey [37, 54].
For most nitrogen containing molecules the conformers were optimized at different levels of theory and afterwards the NQCCs calculated by single point electric field gradient calculations at the B3PW91/6-311+G(df,pd) level of theory. The results were multiplied with a calibration factor of eQh^{-1} of 4.5586(40) MHz a.u.$^{-1}$.
For π-conjugated systems single point calculations at the B3PW91/6-311+G(d,p) level of theory with a calibration factor of eQh^{-1} of 4.599(12) MHz a.u.$^{-1}$ show better results. This method specified for π-conjugated systems was developed within the work on N-vinylformamide in cooperation with W. C. Bailey and is explained in detail in chapter 6.
This method has proofed to be very helpful in many investigations on nitrogen containing molecules [55, 56] as it delivered very precise NQCCs, which are helpful in the assignment process, due to a good prediction of hyperfine structures.

Part I

Formamides

Chapter 5

Introduction

Amides are nitrogen containing functional groups of general interest in chemistry and molecular biology. Due to conjugation between the carbonyl π-electrons and the lone electron pair of the nitrogen, their electronic configurations are rather complex. Formamides are a sub-class of amides which contain the planar sub-unit H(C=O)N. Spectroscopic investigations of several formamides have been reported, aimed at determining their rotational structures. The simplest amide, formamide [3], as well as N-methylformamide [4], N-ethylformamide [5], N,N-dimethylformamide [57], and N,N-methylethylformamide [58] were thoroughly studied. Reports on the microwave spectra of three unsaturated formamides, N-phenylformamide [59, 60], N-vinylformamide [61], and diformamide [62] are available in the literature. Such unsaturated molecules are very interesting, since π-electron conjugation between the double bond(s), the lone electron pair of the nitrogen, and the carbonyl bond is possible.

In the following the results of microwave and quantum chemical investigations on N-vinylformamide (chapter 6) and N-*tert*-butylformamide (chapter 7) are shown. These molecules differ only in the substituent at the nitrogen. The vinyl group provides an extension of the already existing π-conjugation of the amide bond, which makes it interesting to investigate this influence on the quadrupole coupling. The *tert*-butyl group on the other hand provokes not only a large sterical but also a remarkable positive inductive effect, surely to influence the electronic situation at the nitrogen nucleus and therefore the quadrupole coupling as well.

Chapter 6

N-Vinylformamide - VFA

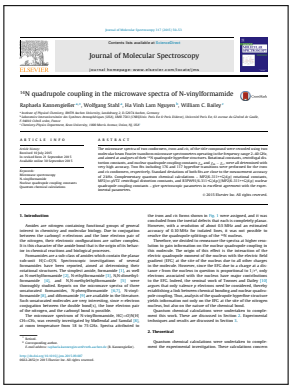
Journal of Molecular Spectroscopy

^{14}N quadrupole coupling in the microwave spectra of N-vinylformamide

Parts of this chapter have already been published in the Journal of Molecular Spectroscopy:

R. KANNENGIEßER, W. STAHL, H.V.L. NGUYEN and W.C. BAILEY ^{14}N quadrupole coupling in the microwave spectra of N-vinylformamide *J. Mol. Spectrosc.*, 2015, **317**, 50-53.

The measurements, quantum chemical calculations, spectrum analysis, spectrum assignment, fits and manuscript preparation on these parts is the work of R. Kannengießer. The coworkers took mostly part in a supporting way especially during corrective work in the publication process. W.C. Bailey carried out the calibration for unsaturated and saturated amides.

6.1 Introduction

The microwave spectrum of N-vinylformamide, HC(=O)N(H)CH=CH_2, was recently investigated by Møllendal and Samdal [61], at room temperature from 18 to 75 GHz. Spectra attributed to the *trans* and *cis* forms shown in Figure 6.1 were assigned, and it was concluded from the inertial defects that each is completely planar. However, with a resolution of about 0.5 MHz and an estimated accuracy of 0.10 MHz for isolated lines, it was not possible to resolve the quadrupole splittings of the ^{14}N nucleus.

Therefore, in the scope of this dissertation the spectra were remeasured at higher resolution to gain information on the nuclear quadrupole coupling in this molecule. Additionally, further calculation methods of nitrogen containing molecules in terms of quadrupole coupling were developed. This molecule was investigated as a special situation is present in N-vinylacetamide, where the π-conjugation of the carbonyl π-electrons and the lone pair of the nitrogen is extended by the vinyl group.

6.2 Theoretical

Quantum chemical calculations were undertaken to predict spectroscopic constants of sufficient accuracy to assist with assignment of the experimental spectra. These are the rotational constants, inertial axes components of the ^{14}N nuclear quadrupole coupling constants (NQCCs), and quartic centrifugal distortion constants (CDCs).

6.2.1 Conformational Preferences

Quantum chemical calculations by Møllendal and Samdal identified four stable conformers, which were recalculated here and are shown in Figure 6.1. Only the two most stable ones *trans*-I and *cis*-I (see left Figure 6.1) were found in their experimental spectrum - and in ours. These conformers are from now on denoted as *trans* and *cis* only.

At the B3LYP and CCSD(T) levels of theory, each in conjunction with cc-pVTZ bases, Møllendal and Samdal calculate the *cis* conformer more stable than the *trans* by 0.3 and 2.8 kJ·mol^{-1}, respectively.
In this work, at the MP2/6-311++G(d,p) level, *trans* is found more stable by 1.9 kJ·mol^{-1}. The results of these and several other calculations are shown in Table 6.1. The MP2 optimized atomic coordinates in the principal inertial axis system are given in the Appendix A in Table A.1 and Table A.2.
This point of the incoherence in the calculated energetical order will be revisited in the section 6.3 with regard to the experimental circumstances.

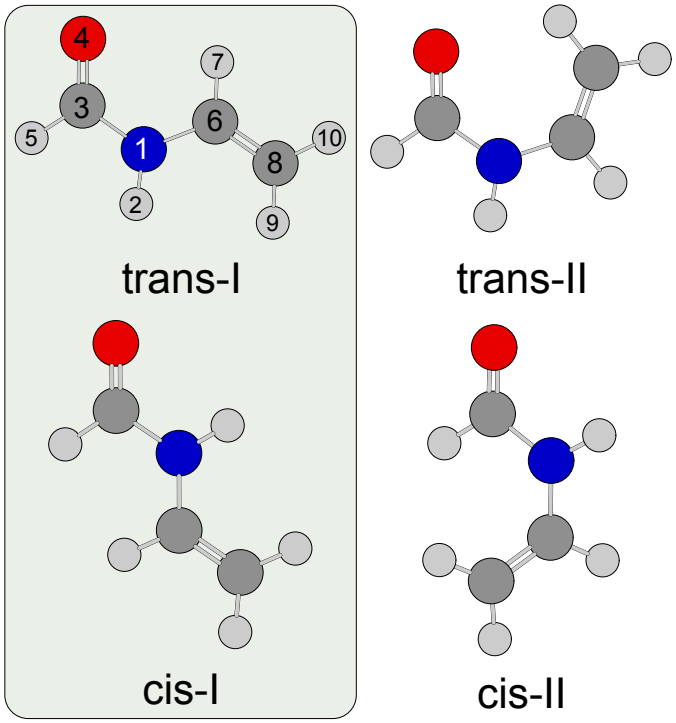

Figure 6.1: Calculated conformers of N-vinylacetamide. Observed conformers *trans*-I and *cis*-I are on the left.

Table 6.1: Energies in Hartree calculated at different levels of theory for the two lowest energy conformers *trans*- and *cis*-N-vinylformamide and their energetical difference in kJ·mol^{-1}.

method	E_{trans} [a]	E_{cis} [a]	$\Delta E_{c.-t.}$
B3LYP/cc-pVTZ [b]	−247.308956	−247.309062	−0.3
CCSD(T)/cc-pVTZ [b]	–	–	−2.8
MP2/6-311++G(d,p)	−246.594672	−246.594013	1.7
MP2/6-311+G(d,p)	−246.594048	−246.593431	1.6
MP2/6-311G(d,p)	−246.582470	−246.582031	1.2
MP2/6-31++G(d,p)	−246.503820	−246.503242	1.5
MP2/6-31+G(d,p)	−246.503087	−246.502491	1.6
B3LYP/6-311++G(3df,2pd)	−247.308417	−247.308386	0.1
B3LYP/6-311++G(d,p)	−247.289805	−247.289571	0.6
B3LYP/6-311+G(d,p)	−247.289717	−247.289476	0.6
B3LYP/6-311G(d,p)	−247.282251	−247.281982	0.7

[a] Sum of electronic and zero-point energies [b] Calculated by Møllendal and Samdal [61].

6.2.2 Nuclear Quadrupole Coupling Constants

Components of the NQCC tensor, χ_{ij} are related to those of the EFG tensor, q_{ij} by

$$\chi_{ij}\ (\text{MHz}) = (eQ/h) \times q_{ij}\ (\text{a.u.}), \tag{6.1}$$

where e is the fundamental electric charge, Q is the electric quadrupole moment of the nucleus, and h is Planck's constant. Calibration of a particular computational model for the calculation of NQCCs is achieved by taking the coefficient eQ/h as a best-fit parameter determined by linear regression analysis of calculated q_{ij} on the experimental structures of a number of molecules versus the corresponding experimental χ_{ij} [54]. The premise that underlies this procedure is that errors inherent in the level of theory are systematic and can be corrected, at least in part, by the best fit parameter eQ/h. Thus was undertaken calibration of the B3PW91/6-311+G(d,p) model, the result of which is illustrated in Figure 6.2. The best-fit parameter eQ/h, the slope of the line shown in the figure, is 4.599(12) MHz/a.u..

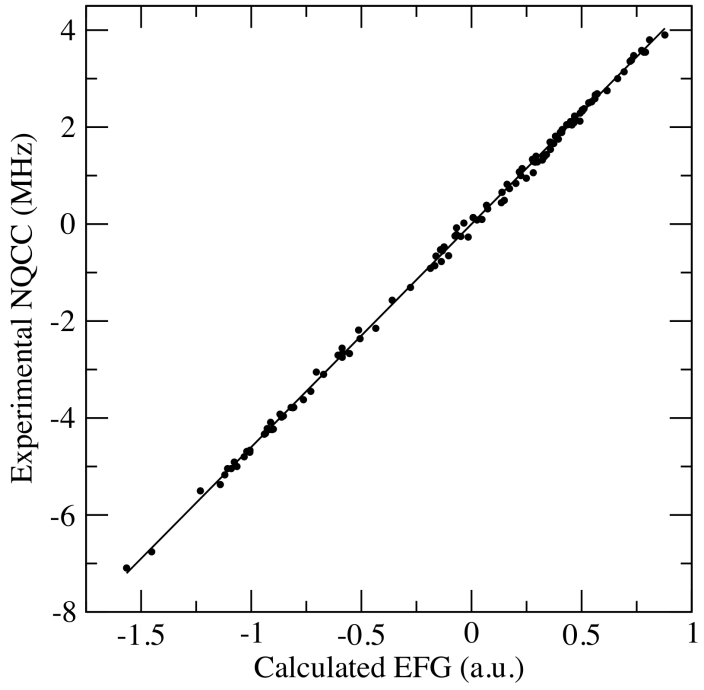

Figure 6.2: Linear regression of experimental NQCCs, χ_{ii} versus B3PW91/6-311+G(d,p) calculated EFGs, q_{ii}. The slope, eQ/h is 4.599(12) MHz/a.u. Standard deviation of the residuals is 0.086 MHz (3.8 % of average $|\chi_{ii}|$).

This model was used here for calculation of the NQCCs on MP2/6-311++G(d,p) optimized structures of both *trans* and *cis* conformers of N-vinylformamide. The results of calculations on this and several other MP2, B3LYP, and HF optimized structures are shown in Table 6.2.

The root mean square deviations for the *trans* conformer were in general lower compared to *cis*. High rms values were mostly found for both *cis* and *trans* with the Hartree Fock method, which is probably due to the simplicity of this method. However with the quite extensive basis set of 6-311++G(3df,3pd) also high rms were obtained in almost all cases.

Table 6.2: ^{14}N inertial axes nuclear quadrupole coupling constants (MHz) in N-vinylformamide, and root mean square (rms) differences between calculated and experimental coupling constants. B3PW91/6-311+G(d,p) calculations of EFGs/NQCCs were made on indicated HF, B3LYP, and MP2 optimized structures.

	χ_{aa}	χ_{bb}	χ_{cc}	rms
trans /experimental	1.70574(90)	1.9358(11)	−3.6416(11)	
HF/6-311++G(d,p)	1.691	1.944	−3.634	0.011
HF/6-311++G(df,pd)	1.684	1.939	−3.623	0.017
HF/6-311++G(3df,3pd)	1.670	1.937	−3.607	0.029
B3LYP/6-311++G(d,p)	1.728	1.948	−3.676	0.025
B3LYP/6-311++G(df,pd)	1.718	1.945	−3.663	0.015
B3LYP/6-311++G(3df,3pd)	1.707	1.941	−3.648	0.005
MP2/6-311++G(d,p)	1.714	1.955	−3.669	0.020
MP2/6-311++G(df,pd)	1.694	1.955	−3.649	0.014
MP2/6-311++G(3df,3pd)	1.676	1.946	−3.622	0.021
cis/experimental	1.8520(14)	1.7876(20)	−3.6396(20)	
HF/6-311++G(d,p)	1.836	1.746	−3.582	0.042
HF/6-311++G(df,pd)	1.825	1.745	−3.570	0.049
HF/6-311++G(3df,3pd)	1.813	1.741	−3.554	0.060
B3LYP/6-311++G(d,p)	1.859	1.754	−3.614	0.024
B3LYP/6-311++G(df,pd)	1.845	1.755	−3.601	0.030
B3LYP/6-311++G(3df,3pd)	1.834	1.752	−3.586	0.039
MP2/6-311++G(d,p)	1.847	1.759	−3.606	0.026
MP2/6-311++G(df,pd)	1.819	1.766	−3.585	0.038
MP2/6-311++G(3df,3pd)	1.805	1.755	−3.560	0.056

6.3 Experimental

At the beginning of the experimental work, some microwave transitions of *cis* and *trans* conformers given in Ref. [61] were remeasured with higher resolution using the MB-FTMW spectrometer operating in the frequency range from 26.5 GHz to 40 GHz.

The hyperfine splittings were calculated using the predicted NQCCs, and could be completely resolved and assigned. We then used the fitted constants χ_{aa} and $\chi_{bb}-\chi_{cc}$ to predict and measure further low J – transitions using the program *XIAM*. Some transitions in the frequency range from 2 GHz to 26.5 GHz were also recorded using the other MB-FTMW spectrometer and included in the fit. The spectrum shown in Figure 6.3 illustrates a typical high resolution measurement of the *trans* conformer with the characteristic hyperfine structure.

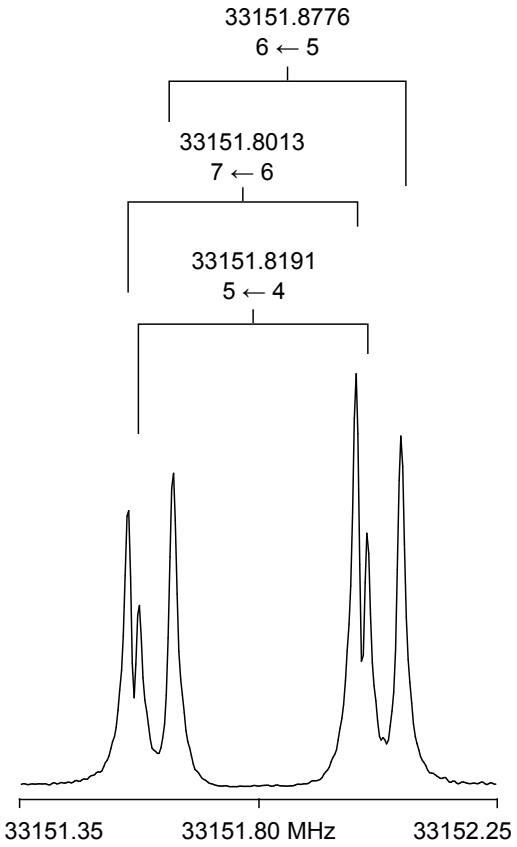

Figure 6.3: Three quadrupole components of the $6_{06} \leftarrow 5_{05}$ transition of the *trans* conformer of N-vinylformamide. The Doppler doublets are marked by brackets. The hyperfine transitions are given by $F' \leftarrow F$. For this spectrum, 225 decays were co-added.

In the spectrum, only few transitions with low J and K quantum numbers could be measured for *cis*, and all transitions belonging to *cis* possess lower intensity in comparison to those of *trans*. We conclude, therefore, that *trans* is the more stable conformer under our molecular beam conditions, which is in agreement with the calculations at different level of theory (see Table 6.1). A list including all assigned transitions of *trans* and *cis* are given in the Table A.3 and Table A.4.

6.4 Results and Discussion

Using the program *XIAM*, excellent fits for the *trans* and *cis* conformers with standard deviations of 2.3 kHz and 2.5 kHz, respectively, could be achieved, which are close to the measurement accuracy of about 2-3 kHz for N-vinylformamide. The results are given in Table 6.3.

Table 6.3: Rotational parameters from the program *XIAM* (exp) compared with theoretical parameters (calc) for the *trans* and *cis* conformers of N-vinylformamide.

		trans		*cis*	
	unit	exp [a]	calc [b]	exp [a]	calc [b]
A	MHz	19 723.244 35(44)	19 820.5	36 996.2(22)	37 208.0
B	MHz	2976.658 70(56)	2943.6	2419.110 90(19)	2400.1
C	MHz	2587.482 51(52)	2562.9	2272.129 89(18)	2254.6
Δ_J	kHz	0.6861(19)	0.681	0.200 45(71)	0.190
Δ_{JK}	kHz	−8.905(11)	−9.05	−4.219(22)	−3.82
Δ_K	kHz	103.32(11)	104.0		274.0
δ_J	kHz	0.139 29(79)	0.139	0.015 64(92)	0.0162
δ_K	kHz	2.53(26)	2.63		1.10
χ_{aa}	MHz	1.705 74(90)	1.714	1.8520(14)	1.847
$\chi_{bb} - \chi_{cc}$	MHz	5.5774(20)	5.624	5.4272(37)	5.365
χ_{bb} [c]	MHz	1.9358(11)	1.955	1.7876(20)	1.759
χ_{cc} [c]	MHz	−3.6416(11)	−3.669	−3.6396(20)	−3.606
σ [d]	kHz	2.3		2.5	
N [e]/N$_q$ [f]		43 / 176		31 / 117	

[a] Parameters are given with one standard uncertainty in parentheses. Watson's A reduction and I^r representation were used. [b] See section 6.2. [c] Derived parameter. [d] Standard deviation of the present fit. [e] Number of rigid rotor transitions used in the least square fit. [f] Number of hyperfine transitions.

In both cases, the rotational constants, centrifugal distortion constants (CDCs), and NQCCs were all determined with high accuracy. Inertial defects for *trans* and *cis*, respectively, are –0.0000873 and –0.0001461 u·Å^2, which confirms that the two conformers are definitely planar. Relative intensities in the spectrum of the *trans* and *cis* transitions clearly indicate that *trans* is the more stable conformer.

The two MP2/6-311++G(d,p) optimized structures yield rotational constants, which differ from the experimental values all by less than 1 %, while B3PW91/6-311+G(d,p) EFGs calculated on these optimized structures give NQCCs in almost exact agreement with the experimentally deduced values, which confirms that this combination of methods is suitable for prediction of NQCCs in π-conjugated amides. MP2/cc-pVTZ calculated CDCs are in good agreement with the experimental results.

Comparing χ_{zz} constants in the several formamides shown in Table 6.4, we note two distinct groups. First, we see that the χ_{zz} values are about the same for N-ethylformamide (No. **2** in Figure 6.4) and N-methylformamide (**3**), as well as for N,N-methylethylformamide (**4**) and N,N-dimethylformamide (**5**), gradually increasing in magnitude from 3.8510(11) MHz in formamide (**1**) to 4.364(2) MHz in N,N-dimethylformamide (**5**). We believe that this change depends on the increasing number of alkyl substitutions attached to the nitrogen atom. In the second group, the two conformers of N-vinylformamide (**6**) possess almost exactly the same χ_{zz} value, which is similar to that of N-phenylformamide (**7**) but different from those of the sat-

Table 6.4: ^{14}N NQCC z-principal axis component, χ_{zz} (MHz) in the formamides given here and shown in Figure 6.4

	χ_{zz}	Ref.
Formamide	−3.8510(11)	[3]
N-Ethylformamide	−3.993(51) [a]	[5]
N-Methylformamide	−4.0358(28)	[4]
N,N-Methylethylformamide	−4.216(31) [a]	[58]
N,N-Dimethylformamide	−4.364(2)	[57]
N-Phenylformamide, *trans*	−3.671(22)	[59, 60]
N-Vinylformamide, *trans*	−3.6416(11)	[b]
N-Vinylformamide, *cis*	−3.6396(20)	[b]
Diformamide, *cis-trans*	−3.41(7)	[62]

[a] Calculated from experimental diagonal components and theoretical off-diagonal components. See http://nqcc.wcbailey.net/Amides.pdf. [37]. [b] This work.

urated formamides (**2** - **5**), and gradually decreasing in magnitude from 3.8510(11) MHz in formamide (**1**) to 3.41(7) MHz in diformamide (**8**). It is likely, in this second group, that π-electron conjugation from the substituent through the lone pair electrons of the nitrogen to the carbonyl bond affects the EFGs at the nitrogen nucleus, which effect is manifested in significant variation of the χ_{zz} constant.

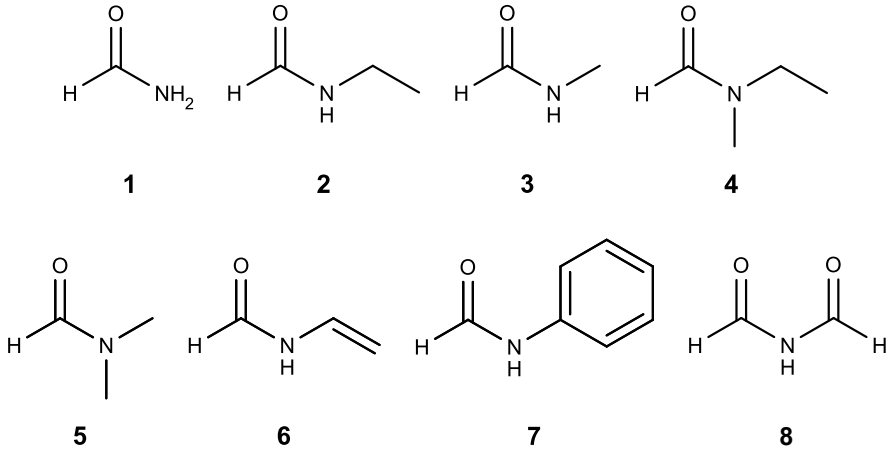

Figure 6.4: 1. Formamide, 2. N-Ethylformamide, 3. N-Methylformamide, 4. N,N-Methylethylformamide, 5. N,N-Dimethylformamide, 6. N-Vinylformamide, 7. N-Phenylformamide, 8. Diformamide

6.5 Conclusion

The quadrupole hyperfine structures in the microwave spectra of the *trans* and *cis* conformers of N-vinylformamide were assigned in the frequency range from 2 to 40 GHz, providing ^{14}N NQCCs with very high accuracy. The NQCCs of the two conformers are almost exactly the same, and are compared with values found for other saturated and unsaturated formamides.

B3PW91/6-311+G(d,p) calculated EFGs, in conjunction with eQ/h = 4.599(12) MHz/a.u., yields more reliable NQCCs for formamides possessing conjugated π-electron systems than does the B3PW91/6-311+G(df,pd) model recommended in [54], whereas this latter performs better for aliphatic formamides [37]. We conclude from this that f-polarization functions on heavy atoms hinder rather than help with modeling of conjugated π-electron systems.

Chapter 7

N-*tert*-Butylformamide - TBFA

The measurements, quantum chemical calculations, spectrum analysis, spectrum assignment, fits and manuscript preparation is the work of R. Kannengießer. B. Fenger helped with the measurements in the frequency range from 2-26.5 GHz, the fit of this data and the quantum chemical calculations.

7.1 Introduction

N-*tert*-butylformamide was measured with low-resolution microwave spectroscopy in 1984 by N. S. True [63]. The measurements were undertaken in the frequency range from 26.5 to 40 GHz. Due to the low resolution an investigation on the quadrupole coupling was not possible. Additionally, due to the high temperatures low J rotational levels were not occupied and could not be measured.

Therefore, N-*tert*-butylformamide was reinvestigated, with the focus on quadrupole coupling in lower rotational levels. Quantum chemical calculations on the conformational landscape and the quadrupole coupling constants were carried out to complement this work, because calculations on such high level were not possible in 1984.

7.2 Theoretical

7.2.1 Conformational landscape and *tert*-butyl rotation

In 1984 two conformers called the *syn* and *anti*-conformers were obtained in the spectrum, where the *anti*-conformer was told to be about 1 kJ·mol^{-1} higher in energy. In the conformational search we used two dihedral angles $\tau = (O_4 - C_3 - N_1 - C_6)$, which defines the rotation of the acetylformate group and $\phi = (C_3 - N_1 - C_6 - C_7)$, which rotates the *tert*-butyl group. First the two conformers from ref. [63] were optimized. Based on these geometries further starting geometries were constructed by rotation of τ and ϕ.
The optimization calculations delivered five stationary points. The results are summarized in Table 7.1. The nuclear coordinates of all five stationary points are given in Table B.1 to Table B.3. Only two of these stationary points were proofed as minima by frequency calculations (see Table 7.1). These are the conformers found by N. S. True in the low resolution spectrum and are shown in Figure 7.1.

Table 7.1: Relative MP2-energies in kJ·mol^{-1}, rotational constants in MHz and dipole moment components in D of the five stationary points of N-*tert*-butylformamide calculated at the MP2/6-311++G(d,p) level of theory. All values refer to the principal axis system. Additionally the number of imaginary frequencies calculated at the same level of theory are given.

	$E_{rel.}$	A	B	C	$\lvert\mu_a\rvert$	$\lvert\mu_b\rvert$	$\lvert\mu_c\rvert$	N_{imag}
syn	0.00	4095.31	1924.46	1840.60	2.839	2.960	0.001	0
anti$_{dist.}$	9.49	4353.97	1579.29	1557.10	4.951	0.517	0.131	0
anti$_{sym.}$	9.61	4356.00	1576.63	1554.19	4.984	0.585	0.001	1
anti$_{ts}$	11.88	4360.65	1558.73	1533.90	5.010	0.771	0.000	1
syn$_{ts}$	14.17	4096.48	1828.31	1747.50	3.131	2.787	0.000	1

For the lowest energy conformer, the *syn*-conformer no imaginary frequency was observed as expected. For the *anti*-conformer the calculations delivered two stationary points, one at 9.49 kJ·mol^{-1} with a slightly distorted geometry ($\mu_c \neq 0$) and one with a symmetric geometry ($\mu_c = 0$) at a slightly higher energy of 9.61 kJ·mol^{-1}. Surprisingly the distorted geometry was proofed as a minimum geometry as no imaginary frequencies were observed, while the symmetric form gave one imaginary frequency.

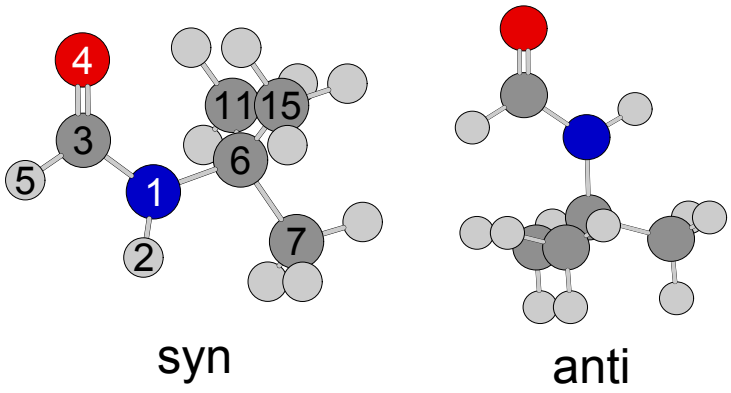

Figure 7.1: Two optimized conformer of N-*tert*-butylformamide, calculated at the MP2/6-311++G(d,p) level of theory.

As the *anti*-conformer has already been measured by N.S. True with low resolution it cannot be a transition state. Therefore, further optimizations and frequency calculations were carried out on this conformer using different methods and basis sets. Starting from both, the distorted and the symmetric geometry, DFT/B3LYP and HF calculations optimized with all used basis sets to the symmetric form giving no imaginary frequencies. With MP2 calculations of the distorted geometry stayed distorted and of the symmetric geometry stayed symmetric, independent of the basis set used in the optimization calculation. We assume therefore that the stable conformation has a symmetric geometry, which somehow causes problems in the calculations with the MP2 method. Thus for the further assignment process the calculated results for the symmetric form of the MP2 calculations were used, despite the calculated imaginary frequency.

The other two stationary points, which were highest in energy had always one imaginary frequency, independent on the method and basis set. They turned out to be the transition states of the rotation of the *tert*-butyl group. The *tert*-butyl group was rotated by 360 degrees in steps of 10 degrees and optimized. The results are shown in Figure 7.2. The barrier of the *tert*-butyl rotation is much lower for the *anti* conformer compared to *syn*, as the barriers are 2.3 kJ·mol^{-1} (192 cm^{-1}) and 14.2 kJ·mol^{-1} (1187 cm^{-1}), respectively. Both transition states could be optimized at the MP2/6-311++G(d,p) level of theory and are included in Figure 7.2.

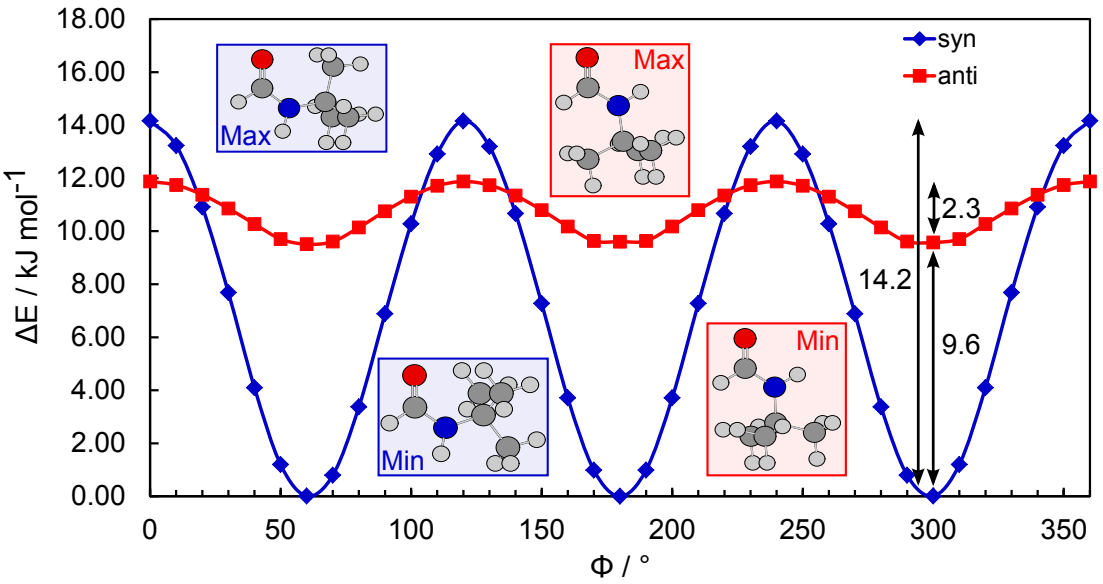

Figure 7.2: Rotation of the *tert*-butyl group ($\Phi = (C_3 - N_1 - C_6 - C_7)$) in the *syn* and the *anti* conformer relative to the energetically lower *syn* conformer.

7.2.2 Nuclear quadrupole coupling

Single point electric field gradient calculation on the *syn*-conformer gave the following nuclear quadrupole coupling constants.

$\chi_{aa} = 1.799641$ MHz, $\chi_{bb} = 2.078843$ MHz, $\chi_{cc} = -3.878484$ MHz,
$\chi_{ab} = 0.092496$ MHz, $\chi_{ac} = 0.001015$ MHz, $\chi_{bc} = -0.000287$ MHz.

For the *anti*-conformer also calculations were carried out and gave the following results.

$\chi_{aa} = 2.121428$ MHz, $\chi_{bb} = 1.971205$ MHz, $\chi_{cc} = -4.092633$ MHz,
$\chi_{ab} = 0.202800$ MHz, $\chi_{ac} = -0.000620$ MHz, $\chi_{bc} = 0.002257$ MHz.

7.3 Experimental

At first measurements in the frequency range from 2 to 26.5 GHz were carried out as the molecule is relatively large. Therefore intense lines were expected in this frequency range. As there were no transitions measured in this frequency range before, predictions had to be made using the program XIAM. For the *syn* conformer

the two rotational parameters $B + C$ and $2A - B - C$, were fitted by N. S. True, which gave us some information about the spectrum. For the *anti* conformer only $B + C$ was available, and therefore no information on the A rotational constant. In Table 7.2 and Table 7.3 the rotational parameters B_J, B_K, and B_- are listed, which are parameters used in XIAM. From the low resolution fits B_J could be calculated for *syn* and *anti*, and B_K for the *syn* conformer. The comparison of the experimental values with the calculated ones already shows a great difference in all three parameters. Thus two predictions of the spectrum were carried out, one based on the experimental values and another one using the MP2 calculated parameters.

Table 7.2: Rotational parameters of the *syn* conformer of N-*tert*-butylformamide obtained by low resolution spectroscopy in comparison with parameters calculated at different level of theory in MHz.

syn	B_J	B_K	B_-
low resolution [a]	1879.5	2185	–
MP2/6-311++G(d,p)	1882.077	2213.368	41.933
B3LYP/6-311++G(d,p)	1858.681	2204.136	41.555
B3LYP/cc-pVTZ	1864.221	2215.987	42.035
HF/6-311++G(d,p)	1876.667	2225.782	40.873

[a] results from N.S. True.

Table 7.3: Rotational parameters of the *anti* conformer of N-*tert*-butylformamide obtained by low resolution spectroscopy in comparison with parameters calculated at different level of theory in MHz.

anti	B_J	B_K	B_-
low resolution [a]	1582.5	–	–
MP2/6-311++G(d,p)	1565.409	2790.591	11.222
B3LYP/6-311++G(d,p)	1553.334	2763.169	11.216
B3LYP/cc-pVTZ	1559.675	2777.409	11.450
HF/6-311++G(d,p)	1579.934	2775.315	11.365

[a] results from N.S. True.

Regarding the predictions, fast scans were carried out in a 10 to 20 MHz range around the predicted lines, taking into account both predictions. This way the first lines of the *syn*-conformer could be found quite fast. They were then remeasured in the high resolution mode to resolve the quadrupole splittings. Parallel to the measurements a first quadrupole assignment could be achieved with the help of the

calculated NQCCs, which simplified the measurement further on. This measurement-assignment procedure was carried out for both the *syn* and the *anti* conformer. However, the measurements for the *syn* conformer turned out to be much easier due to the energetical order. For the *syn* conformer at first only *a*-type transitions were measured, followed by measurements of *b*-type transitions. As the dipole moment in *c*-direction is 0.00 D for both conformers, due to their C_s symmetry no *c*-type lines were observed at all. In the case of the *anti* conformer great attempts to assign *b*-type lines did not succeed. The dipole moment in this direction is only 0.58 D, which is already quite low. Also all measurements on the *anti* conformer were quite challenging, as already mentioned.

A typical picture of the high resolution measurements of the *syn* conformer of N-*tert*-butylformamide is given in Figure 7.3. It shows a clearly resolved hyperfine structure due to the quadrupole coupling. In the case of the *anti* conformer much more decays had to be coadded to get similar signal-to-noise ratios compared to *syn*.

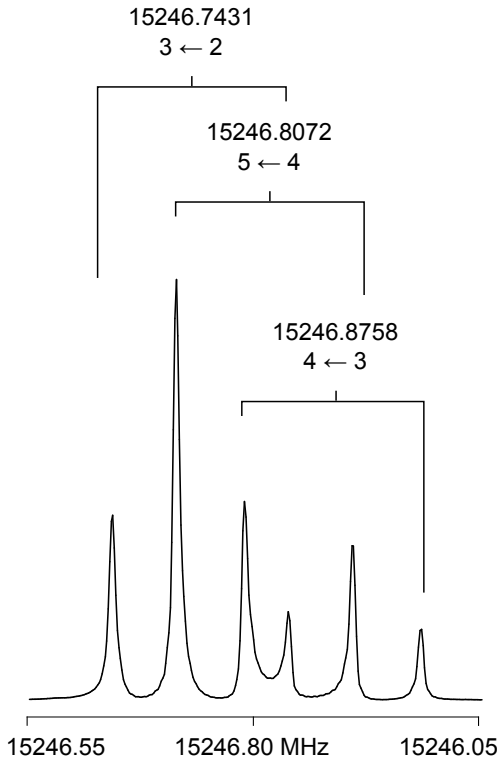

Figure 7.3: High resolution measurement of the $4_{13} \leftarrow 3_{12}$ transition of the *syn* conformer of N-*tert*-butylformamide. Doppler splittings are indicated by brackets, hyperfine components by the respective quantum numbers F' ← F. For this spectrum 1440 decays were coadded.

After both conformers were assigned with the help of the spectrometer operating in the frequency range from 2-26.5 GHz, predictions were carried out in the higher frequency range up to 40 GHz, to measure additional transitions with the second spectrometer. Due to the size of the molecule only few transitions with relatively high J rotational quantum numbers were predicted in this frequency range. However a few *syn*-lines could be observed, by co-addition of a few thousands of decays at the exactly predicted frequencies. For the *anti* conformer no frequencies higher than 26.5 GHz could be measured. The predicted lines were just not intense enough.

7.4 Results and Discussion

The fit results obtained for N-*tert*-butylformamide are given in Table 7.4. All fitted lines are given in Table B.4 for the *syn* and in Table B.5 for the *anti* conformer.

Table 7.4: Rotational fit-parameters from the program XIAM (obs) compared to parameters calculated at the MP2/6-311++G(d,p) level of theory (calc) for the observed conformers of N-*tert*-butylformamide.

		syn		anti	
	Unit	obs [a]	calc	obs [a]	calc
A	MHz	4079.105 661(91)	4095.31	4331.7(26)	4356.00
B	MHz	1927.547 557(43)	1924.46	1579.854 15(40)	1576.63
C	MHz	1843.298 563(41)	1840.60	1558.729 21(44)	1554.19
B_J	MHz	1885.423 060(29)	1879.5 [b]	1569.291 68(29)	1582.5 [a]
B_K	MHz	2193.682 601(87)	2185 [b]	2762.4(26)	2790.59
B_-	MHz	42.124 497(32)	41.93	10.562 47(31)	11.22
D_J	kHz	0.259 00(28)		0.0774(75)	
D_{JK}	kHz	1.272 60(96)		2.326(20)	
D_K	kHz	−0.8719(33)			
d_1	kHz	−0.013 82(18)			
d_2	kHz	0.004 287(50)			
χ_{aa}	MHz	1.803 15(71)	1.7996	2.1345(38)	2.1214
$\chi_{bb} - \chi_{cc}$	MHz	5.7563(17)	5.9573	5.710(11)	6.0638
σ [c]	kHz	1.6		6.3	
N[d]/Nq[e]		69/231		21/88	

[a] Parameters are given with one standard uncertainty in parentheses. Watson's S reduction and I^r representation were used. [b] Experimental value from low resolution measurements. [c] Standard deviation of the fit. [d] Number of rigid rotor transitions. [e] Number of hyperfine transitions.

7.4.1 *syn*-conformer

In total a number of 231 hyperfine components including 69 rotational transitions could be measured for the *syn* conformer of N-*tert*-butylformamide. The fit was obtained with a good standard deviation of 1.6 kHz, which is in the order of the measurement accuracy.
For the *syn*-conformer the direct fit parameters B_J, B_K, B_- were obtained with very high accuracy. They were comparably close to the values taken from the low resolution studies and the calculations.
The three rotational constants A, B, C, which are directly derived from B_J, B_K and B_- are therefore obtained with the same high accuracy.
Additionally, five centrifugal distortion constants D_J, D_{JK}, D_K, d_1 and d_2 and the quadrupole coupling constants χ_{aa} and $\chi_{bb} - \chi_{cc}$ were fitted with high accuracy. As expected the NQCCs were quite close to the calculated values, even though in this case the χ_{aa} constants differed by an unusual high value.

7.4.2 *anti*-conformer

For the *anti*-conformer 88 hyperfine components including 21 rotational transitions were fitted to a standard deviation of 6.3 kHz. This standard deviation is approximately three times the measurement accuracy. This is due to the small number of lines and more important due to the lack of *b*- and *c*-type lines in the fit.
As no *b*-type lines could be fitted for this conformer the B_K-parameter and therefore also the A rotational constant could only be fitted with very poor accuracy. B_J and B_- on the other hand were fitted with the usual high accuracy leading to very accurate B and C rotational constants. Also there is a great difference between the experimental B_K value in our high resolution measurements compared to the low resolution measurements reported by N. S. True.
Only two centrifugal distortion constants D_J and D_{JK} could be fitted in this case. They were obtained with slightly lower accuracy than usual. Attempts to fit the D_K constant lead to a fit with a much lower standard deviation of 2.7 kHz. However, D_K was obtained with an exceptionally great value in the order of MHz instead of kHz. This was most likely also due to the lack of information on the A rotational constant. The D_K constant probably compensated some of this lack.
Due to the fact that the centrifugal distortion can not be well treated in this case

also the quadrupole coupling constants are obtained with slightly lower accuracy, as both effects appear in the same order of magnitude in the spectrum.

7.5 Conclusion

For N-*tert*-butylformamide the two conformers, *syn* and *anti*, which were measured by N. S. True in 1984 with low resolution, were remeasured in this case with high resolution. The measurements lead to a great improvement of the fit, as not only all three rotational constants could be fitted, but also the quadrupole hyperfine structure due to the nitrogen could be resolved. Measurements were carried out giving microwave data in the full frequency range from 2 to 40 GHz.

Part II

Secondary Acetamides

Chapter 8

Introduction

Acetamides form a sub-class of amides, which contain an acetyl group CH3−(C=O) as a basic structure element. Besides mostly unrevealed structural preferences of substituted amides in general, acetamides are especially interesting due to their internal dynamics. The acetylmethyl group undergoes internal rotation with an intermediate or low barrier. The observation of this large-amplitude motion does not only contain information on the intramolecular orientation of the methyl group, and in consequence on the molecular structure, but also on the electronic configuration. The methyl group can be considered as a sensitive probe, whose torsional barrier varies significantly upon changes of the electronic environment induced by structural changes at the other side of the amide bond.

In the family of secondary acetamides, the rotational structure of only one molecule, N-methylacetamide has been reported. N-methylacetamide was first investigated in 1973 by M. Kitano et. al. [64]. Further investigations were then carried out by N. Ohashi et. al. in 2004 revealing the internal rotation barriers of both the acetyl- and the nitrogen-methyl rotation [65]. It was up to now the only secondary acetamide, which was investigated through microwave spectroscopy. Further investigations were only performed on 2-chloroacetamide [66] and α-fluoroacetamide [67], where the internal rotation of the methyl group is prevented due to the substitution of one hydrogen atom of the methyl group with a larger halogen atom.

The secondary amides investigated in this work are N-ethylacetamide (chapter 9), N-*tert*-butylacetamide (chapter 10) and N-vinylacetamide (chapter 11), which only differ in the substituents on the nitrogen atom. N-Ethylacetamide is a small alkyl acetamide, where the alkyl substituent bound to the nitrogen atom is an ethyl group. In N-*tert*-butylacetamide a rather large alkyl substituent was chosen, which

additionally shows a remarkable positive inductive effect. N-Vinylacetamide builds an extended π-electron system with the vinyl-group, which was already introduced and discussed in the work on N-vinylformamide (chapter 6).

Chapter 9

N-Ethylacetamide - EAA

Parts of this chapter have already been published in ChemPhysChem and the Journal of Physical Chemistry A:

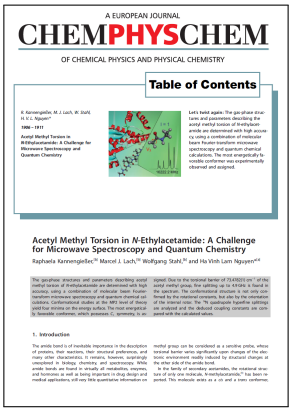

R. KANNENGIEßER, M.J. LACH, W. STAHL and H.V.L. NGUYEN Acetyl Methyl Torsion in N-Ethylacetamide: A Challenge for Microwave Spectroscopy and Quantum Chemistry, *ChemPhysChem*, 2015, **16**, 1906-1911.

R. KANNENGIEßER, W. STAHL, H.V.L. NGUYEN and I. KLEINER ^{14}N Nuclear Quadrupole Coupling and Methyl Internal Rotation in N-*tert*-Butylacetamide As Observed by Microwave Spectroscopy *J. Phys. Chem. A*, 2016, **120**, 3992-3997.

The measurements, quantum chemical calculations, spectrum analysis, spectrum assignment, fits, development of BELGI-C_1-hyperfine, and the manuscript preparation is the work of R. Kannengießer. The coworkers took mostly part in a supporting way especially during corrective work in the publication process. M. J. Lach carried out calculations and measurements on N-ethylacetamide and helped with the XIAM-fit of this molecule. I. Kleiner was involved in the programming process of BELGI-C_1-hyperfine.

9.1 Introduction

N-Methylacetamide exists as a *cis* and a *trans* conformer, where the *cis* conformer possesses a very high energy. In the rotational spectrum, only the *trans* conformer could be observed as the single possible structure, and no discussion on structural preferences is thus necessary.
This becomes already an important question in the structure and dynamics of N-ethylacetamide, since the torsion of the ethyl group around the σ-bond allows different conformations.
For the acetyl methyl torsion, it is known from a series of saturated acetates that the barrier is largely invariant [11, 68, 69]. However, in unsaturated acetates such as vinyl acetate [70], and isopropenyl acetate [71] π-electron conjugation becomes possible and the barrier increases significantly. This leads us to ask, what situation might be found for small acetamides like N-ethylacetamide.

N-Ethylacetamide is found in alcoholic beverages, tea, and wine. It is also a chemical motif in melatonins, for example, the hormone 6-hydroxymelatonin. Its structural properties are therefore of underlying nature to the characteristics observed in larger biofunctional molecules.
With fourteen atoms, N-ethylacetamide is a relatively small biomimetic substance, at the same time being a medium-sized molecule in the realm of precise spectroscopic studies. Determining its structure in a multi-isotopologue study, the atom-by-atom substitution structure method, is already becoming a tedious task for the heavy atom backbone while –in natural abundance– not providing the hydrogen positions. Combining the experimentally deduced molecular parameters with quantum chemical results, a detailed and precise statement on the three-dimensional structure of N-ethylacetamide becomes possible.

9.2 Theoretical

9.2.1 Quantum chemical calculations

In total, 36 different starting geometries were created by varying two dihedral angles $\alpha_1 = (H_2 - N_1 - C_3 - C_5)$ and $\alpha_2 = (H_2 - N_1 - C_9 - C_{12})$ from $-120°$ to $180°$ in a grid of $60°$ (for atom numbers see Figure 9.1).

Optimization yielded four conformers, which were confirmed as stable minima by frequency calculations (see Figure 9.1). Their energy values, rotational constants, and dipole moment components are given in Table 9.1. In the most stable conformers I and II, the oxygen atom is distant from the proton attached to the nitrogen atom. Conversely, the oxygen atom and the proton are in a more hindered *cis* orientation in conformers III and IV. These conformers are thus higher in energy.

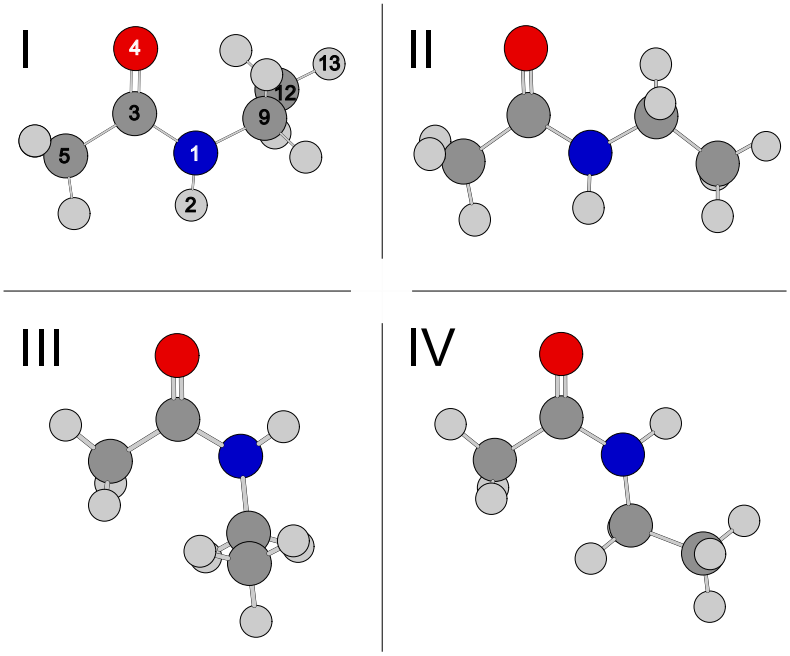

Figure 9.1: Four stable conformers of N-ethylacetamide calculated at the MP2/6-311++G(d,p) level of theory. The two *trans* conformers I and II are lower in energy compared to the *cis* conformers III and IV.

Table 9.1: Relative energy values in kJ·mol^{-1}, rotational constants in GHz, and dipole moment components in D of the four stable conformers of N-ethylacetamide calculated at the MP2/6-311++G(d,p) level of theory.

	$E_{rel.}$	A	B	C	$\lvert\mu_a\rvert$	$\lvert\mu_b\rvert$	$\lvert\mu_c\rvert$
I	0.0	7.093	2.213	1.969	0.43	3.98	0.68
II	2.8	8.294	1.952	1.643	1.62	3.79	0.60
III	11.0	6.353	2.243	1.962	4.13	1.83	0.90
IV	11.4	7.756	1.994	1.651	3.83	2.65	0.37

The most stable conformer I, shown in Figure 9.2, is the one most likely to be observed under molecular beam conditions. Its coordinates in the principal axis system are available in the Appendix C in Table C.1. Conformer II is 2.8 kJ·mol^{-1} higher in energy and might also be identifiable. In contrast, conformers III and IV with much higher relative energies (11.0 and 11.4 kJ·mol^{-1}) are not expected to be seen in the spectrum. Centrifugal distortion constants were calculated at the B3LYP/6-311++G(d,p) level through anharmonic frequency calculations.

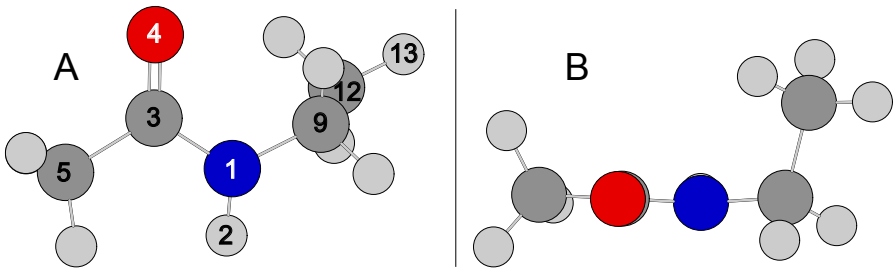

Figure 9.2: The optimized geometry of the most stable conformer I of N-ethylacetamide in the side view (A) and the top view (B). The ethyl group is tilted out of the $C_5 - C_3 - O_4 - N_1$ plane by a small angle of approximately 6°, the ethyl methyl group by 67°.

9.2.2 Nuclear quadrupole coupling

For initial values of the quadrupole coupling constants, single-point electric field gradient calculations were initially carried out at the B3PW91/6-311+G(d,p) level of theory, with a slightly older calibration factor of −4.5617 MHz/a.u., as our investigations on quadrupole coupling in relation with π-conjugated systems were not carried out yet. The calculations delivered values of the quadrupole coupling tensor components of:

$$\chi_{aa} = 1.771217 \text{ MHz}, \chi_{bb} = 1.880003 \text{ MHz}, \chi_{cc} = -3.651225 \text{ MHz},$$
$$\chi_{aa} = 0.168635 \text{ MHz}, \chi_{ac} = 1.435198 \text{ MHz}, \chi_{bc} = -1.065748 \text{ MHz}.$$

With the improved method, using the 6-311+G(df,pd) basis set and the calibration factor of −4.5586 MHz/a.u. the calculation delivered slightly lower values for all quadrupole coupling tensor components:

$$\chi_{aa} = 1.719481 \text{ MHz}, \chi_{bb} = 1.828987 \text{ MHz}, \chi_{cc} = -3.548472 \text{ MHz},$$
$$\chi_{ab} = 0.146234 \text{ MHz}, \chi_{ac} = 1.396616 \text{ MHz}, \chi_{bc} = -1.045763 \text{ MHz}.$$

The lower values calculated with this method, can be explained not only due to the smaller calibration factor but also smaller values calculated with the 6-311+G(df,pd) basis set.

9.2.3 Internal rotation

The acetyl methyl $CH_3 - C = O$ and ethyl methyl group $-CH_2CH_3$ in N-ethylacetamide undergo internal rotation and cause splittings of all rotational transitions [72]. To estimate the order of magnitude of these splittings, the barrier heights were calculated by varying the dihedral angles $\beta_1 = (O_4 - C_3 - C_5 - H_6)$ and $\beta_2 = (N_1 - C_9 - C_{12} - H_{13})$ in a grid of 10°. Due to the C_{3v} symmetry of the methyl group, a rotation of 120° was sufficient.
For the acetyl methyl group, a barrier of 108.64 cm^{-1} was obtained, which is rather low. We thus expected torsional fine splittings of a few hundreds of MHz.
The results for the ethyl methyl group show a much higher barrier of 1187.36 cm^{-1}. From many previous investigations we know that splittings arising from such barriers are very small and cannot be resolved with our spectrometers[73].

In order to improve the accuracy of the internal rotation barrier calculation, attempts to calculate the transition state of the internal rotation were made for the acetyl methyl group. The calculations were carried out at the B3LYP/6-311++G(d,p) level of theory. First the minimum geometry was optimized at this level. Then the acetyl methyl group was manually rotated to the maximally hindered position by a rotation of approx. 60° compared to the minimum and optimized with the TS-Berny algorithm available in GAUSSIAN. The obtained transition state is shown on the left side of Figure 9.3 in comparison to the minimum geometry on the right side. The energy difference between the minimum and the transition state is 138.53 cm^{-1}, which is even higher than the barrier calculated with the simple methyl scan calculation.

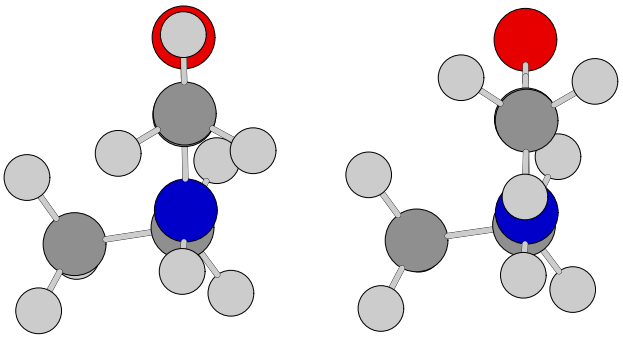

Figure 9.3: Transition state (left) and minimum geometry (right) of the acetyl methyl internal rotation in N-ethylacetamide. The calculations were carried out at the B3LYP/6-311++G(d,p) level of theory.

At the beginning attempts were made to optimize the transition state at a higher level of theory, the MP2/cc-pVTZ level, but failed probably due to the high complexity of the calculation. The minimum geometry however could be optimized at this level of theory and is shown in Figure 9.4. It can be seen that the methyl group is calculated not exactly at an angle of 60° as expected and calculated at the B3LYP/6-311++G(d,p) level of theory, but is slightly shifted to an angle of 51.8° or −64.9°. These angles additionally indicate a distortion of the methyl group in this case.

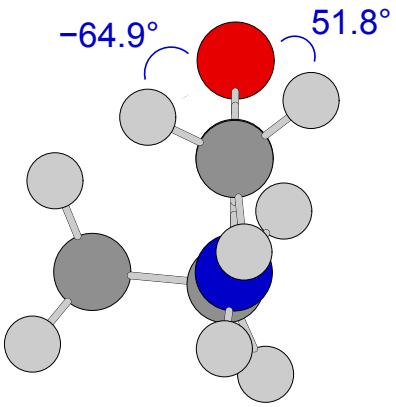

Figure 9.4: Orientation of the acetyl methyl rotor in the minimum geometry calculated at the MP2/cc-pVTZ level of theory.

9.3 Experimental

Two broadband spectra were recorded in the frequency ranges from 10 to 17 GHz and 27 to 38 GHz. All lines appear as multiplets due to the quadrupole coupling of the ^{14}N nucleus. Figure 9.5 illustrates a typical spectrum in the scan mode, where some A–E splittings can be recognized.

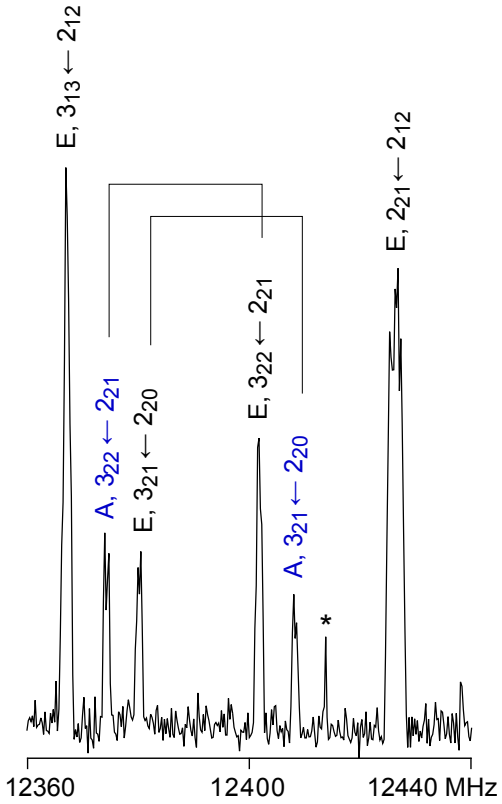

Figure 9.5: Typical spectrum of N-ethylacetamide. The transitions are marked with their corresponding species and quantum numbers J, K_a, K_c, an unassigned line with an asterisk. A–E splittings are indicated by brackets.

Afterwards, measurements in the high-resolution mode were carried out with an intrinsic experimental line width of 2–3 kHz and an experimental accuracy of 0.1 kHz for isolated lines [49]. The experimental accuracy often rises to 2 kHz when the lines are broadened by overlapping transitions due to unresolved splittings from highly hindered internal rotations as well as spin–spin or spin–rotation couplings. Figure 9.6 shows a typical spectrum in the high-resolution mode. Quadrupole hyperfine structure and Doppler splittings can be clearly recognized.

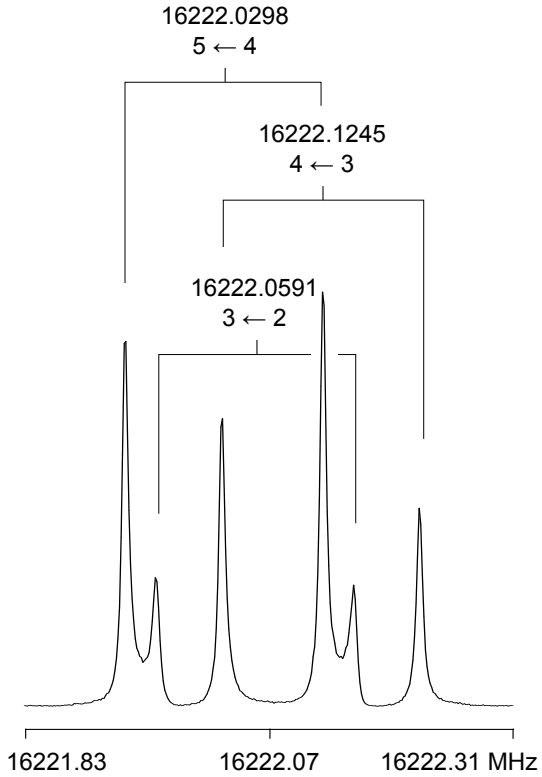

Figure 9.6: Three quadrupole components of the E species $4_{04} \leftarrow 3_{03}$ transition of conformer I. The experimental accuracy is 2 kHz. The brackets indicate the Doppler doublets. The hyperfine transitions are given by $F' \leftarrow F$. For this spectrum, 404 decays were co-added.

The assignment was carried out in three steps. In a first step, the internal rotation and quadrupole coupling effects were neglected and the molecule was treated as a rigid rotor. Using the calculated A, B, and C rotational constants, a first prediction was performed using the program XIAM. The prediction showed a characteristic b-type Q-branch, which was shifted by approximately 1 GHz in the experimental spectrum, but could be assigned by trial and error. Subsequently, further R-branches were included. In total, 6 a- and 16 b-type transitions were fitted using the rigid-rotor model. No c-type lines could be found.

As a second step, the model was extended by considering the quadrupole hyperfine splittings, which are expected to be much smaller than the fine splittings from internal rotation. Using the calculated NQCCs, the quadrupole hyperfine components of all rigid rotor signals could be easily assigned.

In the last step, the internal rotation of the acetyl methyl group was taken into

account. Quantum chemical calculations suggested a barrier height of 108.64 cm^{-1}, which is of the same order of magnitude as the value found for N-methylacetamide (73.468(51) cm^{-1}). In cases with such low barriers to internal rotation, the fine splittings might change dramatically by varying the barrier slightly. To assign the torsional splittings, several XIAM predictions were performed, whereby the V_3 potential was varied in steps of 5.0 cm^{-1} from 70.0 cm^{-1} to 110.0 cm^{-1}. In the region between 70.0 cm^{-1} and 75.0 cm^{-1}, reasonable agreement between the calculated E species and the remaining lines in the spectrum could be found. Afterwards, a much finer step width of 0.067 cm^{-1} (2 GHz) was applied in this region, as illustrated in Figure 9.7. At $V_3 \approx 73.48$ cm^{-1}, the calculated spectrum matched the experimental one best. It should be noted that by varying the V_3 potential, the A–E splittings of *a*-type transitions changed much less than those of b-type. Thus, we first included *a*- and subsequently *b*-type lines in the fit. Finally, 150 A and 121 E-species torsional and hyperfine components were assigned. The fit results are given in Table 9.2. The frequency list of all fitted transitions is available in Table C.2.

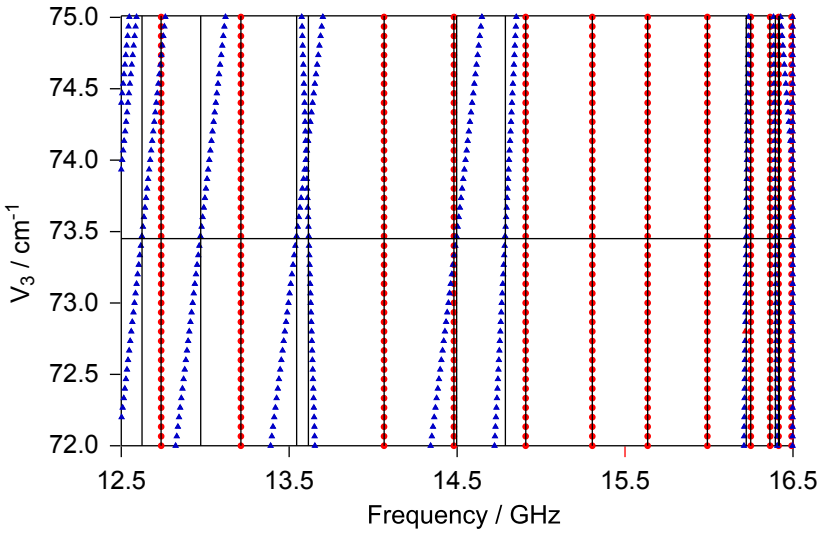

Figure 9.7: Calculated frequencies of the A and E species between 12.5 and 16.5 GHz depending on the V_3 potential. Observed A species transitions were fitted at different values of V_3, while all other internal rotation parameters were fixed. Based on this fit, the A (●) and E (▲) species frequencies were predicted. All measured transitions are represented by black vertical lines. The red dots are located exactly on the measured A species lines. The observed and predicted E species transitions match best at 73.48 cm^{-1} (indicated by the horizontal line)

9.4 Results and Discussion

In total, 271 hyperfine components could be assigned to conformer I of N-ethylacetamide by fitting 18 molecular parameters with the program XIAM: the rotational constants A, B, and C, the centrifugal distortion constants Δ_J, Δ_{JK}, Δ_K, δ_J, and δ_K, the V_3 potential, the polar coordinates of the internal rotor axis in the principal axis system δ and ϵ, the effective parameters D_{pi2J}, D_{pi2K}, and D_{pi2-}, and the NQCCs χ_{aa}, $\chi_{bb} - \chi_{cc}$, χ_{ac}, and χ_{bc}. The NQCC χ_{ab} was fixed to a value

Table 9.2: Molecular parameters of N-ethylacetamide in the principal axis system obtained from the fits using the programs XIAM and BELGI-C_1-hyperfine and from quantum chemical calculations at the MP2/6-311++G(d,p) level of theory.

Parameter	Unit	Fit XIAM [a], [b]	Fit BELGI [a], [c]	Calc [d]
A	MHz	7270.2759(93)	7276.8825(52)	7.093
B	MHz	2183.5536(24)	2182.5468(55)	2.213
C	MHz	1938.7113(18)	1938.6438(14)	1.969
Δ_J	kHz	1.0227(89)	1.2533(45)	2.57
Δ_{JK}	kHz	1.387(90)		3.88
Δ_K	kHz	10.66(96)		13.22
δ_J	kHz	0.1101(74)		0.04
δ_K	kHz	−6.37(44)		−33.23
χ_{aa}	MHz	1.7508(32)	1.7524(40)	1.7713
$\chi_{bb} - \chi_{cc}$	MHz	5.4174(83)	5.4122(57)	5.5303
χ_{ab}	MHz	0.1686 [e]	−0.5576(87)	0.1686
χ_{ac}	MHz	−1.651(71)		−1.4352
χ_{bc}	MHz	0.595(59)		1.0657
V_3	cm^{-1}	73.4782(1)	73.081 59(26)	108.64
F_0	GHz	158.0 [e]	158.079 656(41)	
D_{pi2J}	kHz	−33.59(33)		
D_{pi2K}	kHz	1.4506(19)		
D_{pi2-}	kHz	−91.06(88)		
<(i,a)	deg	27.7216(2)	27.842 94(55)	30.1
<(i,b)	deg	67.2076(5)	67.129 58(48)	65.67
<(i,c)	deg	75.0772(6)	74.988 49(34)	73.38
σ [f]/rms [g]	kHz	9.8	2.7	
N_A / N_E / Nq [h]		150/121/271	150/125/275	

[a] All parameters refer to the principal axis system. Statistical uncertainties are given as one standard uncertainty in the last digit. [b] Watson's A reduction and I^r representation were used. [c] BELGI-C_1-hyperfine parameters transformed into the principal axis system. [d] see section 9.2. [e] Fixed value. [f] standard deviation of the XIAM fit. [g] Root-mean-square deviation of the BELGI fit. [h] Number of A and E species transitions as well as hyperfine components.

of 0.1686 MHz, the rotational constant of the methyl rotor F_0 to 158 GHz, corresponding to a moment of inertia $I_\alpha = 3.2\ u\text{Å}^2$.

The fitted rotational constants B and C are quite close to the calculated values. On the other hand, the calculated and experimental A rotational constants differ by 177 MHz. This difference is very large compared to many other investigations on molecules of a similar size [74, 75], where the same method and basis set were used and it causes the shift of approximately 1 GHz between the predicted and experimental b-type Q-branch transitions. We additionally optimized the structure of conformer I using various method/basis set combinations. The results are summarized in Table C.3. In all calculations, the A rotational constant is not satisfactorily close to the experimental value, except for the calculation at the MP2/6-311++G(2df,2pd) level. The B and C rotational constants are always in good agreement with the experimental values.

In the upper diagram of Figure 9.8, the experimentally determined rotational constants A, B, and C are plotted as straight horizontal lines. These can be compared with the calculated values of the four stable conformers found in our quantum chemical calculations, which are given as dots. Conformers I and III possess similar B and C rotational constants, but the A rotational constant of conformer III does not match the experimental value as well as that of conformer I. However, since the calculated A rotational constant varies in a wide range, depending on the chosen method and basis set, it is still possible that conformer III is the assigned one. By considering the calculated energies indicated in the middle of Figure 9.8, this assumption seems unlikely as conformer III is much higher in energy (11 kJ·mol^{-1}). Finally, the calculated angles of the internal rotor axis with respect to the principal axes of inertia illustrated in the lower part of Figure 9.8 confirm unambiguously that the assigned conformer is conformer I. The calculated angles of conformer I perfectly match the experimental values, whereas those of conformer III show a completely different orientation of the acetyl methyl rotor.
Conformer II is calculated to be only 2.8 kJ·mol^{-1} higher in energy than conformer I and might also exist in the spectrum. However, almost all measured lines found in the scan belong to conformer I, and only some weak lines remain unassigned.
Therefore, we conclude that only the most stable conformer I could be observed. The experimental V_3 potential of 73.4782(1) cm^{-1} is quite low and accordingly, large A–E splittings up to 4.9 GHz occurred in the spectrum. In the contrary, the hyperfine splittings from the ^{14}N nucleus are only in the order of a few hundreds of

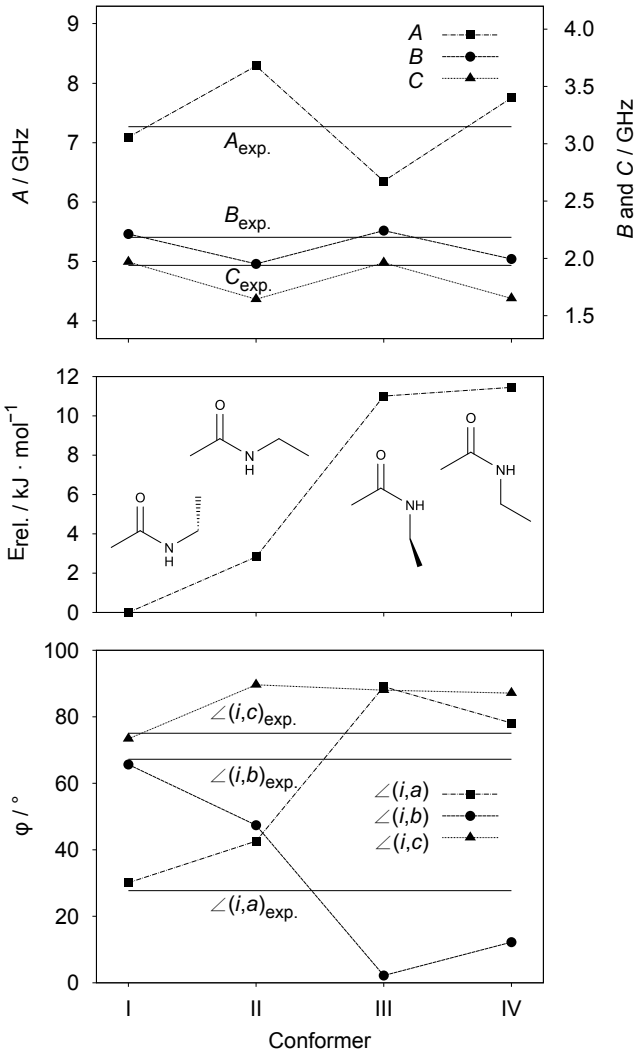

Figure 9.8: Comparison of quantum chemical calculation and experimental results to identify the assigned conformer of N-ethylacetamide. The experimental rotational constants ($A_{exp.}$, $B_{exp.}$, and $C_{exp.}$) are indicated as horizontal lines in the upper diagram, the calculated values as separated points connected by dashed or dotted lines, which are only present for a better tracing. The energy values are shown in the middle together with the structural formulas. In the lower part, the angles between the internal rotor axis and the principal axes $\varphi =< (i, n), n = a,\ b,\ c$ are plotted. The directions of the principal axes were chosen in a way to assure angles between 0° and 90°.

kHz. Therefore, the fit is much more sensitive to variation of the internal rotation parameters than of the NQCCs. Since the quadrupole coupling effect is negligible if compared to the effect of internal rotation, only the absolute line positions of the

quadrupole components with the highest predicted intensity [7] were fitted. For the other quadrupole components, we fitted the splittings relative to these transitions.

The diagonal NQCCs χ_{aa} and $\chi_{bb}-\chi_{cc}$ could be calculated almost exactly, as found in many other investigations on nitrogen containing molecules where Bailey's approach has been applied. Additionally, the two off-diagonal elements of the quadrupole coupling tensor χ_{ac} and χ_{bc} could be determined while the third element χ_{ab} was fixed to the calculated value. The deviations between the observed and calculated values were therefore slightly higher than those of the diagonal elements. Fitting all three off-diagonal elements simultaneously led to high correlations.
Not only the V_3 potential and the polar coordinates of the internal rotor axis δ and ϵ, where δ is the angle between the internal rotation axis and the principal a axis and ϵ the angle between the principal b axis and the projection of the internal rotation axis onto the bc-plane, but also three higher-order terms D_{pi2J}, D_{pi2K}, and D_{pi2-} were needed to reproduce the spectrum. The standard deviation of the fit is about 10 kHz, five times larger than our experimental resolution. Further attempts to reduce the standard deviation using XIAM failed and we therefore conclude that some higher order terms are missing in XIAM, which could be useful in this case. However, since only a few parameters can be fitted with the program XIAM and the barrier to internal rotation is quite low, the fit is already much better than in many other cases with comparably low barriers [76, 77].
Also four E species transitions ($2_{11} \leftarrow 1_{11}, 2_{12} \leftarrow 1_{01}, 3_{03} \leftarrow 2_{12}, 3_{13} \leftarrow 2_{02}$) were excluded from the fit because of their large observed-minus-calculated values (see the frequency list given in Table C.2). Thus, we decided to try and use the newly developed BELGI-C_1-hyperfine program on N-ethylacetamide. The idea was to include a number of higher order terms to deal with the problem of the high standard deviation. Furthermore, BELGI is known to be especially good in the treatment of low barrier cases, which gave hope to be able to include also the problematic E species, which had to be excluded from the XIAM fit.

The use of the BELGI-C_1-hyperfine code was as successful as expected, because it could fit the same data set as with XIAM, but including the four problematic E species transitions to a rms deviation of 2.7 kHz. We floated 20 parameters, which are listed in Table 9.3. It should be noted that the out-of-plane D_{aci} and D_{acJi} parameters, which multiply the $P_aP_c+P_cP_a$ and $P^2(P_aP_c+P_cP_a)$ terms, respectively, are well determined, while the D_{bci} parameter (multiplying the $P_bP_c + P_cP_b$ term) could not be fitted and was set to zero. All fitted transitions of EAA along with

their residuals are available in Table C.2 for both the XIAM and the BELGI fit. In order to compare the results from both fits, XIAM and BELGI, parameters were transformed into the principal axis system if possible. The results are given as *Fit BELGI* in Table 9.2.

Table 9.3: Spectroscopic constants of N-ethylacetamide in the rho-axis system obtained with the program BELGI-C_1-hyperfine.

Parameter [a]	Unit	EAA	Operator
A	MHz	7158.6153(12)	P_a^2
B	MHz	2277.9833(32)	P_b^2
C	MHz	1961.4748(10)	P_c^2
D_{ab}	MHz	715.186(18)	$\{P_a, P_b\}$
D_{aci}	MHz	−291.1414(50)	$\{P_a, P_c\}$
D_{acJi}	kHz	2.611(85)	$P^2\{P_a, P_c\}$
Δ_J	kHz	1.2533(45)	$-P^4$
Δ_{JK}	kHz	−0.885(21)	$-P^2P_a^2$
Δ_K	kHz	17.23(19)	$-P_a^4$
δ_J	kHz	0.0724(42)	$-2P^2(P_b^2 - P_c^2)$
δ_K	kHz	−7.136(69)	$-\{P_a^2, (P_b^2 - P_c^2)\}$
χ_{aa}	MHz	3.8943(62)	
χ_{bb}	MHz	3.6666(62)	
χ_{cc}	MHz	−7.5609 [b]	
χ_{ab}	MHz	−1.257(19)	
V_3	cm^{-1}	73.081 59(26)	$(1/2)(1 - cos3\gamma)$
ρ	unitless	0.040 828 24(25)	P_aP_γ
F	cm^{-1}	5.4845 [c]	P_γ^2
d_{ab}	MHz	−7.383(48)	$(1 - cos3\gamma)\{P_a, P_b\}$
k_1	MHz	0.1512(25)	$(P_aP_\gamma)P_a^2$
c_1	MHz	−0.016 42(30)	$P_\gamma^2(P_b^2 - P_c^2)$
G_v	MHz	−0.022 19(55)	$P_\gamma^2P^2$
N_A / N_E / N_q [d]		150/125/275	
rms A / E [e]	kHz	1.7/3.5	

[a] All parameters refer to the rho-axis system and cannot be directly compared to those referred to the principal axis system. P_a, P_b, and P_c are the components of the overall rotation angular momentum, P_γ is the angular momentum of the internal rotor rotating around the internal rotor axis by an angle γ. {u,v} is the anti-commutator uv + vu. The product of the parameter and operator from a given row yields the term actually used in the vibration-rotation-torsion Hamiltonian, except for F, ρ, and A, which occur in the Hamiltonian in the form $F(P_\gamma - \rho P_a)^2 + AP_a^2$. Statistical uncertainties are shown as one standard uncertainty in the last digit. [b] parameter derived from the linear combination $\chi_{cc} = -(\chi_{aa} + \chi_{bb})$. [c] Fixed to the value from the XIAM fit. [d] Number of A and E-species transitions as well as hyperfine components. [e] Root-mean-square deviations of the A and E-species.

The fitted rotational constants from the BELGI fit were obtained with very high accuracy and are in close agreement with the XIAM results. Also the quadrupole coupling constants were obtained with values close to the ones from XIAM. Both fits are perfectly coherent and give basically the same set of parameters.

The obtained V_3 potential of 73.4782(1) cm^{-1} of N-ethylacetamide is essentially the same value of 73.468(51) cm^{-1} found for N-methylacetamide. Furthermore, these barriers are one order of magnitude lower than those found in the tertiary acetamides, which seems mainly influenced by a change in the electronic environment, introduced by the presence of a proton at the nitrogen atom in the secondary acetamides. This point will be revisited in the discussion of all investigated amides (chapter 17).

9.5 Conclusion

The microwave spectrum of the lowest-energy conformer of N-ethylacetamide was studied using a combination of molecular beam microwave technique and quantum chemistry. The ethyl methyl group is tilted out of the molecular plane by an angle of 67°. Hyperfine splittings were found for all transitions due to the electric quadrupole coupling of the ^{14}N nucleus. The acetyl methyl group undergoes internal rotation, which causes large fine splittings up to 4.9 GHz. The torsional barrier is approximately 73 cm^{-1}, which is the same value as found for N-methylacetamide, whereas a significantly different barrier was expected. Two fits using the programs XIAM and BELGI-C_1-hyperfine, including both, the internal rotation and the quadrupole coupling effect, were carried out and yielded molecular parameters with high accuracy.

Chapter 10

N-*tert*-Butylacetamide - TBAA

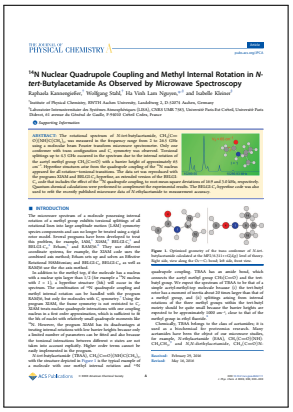

Parts of this chapter have already been published in J. Phys. Chem. A:

R. KANNENGIEßER, W. STAHL, H.V.L. NGUYEN and I. KLEINER ^{14}N Nuclear Quadrupole Coupling and Methyl Internal Rotation in N-*tert*-Butylacetamide As Observed by Microwave Spectroscopy *J. Phys. Chem. A*, 2016, **120**, 3992-3997.

The measurements, quantum chemical calculations, spectrum analysis, spectrum assignment, fits, development of BELGI-C_1-hyperfine, and the manuscript preparation is the work of R. Kannengießer. The coworkers took mostly part in a supporting way especially during corrective work in the publication process. I. Kleiner was involved in the programming process of BELGI-C_1-hyperfine.

10.1 Introduction

N-*tert*-Butylacetamide, $CH_3(C{=}O)(NH)C(CH_3)_3$, with the structure shown in Figure 10.1 is another typical example of a secondary amide. It has an amide bond, which connects an acetyl methyl group $CH_3(C{=}O)$ and a *tert*-butyl group. We expect the spectrum of TBAA to be that of a simple acetyl-methyl-top molecule since: (i) the *tert*-butyl rotor has a moment of inertia about 20 times larger than that of a

methyl group, and (ii) splittings arising from internal rotations of the three methyl groups within the *tert*-butyl moiety should be quite small, since the barrier heights are expected to be approximately 1000 cm^{-1}, similar to that of the methyl group in ethyl fluoride [78]. Chemically, TBAA belongs to the class of acetamides; it is used as a biochemical for proteomics research.

In our investigation on EAA (chapter 9), we observed only one conformer with C_1 symmetry under molecular beam conditions. The microwave spectrum with 150 A and 121 E species torsional and hyperfine components was fitted using the program XIAM to a standard deviation of 9.8 kHz. Attempts to reduce the standard deviation to measurement accuracy of 2 kHz failed using XIAM. However, with the new BELGI-C_1-hyperfine program the standard deviation could be reduced to almost measurement accuracy. Since the barrier height of the acetyl methyl group in TBAA is expected to be close to that found in EAA, the same problem might occur by fitting the spectrum of TBAA using the program XIAM. In many previous investigations, we succeeded to fit the microwave spectra of molecules with C_s symmetry and one methyl top with low barrier height to experimental accuracy using the program BELGI-C_s, e.g. ethyl acetate [11], vinyl acetate [70], and methyl neopentyl ketone [79]. The program BELGI in the C_1 version also shows its efficiency for molecules like allyl acetate [76], linalool [74], isoamylacetate [80], butyl acetate [12], pentyl acetate [81], and hexyl acetate [69]. Since the program BELGI-C_1 is an extended version of the program BELGI-C_s, it is possible to use the BELGI-C_1-hyperfine code to fit the spectra of molecules with C_s symmetry by setting all the out-of-plane terms to zero. As we shall see below, this program was thereby successfully applied to TBAA, where a C_s symmetry is present.

10.2 Theoretical

10.2.1 Conformational analysis

In TBAA, the rotation about the C_3-C_5 bond (for atom numbering see Figure 10.1) by varying the dihedral angle $\gamma = <(O_4\text{-}C_3\text{-}C_5\text{-}H)$ corresponds to the internal rotation of the acetyl methyl group. The rotations about the C_9-C_{10}, C_9-C_{14}, and C_9-C_{18} bonds correspond to internal rotations of the three *tert*-butyl methyl groups. The rotation about the C_3-N_1 bond by varying the dihedral angle $\varphi_1 = <(O_4\text{-}C_3\text{-}N_1\text{-}C_9)$

creates *trans* and *cis* amides. A stable *cis* and a stable *trans* conformation were found, which will be called the *cis* and the *trans* conformer from now on. They are shown in Figure 10.1.

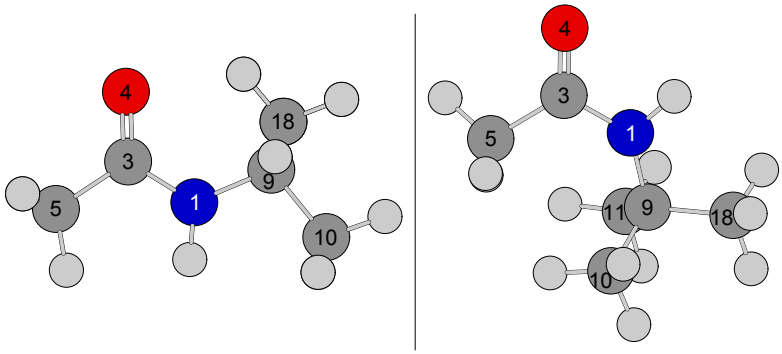

Figure 10.1: Optimized geometry of the *trans* and *cis* conformers of N-*tert*-butylacetamide calculated at the MP2/6-311++G(d,p) level of theory. Right hand side: *trans*, left hand side: *cis*.

The *cis* conformer has the rotational constants A = 3159.3 MHz, B = 1362.5 MHz, and C = 1216.1 MHz, as well as the dipole moment components μ_a = 4.19 D, μ_b = 2.18 D, and μ_c = 0.11 D. The *trans* conformer, shown in Figure 10.2, has C_s symmetry. Its rotational constants are A = 3307.1 MHz, B = 1365.5 MHz, and C = 1237.8 MHz, and the dipole moment components μ_a = 1.04 D, μ_b = 3.81 D, and μ_c = 0.00 D. The Cartesian coordinates of both conformers are given in Table D.1 in Appendix D. It should be noted that the *trans* conformer is 21.15 kJ·mol^{-1} lower in energy than the *cis* conformer. Therefore, we do not expect to observe the *cis* conformer in our spectrum under molecular beam conditions, and only focus on the *trans* conformer.

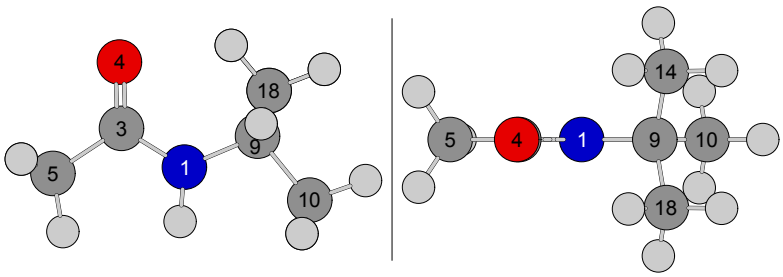

Figure 10.2: Optimized geometry of the *trans* conformer of N-*tert*-butylacetamide calculated at the MP2/6-311++G(d,p) level of theory. Right hand side: view along the $O_4 - C_3$ bond, left hand side: front view.

10.2.2 Nuclear quadrupole coupling

The single point EFG calculations on TBAA yielded a nuclear coupling tensor with the diagonal elements $\chi_{aa} = 1.9833$ MHz, $\chi_{bb} = 2.0254$ MHz, and $\chi_{cc} = -4.0087$ MHz, as well as the off-diagonal elements $\chi_{ab} = -0.1255$ MHz, $\chi_{ac} = -0.0001$ MHz, and $\chi_{bc} = 0.0016$ MHz. Predictions based on these values delivered a typical hyperfine structure of nitrogen nuclei with splittings in the order of a few tens to hundreds of kHz.

10.2.3 Internal rotation

The barrier to internal rotation of the acetyl methyl group was expected to be in the same order of that of EAA (see subsection 9.2.3) of about 75 cm^{-1}. Quantum chemical calculations were additionally carried out to gain further information on the nature of the methyl internal rotation in TBAA.

First an ab initio barrier height of 119 cm^{-1} was obtained by rotating the acetyl methyl group in a grid of 10 degrees, and the structure was optimized except for the frozen dihedral angle γ defining the torsional coordinate.

Additionally, calculations were carried out at the B3LYP/6-311++G(d,p) level of theory. Starting from the minimum geometry optimized at this level of theory, the transition state was calculated. The transition state lies 1.57 kJ·mol$^{\check{}}$1 higher in energy, which corresponds to an internal rotation barrier of 133 cm^{-1} not considering the zero-point energy. The internal rotation of the *tert*-butyl group was not calculated in detail for TBAA as the investigations on TBFA (subsection 7.2.1) already showed, that no splittings due to internal rotation of the *tert*-butyl group is observable with microwave spectroscopy.

10.3 Experimental

10.3.1 Measurements and spectrum assignment

At first, a broadband scan from 9.0 to 12.8 GHz was carried out, where overlapping spectral segments were recorded in a step width of 0.25 MHz. All lines from the

scans were remeasured in higher resolution. They indicated characteristic hyperfine structures due to the nuclear quadrupole coupling of the nitrogen nucleus. A section of the broadband scan is shown in Figure 10.3, a typical measurement at high resolution in Figure 10.4.

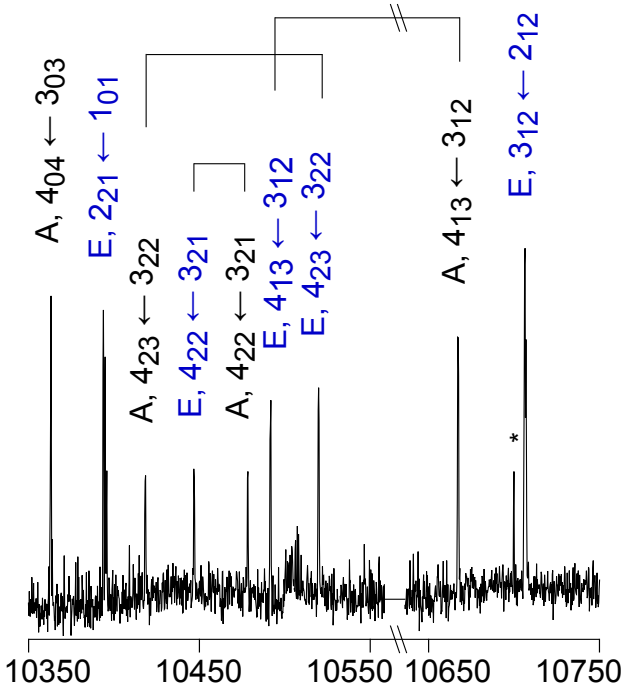

Figure 10.3: A section of the broadband scan of N-*tert*-butylacetamide in the frequency range from 10350 to 10750 MHz. The transitions are marked with their respective quantum numbers and LAM symmetry species; the asterisk marks an unassigned line. A-E splittings are indicated by brackets. Additional splittings arise from the quadrupole coupling of the ^{14}N nucleus.

We often begin the spectrum assignment with a rigid rotor model in which the effects of internal rotation and nuclear quadrupole coupling are neglected. However, from some previous investigations, especially those on N-vinylformamide (chapter 6), N-*tert*-butylformamide (chapter 7), and N-ethylacetamide (chapter 9) we know that the NQCCs can be calculated in almost exact agreement with the experimental values using the method of W. C. Bailey. Therefore, in the case of TBAA we took into account the effect of ^{14}N quadrupole coupling directly at the beginning, and assigned the observed hyperfine structure by comparing it with the calculated hyperfine frequencies. Some A species Q-branch transitions with their characteristic patterns could be readily identified and fitted. Afterward, the number of assigned A species transitions was gradually increased to 26 with 110 hyperfine components.

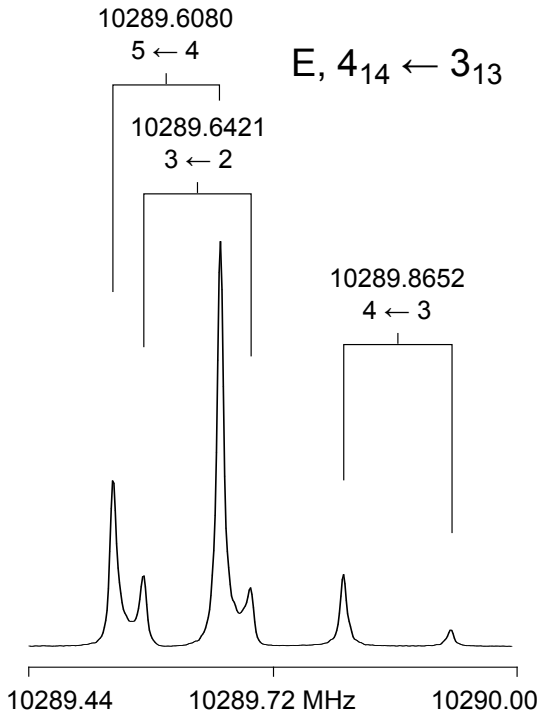

Figure 10.4: A high resolution spectrum of the $4_{14} \leftarrow 3_{13}$ E species transition of N-*tert*-butylacetamide. The Doppler doublets are marked by brackets. Hyperfine transitions are given by the respective F' ← F quantum numbers. For this spectrum, 380 decays were co-added.

As a next step, we removed all assigned A species transitions from the broadband scan and used the same procedure as reported for EAA section 9.3 to assign the E species lines. Because we expected the barrier height in TBAA to be close to that found in EAA (73.4782(1) cm^{-1}), several XIAM predictions were performed, where we varied the barrier to internal rotation from 50 to 100 cm^{-1} with a step width of 5 cm^{-1}. Good agreement between the calculated E species frequencies and the frequencies of the remaining lines in the scan was observed at 65 cm^{-1}.
A global fit of TBAA including 26 A and 35 E species transitions with a total of 250 hyperfine components was carried out with the program XIAM. The root-mean-square (rms) deviation is 16.9 kHz. The same data set was refitted using the BELGI-C_1-hyperfine code to a rms deviation close to the measurement accuracy of 2 kHz. The fit results are given in Table 10.1, the frequency list is available in Table D.2 in the Appendix D.

10.4 Results and Discussion

The microwave spectrum of the C_s *trans* conformer of TBAA was assigned and fitted with the programs XIAM and BELGI-C_1-hyperfine.

Using the program XIAM, we fitted the transition frequencies to determine 14 parameters, which are three linear combinations of the rotational constants B_J, B_K, B_-, three quartic centrifugal distortion constants D_J, D_{JK}, and d_1, the NQCCs χ_{aa}, $\chi_{bb} - \chi_{cc}$, and χ_{ab}, as well as five internal rotation parameters (the barrier to internal rotation V_3, three higher order terms D_{pi2J}, D_{pi2K}, D_{pi2-}, and the angle δ between

Table 10.1: Molecular parameters of the observed *trans* conformer of N-*tert*-butylacetamide in the principal axis system obtained from fits using the programs XIAM and BELGI-C_1-hyperfine and from quantum chemical calculations at the MP2/6-311++G(d,p) level of theory.

Parameter	Unit	Fit XIAM [a,b]	Fit BELGI [a,c]	Calc [d]
A	MHz	3302.4457(46)	3304.8012(16)	3307.1
B	MHz	1365.5902(17)	1364.2402(14)	1365.5
C	MHz	1238.8312(14)	1238.480 89(62)	1237.8
D_J	kHz	0.1042(81)	0.1016(20)	0.0872
D_{JK}	kHz	0.529(80)		0.4594
d_1	kHz	−0.0169(66)		−0.0055
χ_{aa}	MHz	2.0129(72)	2.0118(35)	1.9833 [e]
$\chi_{bb} - \chi_{cc}$	MHz	5.827(18)	5.8278(58)	6.0342 [e]
χ_{ab}	MHz	−0.144(28)	−0.1395(37)	−0.1255 [e]
V_3	cm^{-1}	65.5668(1)	64.915 48(41)	119
F_0	GHz	158.0 [f]	158.062 356(27)	
D_{pi2J}	kHz	−52.27(17)		
D_{pi2K}	kHz	529.1(12)		
D_{pi2-}	kHz	−28.01(35)		
<(i,a)	deg	32.4448(1)	32.563 56(15)	34.95
<(i,b)	deg	57.5552(1)	57.436 44(15)	55.05
<(i,c)	deg	90.0 [f]	90.0 [f]	90
rms [g]	kHz	16.9	3	
N_A / N_E / Nq [h]		110/140/250	110/140/250	

[a] All parameters refer to the principal axis system. Statistical uncertainties are given as one standard uncertainty in the last digit. [b] Watson's S reduction and I^r representation were used. [c] Obtained by transformation from the rho axis system to the principal axis system. [d] Geometry parameters calculated at the MP2/6-311++G(d,p) level, centrifugal distortion constants at the B3LYP/6-311++G(d,p) level. [e] Electric field gradient single point calculation at the B3PW91/6-311+(df,pd) level of theory. [f] Fixed value. [g] Root-mean-square deviation of the fit. [h] Number of A and E species transitions as well as hyperfine components.

the internal rotor axis and the principal a axis). The results are given as Fit XIAM in Table 10.1.

Using the BELGI-C_1-hyperfine code, 17 parameters were floated (with the rotational constant F of the internal rotor fixed at the value from the XIAM fit), that is, the NQCCs χ_{aa}, χ_{bb}, and χ_{ab}, together with the three rotational constants A, B, C, four centrifugal distortion constants Δ_J, Δ_K, δ_J, and δ_K, the D_{ab} parameter (multiplying the off-diagonal $P_aP_b + P_bP_a$ term), the potential barrier height V_3, the rotation-torsion coupling term ρ, and four higher order terms that represent the rotation-torsion interaction. All out-of-plane terms were set to zero due to the C_s symmetry of TBAA. The rms deviation of all 250 hyperfine components is 3.0 kHz, which is close to the measurement accuracy. Parameters that can be transformed into the principal axis system are given as Fit BELGI in Table 10.1. The BELGI-C_1-hyperfine parameters in the rho-axis system are summarized in Table 10.2.

The rotational constants A, B, C deduced from the XIAM and BELGI-C_1-hyperfine fits are of high accuracy and in excellent agreement with the values calculated at the MP2/6-311++G(d,p) level of theory. The centrifugal distortion constants calculated using anharmonic frequency calculations are also close to the experimental values. The NQCCs determined in both fits are essentially the same and are as expected very well-calculated.

The barrier to internal rotation of the acetyl methyl group in TBAA was fitted by the program XIAM to be 65.5668(1) cm^{-1}, which is close to the barrier of 64.91548(41) cm^{-1} obtained with BELGI-C_1-hyperfine. In comparison to the values of 73.468(51) and 73.4782(1) cm^{-1} found for N-methylacetamide [65] and EAA, respectively, the barrier in TBAA decreases by about 8 cm^{-1}. This is strange, because we expect that the bulky *tert*-butyl group increases the acetyl methyl barrier height because of the sterical effect, as already observed in esters by comparing methyl acetate (102.413(20) cm^{-1}) [68] and ethyl acetate (101.606(23) cm^{-1}) [11] with *tert*-butyl acetate (112.983(13) cm^{-1}) [82]. However, because electronic effects might have a much stronger influence on the barrier to internal rotation of the acetyl methyl group than the sterical hindrance, as discussed in chapter 9, we suspect that sizable electronic effects occurring from the orientation of the *tert*-butyl group connected to the amide bond lead to the decrease of the potential barrier in TBAA. On the other hand, it is interesting that the barrier to internal rotation of the acetyl methyl group in TBAA is almost the same as those of two conformers of ethylacetamidoacetate (63.695(61) and 64.756(63) cm^{-1}) [83] and that of 64.96(4) cm^{-1} found for N-acetyl

Table 10.2: Spectroscopic constants of N-*tert*-butylacetamide in the rho-axis system obtained with the program BELGI-C_1-hyperfine.

Parameter [a]	Unit	TBAA	Operator
A	MHz	3178.6949(12)	P_a^2
B	MHz	1490.346 57(62)	P_b^2
C	MHz	1238.480 91(62)	P_c^2
D_{ab}	MHz	478.3453(24)	$\{P_a, P_b\}$
Δ_J	kHz	0.1016(20)	$-P^4$
Δ_K	kHz	2.00(13)	$-P_a^4$
δ_J	kHz	0.0254(21)	$-2P^2(P_b^2 - P_c^2)$
δ_K	kHz	−0.468(59)	$-\{P_a^2, (P_b^2 - P_c^2)\}$
χ_{aa}	MHz	4.1477(60)	
χ_{bb}	MHz	3.6919(67)	
χ_{cc}	MHz	−7.8396 [b]	
χ_{ab}	MHz	−0.1916(80)	
V_3	cm^{-1}	64.915 48(41)	$(1/2)(1 - cos3\gamma)$
ρ	unitless	0.017 955 53(18)	$P_a P_\gamma$
F	cm^{-1}	5.3641 [c]	P_γ^2
d_{ab}	MHz	−3.6271(58)	$(1 - cos3\gamma)\{P_a, P_b\}$
c_4	MHz	−0.001 40(24)	$(1 - cos3\gamma)P_a^2$
F_v	MHz	0.5748(15)	$(1 - cos3\gamma)P^2$
L_v	MHz	0.002 33(12)	$(P_a P_\gamma)P^2$
N_A / N_E / N_q [d]		110/140/250	
rms A / E [e]	kHz	2.5/3.3	

[a] All parameters refer to the rho-axis system and cannot be directly compared to those referred to the principal axis system. P_a, P_b, and P_c are the components of the overall rotation angular momentum, P_γ is the angular momentum of the internal rotor rotating around the internal rotor axis by an angle γ. {u,v} is the anti-commutator uv + vu. The product of the parameter and operator from a given row yields the term actually used in the vibration-rotation-torsion Hamiltonian, except for F, ρ, and A, which occur in the Hamiltonian in the form $F(P_\gamma - \rho P_a)^2 + AP_a^2$. Statistical uncertainties are shown as one standard uncertainty in the last digit. [b] parameter derived from the linear combination $\chi_{cc} = -(\chi_{aa} + \chi_{bb})$. [c] Fixed to the value from the XIAM fit. [d] Number of A and E-species transitions as well as hyperfine components. [e] Root-mean-square deviations of the A and E-species.

alanine methyl ester [84]. Unfortunately, unlike in the case of acetates [85], the limited number of data points is not sufficient to give any definitive statement on the acetyl internal rotation barrier in acetamides yet.

The ab initio barrier height of 119 cm^{-1} is almost twice the experimental value. Many previous investigations have shown that calculating the potential barriers is a difficult task. The predicted values vary in a wide range and depend strongly

on the level of theory in use [85, 86]. Considering the zero-point energy correction might improve the results [84]. Nevertheless, it requires frequency calculations for the transition states. This could not be performed at very high level of theory due to the limitation of our computational resources. The calculations were however possible at the B3LYP/6-311++G(d,p) level of theory and yielded a barrier height of 133 cm^{-1}. Furthermore, a level that yields reasonable value for one specific methyl group may fail for another methyl group, even in the same molecule (for example see Table 7 in ref [84]). High level quantum chemical methods such as diffusion quantum Monte Carlo and coupled cluster are not necessarily in best agreement with the experiments as will be discussed in section 15.4. Currently, no general methods exist to calculate the methyl barrier height. However, results from quantum chemical calculations often give the correct order of magnitude (low, intermediate, or high) of the barrier heights, which is sufficient to hint the authors in the spectral assignment step. It is worth noting that almost all lines observed in the broadband scan could be assigned to the *trans* conformer of TBAA. The *trans* conformer is thus the only conformer, which can be observed under our measurement conditions.

10.5 Conclusion

The microwave spectrum of N-*tert*-butylacetamide was measured between 2 and 26.5 GHz using a molecular beam Fourier transform microwave spectrometer with a measurement accuracy of 2 kHz. Only one conformer with *trans* configuration and C_s symmetry was observed in the spectrum. The data set was fitted using the programs XIAM and BELGI-C_1-hyperfine to rms deviations of 16.9 and 3.0 kHz, respectively. Both XIAM and BELGI fits included 26 A and 35 E species transitions with a total of 250 hfs components, determining 14 and 17 molecular parameters, respectively. All comparable fitted parameters were in excellent agreement. The barrier to internal rotation of the acetyl methyl group was approximately 65 cm^{-1}, surprisingly lower than that of about 73 cm^{-1} found in N-methylacetamide and N-ethylacetamide but close to that found in ethylacetamidoacetate and N-acetyl alanine methyl ester.

Chapter 11

N-Vinylacetamide - VAA

The measurements, quantum chemical calculations, spectrum analysis, spectrum assignment, and the fit is the work of R. Kannengießer.

11.1 Introduction

N-Vinylacetamide (VAA) is another secondary acetamide, which was expected to have a spectrum of a system with one internal rotor and one coupling nucleus. It is already known from the investigations on quadrupole coupling of N-vinylformamide that the vinyl group has some influence on the electronic effects in the molecule, due to the π-conjugation, and therefore on the quadrupole coupling. These investigations on N-vinylacetamide were therefore carried out to gain further information especially on the influence of the vinyl group not only on the quadrupole coupling but also on the internal rotation of the acetyl methyl group.

Chemically N-vinylacetamide is commonly known, as it serves as a water soluble monomer in a polymerization to polyvinylacetamide [87]. Polyvinylacetamide itself can be water soluble, despite it is a polymer. It shows hydrophilic and hydrophobic properties.

11.2 Theoretical

11.2.1 Quantum chemical calculations

For the conformational analysis of N-vinylacetamide two dihedral angles $\alpha_1 = (H_2 - N_1 - C_3 - C_5)$ and $\alpha_2 = (H_2 - N_1 - C_9 - C_{11})$ were rotated analog to the treatment of EAA (subsection 9.2.1), forming 36 starting geometries. For atom numbering see Figure 11.1.

The optimization delivered four stable conformers. Their relative energies, rotational constants, and dipole moment components are given in Table 11.1.

Table 11.1: Relative energy values in kJ·mol^{-1}, rotational constants in MHz, and dipole moment components in D of four stable conformers of N-vinylacetamide calculated at the MP2/6-311++G(d,p) level of theory.

	$E_{rel.}$	A	B	C	$\lvert\mu_a\rvert$	$\lvert\ \mu_b\rvert$	$\lvert\mu_c\rvert$
I	0.0	9292.26	2083.94	1720.99	0.14	3.92	0.07
II	5.4	8524.90	2139.40	1729.85	2.49	2.45	0.01
III	8.2	8309.08	2503.06	1948.78	1.06	4.24	0.20
IV	16.9	7272.50	2564.35	1965.02	3.43	0.70	0.68

The geometries of the four conformers are shown in Figure 11.1. Comparing these conformations with the ones obtained for EAA one sees immediately that due to the extended π-conjugation of the amide bond and the vinyl group, all stable conformers are forced to planarity. This can be easily seen from the dihedral angles in Table 11.2. Only conformer IV, which is the highest in energy shows a slight tilt out of plane by 28 degrees. This also gives rise to a slightly higher dipole moment in *c*-direction for conformer IV compared to the others, which possess basically no dipole moment in this direction.

The lowest energy conformer, conformer I, has a *trans* configuration where the acetyl oxygen is most distinct from the hydrogen atom bound to the nitrogen. It is the VAA analogon to the second conformer of EAA. The nuclear coordinates of this conformer are given in Table E.1.

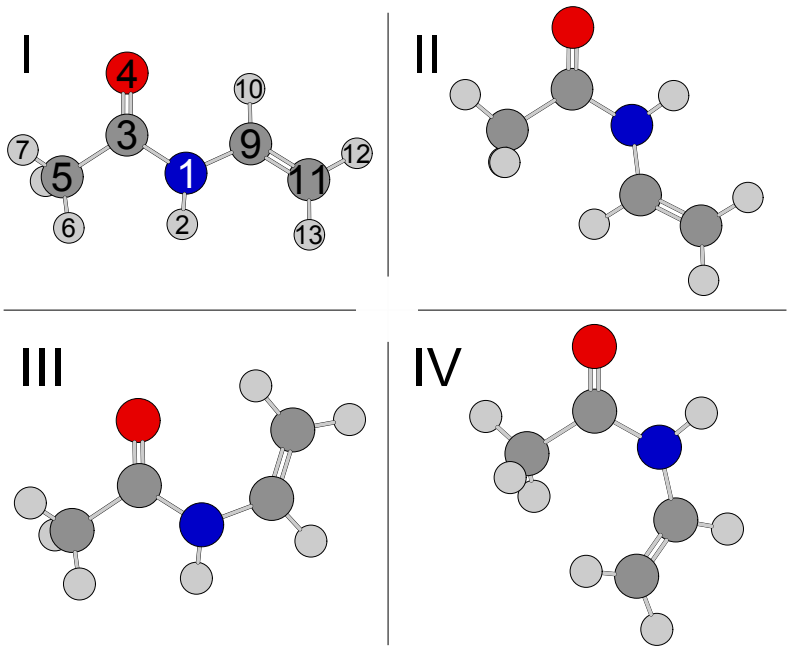

Figure 11.1: Four stable conformers of N-vinylformamide calculated at the MP2/6-311++G(d,p) level of theory.

Table 11.2: Calculated dihedral angles in N-vinylacetamide and N-ethylacetamide.

	VAA			EAA	
	α_1	α_2		α_1	α_2
I	−1.025	−2.538	II	−11.637	35.342
II	−178.044	−1.070	IV	172.547	36.684
III	2.274	176.670	I	9.556	86.799
IV	172.614	154.095	III	−174.635	73.296

11.2.2 Nuclear quadrupole coupling

The vinyl group in VAA makes this molecule a large π-conjugated system for which the calculation of the quadrupole coupling constants is slightly different compared to most other molecules in this dissertation. The exact procedure was described in subsection 6.2.2. The calculated NQCCs are $\chi_{aa} = 1.862407$ MHz, $\chi_{bb} = 1.950767$ MHz, $\chi_{cc} = -3.813175$ MHz, $\chi_{ab} = -0.089501$ MHz, $\chi_{ac} = -0.076024$ MHz, and $\chi_{bc} = 0.077611$ MHz.

11.2.3 Internal rotation

For the internal rotation of the acetyl methyl group, we assumed a small barrier in the order of the ones obtained for EAA (73.4782(1) cm^{-1}) and TBAA (65.5668(1) cm^{-1}). However, the prediction of the barrier is quite difficult as the influence of the π-conjugation on electronic effects and thereby the barrier height of the methyl internal rotation is hardly foreseeable.
Quantum chemical calculations on the barrier delivered a barrier height of only 52.6 cm^{-1}, which is already quite low comparing to the barriers of 109 and 119 cm^{-1}, calculated for EAA and TBAA, respectively, using the same calculation method.

11.3 Experimental

The measurements on VAA turned out to be quite challenging. VAA is a solid substance with a remarkably low vapor pressure of 0.222 torr at 25°C. This is the lowest vapor pressure of all substances measured in this work.
As a result, the substance had to be heated during the measurement to increase the vapor pressure and thereby the concentration of VAA in the gas phase. Therefore, the stainless steel tube containing the substance was heated to 80-100°C.

At first a scan was carried out in the frequency range from 8-16 GHz. An overview of this scan in the whole measured range is available in Figure 11.2. In this frequency range only a small number of low intense lines could be observed. This might be explained as only few lines were predicted in this range due to the planarity of the molecule. Additionally, only a small concentration of the substance in the cavity could be observed, due to the low vapor pressure.

The small number of observed lines turned out to be challenging for the assignment process. At first, all effects causing additional splittings in the spectrum as the internal rotation of the acetyl methyl group and the quadrupole coupling were neglected and it was tried to assign the spectrum as an assumed rigid rotor spectrum, using the data from the scan. As these attempts failed, due to the lack of possibilities, high resolution measurements were carried out to be able to analyze the experimental hyperfine structures, to help and assist with the assignment. With the help of the calculated NQCCs it was finally possible to find some characteristic Q-branch patterns giving seven hyperfine components instead of the five components typically

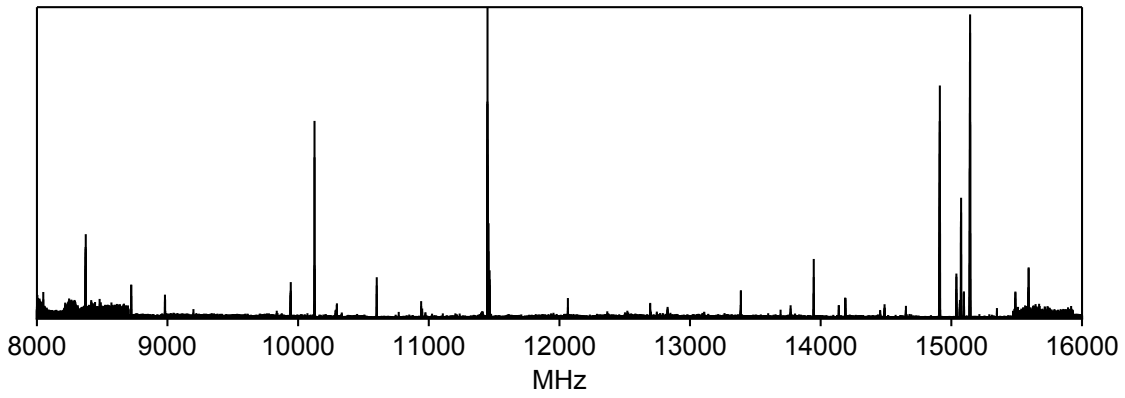

Figure 11.2: Overview of the broadband scan in the frequency range from 8 to 16 GHz.

arising for R-branches. This directed us to the correct assignment of the quadrupole hyperfine splittings and thereby also of the rotational transitions. In total 74 hyperfine components including 16 rotational transitions could be assigned and fitted this way. The results are given in Table 11.3.

After the assignment of the quadrupole coupling and the A species, attempts to fit the E species were made. Several predictions with varying V_3 potentials from 33-100 cm^{-1} (1000-3000 GHz) were carried out with XIAM and compared to the remaining experimental lines. Unfortunately no convincing assignment could be obtained with this procedure up to now. Several approaches were promising when only fitting the internal rotation parameters but failed, when trying to include the quadrupole coupling in the fit. But as the quadrupole coupling could be perfectly fitted for only A species, this shows us that the correct assignment of the E species is still missing. A frequency list of all fitted transitions are available in Table E.2.

11.4 Results and Discussion

The results from the A species in Table 11.3 show already problems in the determination of the rotational constants and the centrifugal distortion constants from the spectrum. The rotational constants are obtained with an unusual low accuracy. Also a very great discrepancy between the fitted and calculated A rotational constant was observed. Usually differences in the order of a few MHz are found. In this case the

difference between the experimental and the calculated value is 240.19 MHz. This corresponds to a difference of 2.5% of the experimental value. In the case of TBAA for example (Table 10.1) a difference of 0.15% was obtained.

Table 11.3: Rotational parameters from the A-species fit (exp) compared with theoretical parameters (calc) of N-vinylacetamide.

		exp [a]	calc	exp-calc
A	MHz	9532.45(89)	9292.26	240.19
B	MHz	2099.02(31)	2083.94	15.08
C	MHz	1731.37(20)	1720.99	10.38
Δ_J	kHz	0.1611(76)	0.1706	−0.0095
Δ_{JK}	kHz	−6.194(66)	3.6519	−9.8457
Δ_K	kHz	−48.74(22)	6.4396	−55.1831
χ_{aa}	MHz	1.8650(15)	1.8624	0.0026
χ_{-}	MHz	5.6807(32)	5.7639	−0.0833
σ	kHz	2.7		
N [b]/N_q [c]		16/74		

[a] Parameters are given with one standard uncertainty in parentheses. Watson′s A reduction and I^r representation were used. [b] Number of rigid rotor transitions used in the least square fit. [c] Number of hyperfine transitions.

The centrifugal distortion constants are determined with a good accuracy considering the low number of lines included in the fit. However, it is only possible to include the three distortion constants Δ_J, Δ_{JK}, and Δ_K. The constants δ_J and δ_K could not be fitted. In comparison with the calculated values the experimental value of Δ_J is close to the calculated one. For the other distortion constants much higher differences were observed. Therefore, we assume that more lines and especially the E species lines have to be included in the fit in order to fit the centrifugal distortion properly. However, a fit excluding the centrifugal distortion lead to a much higher standard deviation of 86 kHz. Including the centrifugal distortion was therefore necessary and lead to a standard deviation of only 2.7 kHz, which is close to the measurement accuracy.

In total 74 hyperfine components of 16 rotational transitions were included in the fit. The fitted quadrupole coupling constants could not only be fitted with high accuracy, the fitted values are additionally in very good agreement with the calculations. This again confirms the predictive power of the EFG calculations with the new method for π-conjugated systems, which was developed in the work on VFA

(subsection 6.2.2). The quadrupole coupling in the spectrum is therefore supposed to be treated sufficiently in the fit. Thus the predictions of the hyperfine structures of the yet unassigned E species transitions should be very accurate and hint to the correct assignment. Unfortunately this was not the case and therefore we assume some additional problem with the E species.

11.5 Conclusion

The microwave spectrum of N-vinylacetamide was measured in the frequency range from 8 to 16 GHz. The A species of the lowest energy conformer could be assigned. The assignment of the respective E species and therefore the determination of internal rotation parameters was not successful. The fit included 16 A species transitions with a total of 74 hyperfine components.
The quadrupole coupling effect of the ^{14}N nucleus was analyzed in detail and the quadrupole hyperfine structure could be assigned with high accuracy. The NQCCs were fitted to values of $\chi_{aa} = 1.8650(15)$ MHz and $\chi_{-} = 5.6807(32)$ MHz.

Part III

Tertiary Propion- and Acetamides

Chapter 12

Introduction

The basic structure element in tertiary amides is $R_1-(C{=}O)-NR_2R_3$, where all three rests R can be methyl- or lager alkyl groups. For methyl internal rotation two different situations are therefore possible: the acetyl methyl rotation and the nitrogen-methyl rotation, both being sensitive to the electronic changes in the environment of the amide bond, due to sterical and inductive effects of different alkyl substituents on the nitrogen atom (R_2, R_3). If the rests R are larger alkyl groups the importance of the conformational analysis increases as larger alkyl groups offer more opportunities for conformationally stable arrangements.
Only one tertiary amide, in particular one acetamide, N,N-dimethylacetamide was studied by microwave spectroscopy so far by M. Fujitake et al. [88]. The V_3 potential of the acetyl methyl group was found to be 677 cm^{-1}. The internal rotation barriers of the nitrogen methyl groups, however, could not be assigned unambiguously. The reported values of the barriers are 183 cm^{-1} and 273 cm^{-1}.

Here, four tertiary amides, the two propionamides N,N-diethylpropionamide (chapter 13) and N,N-dimethylpropionamide (chapter 14), and the two acetamides N,N-diethylacetamide (chapter 15) and N-methyldiacetamide (chapter 16) were investigated.
In N,N-diethylpropionamide all three rests R are ethyl groups offering multiple opportunities for conformational minimum geometries. We assume therefore a high number of stable conformers. However, as methyl internal rotation in ethyl groups is usually highly hindered [55], no internal rotation effects are expected for DEPA.
In N,N-dimethylpropionamide both rests bound to the nitrogen, R_2 and R_3, are methyl groups and should therefore show internal rotation splittings in the spec-

trum. The R_1 group is an ethyl group and provides possibilities for multiple conformations.

In N,N-diethylacetamide, the internal rotation due to the acetyl methyl group should be observable. The nitrogen substituents R_2 and R_3 are ethyl groups, which can be oriented in different directions.
Also N-methyldiacetamide should show internal rotation splittings as all three R-groups are methyl groups in this case. Thus, N-methyldiacetamide contains three internal rotors, one nitrogen methyl rotor and two acetyl methyl rotors, where all three rotors can possibly lead to internal rotation splittings in our spectrum.

Chapter 13

N,N-Diethylpropionamide - DEPA

Parts of this chapter have already been published in the Journal of Physical Chemistry A:

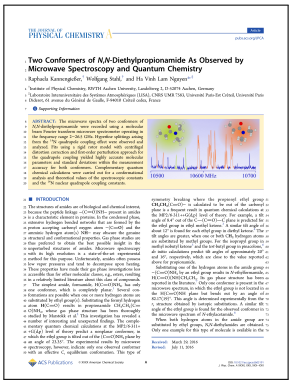

R. KANNENGIEßER, W. STAHL, and H.V.L. NGUYEN Two Conformers of N,N-Diethylpropionamide As Observed by Microwave Spectroscopy and Quantum Chemistry *J. Phys. Chem. A*, 2016, **120**, 5979-5984.

The measurements, quantum chemical calculations, spectrum analysis, spectrum assignment, fits, and the manuscript preparation is the work of R. Kannengießer. The coworkers took mostly part in a supporting way especially during corrective work in the publication process.

13.1 Introduction

This chapter is on N,N-diethylpropionamide (DEPA), where all the three rests R in $R_1-(C{=}O)-NR_2R_3$ are substituted by ethyl groups. A related molecule, that was already investigated is the propionamide $CH_3CH_2(C{=}O)NH_2$ containing only one ethyl group attached to the acetyl group. Its gas phase structure has been thoroughly studied by Marstokk et al [89]. This investigation has revealed a number of interesting and unexpected results. Quantum chemical calculations at the MP2/6-311++G(d,p) level of theory predict a non-planar conformer, in which the ethyl group is tilted out of the $(C{=}O)NH_2$ plane by an angle of 23.35°.

The experimental results by microwave spectroscopy on the other hand indicate only one observed conformer with an effective C_s equilibrium conformation. This type of symmetry breaking, where the propionyl ethyl group $CH_3CH_2(C{=}O)-$ is calculated to be out of the carbonyl plane, is a frequent result in quantum chemical calculations at the MP2/6-311++G(d,p) level of theory. For example, a tilt angle of 8.4° out of the C−(C=O)−C plane is predicted for the ethyl group in ethyl methyl ketone [77]. A similar tilt angle of about 12° is found for each ethyl group in diethyl ketone [90]. The tilt angles are greater, when one or both CH_2 hydrogen atoms are substituted by methyl groups. For the isopropyl group in methyl isobutyl ketone [75] and the *tert*-butyl group in pinacolone [91], ab initio calculations predict tilt angles of approximately 20° and 16°, respectively, which are close to the value reported above for propionamide. This leads us to ask a few questions on what conformational situation will be found in N,N-diethylpropionamide not only for the propionyl ethyl group but also both nitrogen ethyl groups.

(i) How many conformers of DEPA will be observable in the microwave spectrum?
(ii) Which orientations of the three ethyl groups will be present in the most stable conformer?
(iii) Will a conformer with a planar propionyl group exist?

Besides the interesting conformational landscape, DEPA shows ^{14}N nuclear quadrupole coupling giving information on the electronic environment of the nitrogen nucleus in the amide bond, which is expected to be sensitive to the sort of alkyl substituents at the nitrogen.

13.2 Theoretical

13.2.1 Conformational Preferences

For a conformational analysis, $6^4 = 1296$ starting geometries were automatically generated by a program from V. Van varying the four dihedral angles $\angle(N_1, C_4, C_6, C_7)$, $\angle(C_4, N_1, C_2, C_{15})$, $\angle(C_4, N_1, C_3, C_{11})$, and $\angle(O_5, C_4, N_1, C_3)$ (for atom numbering see Figure 13.1) over a grid of 60°, and fully optimized at the MP2/6-311++G(d,p) level of theory. The optimizations yielded ten conformers, which were confirmed as minima on the potential energy surface by frequency calculations. The rotational

constants, dipole moment components, and energies relative to that of the lowest energy conformer are given in Table 13.1.

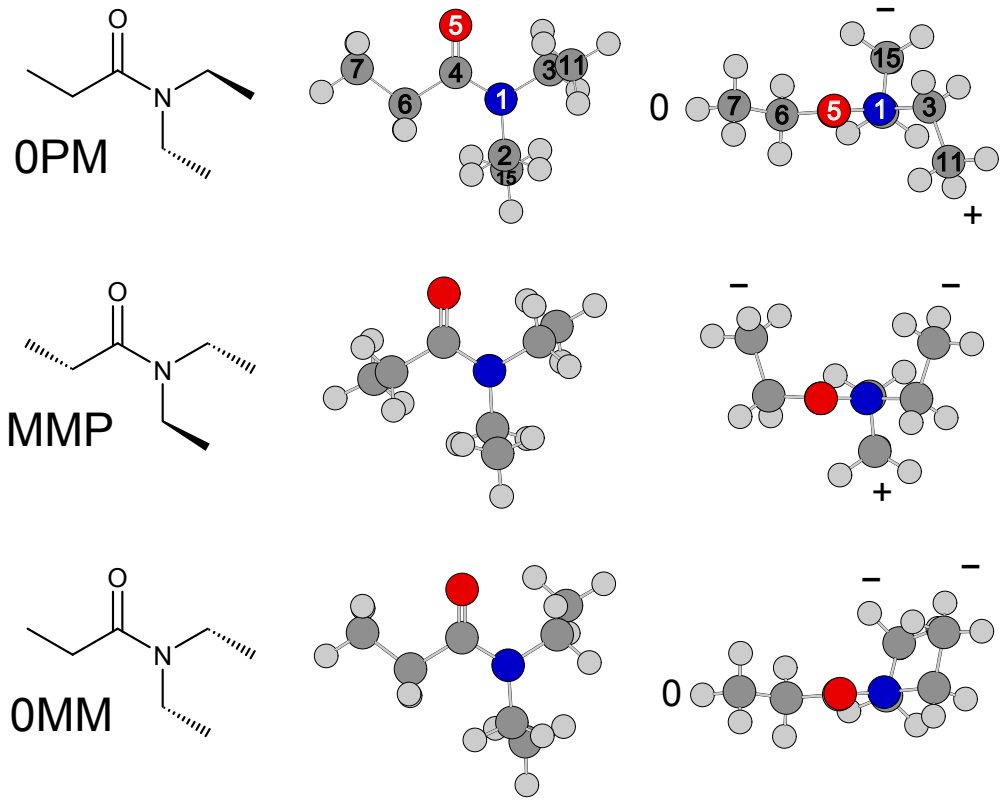

Figure 13.1: Optimized geometries of the three most stable conformers of N,N-diethylpropionamide. Ethyl groups, that are out of the (C=O)N plane, are characterized with P (+) or M (–); ethyl groups located in or almost in this plane with 0. Left hand side: Natta projections, middle: front view, right hand side: view along the O_5-C_4 bond.

To determine the energetically most favorable conformers, not only the calculated electronic energies, but also the zero point energies (ZPE) were considered. We took the ZPE correction into account for all method/basis set combinations except for the MP2/cc-pVTZ and MP2/6-311++G(3df,2pd) levels, where our computational resources did not allow frequency calculations. Therefore, theses two levels of theory are suitable to obtain accurate rotational constants, but they cannot be used to estimate the relative abundances of different conformers in the molecular beam.

Table 13.1: MP2-energies with zero-point corrections in Hartree, relative energies in kJ·mol^{-1}, rotational constants in MHz and dipole moment components in D of the ten stable conformers of N,N-diethylpropionamide calculated at the MP2/6-311++G(d,p) level of theory. All values refer to the principal axis system. Conformers **0PM** and **0MM** - emphasized with bold letters - are the observed conformers.

	$E_{MP2+ZPE}$	E_{rel}	A	B	C	$\lvert\mu_a\rvert$	$\lvert\mu_b\rvert$	$\lvert\mu_c\rvert$
0PM	**−404.456457**	**0.00**	**1915.4**	**1220.8**	**833.7**	**1.625**	**3.514**	**1.422**
MMP	−404.455836	1.63	1698.7	1344.2	948.8	0.826	3.695	1.927
0MM	**−404.455575**	**2.32**	**2071.2**	**1177.1**	**856.3**	**1.775**	**3.676**	**0.331**
PMM	−404.454657	4.73	1989.1	1268.8	892.3	0.504	4.158	0.529
PPP	−404.454284	5.71	1825.3	1371.9	961.3	0.564	4.166	0.576
MPM	−404.454005	6.44	1857.5	1361.2	890.8	0.440	3.935	1.491
MMM	−404.453733	7.15	1929.1	1283.3	947.3	0.963	3.957	0.602
0P0	−404.453661	7.34	2296.9	1076.4	811.0	2.077	3.259	1.109
0PP	−404.453597	7.51	2125.6	1184.8	866.8	1.448	3.707	0.943
P0M	−404.452639	10.02	2005.6	1157.6	940.8	1.293	3.689	1.480

The structures of the three most energetically favorable conformers are given in Figure 13.1; the nuclear coordinates in the principal axis system are available in Table F.1 and Table F.2. They differ by up to 2 kJ·mol^{-1} in energy. On the contrary, their calculated total dipole moments have similar values of approximately 4.1 Debye. All of them might be present in the experimental spectrum under our molecular beam conditions using helium as carrier gas, because the rotational cooling is not as effective as with neon or argon and higher energy conformers could be still populated. The other seven conformers are much higher in energy and are presumably not observable. The lowest energy conformer, which is henceforth called 0PM, has the propionyl ethyl group almost located on the (C=O)N plane (marked with 0) and the other two ethyl groups bending into opposite sides of this plane (marked with plus/P and minus/M). In the same manner, the other two conformers are named MMP and 0MM.

The MP2/6-311++G(d,p) level of theory predicts that the conformer MMP is 0.7 kJ·mol^{-1} lower in energy than conformer 0MM. Re-optimizations using other basis sets including diffuse functions yielded the same results. On the other hand, if the diffuse functions are omitted, 0MM becomes more stable than MMP, which is also the result of HF and DFT calculations (see Table 13.2). This disagreement in energy calculations at different levels of theory challenged the assignment process, as will be revisited in section 13.3 and section 13.4.

Table 13.2: Sum of the electronic and zero-point energies of the three most stable conformers of DEPA calculated at different levels of theory. Energies relative to the lowest energy conformer 0PM are given in kJ·mol^{-1}, absolute energies of conformer 0PM in Hartree.

	$\boldsymbol{E}_{0PM}$	$\boldsymbol{E}_{0MM}$	$\boldsymbol{E}_{MMP}$	Δ_E [a]
MP2				
cc-pVTZ [b]	−404.935066	2.17	2.24	0.07
6-311++G(3df,2pd) [b]	−404.940760	2.33	1.12	−1.21
6-311++G(d,p)	−404.456455	2.32	1.63	−0.69
6-311+G(d,p)	−404.455308	2.29	1.74	−0.55
6-311G(d,p)	−404.443380	2.40	3.67	1.27
6-31++G(d,p)	−404.314998	2.66	1.76	−0.91
6-31+G(d,p)	−404.312833	2.67	1.85	−0.83
6-31G(d,p)	−404.291421	2.46	4.48	2.03
B3LYP				
cc-pVTZ	−405.717289	3.15	4.30	1.16
6-311++G(3df,2pd)	−405.708972	3.15	4.24	1.09
6-311++G(d,p)	−405.679848	3.07	4.30	1.23
6-311+G(d,p)	−405.679675	3.07	4.29	1.22
6-311G(d,p)	−405.674322	2.97	5.50	2.53
6-31++G(d,p)	−405.594573	3.17	4.21	1.04
6-31+G(d,p)	−405.594306	3.20	4.23	1.03
6-31G(d,p)	−405.580069	2.76	5.84	3.08
HF				
cc-pVTZ	−403.056920	3.75	4.33	0.58
6-311++G(3df,2pd)	−403.049900	3.78	4.36	0.58
6-311++G(d,p)	−403.015421	3.64	4.42	0.78
6-311+G(d,p)	−403.015159	3.66	4.41	0.75
6-311G(d,p)	−403.010816	3.69	5.36	1.67
6-31++G(d,p)	−402.938265	3.74	4.32	0.59
6-31+G(d,p)	−402.937899	3.71	4.27	0.56
6-31G(d,p)	−402.931247	3.59	5.53	1.94

[a] E_{MMP}-E_{0MM}. [b] No frequency calculation at this level of theory. Therefore, only the electronic contribution without zero-point correction is used.

13.2.2 Nuclear quadrupole coupling

From the optimized structure at the MP2/6-311++G(d,p) level, we carried out a single point EFG calculation at the B3PW91/6-311+(df,pd) level of theory using a

calibration factor of eQ/h = 4.5586(40) MHz a.u.$^{-1}$ given by Bailey. The calculation results in a nuclear quadrupole coupling tensor with the diagonal elements χ_{aa} = 1.9490 MHz, χ_{bb} = 1.1471 MHz, and χ_{cc} = −3.0961 MHz, as well as the off-diagonal elements χ_{ab} = −0.2437 MHz, χ_{ac} = −0.5440 MHz, and χ_{bc} = 2.6623 MHz for conformer 0PM. For conformer 0MM values of χ_{aa} = 1.8180 MHz, χ_{bb} = 2.3961 MHz, χ_{cc} = −4.2142 MHz, χ_{ab} = −0.0566 MHz, χ_{ac} = −1.0620 MHz, and χ_{bc} = −0.3363 MHz were found.

13.3 Experimental

A broadband scan in the frequency range 8.5 - 16.0 GHz revealed a rich and complex spectrum. All lines in the scan have line widths of a few MHz due to quadrupole interaction. A portion of 7.5 GHz of the scan is given in Figure 13.2; a portion of 50 MHz in Figure 13.3.

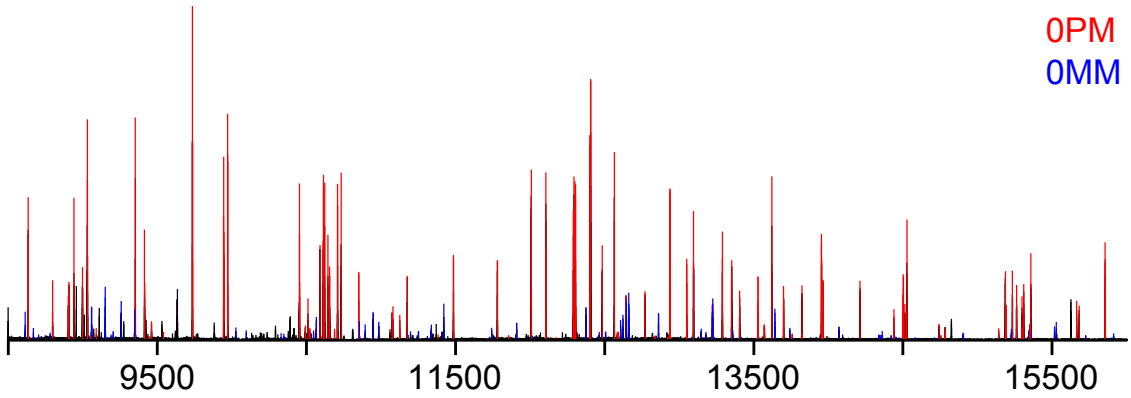

Figure 13.2: Broadband scan from 8500 MHz to 16000 MHz of N,N-diethylpropionamide showing that (i) the transitions of conformer 0PM are much more intense than those of conformer 0MM and (ii) only some weak unassigned lines are present in the spectrum.

All lines were subsequently remeasured at higher resolution, indicating completely resolved hyperfine splittings, arising from the nitrogen nucleus. Figure 13.4 shows a typical spectrum of DEPA measured at high resolution. The line widths are 14 – 30 kHz, corresponding to a measurement accuracy of 2 kHz.

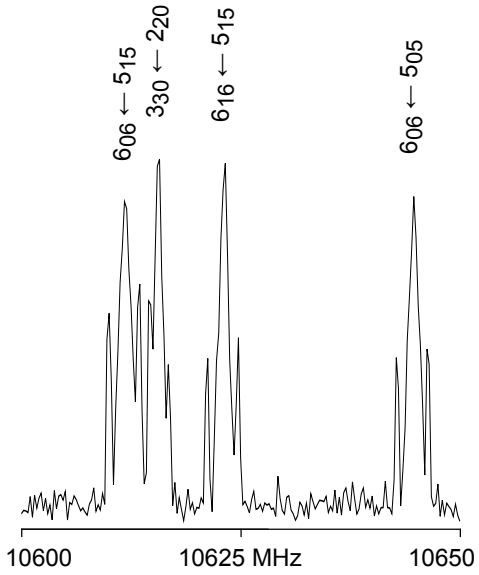

Figure 13.3: Portion of 50 MHz of the broadband scan of N,N-diethylpropionamide. All indicated transitions belong to conformer 0PM and are marked with their rigid rotor quantum numbers J, K_a, K_c. The lines are broadened or split because of the quadrupole coupling, arising from the ^{14}N nucleus.

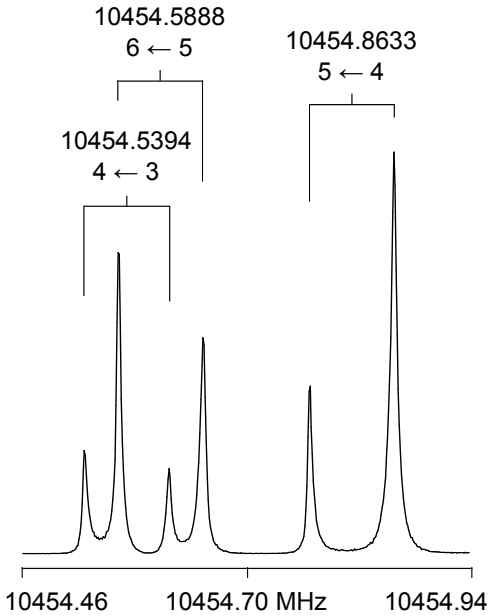

Figure 13.4: Typical spectrum of the $5_{14} \leftarrow 4_{13}$ transition of conformer 0PM of DEPA with three quadrupole components given by $F' \leftarrow F$. Brackets indicate the Doppler doublets. For this spectrum, 1000 decays were coadded.

13.3.1 Conformer 0PM

We started the assignment with the spectrum of the lowest energy conformer 0PM. As a first step, we neglected quadrupole coupling and used a rigid-rotor program to calculate the theoretical spectra. The most intense lines in the spectrum were readily assigned to conformer 0PM by comparing their frequencies with the predicted spectrum. Thereafter, hyperfine splittings were calculated using the NQCCs from subsection 13.2.2. In total, 91 rotational transitions with 368 hyperfine components were assigned and fitted with the program XIAM. The standard deviation of this fit is 2.2 kHz, close the measurement accuracy.

13.3.2 Conformer 0MM

After conformer 0PM was assigned, many weaker lines remained in the spectrum, which might belong to conformer MMP and/or 0MM. By trial and error, 56 lines in the broadband scan could be assigned to conformer 0MM. They contain 220 quadrupole components and were fitted to a standard deviation of 1.7 kHz. The molecular parameters of both conformers 0PM and 0MM are summarized in Table 13.3; the transition frequencies are collected in Table F.3 and Table F.4, respectively. It should be noted that after excluding all transitions belonging to conformer 0PM and 0MM, some weaker lines remain in the spectrum. Hard efforts to assign these lines to conformer MMP did not lead to success. We thus conclude that only conformers 0PM and 0MM are present in our spectrum, where conformer 0PM is lower in energy than conformer 0MM.

Splittings due to internal rotation of the three ethyl methyl groups were not observed for both conformers. The barriers of internal rotation of such groups are usually higher than 1000 cm^{-1}, and the resulting splittings are not resolvable with our spectrometer [55, 78, 92].

13.4 Results and Discussion

The microwave spectra of two conformers of DEPA, called 0PM and 0MM, with 368 and 220 hyperfine transitions were assigned and fitted with excellent standard

deviations of 2.2 kHz and 1.7 kHz, respectively. The rigid rotor model with centrifugal distortion correction and a first order perturbation approach for ^{14}N nuclear quadrupole coupling was sufficient to reproduce the experimental spectra to measurement accuracy of 2 kHz. All parameters were determined with very high accuracy as shown in Table 13.3.

Table 13.3: Molecular parameters of the observed conformers **0PM** and **0MM** of DEPA obtained from the fits using the program XIAM (obs) and from quantum chemical calculations at the MP2/6-311++G(d,p) level of theory (calc).

		0PM		**0MM**	
Par.	Unit	obs [a]	calc	obs [a]	calc
A	MHz	1924.215 84(15)	1915.4	2070.069 10(24)	2071.2
B	MHz	1214.565 984(56)	1220.8	1180.371 868(71)	1177.1
C	MHz	832.070 891(42)	833.7	857.533 403(51)	856.3
D_J	kHz	0.106 99(53)	0.1318	0.186 48(54)	0.1482
D_{JK}	kHz	0.6118(26)	0.6399	0.3234(30)	0.5969
D_K	kHz	−0.0874(60)	0.1274	0.850(18)	0.4089
d_1	kHz	−0.062 18(32)	−0.0771	−0.052 80(38)	−0.0434
d_2	kHz	−0.023 84(16)	−0.026	−0.014 35(21)	−0.0157
χ_{aa}	MHz	1.970 18(79)	1.9490 [b]	1.798 61(93)	1.8180 [b]
$\chi_{bb} - \chi_{cc}$	MHz	4.2749(14)	4.2432 [c]	6.6695(15)	6.6103 [c]
χ_{bb} [c]	MHz	1.152 36(40)	1.1471 [b]	2.435 44(47)	2.3961 [b]
χ_{cc} [c]	MHz	−3.2255(88)	−3.0961 [b]	−4.2340(10)	−4.2142 [b]
σ [d]	kHz	2.2		1.7	
N/N$_q$ [e]		91/368		56/220	

[a] Parameters are given with one standard uncertainty in parentheses. Watson's S reduction and I^r representation were used. [b] See subsection 13.2.2. [c] Derived. [d] Standard deviation of the fit. [e] Number of rotational N and hyperfine transitions N$_q$.

As mentioned in the subsection 13.2.1, calculations at different levels of theory point out that the MP2 method in combination with diffuse functions calculate conformer MMP to be lower in energy than conformer 0MP (see Table 13.2). The experimental results clearly show the contrary. This combination, which includes our most frequently used MP2/6-311++G(d,p) level of theory, might not be suitable for calculating the conformational energies of molecules like DEPA. On the other hand, the rotational constants predicted for both conformers at the MP2/6-311++G(d,p) level are very close to the experimental values. The differences are within 0.5%, which was extremely helpful for the assignment process. The centrifugal distortion constants agree reasonably with the experimental values.

The propionyl ethyl group possesses a dihedral angle $\angle(N_1, C_4, C_6, C_7)$ of $-168.6°$ and $-171.0°$ for conformer 0PM and 0MM, respectively. Correspondingly, the ethyl group is slightly tilted out of the (C=O)N plane by a respective angle of 11.4° and 9.0°. This is almost the same as the angle found for the propionyl ethyl group in ethyl methyl ketone (8.4°) [77] and diethyl ketone (12°) [90]. The ethyl groups attached to the nitrogen in the more stable conformer point in opposite directions, whereas in the other conformer they are oriented in the same direction. In 0PM, the dihedral angles $\angle(C_4, N_1, C_3, C_{11})$ and $\angle(C_4, N_1, C_2, C_{15})$ are 98.2° and 84.3°, respectively. In 0MM, we found that $\angle(C_4, N_1, C_3, C_{11}) = 107.7°$ and $\angle(C_4, N_1, C_2, C_{15}) = -75.9°$.

The experimental NQCCs are as expected in almost exact agreement with the values calculated with the method given in subsection 13.2.2. The NQCC z-principal axis components χ_{zz} of conformers 0PM and 0MM are similar (see Table 13.4), i.e. the orientations of the ethyl groups do not affect the electronic environment at the site of the nitrogen nucleus.

Table 13.4: ^{14}N NQCC z-principal axis component χ_{zz} (in MHz) of DEPA and related amides.

		χ_{zz}	Ref.
Formamide	H(C=O)NH_2	−3.8510(11)	[93]
Propionamide	$\mathbf{CH_3CH_2}$(C=O)NH_2	−3.9762(48)	[94]
N-Ethylformamide	H(C=O)(NH)$\mathbf{CH_2CH_3}$	−3.993(51)	[5]
N-Methylpropionamide	$\mathbf{CH_3CH_2}$(C=O)(NH)$\mathbf{CH_3}$	−4.168(19)	[95]
N-Ethylacetamide	$\mathbf{CH_3}$(C=O)(NH)$\mathbf{CH_2CH_3}$	−4.118(39)	[92]
N,N-Diethyl-	$\mathbf{CH_3CH_2}$(C=O)N$\mathbf{(CH_2CH_3)_2}$	−4.455(55) [a] / [c]	
propionamide		−4.432(34) [b]	

[a] Calculated through diagonalization of the quadrupole tensor with the off-diagonal elements χ_{ab} = 0.243(69), χ_{ac} = 0.544(69), and χ_{bc} = 2.662(69). The estimated uncertainty of the off-diagonal elements is 2x the root mean square difference between calculated and experimental diagonal components. [b] χ_{ab} = 0.057(97), χ_{ac} = 0.1062(97), and χ_{bc} = 0.336(97). [c] This work.

Comparing the χ_{zz} values of amides related to DEPA , we found that (i) χ_{zz} gradually increases from 3.8510(11) MHz in formamide to 4.455(28) MHz in DEPA; (ii) different conformers possess the same χ_{zz} values (within the errors); (iii) χ_{zz} becomes larger with an increase in the +I effect of the alkyl substituents (H− < CH_3− < CH_3CH_2−); and (iv) different molecules with the same alkyl substituents attached to the (C=O)−N frame have essentially the same χ_{zz} values, independent of the place of substitution.

13.5 Conclusion

The microwave spectra from 8.5 to 16.0 GHz of two conformers of N,N-diethylpropionamide showing ^{14}N quadrupole coupling were assigned and fitted using the program XIAM. The standard deviations are within the measurement accuracy of 2 kHz. In both conformers, the propionyl ethyl group is located in (or almost in) the (C=O)N plane, while the other two ethyl groups are tilted out. In the more stable conformer, the latter ethyl groups are oriented in opposite directions, whereas in the other conformer they point in the same direction.

The molecular parameters could be determined with very high accuracy. Calculations at the MP2/6-311++G(d,p) level yielded excellent values for the rotational constants and centrifugal distortion constants. In combination with the B3PW91/6-311+(df,pd) single point EFG calculation and the calibration factor of eQ/h = 4.5586(40) MHz a.u.$^{-1}$, this level of theory results in ^{14}N NQCCs in almost exact agreement with the experimental values. However, energy calculations at this level turn out to be unreliable.

Comparison of the ^{14}N NQCC z-principal axis component χ_{zz} of N,N-diethylpropionamide and related amides indicates that the increasing +I effect of the alkyl substituents at the (C=O)−N frame slightly increase the χ_{zz} value.

Chapter 14

N,N-Dimethylpropionamide - DMPA

The measurements, quantum chemical calculations, spectrum analysis, spectrum assignment, and the fits are the work of R. Kannengießer.

14.1 Introduction

In this chapter the investigations on N,N-dimethylpropionamide (DMPA) are presented. In DMPA both substituents on the nitrogen are methyl groups, and can therefore perform internal rotation.
A related propionamide, the N-methylpropionamide, which contains only one nitrogen-methyl rotor was already investigated by Y. Kawashima et. al. [95]. It was found with an almost planar geometry. The barrier to internal rotation of the nitrogen-methyl group was found to be 80.06487(14) cm^{-1}. Surprisingly, they also succeeded to assign splittings of the internal rotation due to the ethyl-methyl group. The fitted barrier height is with a value of 796(21) cm^{-1} quite high and produced therefore small A-E-splittings. However, this barrier is much lower compared to most other ethyl methyl internal rotations, where barriers > 800 cm^{-1} are calculated. Thus the internal rotation splittings are too small to be observable [11, 55].

14.2 Theoretical

14.2.1 Conformational Preferences

For a conformational analysis, starting geometries were generated by varying the two dihedral angles $\angle(N_1, C_2, C_4, C_7)$ and $\angle(O_3, C_2, N_1, C_{11})$, (for atom numbering see Figure 14.1) over a grid of 60°. Thereby $6^2 = 36$ starting geometries were optimized at the MP2/6-311++G(d,p) level of theory.

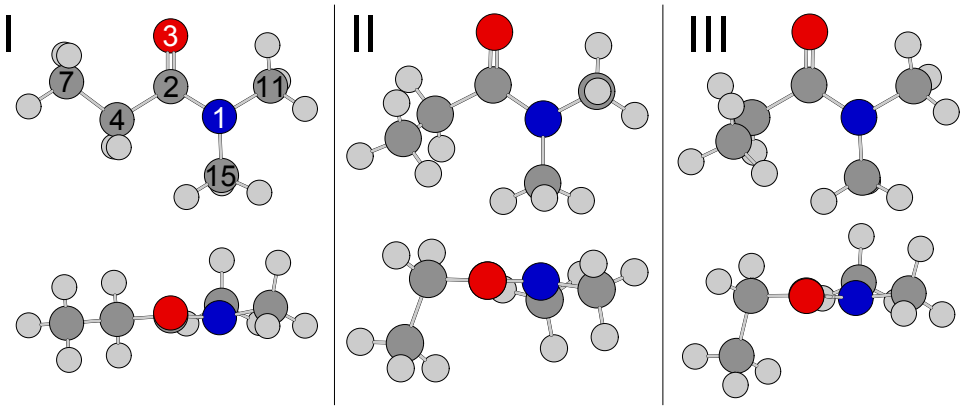

Figure 14.1: Three stable conformers of N,N-dimethylpropionamide calculated at the MP2/6-311++G(d,p) level of theory.

Three stable conformers were found through the optimization calculations. They were confirmed as energy minima by frequency calculations. The rotational constants, dipole moment components, and energies relative to that of the lowest energy conformer are given in Table 14.1.

Table 14.1: Energies in kJ·mol^{-1} relative to the lowest energy conformer with $E_{MP2} = -326.27663$ Hartree, rotational constant in MHz and dipole moment components in Debye.

	E_{MP2}	$E_{MP2+ZPE}$	A	B	C	$\lvert\mu_a\rvert$	$\lvert\mu_b\rvert$	$\lvert\mu_c\rvert$
I	0.00	0.00	4666.0	1838.2	1368.5	1.546	3.695	0.116
II	2.98	3.72	3739.6	2134.8	1536.5	0.122	4.145	0.237
III	3.02	3.53	3680.8	2131.9	1544.1	0.197	4.146	0.361

The lowest energy conformer, conformer I, shows a nearly planar geometry, where the propionyl group lies in the (C=O)N plane, which results in a *c*-dipole moment component of almost zero. The orientation of the propionyl group resembles the one found for the most stable conformers of N,N-diethylpropionamide (subsection 13.2.1), 0PM and 0MM.
In the higher energy conformers of DMPA the propionyl ethyl group is tilted out of the plane to one side of the molecule. These conformers only differ by the orientation of the methyl groups attached to the nitrogen atom. They are about 3 kJ·mol^{-1} higher in energy compared to conformer I. Taking into account the zero-point correction, the energetical order of conformer II and III changes. The corrected relative energies are 3.72 kJ·mol^{-1} and 3.53 kJ·mol^{-1} for conformer II and III, respectively.

14.2.2 Nuclear quadrupole coupling

The quadrupole coupling constants were calculated by EFG single point calculations based on the conformers optimized at the MP2/6-311++G(d,p) level of theory. The results are given in Table 14.2.

Table 14.2: Nuclear quadrupole coupling constants of the three stable conformers of N,N-dimethylacetamide.

	I	II	III
χ_{aa}	2.031	1.702	1.686
χ_{bb}	2.476	2.399	2.181
χ_{cc}	−4.508	−4.101	−3.868
χ_{ab}	−0.049	0.116	−0.159
χ_{ac}	0.275	−1.524	−1.571
χ_{bc}	0.488	−0.169	−1.298

14.2.3 Internal rotation

The internal rotation barriers of all three methyl groups present in DMPA, both nitrogen methyl groups and the propionyl methyl group, were calculated. For the calculation the dihedral angles of the methyl rotation for example $\angle(C_2, C_4, C_7, H_8)$ for the propionyl methyl group were rotated through 360° in steps of 10°. All other than the respective dihedral angle of the methyl rotation were optimized.

Nitrogen methyl rotation

For the calculation on the nitrogen methyl rotations we expected normal threefold potentials with minima at about 40°, 160°, and 280° for the C_{11}-rotation and 80°, 200°, and 320° for the C_{15}-rotation, as these are the angles found for the three hydrogen atoms of the methyl groups in the optimized minimum geometry.
However, the calculations did not deliver the usual threefold potentials, but irregular progressions, with distinct jumps in energy. These jumps can be explained by an influence of the rotation of one nitrogen methyl group on the other one. When one of these methyl groups rotates, the other one, which was not fixed during the calculation, also changes its direction. The results are shown in Figure 14.2.
Due to the coupling of the nitrogen methyl rotors the barrier of the internal rotation of both groups can only be estimated very roughly from Figure 14.2. They are in the order of 200-300 cm^{-1}, whereat the internal rotation barrier of the C_{11}-methyl group appears to be slightly lower compared to the C_{15}-methyl rotation.

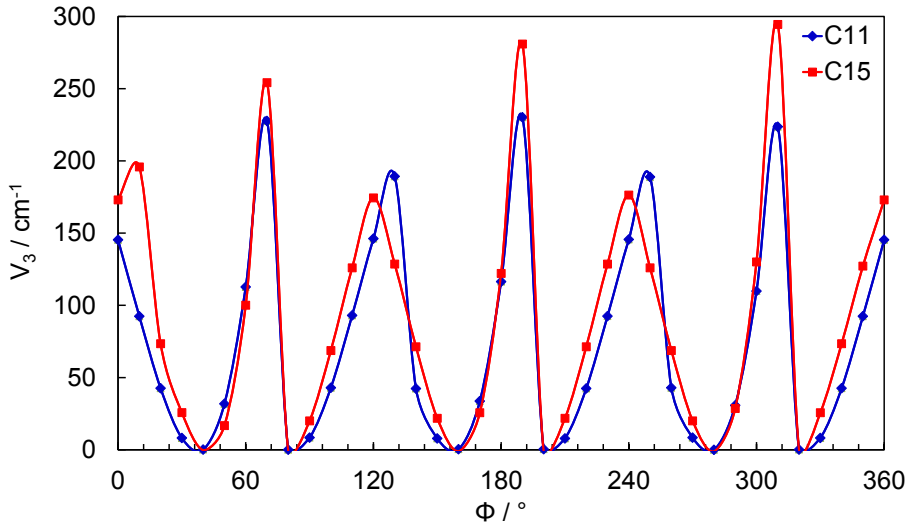

Figure 14.2: Rotation of the nitrogen methyl groups calculated by the rotation of the angles $\angle(C_2, C_1, C_{11}, H_{12})$ and $\angle(C_2, C_1, C_{15}, H_{16})$, respectively.

Additional calculations were carried out, where one methyl group was fixed to its dihedral angle in the minimum geometry, while rotating the other one. Thereby the coupling between the two methyl rotations is suppressed to some extent in the calculation. The results are shown in Figure 14.3.

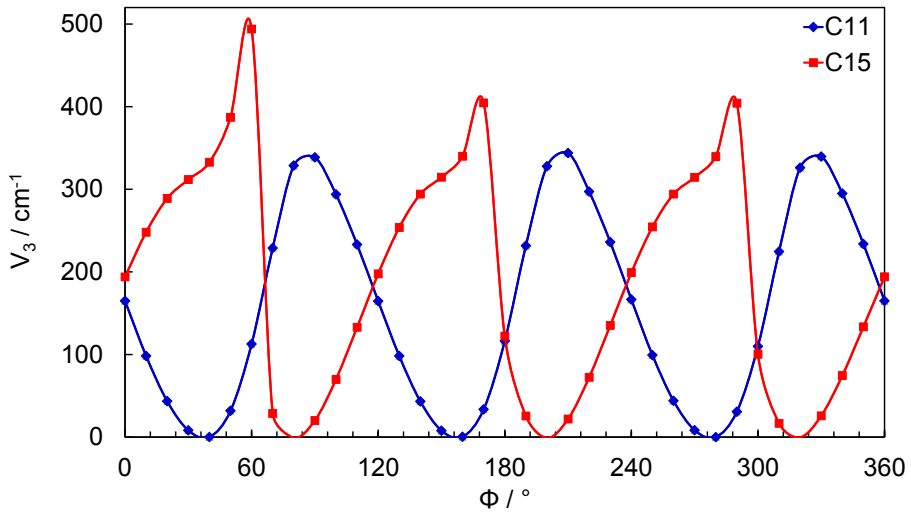

Figure 14.3: Rotation of the nitrogen methyl groups calculated by the rotation of the angles $\angle(C_2, C_1, C_{11}, H_{12})$ or $\angle(C_2, C_1, C_{15}, H_{16})$, respectively, while keeping the other one fixed.

For the C_{11}-rotation an almost symmetric threefold potential was observed, while for the C_{15}-rotation a more distorted potential was calculated. However, the calculated minima are obtained at the expected angles of 40°, 160°, and 280° for the C_{11}-rotation and 80°, 200°, and 320° for the C_{15}-rotation. The obtained barriers are 340 cm^{-1} and 405-495 cm^{-1} for the C_{11}- and the C_{15}-methyl rotation, respectively.

Propionyl methyl rotation

The internal rotation of the propionyl methyl group was calculated in order to estimate the size of the barrier to reason, weather internal rotation splittings of the propionyl methyl rotation will be observable. In the case of N-methylpropionamide the propionyl methyl rotation gave observable splittings in the spectrum. Therefore, a similar situation was at first also assumed for DMPA, where the propionyl methyl rotation could have a barrier of similar order and give therefore internal rotation splittings of similar and, most importantly, observable size.
The calculations delivered a barrier of 1002.5 cm^{-1} at the MP2/6-311++G(d,p) level of theory, which is much higher compared to the experimentally found barrier in N-methylpropionamide of 796(21) cm^{-1}.
The calculated energy curve is shown in Figure 14.4. It shows the usual threefold potential, which is often observed for methyl groups not giving any hint that the

propionyl methyl rotation is influenced or coupled with the methyl rotation of the nitrogen methyl groups.

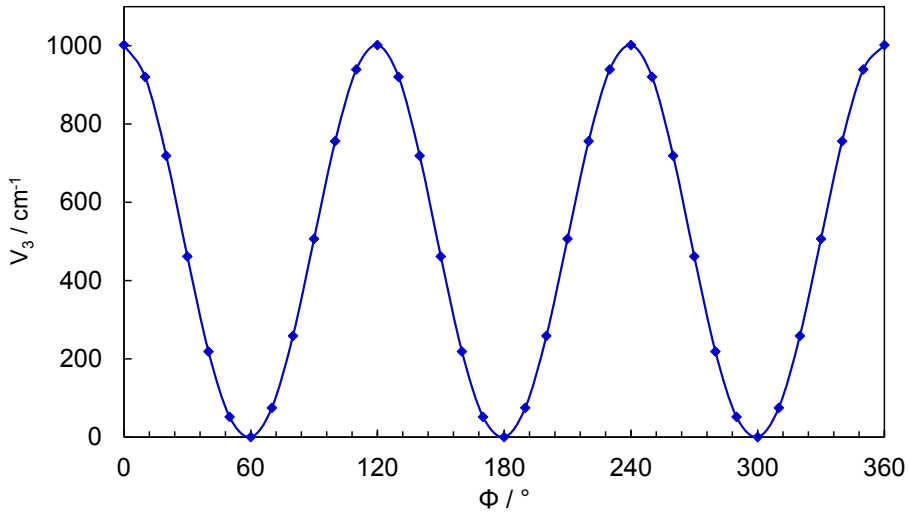

Figure 14.4: Rotation of the propionyl methyl group calculated by the rotation of the angle $\Phi = \angle(C_2, C_4, C_7, H_8)$.

14.3 Experimental

At first, scan measurements were carried out. The scans often showed sets of five lines in adjacency. A typical part of the scan showing these five splittings are given in Figure 14.5.

Closer investigation of these lines with high resolution measurements showed almost the same hyperfine structure for each of these lines, which indicates that they most likely belong to the same rotational transition. Thus the five lines are the five internal rotation species that are typical for systems with two internal rotors. With this a first rough fit could be obtained, where the molecule was treated as a rigid rotor and therefore all internal rotation and quadrupole hyperfine splittings were neglected. With this fit predictions of new lines in the scan range were possible with an accuracy of about 20 MHz. Therefore, small scans of about 50 MHz were carried out around the predicted lines. In total, measurements were carried out in the full range from 9 to 16 GHz.

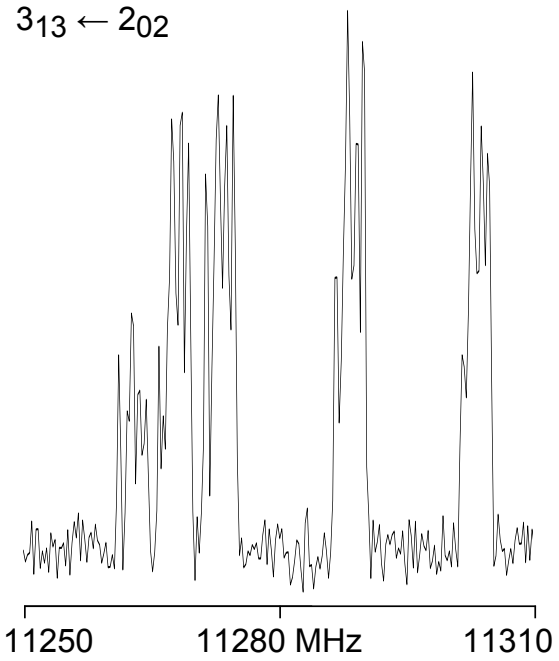

Figure 14.5: Portion of 60 MHz of the broadband scan of N,N-dimethylpropionamide. All five indicated transitions belong to the transition $3_{13} \leftarrow 2_{02}$. The lines are broadened or split because of the quadrupole coupling, arising from the ^{14}N nucleus.

14.3.1 Assignment

In a first step the rigid rotor approach was extended by including the hyperfine splittings. This way a fit of 128 lines including 29 different rotational transitions could be obtained with a standard deviation of 2.8 kHz. The results of the fit are given as *A-species-fit* in Table 14.3. The frequency list can be found in Table G.2.

In the second step we treated the spectrum as a simple one-rotor system, where only the typical splitting into only two species appear. This attempt was carried out for the C_{11}- and the C_{15}- internal rotation independently, giving two separate fits. These fits are also included in Table 14.3 as *C_{11}-fit* and *C_{15}-fit*. They were obtained with standard deviations of 33.0 and 8.2 kHz for the C_{11}- and the C_{15}- rotor, respectively. Even though these are comparably low standard deviations, the fits are not very reliable as only a few splittings could be assigned in both cases so far. Additionally, very high values for the higher order terms D_{pi2J}, D_{pi2K}, and D_{pi2-} were obtained, which leads us to suspect that these terms compensate some miss-assignments. The possibility of miss-assignments is exceptionally high in this case as the two rotors

possess barriers to internal rotation in the same order. Therefore, the splittings of both rotors are quite small and of the same size. Thus, the expected five internal rotation species can easily be confused. Miss-assignments are therefore surely to be expected in the present fits. Unfortunately, they cannot easily be identified and probably also hinder the addition of further transitions to the fit.

In the last step we tried to assign all five symmetry species, which occur for two-top systems in a global fit. This was, however, not successful on a convincing level so far. To make a global fit possible, further measurements are needed. Also it will take a lot of effort to identify present and also to not include further miss-assignments to the fit. However, all attempted fits gave the barriers to internal rotation in the same size as obtained with the separate fits of only one rotor at a time (see Table 14.3).

14.4 Results and Discussion

The assigned *A-species-fit* with a standard deviation of only 2.8 kHz is very reliable, as this is almost within our measurement accuracy, however a few lines show unusual high *obs-calc* deviations. The rotational constants A, B, and C were obtained with the usual high standard deviation. Additionally, all five centrifugal distortion constants D_J, D_{JK}, D_K, d_1, and d_2 could be fitted with a high accuracy, as well as the quadrupole coupling constants χ_{aa} and $\chi_{bb} - \chi_{cc}$.
In the case of the one-rotor-fits not only the standard deviations increase, but also the accuracy of the obtained parameters decreases. The fit of centrifugal distortion constants was only possible for the two constants D_{JK} and D_K in the case of the C_{15}-rotor and not possible at all for the C_{11}-rotor. Thus, the accuracy of the quadrupole coupling constants appeared to be accordingly poor.
However, we believe that the obtained barriers to internal rotation are quite reliable as they were consistent throughout the assignment process.

Table 14.3: Molecular parameters of the three fits carried out for DMPA using the program XIAM.

par.	unit	A-species-fit [a,b]	C_{11}-fit [a,c]	C_{15}-fit [a,d]
A	MHz	4691.961 87(43)	4700.6(28)	4680.0(69)
B	MHz	1826.882 54(22)	1827.87(63)	1844.1(15)
C	MHz	1358.782 56(17)	1358.31(23)	1358.44(53)
D_J	kHz	0.1884(30)		
D_{JK}	kHz	0.720(14)		0.834(60)
D_K	kHz	0.807(45)		0.68(18)
d_1	kHz	−0.0812(24)		
d_2	kHz	−0.0100(17)		
χ_{aa}	MHz	2.0997(15)	2.101(18)	2.0971(26)
$\chi_{bb} - \chi_{cc}$	MHz	7.2533(31)	7.276(39)	7.2433(54)
F_0	GHz		158.0 [e]	158.0 [e]
V_3	cm^{-1}		226.33(53)	137.81(33)
$\angle(i,a)$	°		44.90(45)	72.77(40)
$\angle(i,b)$	°		45.93(44)	19.81(36)
$\angle(i,c)$	°		83.084(55)	80.524(51)
D_{pi2J}	MHz		−0.051(37)	−1.657(71)
D_{pi2K}	MHz		−1.25(31)	3.4(12)
D_{pi2-}	MHz		−0.109(44)	−1.77(17)
σ^f	kHz	2.9	33.0	8.2
N^g		128	67	156

[a] Parameters are given with one standard uncertainty in parentheses. Watson's S reduction and I^r representation were used. [b] Fit of the A-species. [c] Fit including the internal rotation of the C_{11}-rotor. [d] Fit including the internal rotation of the C_{15}-rotor. [e] Fixed. [f] Standard deviation of the fit. [g] Number of lines.

14.5 Conclusion

The microwave spectroscopic measurements of N,N-dimethylpropionamide were carried out in the frequency range from 9 to 16 GHz. Parts of the obtained transitions were thereby measured with high resolution.

The quadrupole hyperfine splittings caused by the ^{14}N nucleus could be fully resolved and assigned. The respective quadrupole coupling constants χ_{aa} and $\chi_{bb} - \chi_{cc}$ could be fitted with high accuracy to values of 2.0997(15) MHz and 7.2533(31) MHz, respectively.

The assignment of the internal rotation of the two nitrogen methyl groups turned out to be quite challenging as the two rotors appear to have similar barriers to internal rotation of 226.33(53) cm^{-1} and 137.81(33) cm^{-1}. A global fit could not be obtained so far.

Chapter 15

N,N-Diethylacetamide - DEAA

Parts of this chapter have already been published in the Journal of Chemical Physics:

R. KANNENGIEßER, S. KLAHM, H.V.L. NGUYEN, A. LÜCHOW, and W. STAHL The Effects of Methyl Internal Rotation and ^{14}N Quadrupole Coupling in the Microwave Spectra of two Conformers of N,N-Diethylacetamide *J. Chem. Phys.*, 2014, **141**, 204308.

The measurements, quantum chemical calculations, spectrum analysis, spectrum assignment, fits, and the manuscript preparation is the work of R. Kannengießer. The coworkers took mostly part in a supporting way especially during corrective work in the publication process. The part on the high level calculations on the internal rotation is the work of A. Lüchow and S. Klahm.

15.1 Introduction

N,N-Diethylacetamide emerges in a condensation reaction between acetic acid and diethyl amine. Many molecules, which have important influence on biological processes in human organisms contain N,N-diethylacetamide as a substructure (see Figure 15.1). For example, entacapone (**1**) is a drug used in the medical treatment

for Parkinson's disease, which operates as an enzyme (catechol-O-methyl transferase (COMT)) inhibitor [96]. D-lysergic acid diethylamide (LSD) (**2**) is a well-known illegal drug and a very strong hallucinogen [97]. N–glycine-sulfonamide (**3**) acts as a potent and selective receptor antagonist for the neuropeptides orexin 1 and orexin 2, which play an important role in the regulation of the sleep-wake cycle [98]. The structure and dynamics of N,N-diethylacetamide can thus reveal a part of the structures of larger biological molecules.

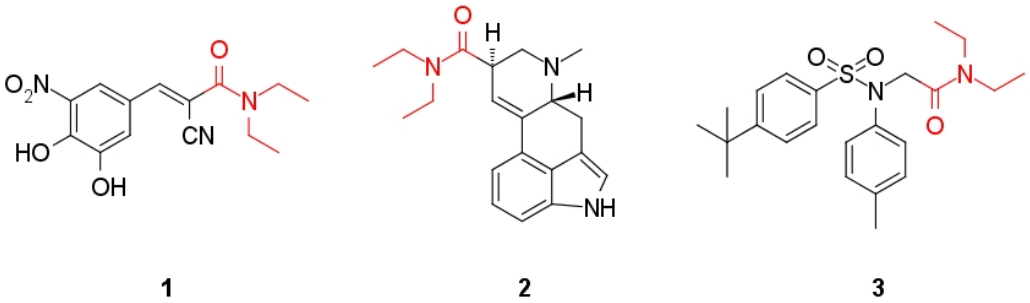

Figure 15.1: Examples of biological molecules containing N,N-diethylacetamide as a substructure. (**1**) Entacapone, (**2**) LSD (D-lysergic acid diethylamide), and (**3**) 2-[(4-tert-butyl-benzene-sulfonyl)-p-tolyl-amino]-N,N-diethylacetamide.

In N,N-dimethylacetamide, the V_3 potential of the acetyl methyl group was found to be 677 cm^{-1} [88]. Since it is a closely related molecule of N,N-diethylacetamide, we expect the V_3 potential of N,N-diethylacetamide to be similar. The splittings due to internal rotation are thus estimated to be in the order of a few hundreds of kHz. Since the determination of the V_3 potentials in N,N-dimethylacetamide was stated to be ambiguous, some higher level theoretical calculations were carried out for N,N-diethylacetamide, in particular Diffusion Quantum Monte Carlo (DMC) and Coupled Cluster (CC) calculations by S. Klahm and A. Lüchow. The V_3 potentials of the two ethyl methyl groups are expected to be higher than 1000 cm^{-1} and cannot be resolved in the microwave spectrum, similar to the case of triethyl amine [55].
In many previous studies on nitrogen containing molecules carried out in Aachen such as diethyl amine [56], triethyl amine [55], quinuclidine [99], and morpholine [100], hyperfine splittings in the order of 0.5–1.0 MHz were observed due to the electric quadrupole moment of the ^{14}N nucleus. Therefore, we expected hyperfine splittings in the order of a few hundreds of kHz for N,N-diethylacetamide, which are in the same order of magnitude as the internal rotation fine splittings of the acetyl methyl group.

15.2 Quantum Chemical Calculations

15.2.1 Conformational Analysis

The conformational analysis was carried out at the second order Møller-Plesset perturbation theory and the basis set 6-311++G(d,p). Despite the problems in the calculation of the energetical order of the conformers of DEPA (subsection 13.2.1), this level of theory was chosen because it yielded reasonable rotational constants in many previous studies in the spectroscopic community [101, 102, 103, 104]. The starting geometries were defined by varying three dihedral angles $\phi_1 = \angle(C_4, C_2, N_1, C_8)$, $\phi_2 = \angle(C_2, N_1, C_8, C_{11})$, and $\phi_3 = \angle(C_2, N_1, C_{15}, C_{18})$ in a step width of 60° (for atom numbers see Figure 15.2). Due to the planarity of the acetyl group ($C_4-(C_2 = O_3)$), only a rotation of ϕ_1 to 0°, 60°, and 120° was necessary, whereby $3\times6\times6 = 108$ starting geometries were created. The rotation of ϕ_1 to −60°, −120°, and 180° was omitted because it would lead to enantiomers, which cannot be distinguished with our experimental method.

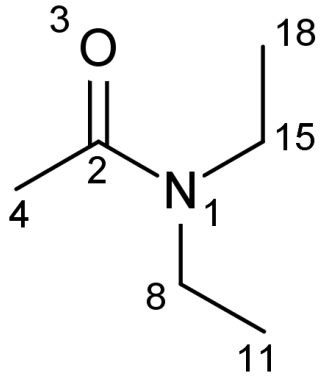

Figure 15.2: N,N-diethylacetamide. Only the heavy atoms are numbered.

From the 108 starting geometries five stationary points on the potential energy surface could be found. Frequency calculations were carried out and yielded no imaginary frequencies, i.e., the optimized geometries are located in real energetic minima. The energies relative to the most stable conformer (conformer I) are indicated in Figure 15.3. Energy values, rotational constants, and dipole moment components of all conformers are summarized in Table 15.1.

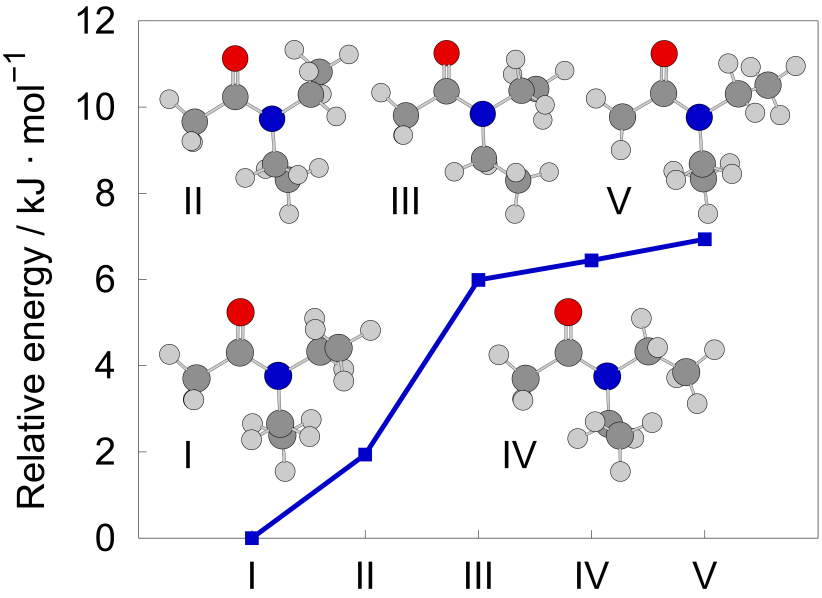

Figure 15.3: Five stable conformers of N,N-diethylacetamide (named according to their order in energy) calculated at the MP2/6-311++G(d,p) level of theory. The energy values are relative to the most stable conformer I (−365.4789 Hartree). All conformers have C_1 symmetry and exist as enantiomeric pairs. For each conformer, only one enantiomer is indicated.

Table 15.1: Energy values, rotational constants, and dipole moment components of the stable conformers of N,N-diethylacetamide calculated at the MP2/6-311++G(d,p) level of theory. Relative energies are given in kJ·mol^{-1}, rotational constants A, B, C are given in GHz, and dipole moment components are given in D.

	$E_{rel.}$	A	B	C	$\lvert\mu_a\rvert$	$\lvert\mu_b\rvert$	$\lvert\mu_c\rvert$
I	0.0	2.072	1.939	1.159	3.489	2.134	1.465
II	1.9	2.207	1.915	1.188	3.024	3.037	0.491
III	6.0	2.404	1.727	1.145	2.997	2.784	1.109
IV	6.4	2.461	1.674	1.155	2.193	3.423	1.259
V	6.9	2.178	1.946	1.216	1.096	4.041	0.936

Conformer I (shown in Figure 15.4) is calculated to be the most stable conformer and expected to be observed in the microwave spectrum under molecular beam conditions. Conformer II is 1.9 kJ·mol^{-1} higher in energy and might therefore also be present in the spectrum.

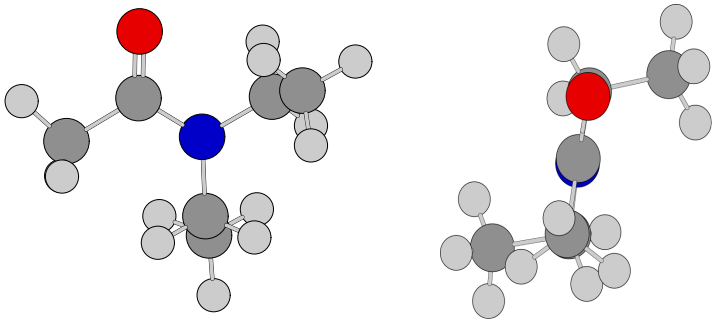

Figure 15.4: The optimized geometry of conformer I of N,N-diethylacetamide calculated at the MP2/6-311++G(d,p) level of theory (left: front view and right: side view). The two ethyl groups are tilted out of the $N-C=O$ plane against each other by the same angle of approximately 110°.

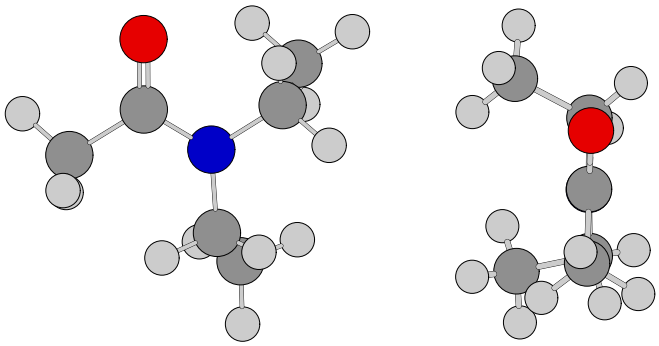

Figure 15.5: The optimized geometry of conformer II of N,N-diethylacetamide calculated at the MP2/6-311++G(d,p) level of theory (left: front view and right: side view). The two ethyl groups are tilted out of the $N-C=O$ plane in the same direction.

In conformer I and II, all heavy atoms except C_{11} and C_{18} of the ethyl groups are almost located in a plane. In Conformer I the two ethyl groups are tilted out of this plane against each other in the same manner as in the lowest energy conformer 0PM of N,N-diethylpropionamide. The ethyl groups are tilted out by the same angle of approximately 110°. Whereas in conformer II the ethyl groups are tilted out in the same direction as presented in Figure 15.5. This orientation of the ethyl group correlates with the one in conformer 0MM of N,N-diethylpropionamide. The Cartesian coordinates of conformer I and II in the principal axis system are available in Table H.1 in the Appendix H.

In Table H.2, energy values and rotational constants optimized at different levels of theory are given for conformer I. Conformer III, IV, and V are about 6 kJ·mol^{-1} higher in energy. From our experience, they cannot be observed under our molecular beam conditions. In these conformers, the C_8 and C_{15} atoms are out of the $C_4 - (C_2 = O_3) - N_1$ plane.

15.2.2 Nuclear quadrupole coupling

At first we carried out EFG calculations at the B3PW91/6-311+G(d,p)//MP2/6-311+G(df,pd) level of theory using the calibration factor of eQ/h of 4.5617(43) MHz/a.u., as by the time of the first assignment, this was the current calculation method and calibration value. The calculations yielded quadrupole coupling constants which are in almost exact agreement with the experimental values (Table 15.2).

Table 15.2: The calculated quadrupole coupling constants χ_{aa} and $\chi_{bb} - \chi_{cc}$ as well as their deviations from the experimental values (expt.) (in MHz) of the ^{14}N nucleus in N,N-diethylacetamide. The electric field gradient was calculated at the B3PW91/6-311+G(d,p) level of theory based on structures optimized with the MP2 method and different basis sets. Values are given with one standard uncertainty in parentheses.

	χ_{aa}	$\Delta\chi_{aa}$	$\chi_{bb} - \chi_{cc}$	$\Delta(\chi_{bb} - \chi_{cc})$
Conf. I / expt.	1.06868(58)		5.07830(82)	
6-311++G(d,p)	1.1121	0.0434	5.2096	0.1313
6-311++G(df,pd)	1.1090	0.0403	5.1727	0.0944
6-311+G(d,p)	1.1199	0.0512	5.2076	0.1293
6-311+G(df,pd)	1.1139	0.0452	5.1704	0.0921
Conf. II / expt.	1.49797(61)		6.2522(11)	
6-311++G(d,p)	1.5923	0.0943	6.3038	0.0516
6-311++G(df,pd)	1.5821	0.0841	6.2707	0.0185
6-311+G(d,p)	1.5964	0.0984	6.3031	0.0509
6-311+G(df,pd)	1.5843	0.0863	6.2694	0.0172

15.2.3 Internal rotation

The barriers to internal rotation of the acetyl methyl group of conformer I and II were determined by standard B3LYP and MP2 as well as highly accurate CCSD(T) and DMC methods by S. Klahm. To calculate the rotational barrier, the methyl group was rotated out of the equilibrium geometry while the rest of the molecule was free in relaxation. The molecular geometries for the DMC single point calculations were obtained at the B3LYP/aug-cpVTZ level of theory. All geometry optimizations were performed with the program GAUSSIAN.

For the DMC calculations, a Slater-Jastrow ansatz was used,

$$\Psi = e^{U}\Phi_{SD} \tag{15.1}$$

where Φ_{SD} is a single Slater determinant and U is a correlation function first used by Schmidt and Moskowitz [105] that includes electron-electron, electron-nucleus, and electron-electron-nucleus terms. The Slater determinant was composed of Kohn-Sham orbitals generated with a B3LYP/cc-pVTZ single point calculation. All B3LYP, MP2, and CC single point calculations were also carried out with the program GAUSSIAN. For the sake of clarity, the calculation level is given in the form *single point calculation level // geometry optimization level.*
The parameters of the correlation factor U were optimized with respect to the energy [106]. The DMC energies are extrapolated to zero time step in the fixed node approximation [107]. The DMC calculations were carried out with the program AMOLQC [108]. For B3LYP and MP2, an extrapolation of the energy to the complete basis set (CBS) was performed using Eq. (2) of Ref. [109] and cc-pVXZ basis sets up to $X = 5$. All energies are stationary points of the potential energy surface. Transition states of the methyl rotation were confirmed with frequency analyses.
Recent investigations on a similar level of theory showed for a series of smaller molecules that the current approach leads to agreement with experimental data within about 0.5 kJ·mol^{-1} [110], which is the reason why it was chosen by S. Klahm for the present investigation on DEAA. The results for the B3LYP, MP2, CCSD(T), and DMC calculations are given in Table 15.3.

Table 15.3: B3LYP, MP2, CC, and DMC rotational barriers for conformers I and II in kJ·mol^{-1}. Values are given with one standard uncertainty in parentheses.

	Conf. I	Conf. II
B3LYP/cc-pVTZ//B3LYP/cc-pVTZ	4.0	
B3LYP/aug-cc-pVTZ//B3LYP/aug-cc-pVTZ	4.0	4.4
B3LYP/CBS//B3LYP/cc-pVTZ	3.9	
MP2/cc-pVTZ//MP2/cc-pVTZ	4.5	
MP2/aug-cc-pVTZ//MP2/aug-cc-pVTZ	4.6	
MP2/CBS//MP2/cc-pVTZ	4.4	
CCSD(T)/cc-pVTZ//B3LYP/aug-cc-pVTZ	4.6	5.1
CCSD(T)/cc-pVTZ//MP2/aug-cc-pVTZ	4.5	
DMC//B3LYP/aug-cc-pVTZ	4.4(4)	

15.3 Experimental

At the beginning, a broadband scan was carried out in the frequency range from 9 to 15 GHz. A part of the scan is shown in Figure 15.6. In total, 75 molecular signals

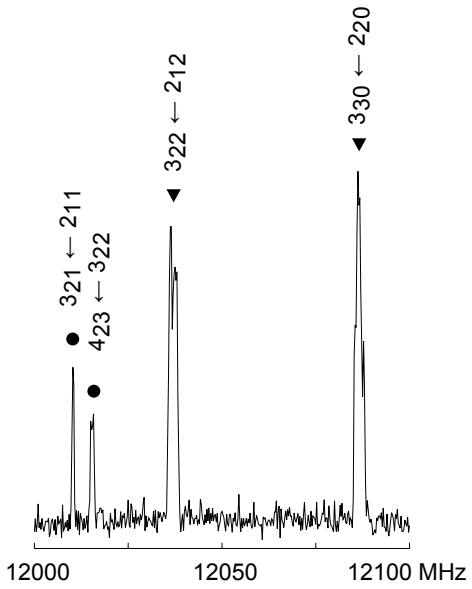

Figure 15.6: A broadband scan of N,N-diethylacetamide in the frequency range-from 12000 to 12100 MHz. The transitions of conformer I are marked with triangles and those of conformer II by circles. Additional splittings arise from the quadrupole coupling of the ^{14}N nucleus.

could be observed in this region. Almost all of them already appeared as multiplets in the scan mode due to the quadrupole splittings of the ^{14}N nucleus.

Figure 15.6 show lines assigned to two different conformers, whereby one conformer, which is therefore probably the lowest energy conformer, shows comparably larger intensities.

With high resolution measurements multiplets were found which contain an excessively high number of splittings in a comparably small frequency range. This is due to the fact that these splittings are caused by three different effects: the fine splittings from internal rotation of the acetyl methyl group, the quadrupole hyperfine splittings, and splittings due to the Doppler effect. A typical spectrum in the high resolution mode is illustrated in Figure 15.7.
Internal rotation splittings in this order of magnitude appear for internal rotors with high barriers, which gives a good hint for the assignment process.

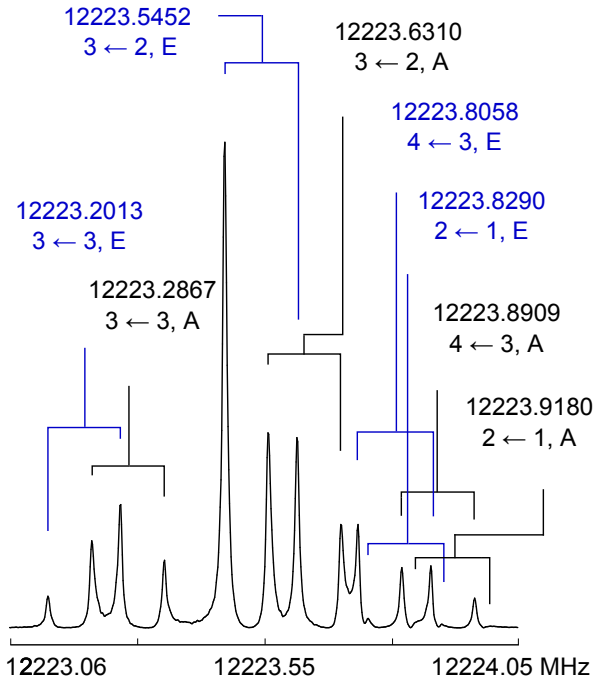

Figure 15.7: The torsional and quadrupole components of the $3_{31} \leftarrow 2_{21}$ transition of conformer I of N,N-diethylacetamide. The experimental resolution is 2 kHz. Doppler doublets are marked by brackets. The A species is indicated in black and the E species in blue. The hyperfine transitions are given by F' ← F. For this spectrum, 800 decays were co-added.

15.3.1 Conformer I

The assignment was carried out in three steps. As a first step, the internal rotation and quadrupole coupling effects were neglected and the molecule was treated as a rigid rotor. Using the A, B, and C rotational constants calculated at the MP2/6-311++G(d,p) level of theory (see subsection 15.2.1), a first prediction was made using the program XIAM.

The predicted spectrum showed characteristic patterns which could be recognized from the spectrum in the scan mode. These lines enabled the initial assignment and fit. The rotational constants were improved and further a-, b-, and c-type transitions could be assigned. The calculated dipole moment in c-direction is smaller than those in a- and b- direction (see Table 15.1). Accordingly, only five c-type transitions with small J quantum numbers, which showed considerably lower intensities, could be measured. In total, the rigid-rotor fit included 47 transitions with a standard deviation of 450 kHz.

In a second step, the rigid rotor model was extended by adding the quadrupole coupling effect. We began with this effect as, from our experience, the quadrupole coupling constants can be calculated almost exactly with EFG calculations using Bailey's method (see subsection 15.2.2). Using the calculated quadrupole coupling constants at the B3PW91/6-311+G(d,p)//MP2/6-311++G(d,p) level of theory (see Table 15.2), reasonable predictions of the hyperfine structures were carried out, which enabled the assignment of some hyperfine transitions of the $J = 3 \leftarrow 2$ R-branches. Afterwards, hyperfine components of all transitions in the rigid rotor fit could be included.

In the last step of the analysis, the internal rotation of the acetyl methyl group was taken into account. The initial value of the V_3 potential to internal rotation was set to 600 cm^{-1}, which is approximately the value of 677 cm^{-1} found in N,N-dimethylacetamide. The polar coordinates of the internal rotor axis in the principal axis system, δ and ϵ, were calculated from the optimized geometry obtained from quantum chemical calculations at the MP2/6-311++G(d,p) level of theory. δ is the angle between the internal rotation axis and the a-axis and ϵ is the angle between the b-axis and the projection of the internal rotation axis onto the bc-plane.

A reliable and unambiguous assignment of the quadrupole hyperfine and internal rotation fine structure was difficult because both effects cause splittings in the same

order of a few tens to a few hundreds of kHz. The starting values played a significant role and an analysis of the splitting pattern had to be carried out very carefully. It should be mentioned that the hyperfine pattern appears twice in the spectrum, once for the A and once for the E species. Also the same A-E splittings appear for each transition in the quadrupole hyperfine structure, as shown in Figure 15.8. However this is only the case for DEAA as both effect are small in this case and do not influence each other. This has not always to be the case, especially when dealing with small internal rotation barriers. Here, the same A-E splitting of about 90 kHz can be found for the transitions $F' \leftarrow F$: $3 \leftarrow 3$, $3 \leftarrow 2$, $4 \leftarrow 3$, $2 \leftarrow 1$, and $2 \leftarrow 2$. Finally, 345 torsional and hyperfine components could be assigned for conformer I and fitted using 12 molecular parameters to a standard deviation of 1.4 kHz. All fitted parameters are given in Table 15.4 . A list of all frequencies along with the residuals are available in Table H.3.

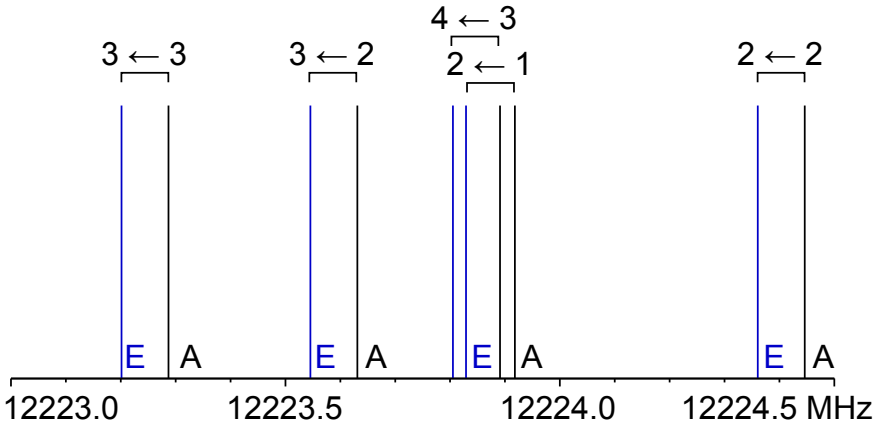

Figure 15.8: The stick spectrum of the $3_{31} \leftarrow 2_{21}$ transition of conformer I of N,N-diethylacetamide. The same A-E splitting of about 90 kHz can be found for all hyperfine components F' ← F and are marked with brackets. For the A species (black) and the E species (blue) the same hyperfine structure was found.

15.3.2 Conformer II

After conformer I was assigned, a number of lines with significantly lower intensity remained in the scan, which belong to conformer II (1.9 kJ·mol^{-1} higher in energy, see subsection 15.2.1). The assignment process followed the three steps carried out

for conformer I. At first, four transitions $5_{14} \leftarrow 4_{13}$, $5_{24} \leftarrow 4_{23}$, $5_{14} \leftarrow 4_{23}$, and $5_{24} \leftarrow 4_{13}$, which form a closed loop, were recognized in the spectrum. Afterwards, all remaining lines in the scan could be assigned to 29 rigid rotor transitions of conformer II. In total, 247 torsional and hyperfine components were assigned for conformer II and fitted using 13 molecular parameters to a standard deviation of 1.6 kHz. The frequency list of all fitted transitions are available in Table H.4.

15.4 Results and Discussion

Using the program XIAM, 345 torsional and hyperfine components of conformer I and 247 components of conformer II of N,N-diethylacetamide were fitted by floating the rotational constants A, B, C, the centrifugal distortion constants D_J, D_{JK}, D_K, d_1, d_2, the V_3 potential, the polar coordinates of the internal rotation axis in the principal axis system δ and ϵ, and the quadrupole coupling constants χ_{aa} and $\chi_{bb} - \chi_{cc}$. The angles between the acetyl methyl group and the principal axes were derived from δ and ϵ. The moment of inertia I_α was kept fixed to 3.2 $u\text{Å}^2$, corresponding to F_0 = 158 GHz, a value often found for methyl groups. Since only torsional ground state transitions were measured, floating I_α led to a strong correlation with V_3. The spectrum could be reproduced within the experimental resolution with a standard deviation of 1.4 kHz and 1.6 kHz for conformer I and II, respectively.

The experimental rotational constants are in reasonable agreement with the values from quantum chemical calculations at different levels of theory (Table H.2). Calculations at the MP2/6-31++G(d,p) level of theory yielded the most accurate rotational constants with deviations of 4 MHz, −7 MHz, and 1 MHz for the A, B, and C rotational constant, respectively. Also calculations at the MP2/6-31+G(d,p) and MP2/6-311++G(d,p) level of theory revealed rotational constants in a similar quality. A better agreement cannot be expected, as results from quantum chemical calculations refer to the equilibrium structure, whereas the experimental data yield rotational constants for the ground vibrational state and no corrections have been made. This accuracy is in good agreement with the calculations carried out for other molecules of similar size like linalool [74] and ethyl methyl ketone [77].

The comparison of the calculated torsional barriers of the acetyl methyl group for conformer I showed a clear agreement at all different levels of theory. The MP2,

Table 15.4: Rotational and torsional parameters from the program XIAM (obs) compared to parameters calculated at the MP2/6-311++G(d,p) level of theory (calc) for the observed conformers of N,N-diethylacetamide.

		Conformer I		Conformer II	
	Unit	obs [a]	calc	obs [a]	calc
A	MHz	2065.943 25(15)	2072	2181.252 31(20)	2207
B	MHz	1946.434 197(70)	1939	1933.673 393(99)	1915
C	MHz	1157.141 719(42)	1159	1191.944 060(91)	1188
D_J	kHz	0.3344(16)		0.8942(32)	
D_{JK}	kHz	0.0 [b]		−3.201(12)	
D_K	kHz	1.1214(90)		4.231(15)	
d_1	kHz	−0.1646(10)		−0.2884(19)	
d_2	kHz	−0.031 49(30)		0.0535(12)	
χ_{aa}	MHz	1.068 68(58)	1.1121	1.497 97(61)	1.5923
$\chi_{bb} - \chi_{cc}$	MHz	5.078 30(82)	5.2096	6.2522(11)	6.3038
F_0	GHz	158.0 [b]		158.0 [b]	
V_3	cm^{-1}	517.04(13)		619.48(91)	
	$kJ{\cdot}mol^{-1}$	6.1852(15)	6.1 [d]	7.411(11)	6.8[c]
I_α	u^2	3.2 [c]		3.2 [c]	
$\angle(i,a)$	deg	44.446(91)	48.07	60.58(48)	67.73
$\angle(i,b)$	deg	50.634(99)	49.25	32.45(49)	25.57
$\angle(i,c)$	deg	72.740(69)	69.1	77.53(20)	78.07
σ	kHz	1.4		1.6	
$N_A/N_E/N$ [e]		43/43/345		25/28/247	

[a] Parameters are given with one standard uncertainty in parentheses. Watson's S reduction and I^r representation were used. [b] Fixed value. [c]Derived parameter. [d] Rigid rotor approach. [e] Number of A-species, E-species, and total number of lines.

CCSD(T), and DMC methods led to almost the same results, while DFT calculations produced slightly lower barriers. Because of the consistency of all results for conformer I, the calculations for conformer II were restricted to B3LYP and CCSD(T) calculations, where we expected the CCSD(T) result to be more reliable than the result obtained by B3LYP. The experimental V_3 potential was fitted to 517.04(13) cm^{-1} (6.1852(15) $kJ{\cdot}mol^{-1}$) and 619.48(91) cm^{-1} (7.411(11) $kJ{\cdot}mol^{-1}$) for conformer I and II, respectively.

Comparing the experimental V_3 values with the calculated rotational barriers, one can state significant differences of more than 2 $kJ{\cdot}mol^{-1}$, which cannot be explained with limitations of the electronic structure calculations. The diffuse functions in the basis set and the extrapolation to the CBS show no effect on the barrier. Due to

the agreement of the DMC, MP2, and CCSD(T) results, no effect of higher order excitations is expected and, finally, the T_1 diagnostics [111] confirms the lack of statical correlation.
We assume that the difference between the calculated barrier and the experimental V_3 value is due to the fact that a rigid rotor model for internal rotation is used in the fit of the microwave data whereas the calculated barrier is obtained from full geometry relaxation. To test this conjecture, we repeated the CCSD(T)/cc-pVTZ//B3LYP/aug-cc-pVTZ calculations with a fixed methyl rotor. For this purpose, all C−H and C−C bonds, C−C−H angles, as well as all H−C−C−H dihedral angles of the methyl group were averaged using the geometries of the minimum and the transition state of the rotation.
Freezing the constructed methyl rotors, the geometry of the potential energetic minimum and the transition state were optimized. For the fixed methyl group, the barriers of conformer I and II change to 6.1 kJ·mol^{-1} and 6.8 kJ·mol^{-1}, respectively. Taking only the geometries of the energetic minima or of the transition states as basis for the construction of the rigid rotors, the rotational barriers change by less than 0.05 kJ·mol^{-1}. The calculated rotational barrier and the experimental V_3 potential differ by 0.1 kJ·mol^{-1} and 0.6 kJ·mol^{-1} for conformer I and II, respectively.

For comparison, the same procedure was carried out for acetaldehyde and acetylfluoride, where excellent agreement with experimental data using relaxed methyl rotors was observed [110]. The introduction of rigid rotors for these systems did not change the methyl rotational barriers. The influence of a geometrically fixed methyl rotor seems to be compound specific and leads to good agreements between the calculated rotational barrier and experimental V_3 potential.

The experimental V_3 potential of conformer II matches the V_3 potential of 677 cm^{-1} found for N,N-dimethylacetamide. In Ref. [88], an unambiguous determination of the V_3 potential of the acetyl methyl group could not be made and two possible values, 677 cm^{-1} and 238 cm^{-1}, were given. The potential of 677 cm^{-1} was only supported by comparing with the results from quantum chemical calculations performed at the MP2/6-31G(d,p) level of theory. Our study on N,N-diethylacetamide strongly confirms the assignment for the V_3 potential of the acetyl methyl group in Ref. [88].

From our experience, the V_3 potential of the acetyl methyl group is almost exactly the same for the three conformers of n–butyl acetate [12] and the two conformers of n-pentyl acetate [81]. Therefore, we expected the same V_3 potential for the two

conformers of N,N-diethylacetamide. Contrary to our expectation, the acetyl methyl V_3 potentials of conformer I and II differ by approximately 100 cm^{-1}. However, the acetyl methyl V_3 potentials in acetamides often depends strongly on the substitutions at the other side of the amide bond and can vary in a very wide range from 24 cm^{-1} like in the case of acetamide up to 677 cm^{-1} like in N,N-dimethylacetamide. Significant changes in the V_3 potential could also be found, even when the hydrogen atoms in the amide group are only substituted by deuterium [112]. Therefore, it is not surprising that the V_3 potential also depends on the configuration of the substituents attached to the nitrogen atom.

The experimental angles between the internal rotor axis and the principal axes of conformer I and II differ by a few degrees from the calculated values optimized at the MP2/6-311++G(d,p) level of theory. The $\angle(i,b)$ angle of conformer I and the $\angle(i,c)$ angle of conformer II are in a good agreement with the experimental values. The differences of the other angles of about 4° and 7° for conformer I and II, respectively, are quite high comparing with other studies on internal rotation [12, 69, 76]. However, fixing the values of the internal rotation angles in the fits to theoretical values yielded only minor differences and comparable standard deviations, which means that the fits are not extremely sensitive to these parameters.

The quadrupole coupling constants χ_{aa} and $\chi_{bb} - \chi_{cc}$ could be fitted with very high accuracy. The calculated values match the experimental ones almost exactly. The best results were obtained at the B3PW91/6-311+G(d,p)//MP2/6-311++G(df,pd) and B3PW91/6-311+G(d,p)//MP2/6-311+G(df,pd) level of theory for both conformers.

15.5 Conclusion

Using a MB-FTMW spectrometer in the frequency range from 2 to 26.5 GHz, the torsional fine structure and the quadrupole hyperfine structure in the rotational spectra of two conformers of N,N-diethylacetamide could be fully resolved and analyzed in a global fit with the program XIAM. The spectra could be reproduced within our experimental resolution using 12 fitted parameters for 345 lines with a ratio of 29 lines/parameter for conformer I and 13 fitted parameters for 247 lines with a ratio of 19 lines/parameter for conformer II. The spectroscopic work was

supplemented by quantum chemical calculations.
The acetyl methyl group undergoes internal rotation with a V_3 potential of 517.04(13) cm^{-1} and 619.48(91) cm^{-1} for conformer I and II, respectively. The DMC and CC calculations for the relaxed rotor indicated a methyl rotational barrier which is about 2 $kJ \cdot mol^{-1}$ lower than the experimental V_3 value, whereas the rigid rotor modification showed a very good agreement of 0.1 $kJ \cdot mol^{-1}$ and 0.6 $kJ \cdot mol^{-1}$ for conformer I and II, respectively.
The quadrupole coupling constants of the ^{14}N nucleus were determined with very high accuracy. EFG calculations with Bailey's method could calculate the coupling constants almost exactly to the experimental values.

Chapter 16

N-Methyldiacetamide - MDAA

The measurements, quantum chemical calculations, spectrum analysis, spectrum assignment, and the fits are the work of R. Kannengießer. K. Eibl helped with the measurements, quantum chemical calculations, assignment and fits of this molecule.

16.1 Introduction

In this chapter the results from investigations on the three rotor molecule, N-methyldiacetamide (MDAA) are shown. MDAA contains two acetyl methyl rotors and one methyl rotor attached to the nitrogen atom.
This leads us to ask the following questions:

(i) How many rotors are resolvable?
(ii) Will there be a conformer with equivalent acetyl methyl rotors?
(iii) Will the acetyl methyl rotors have the same barrier height even though they are not equivalent?

N-Methyldiacetamide is, as far as we know, the only molecule with two acetyl groups, which was investigated so far. As it is a tertiary amide we expect the barriers of these acetyl groups to be in the order of 600 cm^{-1} to 750 cm^{-1}.

16.2 Theoretical

16.2.1 Potential energy surface

For the conformational analysis of MDAA the geometry was optimized, whereby the two dihedral angles $\varphi_1 = \angle(C_4, C_2, N_1, C_{14})$ and $\varphi_2 = \angle(C_{10} - C_8 - N_1 - C_{14})$ (for atom numbers see Figure 16.1) were fixed to certain values between -180 and 180 degrees in a step width of 10 degrees. The optimization was carried out with the program GAUSSIAN at the MP2/6-311++G(d,p) level of theory. The resulting energy values calculated with respect to φ_1 and φ_2 are illustrated in Figure 16.2. For this we parameterized the calculated energies using a two-dimensional Fourier expansion. The corresponding coefficients are available in Table I.1. Figure 16.2 shows the local minima on the energy surface indicated through the optimized conformers I, II and III. These conformers were freely optimized, without freezing φ_1 and φ_2, and were afterwards confirmed as minimum geometries through frequency calculations. The nuclear coordinates of these conformers are given in Table I.2 and Table I.3.

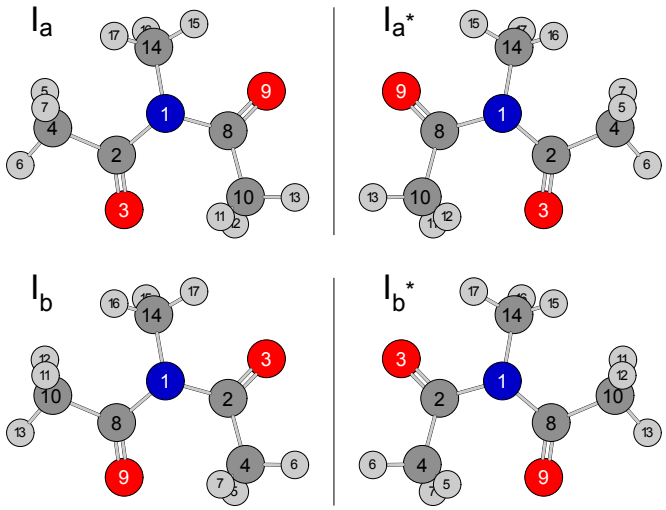

Figure 16.1: Optimized Geometries of the lowest energy conformer of MDAA calculated at the MP2/6-311++G(d,p) level of theory. Enantiomeric geometries are indicated through asterisks.

All conformers are nearly planar and appear as enantiomeric pairs, where the enantiomer is indicated through an asterisk. Additionally, for the conformers I and III two different versions could be optimized, which are indicated through the indices a and b. The index a marks the first version of the conformer, whereas the index

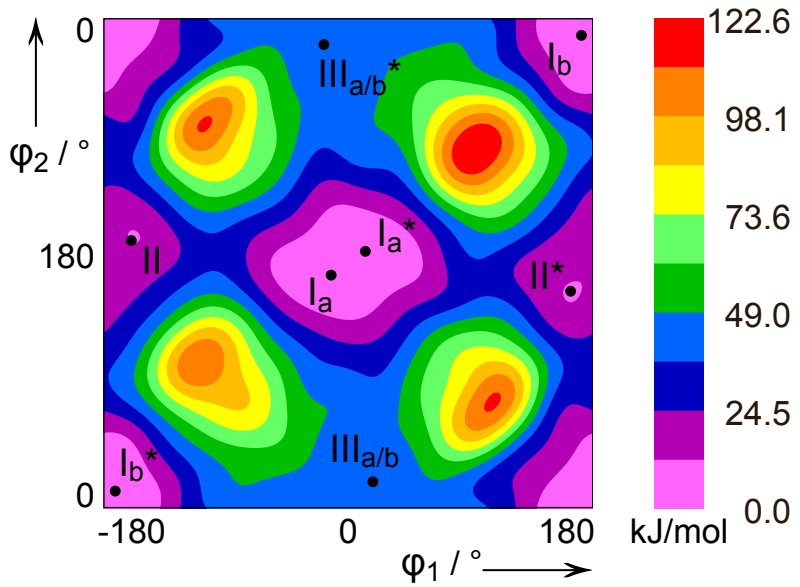

Figure 16.2: Potential energy surface of MDAA with respect to the orientation of the two acetyl groups $\varphi_1 = \angle(C_4, C_2, N_1, C_{14})$ and $\varphi_2 = \angle(C_{10}, C_8, N_1, C_{14})$ calculated at the MP2/6-311++G(d,p) level of theory. The energy values relative to the global minimum (conformer I: $E_{MP2} = -400.181632$ Hartree) are colorcoded.

b marks the second version, where the two structurally identical acetyl groups are exchanged.

Thereby conformer I could be found in four different versions, I_a, I_a*, I_b and I_b* on the energy surface. The respective geometries are shown in Figure 16.1. From a microwave spectroscopic point of view these four versions of conformer I are identical, as they possess the same rotational constants. In Table 16.1 the rotational constants of all three stable conformers are given, in addition to the relative energy values and the dipole moment components. All values refer to the principal axis system.

Conformer I is the lowest energy conformer and therefore most likely to be found in the spectrum. The conformers II and III on the other hand show much higher energies of 11.3 kJ·mol^{-1} and 35.2 kJ·mol^{-1}. Conformers with such high energies usually cannot be measured under our molecular beam conditions. Thus, all measured lines are considered to belong to conformer I.

Table 16.1: Relative MP2-energies in kJ·mol^{-1}, rotational constants in MHz and dipole moment components in D of the five stationary points of N-methyldiacetamide calculated at the MP2/6-311++G(d,p) level of theory. All values refer to the principal axis system.

	$E_{rel.}$	A	B	C	$\lvert\mu_a\rvert$	$\lvert\mu_b\rvert$	$\lvert\mu_c\rvert$
I	0.00	3136.3	1790.3	1179.3	2.899	1.833	0.983
II	11.3	2967.8	1807.7	1192.9	0.303	3.417	0.490
III	35.2	3258.9	1697.1	1189.2	0.173	7.084	0.228

16.2.2 Internal rotation

MDAA is a three rotor molecule, whose methyl rotors cause fine splittings in the microwave spectrum, that strongly depend on the barrier to internal rotation. With the program GAUSSIAN an approximate calculation of these barriers is possible by rotating the dihedral angles $\alpha = \angle(O_3 - C_2 - C_4 - H_5)$, $\beta = \angle(O_9 - C_8 - C_{10} - H_{11})$, and $\gamma = \angle(C_2 - N_1 - C_{14} - H_{15})$, in a grid of 10°. Due to the C_{3v} symmetry of the methyl groups, a rotation of 120° is sufficient.
The calculations delivered a quite small barrier of approx. 116 cm^{-1} for the N-methyl group, which will be called the γ-rotor further on. For the two acetyl methyl rotors much higher barriers of approx. 586 cm^{-1} and 757 cm^{-1} were calculated for the α- and the β-rotor, respectively. We thus expected the torsional fine splittings of the γ-rotor to be in the order of a few MHz, the ones of the α- and β-rotor to be of only a few kHz.
It should be noted, that in the case of N-methyldiacetamide the same distinct energy jumps were obtained, which were already found for N,N-dimethylpropionamide, due to the coupling of the internal rotors.

16.2.3 Nuclear quadrupole coupling

In addition to the numerous splittings expected due to the internal rotation in MDAA, the ^{14}N nucleus causes hyperfine splittings.
By carrying out a single point EFG calculation at the B3PW91/6-311+G(d,p) level of theory based on the structure optimized at the MP2/6-311++G(d,p) level and a calibration factor of eQ/h of 4.599(43) MHz/a.u. the quadrupole coupling constants were calculated:

$$\chi_{aa} = 1.7338 \text{ MHz}, \chi_{bb} = 2.0185 \text{ MHz}, \chi_{cc} = -3.7522 \text{ MHz}$$
$$\chi_{ab} = -0.0302 \text{ MHz}, \chi_{ac} = 0.1198 \text{ MHz} , \chi_{bc} = 0.1581 \text{ MHz}.$$

16.3 Experimental

The microwave spectrum was recorded using the molecular beam Fourier transform microwave spectrometer operating in the frequency ranges of 2-26.5 GHz. At first, a broadband scan was recorded in the frequency range from 9 to 15 GHz. All measured lines showed a characteristic structure and a broadened line width of 1-5 MHz, due to the quadrupole coupling and the internal rotation. Figure 16.3 illustrates a typical part of the broadband scan. In this part of the spectrum already internal rotation splittings do to the γ-rotor can be resolved. These splittings are indicated trough brackets and marked with the respective internal rotation species.

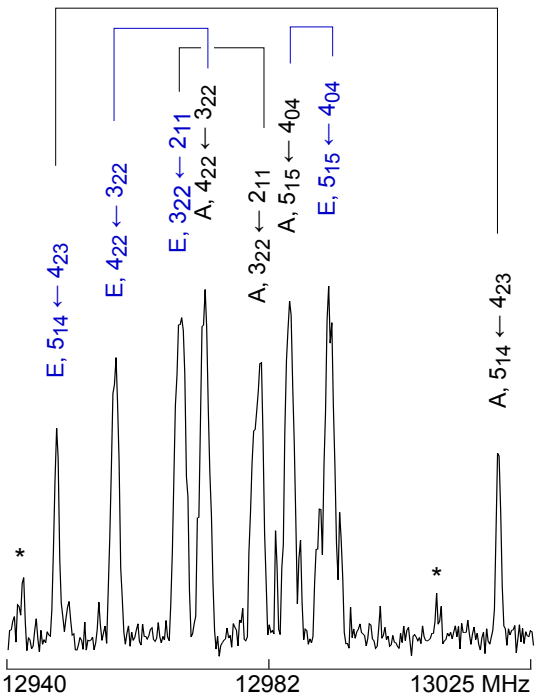

Figure 16.3: Typical part of a broadband scan of MDAA. The transitions are marked with their respective species (A, E) and quantum numbers (J, K_a, K_c). Unassigned lines are marked with asterisks. Brackets indicate internal rotation splittings.

All lines found through measurements in the scan mode of the spectrometer, were afterwards remeasured in the high resolution mode. Figure 16.4 shows a typical spectrum measured in the high resolution mode, showing hyperfine and fine splittings. It can clearly be seen that doublets are observed for the A-species of the γ-rotor and triplets for the E-species. In all cases, only these five symmetry species could be resolved, meaning that only one of the acetyl methyl rotors causes visible internal rotation splittings.

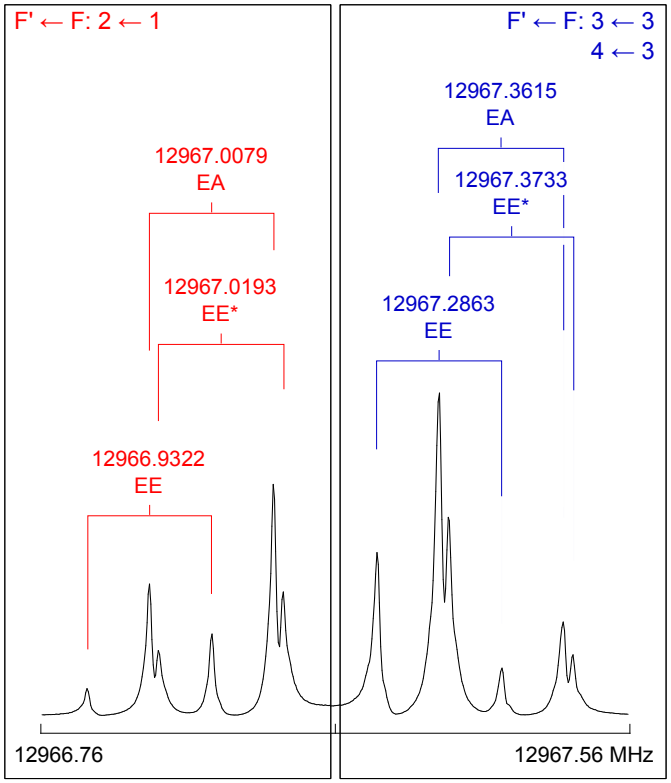

Figure 16.4: Quadrupole hyperfine and internal rotation fine components of the $3_{22} \leftarrow 2_{11}$ transition. The hyperfine transitions are given by $F' \leftarrow F$, the fine components by their respective symmetry species EA, EE and EE*. The Doppler doublets are marked by brackets. For this spectrum, 3012 decays were co-added.

16.3.1 Spectral Assignment

The assignment of the microwave spectrum was carried out using the program XIAM. At first, all internal motions and quadrupole coupling were neglected and the

spectrum was predicted in its rigid rotor model based on the calculated rotational A, B, and C constants. By comparison of the predicted and the measured spectrum a first assignment was possible by fitting the linear combinations of the rotational constants $B_J = \frac{B+C}{2}$, $B_K = A - \frac{B+C}{2}$ and $B_- = \frac{B-C}{2}$.
In a second step, the assignment was extended through the assignment of the first internal rotor. Due to the small calculated barrier of 116 cm^{-1} for the γ-rotor, quite large splittings in the order of a few MHz were expected. For a few transitions, this internal rotation splittings could be easily recognized from the spectrum and assigned with the help of the XIAM-predictions.
As the internal rotation fine splittings of the acetyl methyl groups (α and β) are in the same order of magnitude as the quadrupole hyperfine splittings these both effects were analyzed in the last step of the assignment. The accurate calculation of the NQCCs was thereby essential for this assignment step.

16.4 Results and Discussion

In the end, a global fit of all hyperfine components and the fine components of the α- and the γ-rotor could be carried out by fitting 18 molecular parameters: the linear combinations of the rotational constants B_J, B_K, and B_-, the centrifugal distortion constants Δ_J, Δ_{JK}, Δ_K, δ_J, and δ_K, the NQCCs χ_{aa}, and $\chi_{bb} - \chi_{cc}$, the V_3 potentials and the polar coordinates of the internal rotor axis in the principal axis system δ and ϵ and the effective parameters D_{pi2J}, D_{pi2K}, and D_{pi2-} of the γ-rotor. The ϵ-polar coordinate of the γ-rotor was fixed to 0, the rotational constant of both methyl rotors F_0 to 158 GHz, corresponding to a moment of inertia of $I_\alpha = 3.2\ uA^2$. The results of the fit are summarized in Table 16.2 in comparison to the calculations. The frequency list of the fit can be found in Table I.4.

The calculated rotational constants are quite close to the fitted values, not only at the MP2/6-311++G(d,p) level of theory, but also at different method / basis set combinations. The results of a few calculations with different methods and basis sets are given in Table I.5 in comparison with the experimental values.
As expected, the calculated NQCCs are very close to the experimentally obtained values, as the prediction of the hyperfine structure was already a great help in the assignment process.
By comparison of the V_3 potentials, it is not possible to decide unambiguously,

Table 16.2: Molecular parameters of conformer I of MDAA deduced from the program XIAM (obs) and parameters calculated at the MP2/6-311++G(d,p) level of theory (calc).

Par.	Unit	obs[a]	calc[b]	obs-calc
A	GHz	3.155 450 0(37)	3.136	0.019
B	GHz	1.791 282 2(20)	1.79	0.001
C	GHz	1.170 928 22(40)	1.179	−0.008
Δ_J	kHz	0.0693(19)		
Δ_{JK}	kHz	0.2378(82)		
Δ_K	kHz	−0.057(12)		
δ_J	kHz	0.0148(11)		
δ_K	kHz	0.0 [c]		
χ_{aa}	MHz	1.736 01(75)	1.7197	0.0163
$\chi_{bb} - \chi_{cc}$	MHz	5.8136(12)	5.7239	0.0897
F_0	GHz	158.0 [c]		
Torsional parameters of the γ-methyl rotor				
V_3	cm^{-1}	147.1903(6)	116	
$\angle(i,a)$	°	91.9248(5)	93.94	
$\angle(i,b)$	°	1.9248(5)	4.32	
$\angle(i,c)$	°	90.0 [c]	91.78	
D_{pi2J}	kHz	88.47(15)		
D_{pi2K}	MHz	−56.86(47)		
D_{pi2-}	kHz	84.17(17)		
Torsional parameters of the α-methyl rotor				
V_3	cm^{-1}	679.59(42)	586	
$\angle(i,a)$	°	154.13(36)	150.71	
$\angle(i,b)$	°	64.49(36)	61.06	
$\angle(i,c)$	°	86.019(52)	85.83	
σ^d	kHz	2.2		
N^e		478		

[a] Parameters are given with one standard uncertainty in parentheses. Watson's A reduction and I^r representation were used. [b] See section 16.2. [c] Fixed. [d] Standard deviation of the fit. [e] Number of lines.

which two of the three methyl groups were assigned. Of cause the first rotor, which showed quite large internal rotation splittings and an experimental V_3 potential of 147.1903(6) cm^{-1} is the γ-rotor with a calculated potential of 116 cm^{-1}, but the second rotor with an assigned V_3 potential of 679.59(42) cm^{-1} could either be the α-rotor with a calculated V_3 potential of 586 cm^{-1} or the β rotor with 757 cm^{-1}. For this decision one needs to regard the internal rotation angles $\angle(i,a)$, $\angle(i,b)$

and $\angle(i,c)$. The experimentally fitted values of $\angle(i,a) = 154.13(36)°$, $\angle(i,b) = 64.49(36)°$, and $\angle(i,c) = 86.019(52)°$ agree well with the values of $\angle(i,a) = 150.71°$, $\angle(i,b) = 61.06°$, and $\angle(i,c) = 85.83°$ calculated for the α-rotor. The values calculated for the β-rotor are $\angle(i,a) = 81.29°$, $\angle(i,b) = 12.61°$, and $\angle(i,c) = 80.95°$ and do therefore not come to an agreement with the experimental results.
The standard deviation of the fit is with 2.2 kHz, in the same order as the experimental resolution, which is especially good when considering the complexity of the spectrum.

16.5 Conclusion

The lowest energy conformer of MDAA was found in the gas phase and studied using a combination of microwave spectroscopy and quantum chemistry. The internal rotation of three internal methyl rotors was theoretically and experimentally analyzed. The internal rotation barriers of two of the three methyl rotors could be assigned from the experimentally deduced fine splittings in the rotational spectrum to be 147.1903(6) cm^{-1} and 679.59(42) cm^{-1} for the nitrogen and the acetyl methyl rotor, respectively.

Chapter 17

Comparison and Discussion

In total, two formamides, five acetamides, and two propionamides were investigated in this thesis. The most interesting characteristics and differences of the various molecules were found depending on the substituents at the nitrogen atom. Thereby especially the number of hydrogen substituents at the nitrogen atom plays a crucial role as the group of formamides, secondary, and tertiary amides often shows similar behavior in terms of internal rotation as well as quadrupole coupling.

In Table 17.1 the V_3 potentials of different acetamides are given in order to compare the barrier heights to internal rotation of the acetyl methyl group. For acetamide, a remarkably small barrier of only 24.3 cm^{-1} is reported. The barrier is much lower than those found for other acetyl methyl groups for example in esters like methyl acetate (101.7 cm^{-1}) [68], isopropenyl acetate (135.3 cm^{-1}) [71] or in ketones such as acetone (264.7 cm^{-1}) [114, 115] or ethyl methyl ketone (181.5 cm^{-1}) [77]. It seems that for acetamide there is a special electronic situation, probably due to the amide bond with two hydrogen atoms bound to the nitrogen, which somehow causes such a small acetyl methyl potential.
Substituting one of these hydrogen atoms, one comes to the group of the secondary acetamides, where always small barriers of 65-75 cm^{-1} were found. The barrier height within this group additionally seems to be slightly influenced by the type of substituent exchanging the hydrogen. The smallest barrier was obtained for N-*tert*-butylacetamide with a barrier height of 65.6 cm^{-1}. For N-methyl- and N-ethylacetamide slightly higher barriers of about 73.5 cm^{-1} were found. The differences can probably be explained by the different inductive effects of the substituents. The *tert*-butyl group has a great inductive effect, transferring electronic density through the amide bond. The small methyl and ethyl groups on the other

Table 17.1: V_3 potentials of the acetyl methyl rotation of different acetamides in cm^{-1}.

		V_3(acetyl-CH_3)	ref.	formula
	Acetamide	24.3	[48, 113]	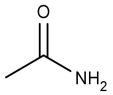
secondary acetamides	N-Methyl-acetamide	73.5	[64, 65]	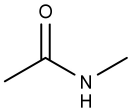
	N-Ethyl-acetamide	73.4	chapter 9	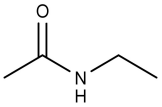
	N-*tert*-Butyl-acetamide	65.6	chapter 10	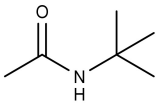
tertiary acetamides	N,N-Dimethyl-acetamide	677	[88]	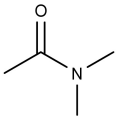
	N,N-Diethyl-acetamide I	517	chapter 15	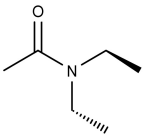
	N,N-Diethyl-acetamide II	619.5		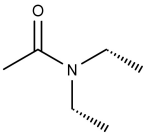
	N-Methyldi-acetamide	679.6/ >800	chapter 16	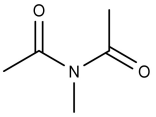

hand have similar and, compared to the *tert*-butyl group, much smaller inductive effects. This phenomenon was also already observed for acetates. In a series of saturated acetates from methyl acetate up to n-hexyl acetate [69], a barrier to internal rotation of approximately 100 cm^{-1} was found, even in cases where the alkyl chain is branched [80]. Only for *tert*-butyl acetate, the bulky *tert*-butyl group caused a slightly higher barrier of 112 cm^{-1} [82]. In vinyl acetate [70] and isopropenyl acetate [71], where the vinyl group is directly bound to the ester group and π-electron con-

jugation, extending from the vinyl double bond to the ester group, is possible, the barrier heights increase significantly to 151.492(34) cm^{-1} and 135.3498(38) cm^{-1}, respectively. This might explain the problems in the assignment of the internal rotation for N-vinylacetamide. Probably the barrier is influenced by the extension of the π-conjugation.
Compared to acetamide it is already remarkable that the substitution of one hydrogen atom results in a barrier increased by about 50 cm^{-1}. When substituting not only one, but both hydrogen atoms the effect is even greater as the barrier increases by one order of magnitude. For all tertiary acetamides, incredibly high barriers in the order of 517-680 cm^{-1} were found. The substitution of both hydrogen atoms in acetamide causes thereby a great hindering of the internal rotation, where obviously, the electronic effect has a much stronger influence on the barrier to internal rotation than sterical hindrances. We assume that in amides a special electronic situation is present, where the electronic density can somehow be easily transported from the nitrogen substituents through the amide bond to the acetyl rotor.
Within the group of the tertiary acetamides the barrier also seems to be influenced by the type of substituents at the nitrogen, which was also found for the secondary acetamides. Moreover, a very interesting effect was observed for N,N-diethylacetamide. In the case of N,N-diethylacetamide, two conformers were assigned whose structures differed only by the orientations of the two ethyl groups. However, quite different V_3 potentials of 517.04(13) cm^{-1} and 619.48(91) cm^{-1} were observed.
In the case of N-methyldiacetamide one of the acetyl barriers increased so much that the splittings were not even observable anymore with our spectrometer. We assume that the barrier height is greater than 800 cm^{-1}, causing splittings too small to be resolvable. This can probably be explained by a coupling between the the methyl groups in N-methyldiacetamide.

In Table 17.2 further V_3 potentials of secondary and tertiary amides are given, whereby the focus is set on the nitrogen methyl rotation. Thereby two different positions are possible for the methyl group. These positions are not always distinguishable from each other. The reported and obtained barriers were therefore ranked by the barrier height in Table 17.2, the smaller barrier was always ranked as I, the higher as II.

Table 17.2: V_3 potentials of the nitrogen methyl rotors of different amides in cm^{-1}.

		$V_3(CH_3\text{-I})$	$V_3(CH_3\text{-II})$	ref.	formula
secondary amides	N-Methyl-formamide	60.1	—	[4]	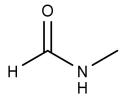
	N-Methyl-acetamide	79.1	—	[65, 64]	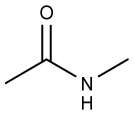
	N-Methyl-propionamide	80.1	—	[95]	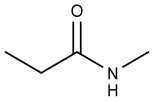
tertiary amides	N,N-Dimethyl-formamide	365.8	771.9	[57]	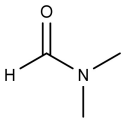
	N,N-Dimethyl-acetamide	183	237	[88]	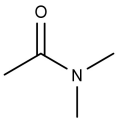
	N,N-Dimethyl-propionamide	134	225.6	chapter 14	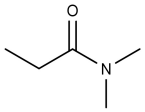
	N-Methyldi-acetamide	147.2	—	chapter 16	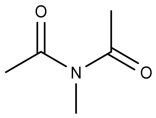
	N,N-Methylethyl-formamide	—	245.2	[58]	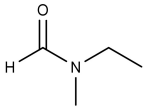

Again, the secondary amides show smaller barriers compared to the tertiary amides, but for the nitrogen methyl rotation this phenomenon is much weaker compared to the acetyl methyl rotation, even though the change in the substituted groups are locally right next to the nitrogen methyl rotors. For the secondary amides, barriers in the same order of magnitude were observed for the nitrogen methyl rotation as for the acetyl methyl rotation of 60-80 cm^{-1}. Thereby the barrier increases slightly with the size of the alkyl groups bound to the carbonyl group from 60 cm^{-1} in N-methylformamide to 80.1 cm^{-1} in N-methylpropionamide. For the tertiary amides, barriers in the order of only one third of the barrier heights obtained for the acetyl

methyl rotation were observed as the barriers are in the order of 150-250 cm^{-1}. Because there are two possible positions for methyl groups two barriers were observed in some cases, which differ by about 50-75 cm^{-1}. The barriers were in the order of 134-183 cm^{-1} and 225-245 cm^{-1} for these two positions. Surprisingly, the barriers to internal rotation of N,N-dimethylformamide are with values of 365.8 cm^{-1} and 771.9 cm^{-1} extremely high compared to all other molecules.

In Table 17.3 the NQCC z-principal axis components χ_{zz} are given in order to compare the quadrupole coupling for the different molecules. The results in this table are sorted by the size of the obtained values for χ_{zz}.

In general the values differ between -3.41 MHz for diformamide up to -4.6461 MHz for N,N-dimethylacetamide, where the primary and secondary amides show smaller values for χ_{zz} compared to the tertiary amides. For all tertiary amides values greater than -4.2 MHz were obtained. Also the primary amides have smaller values compared to their respective secondary amides.

For molecules with extended π-conjugation as diformamide and all vinyl- and phenylamides, the electronic environment at the quadrupole nucleus is highly influences by the π-conjugation, which leads to remarkably small χ_{zz} values.
A similar but slightly weaker effect is observed for *tert* butyl amides. The bulky *tert*-butyl group with its great inductive effect also leads to a decrease in the NQCC z-pricipal axis component.
Small groups like methyl and ethyl groups have only a small influence, which leads to slightly higher values compared to the not methylized or ethylized amides.
For different conformers often similar but not identical values were obtained for χ_{zz}. Surprisingly, the difference between the two conformers of N-*tert*-butylformamide is exceptionally great.

Table 17.3: ^{14}N NQCC z-principal axis component χ_{zz} (in MHz) of form-, acet- and propionamides sorted by the size of χ_{zz}.

		χ_{zz}	ref.
	Formamide	−3.8510(11)	[93]
	Acetamide	−3.9458(22)	[48]
	Propionamide	−3.9762(48)	[94]
secondary amides	Diformamide	−3.41(7)	[62]
	N-Vinylformamide, cis	−3.6396(20)	chapter 6
	N-Vinylformamide, trans	−3.6416(11)	chapter 6
	N-Phenylformamide, trans	−3.671(22)	[59, 60]
	N-Vinylacetamide	−3.7728(17)	chapter 11
	N-*tert*-Butylformamide, syn	−3.7799(11)	chapter 7
	N-Methyldiacetamide	−3.7816(25)	chapter 16
	N-*tert*-Butylacetamide	−3.9199(81)	chapter 10
	N-*tert*-Butylformamide, anti	−3.9220(24)	chapter 7
	N-Ethylformamide	−3.993(51)	[5]
	N-Methylformamide	−4.0358(28)	[4]
	N-Ethylacetamide	−4.118(39)	chapter 9
	N-Methylacetamide	−4.1410(9)	[65]
	N-Methylpropionamide	−4.168(19)	[95]
tertiary amides	N,N-Methylethylformamide	−4.216(31)	[58]
	N,N-Dimethylformamide	−4.364(2)	[57]
	N,N-Diethylacetamide I	−4.389(40)	chapter 15
	N,N-Diethylacetamide II	−4.408(50)	chapter 15
	N,N-Diethylpriopionamide 0MM	−4.432(34)	chapter 13
	N,N-Diethylpriopionamide 0PM	−4.455(55)	chapter 13
	N,N-Dimethylacetamide	−4.6461(16)	[88]
	N,N-Dimethylpropionamide	−4.720(66)	chapter 14

Values for molecules giving an external reference were calculated by W. C. Bailey [37]. Molecules investigated in this work were calculated through diagonalization of the quadrupole tensor with the off-diagonal elements from quantum chemical calculations. The estimated uncertainty of the off-diagonal elements is 2x the root mean square difference between calculated and experimental diagonal components.

Part IV

Appendix

Appendix A

N-Vinylformamide

Table A.1: Nuclear coordinates (in Å) in the principal axis system of the ***trans*** conformer of N-vinylformamide, calculated at the MP2/6-311++G(d,p) level of theory.

	a	*b*	*c*
N_1	0.046250	0.675298	−0.000124
H_2	0.367092	1.633830	−0.000017
C_3	−1.311385	0.454734	0.000043
O_4	−1.839737	−0.641266	0.000092
H_5	−1.880556	1.400444	0.000119
C_6	0.990979	−0.357165	−0.000201
H_7	0.545010	−1.345414	−0.000563
C_8	2.317902	−0.158152	0.000165
H_9	2.753732	0.836198	0.000577
H_{10}	2.986229	−1.009165	0.000060

Table A.2: Nuclear coordinates (in Å) in the principal axis system of the ***cis*** conformer of N-vinylformamide, calculated at the MP2/6-311++G(d,p) level of theory.

	a	*b*	*c*
N_1	−0.021507	−0.269838	−0.000141
H_2	0.000556	−1.283099	−0.000318
C_3	1.197728	0.362713	0.000064
O_4	2.269169	−0.212995	0.000049
H_5	1.098639	1.462533	0.000237
C_6	−1.250412	0.391748	−0.000094
H_7	−1.165962	1.475029	−0.000223
C_8	−2.446476	−0.217325	0.000122
H_9	−2.540792	−1.298256	0.000274
H_{10}	−3.349896	0.377817	0.000118

Table A.3: Observed frequencies ν_{obs} in GHz of the ***trans*** conformer of N-vinylformamide. $\nu_c - \nu_o$ values in kHz are obtained after a fit with the program XIAM. J, K_a, and K_c are the symmetric top rotational quantum numbers, F is the total angular momentum in the coupled basis with $F = J + I$.

No.	J'	K_a'	K_c'	F'	J	K_a	K_c	F	ν_{obs}	$\nu_c - \nu_o$
1	2	1	2	3	1	1	1	2	10.7389720	0.8
2	2	1	2	2	1	1	1	1	10.7395607	−0.2
3	2	1	2	1	1	1	1	0	10.7391908	−1.2
4	2	1	2	2	1	1	1	2	10.7401383	−3.4
5	2	1	2	1	1	1	1	1	10.7377424	2.3
6	2	0	2	3	1	0	1	2	11.1215158	0.3
7	2	0	2	2	1	0	1	1	11.1215710	−1.5
8	2	0	2	1	1	0	1	0	11.1219689	1.8
9	2	0	2	2	1	0	1	2	11.1220844	0.1
10	2	0	2	1	1	0	1	1	11.1206887	0.9
11	2	1	1	3	1	1	0	2	11.5174147	0.8
12	2	1	1	2	1	1	0	1	11.5178829	−1.2
13	2	1	1	1	1	1	0	0	11.5161234	2.6
14	2	1	1	2	1	1	0	2	11.5167936	2.0
15	2	1	1	1	1	1	0	1	11.5188526	0.6
16	5	0	5	6	4	1	4	5	12.6085320	−1.9
17	5	0	5	5	4	1	4	4	12.6078157	−0.3
18	5	0	5	4	4	1	4	3	12.6087598	1.6
19	5	0	5	5	4	1	4	5	12.6092752	−2.5
20	5	0	5	4	4	1	4	4	12.6069184	−2.3
21	3	1	3	4	2	1	2	3	16.1044350	0.4
22	3	1	3	3	2	1	2	2	16.1046260	−0.6
23	3	1	3	2	2	1	2	1	16.1046055	−2.5
24	3	1	3	3	2	1	2	3	16.1057957	−1.4
25	3	1	3	2	2	1	2	2	16.1027861	−1.1
26	3	0	3	4	2	0	2	3	16.6655194	0.3
27	3	0	3	3	2	0	2	2	16.6655738	1.9
28	3	0	3	2	2	0	2	1	16.6656180	0.5
29	3	0	3	3	2	0	2	3	16.6661407	0.0
30	3	0	3	2	2	0	2	2	16.6647323	−0.4
31	3	2	2	4	2	2	1	3	16.6924405	−0.9
32	3	2	2	3	2	2	1	2	16.6929913	1.6

No.	J'	K_a'	K_c'	F'	J	K_a	K_c	F	ν_{obs}	$\nu_c - \nu_o$
33	3	2	2	2	2	2	1	1	16.6921404	3.6
34	3	2	2	3	2	2	1	3	16.6924405	−0.9
35	3	2	2	2	2	2	1	2	16.6929913	1.6
36	3	2	1	4	2	2	0	3	16.7192519	0.3
37	3	2	1	3	2	2	0	2	16.7197685	1.2
38	3	2	1	2	2	2	0	1	16.7189578	3.6
39	1	1	0	2	1	0	1	2	17.1359355	−2.6
40	1	1	0	1	1	0	1	1	17.1343355	1.6
41	1	1	0	2	1	0	1	1	17.1354243	−2.0
42	1	1	0	1	1	0	1	0	17.1356144	1.2
43	1	1	0	0	1	0	1	1	17.1370643	−0.8
44	1	1	0	1	1	0	1	2	17.1348465	0.9
45	3	1	2	4	2	1	1	3	17.2718969	0.1
46	3	1	2	3	2	1	1	2	17.2720221	−0.5
47	3	1	2	2	2	1	1	1	17.2717262	1.3
48	3	1	2	3	2	1	1	3	17.2714042	3.8
49	3	1	2	2	2	1	1	2	17.2726942	1.4
50	2	1	1	3	2	0	2	3	17.5318380	1.6
51	2	1	1	2	2	0	2	2	17.5306458	0.4
52	2	1	1	1	2	0	2	1	17.5324993	1.2
53	2	1	1	3	2	0	2	2	17.5312675	−0.2
54	2	1	1	2	2	0	2	1	17.5315313	1.1
55	2	1	1	2	2	0	2	3	17.5312147	0.5
56	2	1	1	1	2	0	2	2	17.5316154	2.0
57	3	1	2	4	3	0	3	4	18.1382137	−0.5
58	3	1	2	3	3	0	3	3	18.1370958	−0.3
59	3	1	2	2	3	0	3	2	18.1386068	1.3
60	3	1	2	4	3	0	3	3	18.1375972	4.6
61	3	1	2	3	3	0	3	2	18.1379377	2.4
62	3	1	2	2	3	0	3	3	18.1377693	3.0
63	3	1	2	3	3	0	3	4	18.1377206	2.8
64	6	0	6	7	5	1	5	6	18.9413380	−0.2
65	6	0	6	6	5	1	5	5	18.9406296	0.8
66	6	0	6	5	5	1	5	4	18.9415120	0.8
67	4	1	3	5	4	0	4	5	18.9698885	−2.2
68	4	1	3	4	4	0	4	4	18.9687710	−1.7

No.	J'	K_a'	K_c'	F'	J	K_a	K_c	F	ν_{obs}	$\nu_c - \nu_o$
69	4	1	3	3	4	0	4	3	18.9701789	0.8
70	5	1	4	6	5	0	5	6	20.0462173	−2.9
71	5	1	4	5	5	0	5	5	20.0450714	−3.0
72	5	1	4	4	5	0	5	4	20.0464541	0.4
73	6	1	5	7	6	0	6	7	21.3904871	−3.8
74	6	1	5	6	6	0	6	6	21.3893000	−1.9
75	6	1	5	5	6	0	6	5	21.3906920	0.4
76	4	1	4	5	3	1	3	4	21.4649240	0.5
77	4	1	4	3	3	1	3	2	21.4650241	−0.5
78	4	1	4	4	3	1	3	4	21.4663854	0.2
79	4	1	4	3	3	1	3	3	21.4631815	−3.6
80	1	1	1	2	0	0	0	1	22.3105500	2.6
81	1	1	1	1	0	0	0	0	22.3111239	−4.3
82	1	1	1	1	0	0	0	1	22.3111239	−4.3
83	4	0	4	5	3	0	3	4	22.1894502	1.2
84	4	0	4	4	3	0	3	3	22.1895076	1.2
85	4	0	4	3	3	0	3	2	22.1894901	−1.9
86	4	0	4	4	3	0	3	4	22.1901271	−0.9
87	4	0	4	3	3	0	3	3	22.1886521	−0.7
88	4	2	3	5	3	2	2	4	22.2513984	0.2
89	4	2	3	4	3	2	2	3	22.2516343	−1.6
90	4	2	3	3	3	2	2	2	22.2513364	−0.7
91	4	2	3	4	3	2	2	4	22.2516343	−1.6
92	4	2	3	3	3	2	2	3	22.2513364	−0.7
93	4	2	2	5	3	2	1	4	22.3183241	−0.7
94	4	2	2	4	3	2	1	3	22.3185169	−1.2
95	4	2	2	3	3	2	1	2	22.3182710	0.8
96	4	1	3	5	3	1	2	4	23.0211262	0.7
97	4	1	3	4	3	1	2	3	23.0211830	0.0
98	4	1	3	3	3	1	2	2	23.0210650	0.4
99	5	1	5	6	4	1	4	5	26.8189989	0.5
100	5	1	5	5	4	1	4	4	26.8190636	0.3
101	5	1	5	4	4	1	4	3	26.8190636	0.3
102	5	1	5	5	4	1	4	5	26.8205256	0.6
103	5	1	5	4	4	1	4	4	26.8172239	−1.8
104	2	1	2	3	1	0	1	2	27.4854685	3.1

No.	J'	K_a'	K_c'	F'	J	K_a	K_c	F	ν_{obs}	$\nu_c - \nu_o$
105	2	1	2	2	1	0	1	1	27.4861220	−2.2
106	2	1	2	1	1	0	1	0	27.4855799	−2.8
107	2	1	2	2	1	0	1	2	27.4866361	0.2
108	2	1	2	1	1	0	1	1	27.4842998	−3.6
109	5	0	5	6	4	0	4	5	27.6868744	0.6
110	5	0	5	5	4	0	4	4	27.6869390	0.3
111	5	0	5	4	4	0	4	3	27.6869025	5.6
112	5	0	5	5	4	0	4	5	27.6876165	−1.2
113	5	0	5	4	4	0	4	4	27.6860427	−0.6
114	5	2	4	6	4	2	3	5	27.8057908	1.2
115	5	2	4	5	4	2	3	4	27.8059182	−1.2
116	5	2	4	4	4	2	3	3	27.8057719	−4.0
117	5	3	3	6	4	3	2	5	27.8433864	−2.6
118	5	3	3	5	4	3	2	4	27.8436463	3.7
119	5	3	3	4	4	3	2	3	27.8433292	3.6
120	5	2	3	6	4	2	2	5	27.9392626	−2.1
121	5	2	3	5	4	2	2	4	27.9393394	0.8
122	5	2	3	4	4	2	2	3	27.9392549	−2.2
123	5	1	4	6	4	1	3	5	28.7632057	2.3
124	5	1	4	5	4	1	3	4	28.7632390	−1.3
125	5	1	4	4	4	1	3	3	28.7631741	1.6
126	3	2	1	2	4	1	4	3	30.5632513	−2.7
127	3	2	1	3	4	1	4	4	30.5613454	0.6
128	3	2	1	4	4	1	4	5	30.5628632	3.7
129	8	0	8	9	7	1	7	8	31.8170181	−1.0
130	8	0	8	8	7	1	7	7	31.8163948	5.3
131	8	0	8	7	7	1	7	6	31.8171268	−1.2
132	3	1	3	4	2	0	2	3	32.4683891	4.6
133	3	1	3	3	2	0	2	2	32.4691793	1.0
134	3	1	3	2	2	0	2	1	32.4682226	−1.0
135	3	1	3	3	2	0	2	3	32.4697497	2.6
136	3	1	3	2	2	0	2	2	32.4673364	−2.5
137	2	2	1	1	3	1	2	2	32.9665983	−6.9
138	2	2	1	2	3	1	2	3	32.9664239	1.4
139	2	2	1	3	3	1	2	4	32.9664760	1.6
140	2	2	1	2	3	1	2	2	32.9657539	1.5

No.	J'	K_a'	K_c'	F'	J	K_a	K_c	F	ν_{obs}	$\nu_c - \nu_o$
141	2	2	1	3	3	1	2	3	32.9669723	1.5
142	6	0	6	7	5	0	5	6	33.1518013	−1.4
143	6	0	6	6	5	0	5	5	33.1518776	1.5
144	6	0	6	5	5	0	5	4	33.1518191	2.9
145	6	0	6	6	5	0	5	6	33.1526163	−3.6
146	6	0	6	5	5	0	5	5	33.1509197	−1.2
147	6	1	6	7	5	1	5	6	32.1653353	2.1
148	6	1	6	6	5	1	5	5	32.1653781	−4.6
149	6	1	6	5	5	1	5	4	32.1653781	0.0
150	6	1	6	6	5	1	5	6	32.1669089	−0.4
151	6	1	6	5	5	1	5	5	32.1635378	−2.7
152	6	2	5	7	5	2	4	6	33.3545073	−1.2
153	6	2	5	6	5	2	4	5	33.3545942	2.9
154	6	2	5	5	5	2	4	4	33.3545073	−0.1
155	6	2	4	7	5	2	3	6	33.5869292	−1.3
156	6	2	4	6	5	2	3	5	33.5869489	2.3
157	6	1	5	7	5	1	4	6	34.4960791	5.8
158	6	1	5	6	5	1	4	5	34.4961001	−3.5
159	6	1	5	5	5	1	4	4	34.4960525	−1.7
160	2	2	0	1	3	1	3	2	35.3093251	0.7
161	2	2	0	2	3	1	3	3	35.3066002	0.0
162	2	2	0	3	3	1	3	4	35.3085301	−1.4
163	4	1	4	5	3	0	3	4	37.2677931	4.1
164	4	1	4	4	3	0	3	3	37.2686319	2.8
165	4	1	4	3	3	0	3	2	37.2676290	−1.7
166	4	1	4	4	3	0	3	4	37.2692482	−2.5
167	4	1	4	3	3	0	3	3	37.2667896	−1.9
168	7	1	7	8	6	1	6	7	37.5027686	4.2
169	7	1	7	7	6	1	6	6	37.5028060	−0.1
170	7	1	7	6	6	1	6	5	37.5027914	−5.8
171	7	0	7	8	6	0	6	7	38.5790530	−1.2
172	7	0	7	7	6	0	6	6	38.5791383	2.4
173	7	0	7	6	6	0	6	5	38.5790605	−2.0
174	7	2	6	8	6	2	5	7	38.8964410	1.4
175	7	2	6	7	6	2	5	6	38.8964991	0.0
176	7	2	6	6	6	2	5	5	38.8964410	−1.1

Table A.4: Observed frequencies ν_{obs} in GHz of the ***cis*** conformer of N-vinylformamide. $\nu_c - \nu_o$ values in kHz are obtained after a fit with the program XIAM. J, K_a, and K_c are the symmetric top rotational quantum numbers, F is the total angular momentum in the coupled basis with $F = J + I$.

No.	J'	K_a'	K_c'	F'	J	K_a	K_c	F	ν_{obs}	$\nu_c - \nu_o$
1	2	1	2	3	1	1	1	2	9.2353415	0.6
2	2	1	2	2	1	1	1	1	9.2359800	5.5
3	2	1	2	1	1	1	1	0	9.2354956	0.2
4	2	1	2	2	1	1	1	2	9.2365062	−4.6
5	2	1	2	1	1	1	1	1	9.2341545	−0.2
6	2	0	2	3	1	0	1	2	9.3819678	0.7
7	2	0	2	2	1	0	1	1	9.3820104	0.0
8	2	0	2	1	1	0	1	0	9.3824706	2.9
9	2	0	2	2	1	0	1	2	9.3825666	0.6
10	2	0	2	1	1	0	1	1	9.3810799	1.2
11	2	1	1	3	1	1	0	2	9.5294170	−1.3
12	2	1	1	2	1	1	0	1	9.5299380	2.5
13	2	1	1	1	1	1	0	0	9.5280994	−0.3
14	3	1	3	4	2	1	2	3	13.8528824	0.2
15	3	1	3	3	2	1	2	2	13.8530821	1.1
16	3	1	3	2	2	1	2	1	13.8530516	−1.5
17	3	1	3	3	2	1	2	3	13.8542481	−2.8
18	3	1	3	2	2	1	2	2	13.8512312	−2.1
19	3	0	3	4	2	0	2	3	14.0718072	0.4
20	3	0	3	3	2	0	2	2	14.0718344	−0.3
21	3	0	3	2	2	0	2	1	14.0719202	0.1
22	3	0	3	3	2	0	2	3	14.0724335	−0.1
23	3	0	3	2	2	0	2	2	14.0709891	0.7
24	3	2	2	4	2	2	1	3	14.0736700	0.3
25	3	2	2	3	2	2	1	2	14.0742661	1.1
26	3	2	2	2	2	2	1	1	14.0733400	1.0
27	3	2	2	3	2	2	1	3	14.0736700	0.3
28	3	2	2	2	2	2	1	2	14.0742661	1.1
29	3	2	1	4	2	2	0	3	14.0755422	0.6
30	3	2	1	3	2	2	0	2	14.0761299	−1.1
31	3	2	1	2	2	2	0	1	14.0752120	−0.2
32	3	1	2	4	2	1	1	3	14.2938863	0.8

No.	J'	K_a'	K_c'	F'	J	K_a	K_c	F	ν_{obs}	$\nu_c - \nu_o$
33	3	1	2	3	2	1	1	2	14.2940195	−0.3
34	3	1	2	2	2	1	1	1	14.2937190	−1.4
35	3	1	2	3	2	1	1	3	14.2934478	2.6
36	3	1	2	2	2	1	1	2	14.2946164	2.1
37	4	1	4	5	3	1	3	4	18.4700067	0.0
38	4	1	4	4	3	1	3	3	18.4701028	0.0
39	4	1	4	3	3	1	3	2	18.4701090	−0.1
40	4	1	4	4	3	1	3	4	18.4714708	−0.7
41	4	1	4	3	3	1	3	3	18.4682596	−1.7
42	4	0	4	5	3	0	3	4	18.7602196	−0.3
43	4	0	4	4	3	0	3	3	18.7602425	0.5
44	4	0	4	3	3	0	3	2	18.7602705	−1.9
45	4	0	4	4	3	0	3	4	18.7608687	−0.2
46	4	0	4	3	3	0	3	3	18.7594267	0.6
47	4	2	3	5	3	2	2	4	18.7646136	−2.0
48	4	2	3	4	3	2	2	3	18.7648673	−1.7
49	4	2	3	3	3	2	2	2	18.7645510	0.6
50	4	2	3	4	3	2	2	4	18.7648673	−1.7
51	4	2	3	3	3	2	2	3	18.7645510	0.6
52	4	2	2	5	3	2	1	4	18.7692922	−1.2
53	4	2	2	4	3	2	1	3	18.7695385	−0.3
54	4	2	2	3	3	2	1	2	18.7692288	−0.7
55	4	1	3	5	3	1	2	4	19.0579574	−0.9
56	4	1	3	4	3	1	2	3	19.0580117	−1.6
57	4	1	3	3	3	1	2	2	19.0579036	0.3
58	5	1	5	6	4	1	4	5	23.0866338	0.7
59	5	1	5	5	4	1	4	4	23.0866898	−0.3
60	5	1	5	4	4	1	4	3	23.0867021	2.3
61	5	0	5	6	4	0	4	5	23.4467410	0.2
62	5	0	5	5	4	0	4	4	23.4467594	−1.3
63	5	0	5	4	4	0	4	3	23.4467730	1.6
64	5	0	5	5	4	0	4	5	23.4474072	−2.5
65	5	0	5	4	4	0	4	4	23.4459553	−0.2
66	5	2	4	6	4	2	3	5	23.4551973	3.8
67	5	2	4	5	4	2	3	4	23.4553265	−0.5
68	5	2	4	4	4	2	3	3	23.4551848	5.0

No.	J'	K_a'	K_c'	F'	J	K_a	K_c	F	ν_{obs}	$\nu_c - \nu_o$
69	5	2	3	6	4	2	2	5	23.4645526	5.9
70	5	2	3	5	4	2	2	4	23.4646697	−0.3
71	5	2	3	4	4	2	2	3	23.4645390	4.9
72	5	1	4	6	4	1	3	5	23.8215313	−0.2
73	5	1	4	5	4	1	3	4	23.8215587	−1.4
74	5	1	4	4	4	1	3	3	23.8215058	0.7
75	6	0	6	7	5	0	5	6	28.1308961	−4.8
76	6	0	6	6	5	0	5	5	28.1309224	2.0
77	6	0	6	5	5	0	5	4	28.1309224	1.5
78	6	0	6	6	5	0	5	6	28.1315835	−5.8
79	6	0	6	5	5	0	5	5	28.1301126	−3.1
80	6	1	6	7	5	1	5	6	27.7026594	4.4
81	6	1	6	6	5	1	5	5	27.7026926	−0.7
82	6	1	6	6	5	1	5	6	27.7042167	1.5
83	6	1	6	5	5	1	5	5	27.7008713	1.6
84	6	1	5	7	5	1	4	6	28.5844836	0.8
85	6	1	5	6	5	1	4	5	28.5845066	6.2
86	6	1	5	5	5	1	4	4	28.5844624	−5.0
87	6	2	5	7	5	2	4	6	28.1453399	−4.1
88	6	2	5	6	5	2	4	5	28.1454270	2.8
89	6	2	5	5	5	2	4	4	28.1453399	−4.0
90	6	2	4	7	5	2	3	6	28.1617067	−0.7
91	6	2	4	6	5	2	3	5	28.1617748	−0.6
92	6	2	4	5	5	2	3	4	28.1617078	−0.7
93	7	0	7	8	6	0	6	7	32.8122291	−3.5
94	7	0	7	7	6	0	6	6	32.8122554	2.9
95	7	0	7	7	6	0	6	7	32.8129370	−3.9
96	7	0	7	6	6	0	6	6	32.8114399	−2.1
97	7	1	7	8	6	1	6	7	32.3179651	3.6
98	7	1	7	7	6	1	6	6	32.3179892	−0.6
99	7	1	7	6	6	1	6	5	32.3179970	1.2
100	7	1	7	7	6	1	6	7	32.3195503	0.3
101	7	1	7	6	6	1	6	6	32.3161711	−1.1
102	7	1	6	8	6	1	5	7	33.3466832	−1.3
103	7	1	6	7	6	1	5	6	33.3467022	5.3
104	7	1	6	6	6	1	5	5	33.3466725	−1.9

No.	J'	K_a'	K_c'	F'	J	K_a	K_c	F	ν_{obs}	$\nu_c - \nu_o$
105	7	2	6	7	6	2	5	6	32.8350445	−0.4
106	7	2	6	6	6	2	5	5	32.8349960	0.2
107	7	2	5	7	6	2	4	6	32.8611955	−7.2
108	7	2	5	6	6	2	4	5	32.8611675	−1.7
109	8	0	8	9	7	0	7	8	37.4902697	−1.9
110	8	0	8	8	7	0	7	7	37.4902972	4.7
111	8	0	8	7	7	0	7	6	37.4902798	−2.1
112	8	0	8	8	7	0	7	8	37.4910029	2.0
113	8	1	8	9	7	1	7	8	36.9324415	−1.4
114	8	1	8	7	7	1	7	6	36.9324712	2.0
115	8	1	7	9	7	1	6	8	38.1080053	0.0
116	8	1	7	8	7	1	6	7	38.1080192	4.1
117	8	1	7	7	7	1	6	6	38.1079980	0.0

Appendix B

N-*tert*-Butylformamide

Table B.1: Nuclear coordinates (in Å) in the principal axis system of the ***syn*** conformer of N-*tert*-butylformamide, calculated at the MP2/6-311++G(d,p) level of theory.

	syn		
	a	*b*	*c*
N_1	0.332539	0.944007	−0.000125
H_2	0.090544	1.925527	−0.000037
C_3	1.663873	0.653596	0.00012
O_4	2.152951	−0.466722	−0.000053
H_5	2.281441	1.571861	−0.000177
C_6	−0.760323	−0.041349	0.000016
C_7	−2.063857	0.756957	−0.000903
H_8	−2.917555	0.073407	−0.000741
H_9	−2.132953	1.39017	0.890852
H_{10}	−2.132358	1.389078	−0.893472
C_{11}	−0.678728	−0.909102	−1.260308
H_{12}	−1.512047	−1.619528	−1.273746
H_{13}	−0.740924	−0.281254	−2.155101
H_{14}	0.260233	−1.465732	−1.283948
C_{15}	−0.679649	−0.907821	1.261287
H_{16}	−0.742771	−0.279097	2.155399
H_{17}	−1.512798	−1.618449	1.274737
H_{18}	0.259418	−1.464211	1.286273

Table B.2: Nuclear coordinates (in Å) in the principal axis system of the distorted and symmetric form of the ***anti*** conformer of N-*tert*-butylformamide, calculated at the MP2/6-311++G(d,p) level of theory.

	$anti_{dist}$			$anti_{sym}$		
	a	*b*	*c*	*a*	*b*	*c*
N_1	−0.500395	0.490070	−0.136078	0.502321	0.498944	−0.000054
H_2	−0.662556	1.488879	−0.071961	0.664195	1.499081	0.000383
C_3	−1.626787	−0.271937	−0.029540	1.628082	−0.267940	−0.000185
O_4	−2.764609	0.173484	0.011398	2.769148	0.171576	0.000026
H_5	−1.417786	−1.354852	−0.003249	1.414152	−1.350666	−0.000194
C_6	0.879826	0.003919	0.006061	−0.881278	0.003001	0.000024
C_7	1.790363	1.197004	−0.285081	−1.784607	1.236183	0.000164
H_8	2.839049	0.900646	−0.191078	−2.834974	0.931168	0.000424
H_9	1.622472	1.569205	−1.300767	−1.603815	1.846879	0.891297
H_{10}	1.601794	2.010100	0.425136	−1.604150	1.846797	−0.891076
C_{11}	1.126494	−0.505852	1.431674	−1.146986	−0.829893	−1.259614
H_{12}	2.164191	−0.837415	1.545911	−2.191467	−1.158561	−1.281177
H_{13}	0.930375	0.288560	2.158760	−0.945936	−0.234702	−2.155541
H_{14}	0.470190	−1.351200	1.661216	−0.511632	−1.720045	−1.287715
C_{15}	1.154889	−1.105830	−1.014375	−1.146637	−0.830135	1.259581
H_{16}	0.940205	−0.749824	−2.026345	−0.945521	−0.235064	2.155574
H_{17}	2.207056	−1.404021	−0.960495	−2.191013	−1.159131	1.281381
H_{18}	0.546393	−1.993846	−0.822062	−0.510918	−1.720056	1.287329

Table B.3: Nuclear coordinates (in Å) in the principal axis system of the syn_{ts} and $anti_{ts}$ transition states of N-*tert*-butylformamide, calculated at the MP2/6-311++G(d,p) level of theory.

	syn_{ts}			$anti_{ts}$		
	a	b	c	a	b	c
N_1	0.367021	−0.873115	0.000113	0.512962	−0.444550	0.000120
H_2	0.132349	−1.858143	0.000166	0.676362	−1.446376	0.000118
C_3	1.711839	−0.625378	−0.000059	1.658392	0.295163	0.000036
O_4	2.276987	0.455561	0.000029	2.782999	−0.188206	−0.000009
H_5	2.272730	−1.580871	0.000199	1.486582	1.381167	−0.000044
C_6	−0.789089	0.038389	0.000002	−0.887605	−0.008792	0.000000
C_7	−0.366558	1.507447	−0.000792	−0.996814	1.515566	−0.000215
H_8	−1.277937	2.114876	−0.000914	−2.057304	1.784156	−0.000313
H_9	0.224691	1.756142	0.881725	−0.537542	1.953955	0.890676
H_{10}	0.224339	1.755279	−0.883791	−0.537433	1.953709	−0.891171
C_{11}	−1.616586	−0.262164	−1.254983	−1.563792	−0.572336	−1.255261
H_{12}	−2.516461	0.361467	−1.274928	−2.625681	−0.305265	−1.272363
H_{13}	−1.027594	−0.059383	−2.154367	−1.084207	−0.176729	−2.155576
H_{14}	−1.930094	−1.312515	−1.272441	−1.486794	−1.665101	−1.274630
C_{15}	−1.615980	−0.261001	1.255667	−1.563914	−0.571996	1.255346
H_{16}	−1.026543	−0.057398	2.154574	−1.084423	−0.176135	2.155599
H_{17}	−2.515840	0.362660	1.275481	−2.625807	−0.304931	1.272269
H_{18}	−1.929480	−1.311334	1.274245	−1.486904	−1.664755	1.275026

Table B.4: Observed frequencies ν_{obs} in GHz of the ***syn*** conformer of N-*tert*-butylformamide. $\nu_c - \nu_o$ values in kHz are obtained after a fit with the program XIAM. J, K_a, and K_c are the symmetric top rotational quantum numbers, F is the total angular momentum in the coupled basis with $F = J + I$.

No.	J'	K_a'	K_c'	F'	J	K_a	K_c	F	ν_{obs}	$\nu_c - \nu_o$
1	3	1	3	4	2	1	2	3	11.1845504	0.0
2	3	1	3	3	2	1	2	2	11.1847568	0.0
3	3	1	3	2	2	1	2	1	11.1847288	0.9
4	3	1	3	3	2	1	2	3	11.1859706	−1.1
5	3	1	3	2	2	1	2	2	11.1828375	−0.5
6	3	0	3	4	2	0	2	3	11.3027837	0.4
7	3	0	3	3	2	0	2	2	11.3028609	0.3
8	3	0	3	2	2	0	2	1	11.3028840	1.3
9	3	0	3	3	2	0	2	3	11.3034749	−0.4
10	3	0	3	2	2	0	2	2	11.3019270	0.7
11	3	2	2	4	2	2	1	3	11.3123508	0.2
12	3	2	2	3	2	2	1	2	11.3129310	0.8
13	3	2	2	2	2	2	1	1	11.3120303	1.7
14	3	2	2	3	2	2	1	3	11.3123508	0.2
15	3	2	2	2	2	2	1	2	11.3129310	0.8
16	3	2	1	4	2	2	0	3	11.3220571	0.1
17	3	2	1	3	2	2	0	2	11.3225817	0.9
18	3	2	1	2	2	2	0	1	11.3217491	1.8
19	3	2	1	2	2	2	0	2	11.3227054	1.7
20	3	1	2	4	2	1	1	3	11.4373189	−0.2
21	3	1	2	3	2	1	1	2	11.4374554	−2.1
22	3	1	2	2	2	1	1	1	11.4371393	−0.8
23	3	1	2	3	2	1	1	3	11.4368260	3.8
24	3	1	2	2	2	1	1	2	11.4381303	2.0
25	4	1	4	5	3	1	3	4	14.9100372	0.3
26	4	1	4	4	3	1	3	3	14.9101483	0.7
27	4	1	4	3	3	1	3	2	14.9101383	−2.1
28	4	1	4	4	3	1	3	4	14.9115685	−0.4
29	4	1	4	3	3	1	3	3	14.9082203	−1.3
30	4	0	4	5	3	0	3	4	15.0591435	0.0
31	4	0	4	4	3	0	3	3	15.0592321	−0.7
32	4	0	4	3	3	0	3	2	15.0591844	−0.4

No.	J'	K_a'	K_c'	F'	J	K_a	K_c	F	ν_{obs}	$\nu_c - \nu_o$
33	4	0	4	4	3	0	3	4	15.0599237	−1.1
34	4	0	4	3	3	0	3	3	15.0582505	0.0
35	4	2	3	5	3	2	2	4	15.0813227	1.4
36	4	2	3	4	3	2	2	3	15.0815751	−0.8
37	4	2	3	3	3	2	2	2	15.0812571	1.3
38	4	2	3	4	3	2	2	4	15.0815751	−0.8
39	4	2	3	3	3	2	2	3	15.0812571	1.3
40	4	3	2	5	3	3	1	4	15.0878229	−1.4
41	4	3	2	4	3	3	1	3	15.0883452	1.9
42	4	3	2	3	3	3	1	2	15.0876220	1.9
43	4	3	2	3	3	3	1	3	15.0886462	−3.2
44	4	3	1	5	3	3	0	4	15.0880858	−1.0
45	4	3	1	4	3	3	0	3	15.0886037	−0.5
46	4	3	1	3	3	3	0	2	15.0878847	1.8
47	4	3	1	3	3	3	0	3	15.0889116	−1.3
48	4	2	2	5	3	2	1	4	15.1054828	−0.9
49	4	2	2	4	3	2	1	3	15.1056636	1.0
50	4	2	2	3	3	2	1	2	15.1054286	−0.6
51	4	1	3	5	3	1	2	4	15.2468072	0.3
52	4	1	3	4	3	1	2	3	15.2468758	0.2
53	4	1	3	3	3	1	2	2	15.2467431	0.0
54	8	2	7	9	8	1	8	9	8.1379479	−0.3
55	8	2	7	8	8	1	8	8	8.1367986	1.0
56	8	2	7	7	8	1	8	7	8.1380938	0.7
57	9	2	8	9	9	1	9	9	8.5328750	−0.3
58	9	2	8	8	9	1	9	8	8.5341499	1.9
59	10	2	9	11	10	1	10	11	8.9752450	−1.8
60	10	2	9	10	10	1	10	10	8.9741064	−0.2
61	10	2	9	9	10	1	10	9	8.9753611	−0.3
62	3	0	3	4	2	1	2	3	9.2331870	−0.8
63	3	0	3	3	2	1	2	2	9.2326663	1.4
64	3	0	3	2	2	1	2	1	9.2336236	3.1
65	3	0	3	3	2	1	2	3	9.2338786	−1.2
66	3	0	3	2	2	1	2	2	9.2317330	2.4
67	2	1	2	3	1	0	1	2	9.6088075	0.5
68	2	1	2	2	1	0	1	1	9.6094796	−1.3

No.	J'	K_a'	K_c'	F'	J	K_a	K_c	F	ν_{obs}	$\nu_c - \nu_o$
69	2	1	2	1	1	0	1	0	9.6089442	0.8
70	2	1	2	2	1	0	1	2	9.6100214	−0.5
71	2	1	2	1	1	0	1	1	9.6075888	−2.3
72	10	3	7	11	10	2	8	11	10.2679721	−1.1
73	10	3	7	10	10	2	8	10	10.2684014	−0.1
74	10	3	7	9	10	2	8	9	10.2679304	0.2
75	9	3	6	10	9	2	7	10	10.4725104	−0.7
76	9	3	6	9	9	2	7	9	10.4728739	1.0
77	9	3	6	8	9	2	7	8	10.4724720	1.3
78	8	4	4	9	7	5	3	8	10.4508518	−1.0
79	8	4	4	8	7	5	3	7	10.4512517	0.7
80	8	4	4	7	7	5	3	6	10.4507973	−0.9
81	8	3	5	9	8	2	6	9	10.6369714	0.1
82	8	3	5	8	8	2	6	8	10.6372455	1.4
83	8	3	5	7	8	2	6	7	10.6369403	3.3
84	7	3	4	8	7	2	5	8	10.7614169	0.7
85	7	3	4	7	7	2	5	7	10.7615803	0.4
86	7	3	4	6	7	2	5	6	10.7613911	−1.5
87	6	3	3	7	6	2	4	7	10.8493728	0.8
88	6	3	3	6	6	2	4	6	10.8494049	−1.4
89	5	3	2	6	5	2	3	6	10.9067472	2.2
90	5	3	2	5	5	2	3	5	10.9066225	0.5
91	4	3	1	5	4	2	2	5	10.9405859	0.0
92	4	3	1	4	4	2	2	4	10.9402512	−1.1
93	4	3	1	3	4	2	2	3	10.9406719	0.3
94	3	3	0	4	3	2	1	4	10.9579838	1.0
95	3	3	0	3	3	2	1	3	10.9573101	−0.7
96	3	3	0	2	3	2	1	2	10.9582166	−1.4
97	3	3	1	4	3	2	2	4	10.9700793	−0.2
98	3	3	1	3	3	2	2	3	10.9693152	−1.8
99	3	3	1	2	3	2	2	2	10.9703447	−1.6
100	4	3	2	5	4	2	3	5	10.9765820	−0.5
101	4	3	2	4	4	2	3	4	10.9760848	0.4
102	4	3	2	3	4	2	3	3	10.9767091	−1.5
103	5	3	3	6	5	2	4	6	10.9897731	0.5
104	5	3	3	5	5	2	4	5	10.9893957	1.0

No.	J'	K_a'	K_c'	F'	J	K_a	K_c	F	ν_{obs}	$\nu_c - \nu_o$
105	5	3	3	4	5	2	4	4	10.9898506	1.0
106	6	3	4	7	6	2	5	7	11.0127453	0.0
107	6	3	4	6	6	2	5	6	11.0124225	0.9
108	6	3	4	5	6	2	5	5	11.0128013	1.3
109	7	3	5	8	7	2	6	8	11.0490000	1.6
110	7	3	5	7	7	2	6	7	11.0486938	0.0
111	7	3	5	6	7	2	6	6	11.0490407	−1.7
112	7	3	4	8	6	4	3	7	11.0771080	−0.3
113	7	3	4	7	6	4	3	6	11.0774707	1.9
114	7	3	4	6	6	4	3	5	11.0770538	0.5
115	8	3	6	9	8	2	7	9	11.1023142	1.0
116	8	3	6	8	8	2	7	8	11.1020079	1.1
117	8	3	6	7	8	2	7	7	11.1023501	−1.7
118	9	3	7	10	9	2	8	10	11.1766312	1.2
119	9	3	7	9	9	2	8	9	11.1763095	1.0
120	9	3	7	8	9	2	8	8	11.1766664	0.5
121	6	2	4	7	5	3	3	6	11.7911134	1.6
122	6	2	4	6	5	3	3	5	11.7912133	−0.8
123	5	1	4	6	4	2	3	5	12.8894137	−2.6
124	5	1	4	5	4	2	3	4	12.8887820	−1.1
125	5	1	4	4	4	2	3	3	12.8895623	3.4
126	4	0	4	5	3	1	3	4	13.1077798	−1.1
127	4	0	4	4	3	1	3	3	13.1071397	−1.2
128	4	0	4	3	3	1	3	2	13.1080788	1.4
129	4	0	4	4	3	1	3	4	13.1085613	−0.9
130	4	0	4	3	3	1	3	3	13.1061586	0.0
131	3	1	3	4	2	0	2	3	13.2541463	0.4
132	3	1	3	3	2	0	2	2	13.2549522	−0.3
133	3	1	3	2	2	0	2	1	13.2539898	−0.2
134	3	1	3	3	2	0	2	3	13.2555676	0.4
135	3	1	3	2	2	0	2	2	13.2530317	−2.0
136	2	2	1	3	1	1	0	2	14.0805335	1.4
137	2	2	1	2	1	1	0	1	14.0810834	−3.0
138	2	2	1	1	1	1	0	0	14.0791509	−2.3
139	2	2	1	2	1	1	0	2	14.0799527	0.2
140	2	2	1	1	1	1	0	1	14.0819841	−3.9

No.	J'	K_a'	K_c'	F'	J	K_a	K_c	F	ν_{obs}	$\nu_c - \nu_o$
141	2	2	0	3	1	1	1	2	14.1675035	0.7
142	2	2	0	2	1	1	1	1	14.1662965	1.3
143	2	2	0	1	1	1	1	0	14.1687325	−1.4
144	2	2	0	2	1	1	1	2	14.1668856	−2.5
145	2	2	0	1	1	1	1	1	14.1672531	1.6
146	8	3	5	9	7	4	4	8	14.8705855	0.0
147	8	3	5	8	7	4	4	7	14.8708180	−0.1
148	8	3	5	7	7	4	4	6	14.8705595	2.5
149	8	4	4	9	8	3	5	9	15.3125652	0.0
150	8	4	4	8	8	3	5	8	15.3124413	−0.7
151	10	4	7	11	10	3	8	11	15.3160305	−2.0
152	10	4	7	10	10	3	8	10	15.3159292	−0.5
153	10	4	7	9	10	3	8	9	15.3160438	1.0
154	9	4	6	10	9	3	7	10	15.3242086	−1.2
155	9	4	6	9	9	3	7	9	15.3240812	−2.3
156	9	4	6	8	9	3	7	8	15.3242264	2.5
157	7	4	3	8	7	3	4	8	15.3302806	1.6
158	7	4	3	7	7	3	4	7	15.3300867	−0.6
159	8	4	5	9	8	3	6	9	15.3322558	−1.7
160	8	4	5	8	8	3	6	8	15.3320954	−0.1
161	8	4	5	7	8	3	6	7	15.3322763	−1.6
162	7	4	4	8	7	3	5	8	15.3393055	0.7
163	7	4	4	7	7	3	5	7	15.3390897	−0.5
164	7	4	4	6	7	3	5	6	15.3393336	−2.2
165	6	4	2	7	6	3	3	7	15.3412697	−0.4
166	6	4	2	6	6	3	3	6	15.3409875	−1.5
167	6	4	2	5	6	3	3	5	15.3413166	−1.0
168	6	4	3	7	6	3	4	7	15.3449038	−0.3
169	6	4	3	6	6	3	4	6	15.3446103	−0.5
170	6	4	3	5	6	3	4	5	15.3449522	−1.4
171	5	4	1	6	5	3	2	6	15.3477335	1.3
172	5	4	1	5	5	3	2	5	15.3473228	1.5
173	5	4	1	4	5	3	2	4	15.3478185	2.6
174	5	4	2	6	5	3	3	6	15.3489489	−0.8
175	5	4	2	5	5	3	3	5	15.3485327	−0.6
176	5	4	2	4	5	3	3	4	15.3490326	−2.0

No.	J'	K_a'	K_c'	F'	J	K_a	K_c	F	ν_{obs}	$\nu_c - \nu_o$
177	4	4	0	5	4	3	1	5	15.3512860	3.4
178	4	4	0	4	4	3	1	4	15.3506595	0.6
179	4	4	0	3	4	3	1	4	15.3517513	−0.5
180	4	4	1	5	4	3	2	5	15.3515916	3.3
181	4	4	1	4	4	3	2	4	15.3509588	−3.7
182	4	4	1	3	4	3	2	3	15.3517527	3.5
183	4	4	1	4	4	3	2	3	15.3506595	3.1
184	7	2	5	8	6	3	4	7	15.6605957	−0.5
185	7	2	5	7	6	3	4	6	15.6604992	−0.6
186	7	2	5	6	6	3	4	5	15.6606161	1.8
187	4	1	4	5	3	0	3	4	16.8613997	0.3
188	4	1	4	4	3	0	3	3	16.8622391	−0.4
189	4	1	4	3	3	0	3	2	16.8612445	−3.3
190	4	1	4	4	3	0	3	4	16.8629317	0.2
191	4	1	4	3	3	0	3	3	16.8603116	−1.9
192	6	1	5	7	5	2	4	6	16.8977096	−1.4
193	6	1	5	6	5	2	4	5	16.8969783	−2.6
194	6	1	5	5	5	2	4	4	16.8978506	2.4
195	5	0	5	6	4	1	4	5	17.0038854	−1.0
196	5	0	5	5	4	1	4	4	17.0032384	−0.8
197	5	0	5	4	4	1	4	3	17.0041030	3.0
198	5	0	5	5	4	1	4	5	17.0047702	−1.0
199	5	0	5	4	4	1	4	4	17.0021725	−1.5
200	7	2	5	8	6	2	4	7	26.5063026	−2.2
201	7	2	5	7	6	2	4	6	26.5062574	2.3
202	7	2	5	6	6	2	4	5	26.5063169	1.9
203	7	1	6	8	6	1	5	7	26.6557455	1.0
204	7	1	6	7	6	1	5	6	26.6557896	−2.7
205	7	1	6	6	6	1	5	5	26.6557258	−3.6
206	8	1	8	9	7	1	7	8	29.7859748	0.6
207	8	1	8	8	7	1	7	7	29.7860227	−1.4
208	8	1	8	7	7	1	7	6	29.7859981	−1.3
209	8	0	8	9	7	0	7	8	29.9773959	0.3
210	8	0	8	8	7	0	7	7	29.9775272	−0.5
211	9	1	9	10	8	1	8	9	33.4972029	−2.0
212	9	1	9	9	8	1	8	8	33.4972497	−2.8

No.	J'	K_a'	K_c'	F'	J	K_a	K_c	F	ν_{obs}	$\nu_c - \nu_o$
213	9	1	9	8	8	1	8	7	33.4972286	3.8
214	9	0	9	10	8	0	8	9	33.6777953	−0.4
215	9	0	9	9	8	0	8	8	33.6779251	−2.6
216	9	1	8	9	8	1	7	8	34.2356345	−1.7
217	9	1	8	8	8	1	7	7	34.2355703	4.5
218	7	1	7	8	6	0	6	7	27.5126928	2.1
219	7	1	7	7	6	0	6	6	27.5134131	0.6
220	7	1	7	6	6	0	6	5	27.5126104	−0.9
221	6	2	5	7	5	1	4	6	28.5730474	0.8
222	6	2	5	6	5	1	4	5	28.5739168	−0.2
223	6	2	5	5	5	1	4	4	28.5728869	0.5
224	5	3	3	6	4	2	2	5	29.8020844	−0.4
225	5	3	3	5	4	2	2	4	29.8020153	−0.8
226	5	3	3	4	4	2	2	3	29.8021079	4.5
227	8	1	8	9	7	0	7	8	31.0328510	2.5
228	8	1	8	8	7	0	7	7	31.0334922	−1.2
229	8	1	8	7	7	0	7	6	31.0327873	−0.6
230	7	2	6	8	6	1	5	7	32.0927643	1.7
231	7	2	6	6	6	1	5	5	32.0926321	6.9

Table B.5: Observed frequencies ν_{obs} in GHz of the ***anti*** conformer of N-*tert*-butylformamide. $\nu_c - \nu_o$ values in kHz are obtained after a fit with the program XIAM. J, K_a, and K_c are the symmetric top rotational quantum numbers, F is the total angular momentum in the coupled basis with $F = J + I$.

No.	J'	K_a'	K_c'	F'	J	K_a	K_c	F	ν_{obs}	$\nu_c - \nu_o$
1	3	1	3	3	2	1	2	2	9.3840985	−1.4
2	3	1	3	2	2	1	2	1	9.3840522	−0.6
3	3	1	3	3	2	1	2	3	9.3853626	2.0
4	3	0	3	4	2	0	2	3	9.4152267	−2.0
5	3	0	3	3	2	0	2	2	9.4152616	−3.6
6	3	0	3	2	2	0	2	1	9.4153562	−2.2
7	3	0	3	3	2	0	2	3	9.4159560	−2.3
8	3	0	3	2	2	0	2	2	9.4142760	−4.2
9	3	2	2	4	2	2	1	3	9.4155342	0.8
10	3	2	2	3	2	2	1	2	9.4162183	−1.2

No.	J'	K_a'	K_c'	F'	J	K_a	K_c	F	ν_{obs}	$\nu_c - \nu_o$
11	3	2	2	3	2	2	1	3	9.4155342	0.8
12	3	2	2	2	2	2	1	2	9.4162183	−1.2
13	3	2	1	4	2	2	0	3	9.4160183	−2.7
14	3	2	1	3	2	2	0	2	9.4166928	−3.2
15	3	2	1	2	2	2	0	1	9.4156397	−2.6
16	3	2	1	2	2	2	0	2	9.4167163	−4.1
17	3	1	2	4	2	1	1	3	9.4473182	2.7
18	3	1	2	3	2	1	1	2	9.4474780	3.7
19	3	1	2	2	2	1	1	1	9.4471458	4.1
20	3	1	2	3	2	1	1	3	9.4468976	−2.1
21	3	1	2	2	2	1	1	2	9.4480366	1.1
22	4	1	4	5	3	1	3	4	12.5117521	2.2
23	4	1	4	4	3	1	3	3	12.5118620	2.0
24	4	1	4	3	3	1	3	2	12.5118620	2.2
25	4	1	4	4	3	1	3	4	12.5133475	0.0
26	4	1	4	3	3	1	3	3	12.5098556	3.9
27	4	0	4	5	3	0	3	4	12.5530778	−3.9
28	4	0	4	4	3	0	3	3	12.5531088	−4.3
29	4	0	4	3	3	0	3	2	12.5531379	−3.5
30	4	0	4	4	3	0	3	4	12.5538388	−3.9
31	4	0	4	3	3	0	3	3	12.5521509	−5.5
32	4	2	3	5	3	2	2	4	12.5540788	11.9
33	4	2	3	4	3	2	2	3	12.5543715	11.9
34	4	2	3	3	3	2	2	2	12.5540060	14.4
35	4	2	3	4	3	2	2	4	12.5543715	11.9
36	4	2	3	3	3	2	2	3	12.5540060	14.4
37	4	3	2	5	3	3	1	4	12.5542335	−0.2
38	4	3	2	4	3	3	1	3	12.5548609	−3.9
39	4	3	2	3	3	3	1	2	12.5539852	−3.4
40	4	3	2	3	3	3	1	3	12.5551938	1.5
41	4	3	1	5	3	3	0	4	12.5542379	1.6
42	4	3	1	4	3	3	0	3	12.5548706	3.2
43	4	3	1	3	3	3	0	2	12.5539942	2.9
44	4	3	1	4	3	3	0	4	12.5539725	−3.3
45	4	3	1	3	3	3	0	3	12.5551938	−1.2
46	4	2	2	5	3	2	1	4	12.5552771	−5.5

No.	J'	K_a'	K_c'	F'	J	K_a	K_c	F	ν_{obs}	$\nu_c - \nu_o$
47	4	2	2	4	3	2	1	3	12.5555553	−4.9
48	4	2	2	3	3	2	1	2	12.5552044	−5.2
49	4	2	2	4	3	2	1	4	12.5555353	−6.8
50	4	2	2	3	3	2	1	3	12.5552273	−6.7
51	4	1	3	5	3	1	2	4	12.5962917	1.4
52	4	1	3	4	3	1	2	3	12.5963596	2.4
53	4	1	3	3	3	1	2	2	12.5962360	1.5
54	4	1	3	4	3	1	2	4	12.5959394	−2.1
55	4	1	3	3	3	1	2	3	12.5967951	−0.6
56	5	1	5	6	4	1	4	5	15.6394827	1.9
57	5	1	5	5	4	1	4	4	15.6395452	−1.7
58	5	1	5	4	4	1	4	3	15.6395514	−1.3
59	5	1	5	5	4	1	4	5	15.6411426	−1.8
60	5	1	5	4	4	1	4	4	15.6375438	−0.6
61	5	0	5	6	4	0	4	5	15.6904334	−5.7
62	5	0	5	5	4	0	4	4	15.6904615	−8.1
63	5	0	5	5	4	0	4	5	15.6912231	−7.5
64	5	0	5	4	4	0	4	4	15.6895078	−9.0
65	5	2	4	6	4	2	3	5	15.6924907	21.2
66	5	2	4	5	4	2	3	4	15.6926413	16.8
67	5	2	4	4	4	2	3	3	15.6924738	20.3
68	5	2	4	5	4	2	3	5	15.6929299	12.6
69	5	4	2	6	4	4	1	5	15.6926283	0.9
70	5	4	2	5	4	4	1	4	15.6931964	−3.6
71	5	4	2	4	4	4	1	3	15.6924564	0.1
72	5	4	1	6	4	4	0	5	15.6926283	0.9
73	5	4	1	5	4	4	0	4	15.6931964	−3.7
74	5	4	1	4	4	4	0	3	15.6924564	0.1
75	5	3	3	6	4	3	2	5	15.6929866	−6.6
76	5	3	3	5	4	3	2	4	15.6933118	−6.8
77	5	3	3	4	4	3	2	3	15.6929116	−1.4
78	5	3	3	5	4	3	2	5	15.6930563	−1.8
79	5	3	2	6	4	3	1	5	15.6930000	−2.4
80	5	3	2	5	4	3	1	4	15.6933256	−2.0
81	5	3	2	4	4	3	1	3	15.6929197	−2.5
82	5	3	2	5	4	3	1	5	15.6930666	−0.4

No.	J'	K_a'	K_c'	F'	J	K_a	K_c	F	ν_{obs}	$\nu_c - \nu_o$
83	5	2	3	6	4	2	2	5	15.6948918	−5.5
84	5	2	3	5	4	2	2	4	15.6950300	−3.0
85	5	2	3	4	4	2	2	3	15.6948783	−5.2
86	5	1	4	6	4	1	3	5	15.7451238	−2.5
87	5	1	4	5	4	1	3	4	15.7451622	−0.4
88	5	1	4	4	4	1	3	3	15.7451003	0.0

Appendix C

N-Ethylacetamide

Table C.1: Nuclear coordinates (in Å) in the principal axis system of the conformer **I** of N-ethylacetamide, calculated at the MP2/6-311++G(d,p) level of theory.

	a	*b*	*c*
N_1	−0.136448	−0.780541	−0.281853
H_2	−0.010632	−1.743798	−0.010497
C_3	0.890097	0.097121	−0.057068
O_4	0.761483	1.306930	−0.210693
C_5	2.202497	−0.527711	0.376736
H_6	2.427844	−0.191867	1.392088
H_7	2.189458	−1.620045	0.353492
H_8	2.993380	−0.161325	−0.280669
C_9	−1.481451	−0.299840	−0.567588
H_{10}	−1.386037	0.517559	−1.286076
H_{11}	−2.027573	−1.114776	−1.051312
C_{12}	−2.214489	0.184261	0.682041
H_{13}	−1.660798	1.005887	1.141553
H_{14}	−3.216029	0.541440	0.422816
H_{15}	−2.315090	−0.626767	1.409608

Table C.2: Observed frequencies ν_{obs} in GHz of conformer I of N-ethylacetamide. $\nu_{X/B} - \nu_o$ values in kHz are obtained after a fit with the programs XIAM (ν_X) and BELGI(ν_B). J, K_a, and K_c are the symmetric top rotational quantum numbers, F is the total angular momentum in the coupled basis with $F = J + I$.

No.	J'	K_a'	K_c'	F'	J	K_a	K_c	F	sym.	ν_{obs}	$\nu_X - \nu_o$	$\nu_B - \nu_o$
1	3	0	3	4	2	1	2	3	A	7.368828	−7.5	0
2	3	0	3	3	2	1	2	2	A	7.368363	2.0	1
3	3	0	3	2	2	1	2	1	A	7.369229	−0.2	−1
4	3	0	3	3	2	1	2	3	A	7.369516	0.3	−1
5	3	0	3	2	2	1	2	2	A	7.367433	0.6	1
6	2	1	2	3	1	1	1	2	A	8.003482	−0.1	−2
7	2	1	2	1	1	1	1	0	A	8.003667	−0.6	−1
8	2	0	2	3	1	0	1	2	A	8.240999	4.1	1
9	2	0	2	2	1	0	1	1	A	8.241072	−4.5	−4
10	2	0	2	1	1	0	1	0	A	8.241456	1.7	2
11	2	0	2	2	1	0	1	2	A	8.241604	0.8	1
12	2	0	2	1	1	0	1	1	A	8.240137	0.0	2
13	6	1	5	7	5	2	4	6	A	11.224878	5.8	1
14	6	1	5	6	5	2	4	5	A	11.224208	−1.5	0
15	6	1	5	5	5	2	4	4	A	11.225004	−0.5	1
16	4	0	4	5	3	1	3	4	A	11.783164	−6.4	1
17	4	0	4	4	3	1	3	3	A	11.782592	−0.6	0
18	4	0	4	3	3	1	3	2	A	11.783434	−2.0	−1
19	4	0	4	4	3	1	3	4	A	11.783950	0.5	0
20	4	0	4	3	3	1	3	3	A	11.781603	−1.8	0
21	3	1	3	4	2	1	2	3	A	12.000107	2.8	1
22	3	1	3	3	2	1	2	2	A	12.000306	−2.7	−2
23	3	1	3	3	2	1	2	3	A	12.001462	−1.3	−1
24	3	0	3	4	2	0	2	3	A	12.340277	2.0	−2
25	3	0	3	3	2	0	2	2	A	12.340364	3.1	1
26	3	0	3	2	2	0	2	1	A	12.340375	3.2	2
27	3	0	3	3	2	0	2	3	A	12.340968	2.7	0
28	3	2	2	4	2	2	1	3	A	12.374025	3.7	1
29	3	2	2	3	2	2	1	2	A	12.374589	−0.7	0
30	3	2	2	2	2	2	1	1	A	12.373710	−1.8	0
31	3	2	2	3	2	2	1	3	A	12.374025	0.0	1
32	3	2	2	2	2	2	1	2	A	12.374589	−0.7	0

No.	J'	K_a'	K_c'	F'	J	K_a	K_c	F	sym.	ν_{obs}	$\nu_X - \nu_o$	$\nu_B - \nu_o$
33	3	2	1	4	2	2	0	3	A	12.407984	3.9	0
34	3	2	1	3	2	2	0	2	A	12.408486	0.2	0
35	3	2	1	2	2	2	0	1	A	12.407685	0.7	2
36	3	1	2	4	2	1	1	3	A	12.737619	9.0	3
37	3	1	2	3	2	1	1	2	A	12.737752	−4.5	−1
38	3	1	2	2	2	1	1	1	A	12.737442	−7.1	−4
39	3	1	2	3	2	1	1	3	A	12.737164	−1.8	1
40	3	1	2	2	2	1	1	2	A	12.738365	−3.8	0
41	2	1	2	3	1	0	1	2	A	13.212449	13.6	−1
42	2	1	2	2	1	0	1	1	A	13.213074	−2.6	−3
43	2	1	2	1	1	0	1	0	A	13.212600	3.5	2
44	2	1	2	2	1	0	1	2	A	13.213604	0.2	−1
45	2	1	2	1	1	0	1	1	A	13.211276	−3.5	−3
46	7	2	5	8	7	1	6	8	A	13.707604	3.3	−2
47	7	2	5	7	7	1	6	7	A	13.707847	3.4	1
48	7	2	5	6	7	1	6	6	A	13.707573	3.7	2
49	7	2	5	7	7	1	6	6	A	13.707589	−5.0	−1
50	6	2	4	7	6	1	5	7	A	14.065234	−3.1	−1
51	6	2	4	6	6	1	5	6	A	14.065586	1.2	0
52	6	2	4	5	6	1	5	5	A	14.065175	0.4	−1
53	5	2	3	6	5	1	4	6	A	14.481094	−3.9	2
54	5	2	3	5	5	1	4	5	A	14.481516	−4.3	−2
55	5	2	3	4	5	1	4	4	A	14.481005	−2.1	0
56	4	2	2	5	4	1	3	5	A	14.908596	−6.4	1
57	4	2	2	4	4	1	3	4	A	14.909041	1.4	2
58	4	2	2	3	4	1	3	3	A	14.908483	1.4	2
59	3	2	1	4	3	1	2	4	A	15.305109	−5.1	1
60	3	2	1	3	3	1	2	3	A	15.305459	−0.5	1
61	3	2	1	2	3	1	2	2	A	15.304986	−0.2	1
62	2	2	0	3	2	1	1	3	A	15.634742	−1.7	2
63	2	2	0	2	2	1	1	2	A	15.634729	0.0	3
64	2	2	0	1	2	1	1	1	A	15.634746	−3.6	−2
65	2	2	0	3	2	1	1	2	A	15.635328	−4.9	−2
66	2	2	0	2	2	1	1	1	A	15.633804	−5.4	−3
67	4	1	4	5	3	1	3	4	A	15.990591	1.4	1
68	4	1	4	4	3	1	3	3	A	15.990700	−0.3	1

No.	J'	K_a'	K_c'	F'	J	K_a	K_c	F	sym.	ν_{obs}	$\nu_X - \nu_o$	$\nu_B - \nu_o$
69	4	1	4	3	3	1	3	2	A	15.990685	−3.7	−2
70	7	1	6	8	6	2	5	7	A	16.124551	−4.2	2
71	7	1	6	7	6	2	5	6	A	16.123838	−2.6	−1
72	7	1	6	6	6	2	5	5	A	16.124662	−3.1	−1
73	5	0	5	6	4	1	4	5	A	16.248916	−9.9	0
74	5	0	5	5	4	1	4	4	A	16.248350	0.3	0
75	5	0	5	4	4	1	4	3	A	16.249107	−2.4	−3
76	5	0	5	5	4	1	4	5	A	16.249815	−1.1	−3
77	5	0	5	4	4	1	4	4	A	16.247266	−0.1	1
78	2	2	1	3	2	1	2	3	A	16.364264	1.7	1
79	2	2	1	2	2	1	2	2	A	16.362542	−2.7	−1
80	2	2	1	1	2	1	2	1	A	16.365220	0.9	1
81	2	2	1	3	2	1	2	2	A	16.363108	−0.6	1
82	2	2	1	2	2	1	2	1	A	16.364340	−1.7	−1
83	2	2	1	2	2	1	2	3	A	16.363692	−7.7	−6
84	2	2	1	1	2	1	2	2	A	16.363419	−3.3	−3
85	4	0	4	5	3	0	3	4	A	16.414443	4.6	3
86	4	0	4	4	3	0	3	3	A	16.414537	−4.3	−1
87	4	0	4	3	3	0	3	2	A	16.414476	−5.9	−3
88	4	0	4	4	3	0	3	4	A	16.415225	−4.2	−2
89	4	0	4	3	3	0	3	3	A	16.413548	−4.7	−1
90	4	2	3	5	3	2	2	4	A	16.492054	−1.4	−1
91	4	2	3	4	3	2	2	3	A	16.492305	2.0	1
92	4	2	3	3	3	2	2	2	A	16.491990	0.3	0
93	4	2	3	4	3	2	2	4	A	16.492305	2.0	1
94	4	2	3	3	3	2	2	3	A	16.491990	0.3	0
95	3	2	2	4	3	1	3	4	A	16.738180	0.2	−2
96	3	2	2	3	3	1	3	3	A	16.736824	1.5	1
97	3	2	2	2	3	1	3	2	A	16.738656	1.7	0
98	3	2	2	4	3	1	3	3	A	16.736824	1.5	1
99	3	2	2	3	3	1	3	2	A	16.738656	1.7	0
100	3	2	2	3	3	1	3	4	A	16.738180	0.0	−2
101	3	2	2	2	3	1	3	3	A	16.736824	1.5	1
102	3	1	3	4	2	0	2	3	A	16.971557	13.5	1
103	3	1	3	3	2	0	2	2	A	16.972310	0.1	1
104	3	1	3	2	2	0	2	1	A	16.971414	−3.9	−3

No.	J'	K_a'	K_c'	F'	J	K_a	K_c	F	sym.	ν_{obs}	$\nu_X - \nu_o$	$\nu_B - \nu_o$
105	3	1	3	3	2	0	2	3	A	16.972913	−0.6	0
106	3	1	3	2	2	0	2	2	A	16.970474	−4.3	−2
107	4	2	3	5	4	1	4	5	A	17.239647	2.0	1
108	4	2	3	4	4	1	4	4	A	17.238428	−1.9	−1
109	4	2	3	3	4	1	4	3	A	17.239958	−2.0	−1
110	5	2	4	6	5	1	5	6	A	17.870569	−0.8	1
111	5	2	4	5	5	1	5	5	A	17.869414	−1.3	0
112	5	2	4	4	5	1	5	4	A	17.870802	−1.5	−1
113	4	1	4	5	3	0	3	4	A	20.621868	9.9	1
114	4	1	4	4	3	0	3	3	A	20.622646	−1.1	0
115	4	1	4	3	3	0	3	2	A	20.621731	−0.6	1
116	4	1	4	4	3	0	3	4	A	20.623334	−1.1	−1
117	4	1	4	3	3	0	3	3	A	20.620802	−1.4	1
118	6	0	6	7	5	1	5	6	A	20.736418	−14.6	1
119	6	0	6	6	5	1	5	5	A	20.735902	−0.1	1
120	6	0	6	5	5	1	5	4	A	20.736559	−0.7	0
121	2	2	1	3	1	1	0	2	A	24.121593	2.7	2
122	2	2	1	2	1	1	0	1	A	24.122106	−0.7	1
123	2	2	1	1	1	1	0	0	A	24.120290	1.2	3
124	2	2	1	2	1	1	0	2	A	24.121027	−1.2	1
125	2	2	1	1	1	1	0	1	A	24.122983	−0.9	0
126	5	1	5	6	4	0	4	5	A	24.180782	2.8	−1
127	5	1	5	5	4	0	4	4	A	24.181540	1.1	0
128	5	1	5	4	4	0	4	3	A	24.180673	3.5	2
129	2	2	0	3	1	1	1	2	A	24.376261	5.1	2
130	2	2	0	2	1	1	1	1	A	24.375104	−0.9	2
131	2	2	0	1	1	1	1	0	A	24.377419	−5.1	−3
132	2	2	0	2	1	1	1	2	A	24.375654	−2.8	0
133	2	2	0	1	1	1	1	1	A	24.376044	−0.2	1
134	6	1	6	7	5	0	5	6	A	27.671575	−1.8	0
135	6	1	6	6	5	0	5	5	A	27.672286	4.8	5
136	6	1	6	5	5	0	5	4	A	27.671483	−4.3	−4
137	3	2	2	4	2	1	1	3	A	28.000252	−1.9	0
138	3	2	2	3	2	1	1	2	A	28.000843	0.1	1
139	3	2	2	2	2	1	1	1	A	27.999921	−3.3	−3
140	3	2	2	3	2	1	1	3	A	28.000252	0.0	0

No.	J'	K_a'	K_c'	F'	J	K_a	K_c	F	sym.	ν_{obs}	$\nu_X - \nu_o$	$\nu_B - \nu_o$
141	3	2	2	2	2	1	1	2	A	28.000843	0.1	1
142	3	2	1	4	2	1	2	3	A	28.780761	6.8	2
143	3	2	1	3	2	1	2	2	A	28.779501	−1.5	1
144	3	2	1	2	2	1	2	1	A	28.781438	−0.8	1
145	4	2	3	5	3	1	2	4	A	31.754693	−5.9	2
146	4	2	3	4	3	1	2	3	A	31.755393	−2.5	0
147	4	2	3	3	3	1	2	2	A	31.754468	−1.7	0
148	5	2	4	6	4	1	3	5	A	35.385963	−17.4	0
149	5	2	4	5	4	1	3	4	A	35.386735	−1.3	−1
150	5	2	4	4	4	1	3	3	A	35.385782	−3.5	−3
151	2	0	2	3	1	0	1	2	E	8.121143	−32.9	1
152	2	0	2	2	1	0	1	1	E	8.121206	0.2	1
153	2	0	2	1	1	0	1	0	E	8.121552	5.1	7
154	2	0	2	2	1	0	1	2	E	8.121676	0.9	2
155	2	0	2	1	1	0	1	1	E	8.120378	−0.9	0
156	2	1	2	3	1	1	1	2	E	8.287579	34.1	0
157	2	1	2	2	1	1	1	1	E	8.288200	2.4	3
158	2	1	2	1	1	1	1	0	E	8.287082	0.6	0
159	2	1	2	2	1	1	1	2	E	8.288040	−0.5	−1
160	2	1	2	1	1	1	1	1	E	8.287483	−2.5	−1
161	2	1	1	3	2	0	2	3	E	8.407388	1.0	−2
162	2	1	1	2	2	0	2	2	E	8.407027	−0.1	−2
163	2	1	1	2	2	0	2	1	E	8.407856	6.3	4
164	2	1	1	2	2	0	2	3	E	8.407560	4.4	2
165	2	1	1	1	2	0	2	2	E	8.406759	2.6	2
166	3	1	2	4	3	0	3	4	E	8.671701	20.3	3
167	3	1	2	3	3	0	3	3	E	8.671333	0.0	3
168	3	1	2	3	3	0	3	2	E	8.672152	−0.3	1
169	3	1	2	3	3	0	3	4	E	8.671939	−6.7	−5
170	4	1	3	5	4	0	4	5	E	9.086931	16.6	−1
171	4	1	3	4	4	0	4	4	E	9.086438	3.6	3
172	4	1	3	3	4	0	4	3	E	9.087058	−3.2	−5
173	4	1	3	5	4	0	4	4	E	9.086228	1.8	2
174	4	1	3	4	4	0	4	3	E	9.087322	1.5	−1
175	3	0	3	4	2	1	2	3	E	9.759670	102.9*	8
176	3	0	3	3	2	1	2	2	E	9.759815	−3.8	4

No.	J'	K_a'	K_c'	F'	J	K_a	K_c	F	sym.	ν_{obs}	$\nu_X - \nu_o$	$\nu_B - \nu_o$
177	3	0	3	3	2	1	2	3	E	9.760276	−2.8	4
178	3	0	3	2	2	1	2	2	E	9.758996	−8.3	1
179	4	1	4	5	3	1	2	4	E	10.330832	−20.1	−3
180	4	1	4	4	3	1	2	3	E	10.331571	2.7	1
181	4	1	4	3	3	1	2	2	E	10.330664	0.5	−3
182	2	1	2	3	1	0	1	2	E	10.541531	−167.6*	1
183	2	1	2	2	1	0	1	1	E	10.541523	5.2	6
184	2	1	2	1	1	0	1	0	E	10.541979	1.9	4
185	2	1	2	2	1	0	1	2	E	10.541992	−2.7	−2
186	2	1	2	1	1	0	1	1	E	10.540805	−3.1	−2
187	6	1	6	7	5	2	4	6	E	11.380290	10.3	−1
188	6	1	6	6	5	2	4	5	E	11.381424	5.7	8
189	6	1	6	5	5	2	4	4	E	11.380105	0.7	−1
190	3	0	3	4	2	0	2	3	E	12.180058	−40.1	0
191	3	0	3	2	2	0	2	1	E	12.180141	4.4	5
192	3	0	3	3	2	0	2	3	E	12.180664	−0.4	−1
193	3	0	3	2	2	0	2	2	E	12.179313	0.0	1
194	1	1	0	2	0	0	0	1	E	12.311462	−38.1	−1
195	1	1	0	0	0	0	0	1	E	12.311924	−1.5	−3
196	1	1	0	1	0	0	0	1	E	12.311154	0.6	1
197	3	1	3	4	2	1	2	3	E	12.367061	45.1	0
198	3	1	3	3	2	1	2	2	E	12.367353	−0.7	0
199	3	1	3	2	2	1	2	1	E	12.367054	7.6	7
200	3	1	3	3	2	1	2	3	E	12.367814	−0.4	0
201	3	1	3	2	2	1	2	2	E	12.366337	−4.1	−4
202	3	2	1	4	2	2	0	3	E	12.379955	−36.2	−1
203	3	2	1	3	2	2	0	2	E	12.380498	1.7	0
204	3	2	1	2	2	2	0	1	E	12.379644	2.5	2
205	3	2	2	4	2	2	1	3	E	12.401615	29.2	−2
206	3	2	2	3	2	2	1	2	E	12.402124	−0.2	−3
207	3	2	2	2	2	2	1	1	E	12.401319	1.4	0
208	3	2	2	3	2	2	1	3	E	12.401549	0.2	−2
209	3	2	2	2	2	2	1	2	E	12.402213	0.9	−1
210	2	2	1	3	2	1	2	3	E	12.426570	29.2	−6
211	2	2	1	2	2	1	2	2	E	12.425534	6.6	1
212	2	2	1	1	2	1	2	1	E	12.427145	3.7	−3

No.	J'	K_a'	K_c'	F'	J	K_a	K_c	F	sym.	ν_{obs}	$\nu_X - \nu_o$	$\nu_B - \nu_o$
213	2	2	1	3	2	1	2	2	E	12.426109	2.9	−3
214	2	2	1	2	2	1	2	1	E	12.426251	7.0	1
215	2	2	1	2	2	1	2	3	E	12.425995	16.4	10
216	2	2	1	1	2	1	2	2	E	12.426428	−5.9	−12
217	3	1	2	4	2	1	1	3	E	12.444371	−24.4	1
218	3	1	2	3	2	1	1	2	E	12.444437	0.0	1
219	3	1	2	2	2	1	1	1	E	12.444383	2.4	3
220	3	1	2	3	2	1	1	3	E	12.444609	5.5	6
221	3	2	2	4	3	1	3	4	E	12.461124	21.5	0
222	3	2	2	3	3	1	3	3	E	12.460305	5.9	6
223	3	2	2	2	3	1	3	2	E	12.461410	−2.4	−2
224	3	2	2	4	3	1	3	3	E	12.460371	−7.4	−7
225	3	2	2	3	3	1	3	2	E	12.461321	2.5	2
226	3	2	2	3	3	1	3	4	E	12.461057	5.6	5
227	3	2	2	2	3	1	3	3	E	12.460394	6.5	7
228	4	2	3	5	4	1	4	5	E	12.624365	6.8	0
229	4	2	3	4	4	1	4	4	E	12.623504	2.1	1
230	4	2	3	3	4	1	4	3	E	12.624586	1.3	2
231	4	2	3	4	4	1	4	3	E	12.624734	−19.6	2
232	5	2	4	6	5	1	5	6	E	12.973445	−0.2	3
233	5	2	4	5	5	1	5	5	E	12.972462	−3.6	−3
234	5	2	4	4	5	1	5	4	E	12.973645	−1.1	2
235	6	2	5	7	6	1	6	7	E	13.545861	13.7	6
236	6	2	5	6	6	1	6	6	E	13.544744	−6.7	−3
237	6	2	5	5	6	1	6	5	E	13.546049	−6.0	1
238	4	0	4	5	3	1	3	4	E	13.614640	2.9	−8
239	4	0	4	4	3	1	3	3	E	13.614591	10.1	0
240	4	0	4	4	3	1	3	4	E	13.615343	4.9	−5
241	4	0	4	3	3	1	3	3	E	13.613707	0.5	−7
242	2	1	1	3	1	1	1	2	E	14.274579	171.4*	0
243	2	1	1	2	1	1	1	1	E	14.274911	4.7	5
244	2	1	1	1	1	1	1	0	E	14.274242	−4.9	−6
245	2	1	1	1	1	1	1	1	E	14.274643	3.1	4
246	6	0	6	7	5	1	4	6	E	14.497478	14.1	2
247	6	0	6	6	5	1	4	5	E	14.498287	−0.8	−1
248	6	0	6	5	5	1	4	4	E	14.497347	1.6	4

No.	J'	K_a'	K_c'	F'	J	K_a	K_c	F	sym.	ν_{obs}	$\nu_X - \nu_o$	$\nu_B - \nu_o$
249	3	1	3	4	2	0	2	3	E	14.787449	−85.4*	4
250	3	1	3	3	2	0	2	2	E	14.787669	−0.9	4
251	3	1	3	3	2	0	2	3	E	14.788202	−5.8	−1
252	3	1	3	2	2	0	2	2	E	14.786653	−4.1	1
253	3	2	2	4	3	0	3	4	E	15.068515	−29.6	−2
254	3	2	2	3	3	0	3	3	E	15.067842	1.0	0
255	3	2	2	2	3	0	3	2	E	15.068751	−0.1	−2
256	4	0	4	5	3	0	3	4	E	16.222032	−40.1	−2
257	4	0	4	4	3	0	3	3	E	16.222128	−1.2	−4
258	4	0	4	3	3	0	3	2	E	16.222063	−2.2	−4
259	4	0	4	4	3	0	3	4	E	16.222735	−2.1	−6
260	4	0	4	3	3	0	3	3	E	16.221244	−0.1	0
261	4	1	4	5	3	1	3	4	E	16.395141	47.7	−2
262	4	1	4	4	3	1	3	3	E	16.395367	1.0	−1
263	4	1	4	3	3	1	3	2	E	16.395153	5.8	3
264	4	1	4	4	3	1	3	4	E	16.396119	2.0	0
265	4	1	4	3	3	1	3	3	E	16.394137	5.2	2
266	4	2	3	5	3	2	2	4	E	16.558383	33.2	−2
267	4	2	3	4	3	2	2	3	E	16.558566	−0.5	−3
268	4	2	3	3	3	2	2	2	E	16.558330	0.3	−2
269	4	1	4	5	3	0	3	4	E	19.002533	−3.8	−5
270	4	1	4	4	3	0	3	3	E	19.002904	3.6	1
271	4	1	4	4	3	0	3	4	E	19.003511	0.9	−3
272	4	1	4	3	3	0	3	3	E	19.001675	2.8	−1
273	2	1	1	3	1	0	1	2	E	16.528531	−30.8	0
274	2	1	1	2	1	0	1	1	E	16.528234	−2.1	−2
275	2	1	1	1	1	0	1	1	E	16.527966	−3.3	−3

* not included in the fit

Table C.3: Energy values in hartree, rotational constants in GHz and their deviations to the experimental values dev_A, dev_B, dev_C of conformer **I** of N-ethylacetamide optimized at different level of theory.

	E	A	dev_A	B	dev_B	C	dev_C
MP2							
6-31+G(d,p)	−286.9909	7.137	0.134	2.204	−0.021	1.956	−0.017
6-311++G(3d,3p)	−287.1820	7.188	0.082	2.214	−0.031	1.966	−0.028
6-311++G(df,pd)	−287.2096	7.143	0.127	2.226	−0.042	1.979	−0.041
6-311+G(2df,2pd)	−287.2681	7.272	−0.002	2.215	−0.032	1.963	−0.024
6-311+G(d,p)	−287.0946	7.095	0.175	2.213	−0.029	1.968	−0.029
6-311G(d,p)	−287.0831	7.071	0.199	2.208	−0.024	1.970	−0.031
6-31G(2df,2pd)	−287.1696	7.124	0.146	2.243	−0.059	1.992	−0.053
6-31G(3df,3pd)	−287.1948	7.090	0.180	2.249	−0.065	2.000	−0.062
cc-pVDZ	−286.9773	6.935	0.335	2.205	−0.022	1.970	−0.031
B3LYP							
6-311++G(d,p)	−287.9332	7.409	−0.139	2.078	0.106	1.855	0.084
cc-pVTZ	−287.9598	7.443	−0.173	2.090	0.093	1.865	0.074
HF							
6-31+G(3d,3p)	−286.0858	7.446	−0.176	2.153	0.030	1.930	0.009
6-311++G(2df,2pd)	−286.1479	7.524	−0.254	2.155	0.028	1.927	0.011
6-311++G(3d,3p)	−286.1415	7.456	−0.186	2.154	0.029	1.932	0.007
6-311++G(d,p)	−286.1260	7.481	−0.211	2.147	0.036	1.922	0.017
6-311+G(d,p)	−286.1259	7.482	−0.212	2.147	0.036	1.921	0.017
6-311+G(df,pd)	−286.1373	7.524	−0.253	2.151	0.033	1.922	0.016
6-311G(3df,3pd)	−286.1477	7.421	−0.151	2.175	0.008	1.947	−0.008
6-311G(df,pd)	−286.1318	7.485	−0.214	2.159	0.024	1.932	0.007
6-31G(3df,3pd)	−286.0878	7.387	−0.117	2.175	0.009	1.945	−0.006
6-31G(d,p)	−286.0606	7.380	−0.110	2.166	0.018	1.939	0.000
Experiment		7.2702759(93)		2.1835536(24)		1.9387113(18)	

Appendix D

N-*tert*-Butylacetamide

Table D.1: Nuclear coordinates (in Å) in the principal axis system of the ***trans*** and the ***cis*** conformers of N-*tert*-butylacetamide, calculated at the MP2/6-311++G(d,p) level of theory.

	trans			*cis*		
	a	*b*	*c*	*a*	*b*	*c*
N_1	−0.228763	0.676193	0.000006	−0.214485	−0.650511	−0.153353
H_2	−0.279575	1.684478	0.000338	−0.221661	−1.664387	−0.126429
C_3	−1.412621	−0.008867	−0.000003	−1.495202	−0.161740	−0.023786
O_4	−1.485542	−1.234037	−0.000030	−2.446629	−0.938094	0.006943
C_5	−2.658204	0.861687	−0.000025	−1.712138	1.338304	0.004664
H_6	−3.251624	0.612901	0.882865	−2.742083	1.512010	0.315830
H_7	−2.443937	1.933254	0.000006	−1.033370	1.853906	0.685151
H_8	−3.251518	0.612947	−0.883001	−1.572520	1.749501	−0.998956
C_9	1.109306	0.064551	0.000013	1.109060	−0.027356	0.007841
C_{10}	2.109256	1.221249	−0.000267	1.310956	1.147742	−0.955839
H_{11}	1.982510	1.845144	0.891899	0.713890	2.019331	−0.683900
H_{12}	3.130576	0.829919	−0.000317	2.363648	1.449298	−0.939064
H_{13}	1.982292	1.844853	−0.892602	1.051019	0.847118	−1.975560
C_{14}	1.298849	−0.784712	1.261315	1.351168	0.406856	1.459911
H_{15}	2.309687	−1.206377	1.274512	2.359253	0.822253	1.567293
H_{16}	1.168252	−0.165343	2.154880	0.636159	1.170262	1.777193
H_{17}	0.574330	−1.600685	1.286948	1.254697	−0.452335	2.131160
C_{18}	1.298794	−0.785110	−1.261021	2.115007	−1.124272	−0.357805
H_{19}	1.168046	−0.166058	−2.154783	1.976538	−1.439513	−1.396922
H_{20}	2.309720	−1.206579	−1.274141	3.136511	−0.752345	−0.237696
H_{21}	0.574443	−1.601227	−1.286348	1.991207	−1.995687	0.295193

Table D.2: Observed frequencies ν_{obs} in GHz N-*tert*-butylacetamide. $\nu_{X/B} - \nu_o$ values in kHz are obtained after a fit with the programs XIAM (ν_X) and BELGI (ν_B). J, K_a, and K_c are the symmetric top rotational quantum numbers, F is the total angular momentum in the coupled basis with $F = J + I$.

No.	J'	K_a'	K_c'	F'	J	K_a	K_c	F	sym.	ν_{obs}	$\nu_X - \nu_o$	$\nu_B - \nu_o$
1	3	1	2	4	2	1	1	3	A	8.0059200	−6.9	−4
2	3	1	2	3	2	1	1	2	A	8.0060862	−5.4	−2
3	3	1	2	2	2	1	1	1	A	8.0057391	−4.2	−1
4	3	1	2	3	2	1	1	3	A	8.0054819	2.8	6
5	3	1	2	2	2	1	1	2	A	8.0066921	−4.2	−1
6	4	0	4	5	3	1	3	4	A	8.6961228	−9.2	0
7	4	0	4	4	3	1	3	3	A	8.6955903	−8.1	1
8	4	0	4	3	3	1	3	2	A	8.6964026	−5.2	4
9	4	0	4	4	3	1	3	4	A	8.6970833	−7.8	2
10	4	0	4	3	3	1	3	3	A	8.6943846	−8.1	1
11	3	1	3	4	2	0	2	3	A	9.4601087	2.3	−1
12	3	1	3	3	2	0	2	2	A	9.4608950	1.4	−2
13	3	1	3	2	2	0	2	1	A	9.4599758	−0.2	−3
14	3	1	3	3	2	0	2	3	A	9.4616011	2.0	−1
15	3	1	3	2	2	0	2	2	A	9.4588780	−0.4	−4
16	4	1	4	5	3	1	3	4	A	10.1549652	−2.1	0
17	4	1	4	4	3	1	3	3	A	10.1550970	−0.1	2
18	4	1	4	3	3	1	3	2	A	10.1550689	−3.6	−1
19	4	1	4	4	3	1	3	4	A	10.1565880	−1.8	1
20	4	1	4	3	3	1	3	3	A	10.1530543	−3.1	−1
21	4	0	4	5	3	0	3	4	A	10.3631091	−3.1	0
22	4	0	4	4	3	0	3	3	A	10.3632484	−1.5	1
23	4	0	4	3	3	0	3	2	A	10.3631492	−3.9	−1
24	4	0	4	4	3	0	3	4	A	10.3640685	−2.8	0
25	4	0	4	3	3	0	3	3	A	10.3620394	−4.8	−2
26	4	2	3	5	3	2	2	4	A	10.4183974	0.7	4
27	4	2	3	4	3	2	2	3	A	10.4186836	−2.2	1
28	4	2	3	3	3	2	2	2	A	10.4183190	−3.4	0
29	4	2	3	4	3	2	2	4	A	10.4186836	−2.2	1
30	4	2	3	3	3	2	2	3	A	10.4183190	−3.4	0
31	4	2	2	5	3	2	1	4	A	10.4785044	0.1	−1
32	4	2	2	4	3	2	1	3	A	10.4786720	1.0	0

No.	J'	K_a'	K_c'	F'	J	K_a	K_c	F	sym.	ν_{obs}	$\nu_X - \nu_o$	$\nu_B - \nu_o$
33	4	2	2	3	3	2	1	2	A	10.4784490	1.5	1
34	4	1	3	5	3	1	2	4	A	10.6670292	−5.2	−3
35	4	1	3	4	3	1	2	3	A	10.6671199	−4.6	−2
36	4	1	3	3	3	1	2	2	A	10.6669645	−5.1	−2
37	4	1	3	4	3	1	2	4	A	10.6666636	−13.0	−10
38	4	1	3	3	3	1	2	3	A	10.6675716	−2.7	0
39	2	2	1	3	1	1	0	2	A	11.2234888	1.5	4
40	2	2	1	2	1	1	0	1	A	11.2240106	−5.3	−3
41	2	2	1	1	1	1	0	0	A	11.2220797	−3.3	−1
42	2	2	1	2	1	1	0	2	A	11.2228414	1.5	4
43	2	2	1	1	1	1	0	1	A	11.2250197	−3.2	0
44	2	2	0	3	1	1	1	2	A	11.3581561	−3.5	−1
45	2	2	0	2	1	1	1	1	A	11.3568814	−1.0	2
46	2	2	0	1	1	1	1	0	A	11.3594018	−7.5	−5
47	2	2	0	2	1	1	1	2	A	11.3574498	−4.3	−2
48	2	2	0	1	1	1	1	1	A	11.3579813	1.3	4
49	5	0	5	6	4	1	4	5	A	11.4523003	−8.2	0
50	5	0	5	5	4	1	4	4	A	11.4517957	−7.0	1
51	5	0	5	4	4	1	4	3	A	11.4524918	−6.3	2
52	5	0	5	5	4	1	4	5	A	11.4534175	−7.7	1
53	5	0	5	4	4	1	4	4	A	11.4504489	−9.5	−1
54	4	1	4	5	3	0	3	4	A	11.8219491	1.6	−2
55	4	1	4	4	3	0	3	3	A	11.8227522	3.6	−1
56	4	1	4	3	3	0	3	2	A	11.8218246	6.8	3
57	4	1	4	4	3	0	3	4	A	11.8235739	3.9	0
58	4	1	4	3	3	0	3	3	A	11.8207108	1.9	−2
59	5	1	5	6	4	1	4	5	A	12.6834834	−1.1	0
60	5	1	5	5	4	1	4	4	A	12.6835778	−0.3	1
61	5	1	5	4	4	1	4	3	A	12.6835509	−1.3	0
62	5	1	5	5	4	1	4	5	A	12.6852003	−0.3	1
63	5	1	5	4	4	1	4	4	A	12.6815106	−1.8	−1
64	5	0	5	6	4	0	4	5	A	12.9111409	−2.8	−1
65	5	0	5	5	4	0	4	4	A	12.9113006	−0.8	1
66	5	0	5	4	4	0	4	3	A	12.9111639	1.0	3
67	5	0	5	5	4	0	4	5	A	12.9122599	−0.6	1
68	5	0	5	4	4	0	4	4	A	12.9099537	−3.4	−2

No.	J'	K_a'	K_c'	F'	J	K_a	K_c	F	sym.	ν_{obs}	$\nu_X - \nu_o$	$\nu_B - \nu_o$
69	5	2	4	6	4	2	3	5	A	13.0154161	−3.2	1
70	5	2	4	5	4	2	3	4	A	13.0155825	−3.7	1
71	5	2	4	4	4	2	3	3	A	13.0153922	−8.6	−4
72	5	1	4	6	4	1	3	5	A	13.3211072	−1.8	−1
73	5	1	4	5	4	1	3	4	A	13.3211806	−1.1	0
74	5	1	4	4	4	1	3	3	A	13.3210732	−1.8	−1
75	3	2	2	4	2	1	1	3	A	13.7009184	3.2	6
76	3	2	2	3	2	1	1	2	A	13.7015275	−0.3	2
77	3	2	2	2	2	1	1	1	A	13.7005717	−3.2	−1
78	3	2	2	3	2	1	1	3	A	13.7009184	3.2	6
79	3	2	2	2	2	1	1	2	A	13.7015275	−0.3	2
80	7	1	6	8	6	2	5	7	A	13.8156183	9.5	−4
81	7	1	6	7	6	2	5	6	A	13.8149179	10.4	−3
82	7	1	6	6	6	2	5	5	A	13.8157406	16.6	3
83	3	2	1	4	2	1	2	3	A	14.1165530	−5.9	−4
84	3	2	1	3	2	1	2	2	A	14.1151478	−1.2	0
85	3	2	1	2	2	1	2	1	A	14.1173117	0.2	2
86	3	2	1	2	2	1	2	2	A	14.1153429	−8.7	−7
87	5	1	5	6	4	0	4	5	A	14.1423246	4.8	−1
88	5	1	5	5	4	0	4	4	A	14.1430814	4.6	−1
89	5	1	5	4	4	0	4	3	A	14.1422197	2.8	−3
90	5	1	5	5	4	0	4	5	A	14.1440411	5.2	0
91	5	1	5	4	4	0	4	4	A	14.1410144	3.3	−2
92	6	0	6	7	5	1	5	6	A	14.2041162	−6.8	−1
93	6	0	6	6	5	1	5	5	A	14.2036875	−6.1	0
94	6	0	6	5	5	1	5	4	A	14.2042512	−4.1	2
95	6	0	6	6	5	1	5	6	A	14.2054041	−5.6	1
96	6	0	6	5	5	1	5	5	A	14.2021824	−7.2	−1
97	6	1	6	7	5	1	5	6	A	15.2060724	0.3	0
98	6	1	6	6	5	1	5	5	A	15.2061502	0.2	−1
99	6	1	6	5	5	1	5	4	A	15.2061183	−0.5	−1
100	6	0	6	7	5	0	5	6	A	15.4352998	0.8	0
101	6	0	6	6	5	0	5	5	A	15.4354702	1.2	0
102	6	0	6	5	5	0	5	4	A	15.4353118	2.5	2
103	6	2	5	7	5	2	4	6	A	15.6073728	−4.2	1
104	6	2	5	6	5	2	4	5	A	15.6074896	−2.8	2

No.	J'	K_a'	K_c'	F'	J	K_a	K_c	F	sym.	ν_{obs}	$\nu_X - \nu_o$	$\nu_B - \nu_o$
105	6	2	4	7	5	2	3	6	A	15.8067276	12.1	1
106	6	2	4	6	5	2	3	5	A	15.8066821	13.0	2
107	6	2	4	5	5	2	3	4	A	15.8067386	14.0	3
108	6	1	5	7	5	1	4	6	A	15.9657092	3.7	2
109	6	1	5	6	5	1	4	5	A	15.9657827	3.9	3
110	6	1	5	5	5	1	4	4	A	15.9656869	3.7	2
111	2	1	1	3	1	1	1	2	E	8.1160860	48.4	1
112	2	1	1	2	1	1	1	1	E	8.1163437	54.1	6
113	2	1	1	1	1	1	1	0	E	8.1159005	52.4	6
114	2	1	1	2	1	1	1	2	E	8.1162755	38.7	−8
115	2	1	1	1	1	1	1	1	E	8.1160288	48.9	1
116	2	1	1	3	1	0	1	2	E	8.8751480	23.3	0
117	2	1	1	2	1	0	1	1	E	8.8749442	23.3	0
118	2	1	1	1	1	0	1	0	E	8.8756426	23.0	−1
119	2	1	1	2	1	0	1	2	E	8.8753500	26.1	3
120	2	1	1	1	1	0	1	1	E	8.8746338	22.6	−1
121	3	1	3	4	2	0	2	3	E	8.8201695	−11.1	−3
122	3	1	3	3	2	0	2	2	E	8.8207597	−5.9	3
123	3	1	3	2	2	0	2	1	E	8.8200750	1.6	10
124	3	1	3	3	2	0	2	3	E	8.8212269	−12.1	−3
125	3	1	3	2	2	0	2	2	E	8.8193302	−6.4	2
126	4	0	4	5	3	1	3	4	E	9.0123531	16.6	9
127	4	0	4	4	3	1	3	3	E	9.0119170	−2.6	−11
128	4	0	4	3	3	1	3	2	E	9.0125596	17.6	10
129	4	0	4	4	3	1	3	4	E	9.0129886	10.6	3
130	4	0	4	3	3	1	3	3	E	9.0111199	6.8	−1
131	3	2	2	4	2	1	1	3	E	9.3848818	−27.3	1
132	3	2	2	3	2	1	1	2	E	9.3845320	−30.2	−2
133	3	2	2	2	2	1	1	1	E	9.3850389	−32.3	−4
134	2	2	1	3	1	1	1	2	E	9.6359386	7.1	3
135	2	2	1	2	1	1	1	1	E	9.6352969	6.3	2
136	2	2	1	1	1	1	1	0	E	9.6362382	0.2	−3
137	2	2	1	2	1	1	1	2	E	9.6352480	10.2	6
138	2	2	1	1	1	1	1	1	E	9.6363698	0.0	−5
139	4	0	4	5	3	0	3	4	E	10.2138588	6.6	5
140	4	0	4	4	3	0	3	3	E	10.2139495	1.2	0

No.	J'	K_a'	K_c'	F'	J	K_a	K_c	F	sym.	ν_{obs}	$\nu_X - \nu_o$	$\nu_B - \nu_o$
141	4	0	4	3	3	0	3	2	E	10.2138793	1.2	0
142	4	0	4	4	3	0	3	4	E	10.2144936	0.0	−2
143	4	0	4	3	3	0	3	3	E	10.2131437	2.0	1
144	4	1	4	5	3	1	3	4	E	10.2896080	7.6	−1
145	4	1	4	4	3	1	3	3	E	10.2898652	8.2	0
146	4	1	4	3	3	1	3	2	E	10.2896421	9.4	1
147	4	1	4	4	3	1	3	4	E	10.2909221	6.7	−1
148	4	1	4	3	3	1	3	3	E	10.2882151	11.3	3
149	2	2	1	3	1	0	1	2	E	10.3950073	−6.1	8
150	2	2	1	2	1	0	1	1	E	10.3939068	−9.8	5
151	2	2	1	1	1	0	1	0	E	10.3959943	−10.1	4
152	2	2	1	2	1	0	1	2	E	10.3943007	−19.0	−5
153	2	2	1	1	1	0	1	1	E	10.3949751	−20.7	−6
154	4	2	2	5	3	2	1	4	E	10.4471043	−36.2	2
155	4	2	2	4	3	2	1	3	E	10.4473441	−34.4	4
156	4	2	2	3	3	2	1	2	E	10.4470363	−37.4	1
157	4	1	3	5	3	1	2	4	E	10.4919575	−23.0	−3
158	4	1	3	4	3	1	2	3	E	10.4920239	−22.7	−2
159	4	1	3	3	3	1	2	2	E	10.4919726	−20.6	0
160	4	1	3	4	3	1	2	4	E	10.4923436	−23.3	−3
161	4	1	3	3	3	1	2	3	E	10.4915388	−22.2	−2
162	4	2	3	5	3	2	2	4	E	10.5202366	12.8	−2
163	4	2	3	4	3	2	2	3	E	10.5203977	13.1	−2
164	4	2	3	3	3	2	2	2	E	10.5201824	13.7	−1
165	3	1	2	4	2	1	2	3	E	10.7065197	22.2	0
166	3	1	2	3	2	1	2	2	E	10.7061450	22.4	0
167	3	1	2	2	2	1	2	1	E	10.7067939	22.1	0
168	3	1	2	3	2	1	2	3	E	10.7068382	20.5	−1
169	3	1	2	2	2	1	2	2	E	10.7057126	22.3	−1
170	4	1	4	5	3	0	3	4	E	11.4911193	3.3	1
171	4	1	4	4	3	0	3	3	E	11.4918859	0.2	−1
172	4	1	4	3	3	0	3	2	E	11.4909729	4.1	2
173	4	1	4	4	3	0	3	4	E	11.4924314	0.3	−1
174	4	1	4	3	3	0	3	3	E	11.4902395	7.1	5
175	5	0	5	6	4	1	4	5	E	11.5207500	7.2	2
176	5	0	5	5	4	1	4	4	E	11.5202067	9.4	3

No.	J'	K_a'	K_c'	F'	J	K_a	K_c	F	sym.	ν_{obs}	$\nu_X - \nu_o$	$\nu_B - \nu_o$
177	5	0	5	4	4	1	4	3	E	11.5209232	−1.0	−7
178	5	0	5	5	4	1	4	5	E	11.5215187	6.3	1
179	5	0	5	4	4	1	4	4	E	11.5192804	9.5	4
180	3	1	2	4	2	0	2	3	E	11.7235320	7.9	0
181	3	1	2	3	2	0	2	2	E	11.7233750	4.1	−3
182	3	1	2	2	2	0	2	1	E	11.7236843	8.9	1
183	3	1	2	3	2	0	2	3	E	11.7238548	10.4	3
184	3	1	2	2	2	0	2	2	E	11.7229482	9.6	2
185	4	2	3	5	3	1	2	4	E	12.0307134	4.3	−2
186	4	2	3	4	3	1	2	3	E	12.0304100	8.0	1
187	4	2	3	3	3	1	2	2	E	12.0308228	5.1	−2
188	3	2	2	4	2	1	2	3	E	12.2169977	15.0	1
189	3	2	2	3	2	1	2	2	E	12.2161552	15.2	1
190	3	2	2	2	2	1	2	1	E	12.2174344	13.6	0
191	3	2	2	3	2	1	2	3	E	12.2168491	14.0	0
192	3	2	2	2	2	1	2	2	E	12.2163528	13.5	−1
193	2	2	0	3	1	1	0	2	E	12.6586402	−33.5	2
194	2	2	0	2	1	1	0	1	E	12.6583143	−35.6	0
195	2	2	0	2	1	1	0	2	E	12.6579638	−35.8	0
196	5	1	5	6	4	1	4	5	E	12.7671165	10.6	0
197	5	1	5	5	4	1	4	4	E	12.7673009	9.1	−2
198	5	1	5	4	4	1	4	3	E	12.7671432	4.8	−6
199	5	1	5	5	4	1	4	5	E	12.7686155	8.6	−2
200	5	1	5	4	4	1	4	4	E	12.7654950	9.9	−1
201	5	0	5	6	4	0	4	5	E	12.7980142	7.5	1
202	5	0	5	5	4	0	4	4	E	12.7981420	7.2	1
203	5	0	5	4	4	0	4	3	E	12.7980244	9.5	3
204	5	0	5	5	4	0	4	5	E	12.7987817	5.4	−1
205	5	0	5	4	4	0	4	4	E	12.7972163	7.9	2
206	5	2	3	6	4	2	2	5	E	13.0714557	−43.8	3
207	5	2	3	5	4	2	2	4	E	13.0715547	−44.2	3
208	5	2	3	4	4	2	2	3	E	13.0714412	−47.6	−1
209	5	2	4	6	4	2	3	5	E	13.1945549	9.7	0
210	5	2	4	5	4	2	3	4	E	13.1945990	6.6	−3
211	5	2	4	4	4	2	3	3	E	13.1945440	7.8	−2
212	4	1	3	5	3	1	3	4	E	13.3953196	−4.4	−1

No.	J'	K_a'	K_c'	F'	J	K_a	K_c	F	sym.	ν_{obs}	$\nu_X - \nu_o$	$\nu_B - \nu_o$
213	4	1	3	4	3	1	3	3	E	13.3946481	−3.8	0
214	4	1	3	3	3	1	3	2	E	13.3955907	−4.5	−1
215	6	1	5	7	5	2	4	6	E	14.0016653	−41.9	−5
216	6	1	5	6	5	2	4	5	E	14.0020778	−39.1	−3
217	6	1	5	5	5	2	4	4	E	14.0016031	−37.1	0
218	5	1	5	6	4	0	4	5	E	14.0443798	10.0	−1
219	5	1	5	5	4	0	4	4	E	14.0452393	10.0	−1
220	5	1	5	4	4	0	4	3	E	14.0442429	13.8	2
221	5	1	5	5	4	0	4	5	E	14.0458800	9.2	−2
222	5	1	5	4	4	0	4	4	E	14.0434329	10.4	−1
223	4	1	3	5	3	0	3	4	E	14.5968339	−5.7	4
224	4	1	3	4	3	0	3	3	E	14.5966640	−16.6	−6
225	4	1	3	3	3	0	3	2	E	14.5969271	−4.3	6
226	4	1	3	4	3	0	3	4	E	14.5972128	−13.2	−3
227	4	1	3	3	3	0	3	3	E	14.5961830	−12.0	−2
228	5	2	4	6	4	1	3	5	E	14.7333092	35.5	−2
229	5	2	4	5	4	1	3	4	E	14.7329805	32.8	−4
230	5	2	4	4	4	1	3	3	E	14.7333982	37.5	0
231	4	2	3	5	3	1	3	4	E	14.9340751	22.6	−1
232	4	2	3	4	3	1	3	3	E	14.9330310	23.7	0
233	4	2	3	3	3	1	3	2	E	14.9344423	22.6	−1
234	3	2	1	4	2	1	1	3	E	15.2448427	−50.1	1
235	3	2	1	3	2	1	1	2	E	15.2445798	−53.1	−3
236	3	2	1	2	2	1	1	1	E	15.2449665	−58.1	−7
237	6	1	6	7	5	1	5	6	E	15.2491433	13.8	0
238	6	1	6	6	5	1	5	5	E	15.2492787	13.8	0
239	6	1	6	5	5	1	5	4	E	15.2491720	13.0	−1
240	6	0	6	7	5	0	5	6	E	15.3625753	15.8	4
241	6	0	6	6	5	0	5	5	E	15.3627352	15.6	4
242	6	0	6	5	5	0	5	4	E	15.3625753	16.0	4
243	6	1	5	7	5	1	4	6	E	15.6537932	5.9	−4
244	6	1	5	6	5	1	4	5	E	15.6538213	8.7	−1
245	6	1	5	5	5	1	4	4	E	15.6538067	8.2	−2
246	6	2	4	7	5	2	3	6	E	15.7046030	−48.9	4
247	6	2	4	6	5	2	3	5	E	15.7046337	−50.7	2
248	6	2	5	7	5	2	4	6	E	15.8630538	3.9	0

No.	J'	K_a'	K_c'	F'	J	K_a	K_c	F	sym.	ν_{obs}	$\nu_X - \nu_o$	$\nu_B - \nu_o$
249	6	2	5	6	5	2	4	5	E	15.8631026	2.8	−1
250	6	2	5	5	5	2	4	4	E	15.8630456	2.0	−1

Appendix E

N-Vinylacetamide

Table E.1: Nuclear coordinates (in Å) in the principal axis system of conformer **I** of N-vinylacetamide, calculated at the MP2/6-311++G(d,p) level of theory.

	a	*b*	*c*
N_1	−0.296190	−0.477807	−0.036250
H_2	−0.375413	−1.484712	−0.037944
C_3	0.966408	0.085987	−0.017399
O_4	1.146262	1.293658	−0.002889
C_5	2.100762	−0.917548	0.023421
H_6	2.410964	−1.054036	1.063656
H_7	1.820370	−1.889590	−0.389822
H_8	2.945233	−0.511402	−0.534016
C_9	−1.468004	0.282884	0.013970
H_{10}	−1.281968	1.350489	0.051944
C_{11}	−2.703924	−0.241272	0.011234
H_{12}	−2.878267	−1.312184	−0.030458
H_{13}	−3.563406	0.414755	0.054360

Table E.2: Observed frequencies ν_{obs} in GHz of the A species of N-vinylacetamide. $\nu_c - \nu_o$ values in kHz are obtained after a fit with the program XIAM. J, K_a, and K_c are the symmetric top rotational quantum numbers, F is the total angular momentum in the coupled basis with $F = J + I$.

No.	J'	K_a'	K_c'	F'	J	K_a	K_c	F	ν_{obs}	$\nu_c - \nu_o$
1	1	1	0	2	1	0	1	2	7.9865951	−2.9
2	1	1	0	1	1	0	1	1	7.9849066	−0.3
3	1	1	0	2	1	0	1	1	7.9860326	−6.0
4	1	1	0	1	1	0	1	2	7.9854639	−2.5

No.	J'	K_a'	K_c'	F'	J	K_a	K_c	F	ν_{obs}	$\nu_c - \nu_o$
5	1	1	0	1	1	0	1	0	7.9863090	3.4
6	1	1	0	0	1	0	1	1	7.9877335	−2.6
7	2	1	1	3	2	0	2	3	8.3744860	−1.1
8	2	1	1	2	2	0	2	2	8.3732322	0.8
9	2	1	1	1	2	0	2	1	8.3751851	0.3
10	2	1	1	3	2	0	2	2	8.3738409	−3.5
11	2	1	1	2	2	0	2	3	8.3738745	0.4
12	2	1	1	2	2	0	2	1	8.3742328	1.7
13	2	1	1	1	2	0	2	2	8.3741857	0.7
14	4	0	4	5	3	1	3	4	8.4805349	−2.4
15	4	0	4	4	3	1	3	3	8.4799500	−0.7
16	4	0	4	3	3	1	3	2	8.4808261	5.6
17	3	1	2	4	3	0	3	4	8.9813408	2.2
18	3	1	2	3	3	0	3	3	8.9801400	0.7
19	3	1	2	2	3	0	3	2	8.9817596	1.2
20	3	1	2	4	3	0	3	3	8.9806036	−1.6
21	3	1	2	3	3	0	3	2	8.9811324	3.0
22	3	1	2	3	3	0	3	4	8.9808707	−2.0
23	3	1	2	2	3	0	3	3	8.9807702	1.9
24	4	1	3	5	4	0	4	5	9.8360298	1.0
25	4	1	3	4	4	0	4	4	9.8348017	2.8
26	4	1	3	3	4	0	4	3	9.8363416	−3.4
27	4	1	3	4	4	0	4	3	9.8358560	1.2
28	4	1	3	4	4	0	4	5	9.8356358	−3.1
29	4	1	3	3	4	0	4	4	9.8352891	0.0
30	2	2	1	3	3	1	2	4	10.7707633	10.8
31	2	2	1	2	3	1	2	3	10.7706171	−1.9
32	2	2	1	1	3	1	2	2	10.7709229	0.5
33	2	2	1	3	3	1	2	3	10.7712202	1.8
34	2	2	1	2	3	1	2	2	10.7699896	−0.4
35	3	1	3	4	2	1	2	3	10.9417035	0.2
36	3	1	3	3	2	1	2	2	10.9419179	0.6
37	3	1	3	2	2	1	2	1	10.9418770	−0.7
38	3	1	3	3	2	1	2	3	10.9431269	−2.9
39	3	1	3	2	2	1	2	2	10.9399947	3.2
40	5	1	4	6	5	0	5	6	10.9742629	−6.0

No.	J'	K_a'	K_c'	F'	J	K_a	K_c	F	ν_{obs}	$\nu_c - \nu_o$
41	5	1	4	5	5	0	5	5	10.9729720	−1.4
42	5	1	4	4	5	0	5	4	10.9745267	−6.1
43	1	1	1	2	0	0	0	1	11.4490384	−0.4
44	1	1	1	1	0	0	0	0	11.4496181	7.1
45	1	1	1	0	0	0	0	1	11.4481789	−1.6
46	1	1	1	1	0	0	0	1	11.4496181	7.1
47	1	1	1	0	0	0	0	0	11.4481789	−1.6
48	3	0	3	4	2	0	2	3	11.4578802	−1.4
49	3	0	3	3	2	0	2	2	11.4579703	−2.0
50	3	0	3	2	2	0	2	1	11.4579829	1.0
51	3	0	3	3	2	0	2	3	11.4586137	−1.3
52	3	0	3	2	2	0	2	2	11.4569804	−1.7
53	3	1	2	4	2	1	1	3	12.0647364	3.3
54	3	1	2	3	2	1	1	2	12.0648748	−5.4
55	3	1	2	2	2	1	1	1	12.0645561	0.6
56	6	1	5	7	6	0	6	7	12.4345390	−17.3
57	6	1	5	6	6	0	6	6	12.4331632	−15.7
58	6	1	5	5	6	0	6	5	12.4347723	−16.5
59	5	0	5	6	4	1	4	5	12.8282874	−1.2
60	5	0	5	5	4	1	4	4	12.8277092	0.5
61	5	0	5	4	4	1	4	3	12.8284914	2.2
62	5	0	5	5	4	1	4	5	12.8292506	−1.2
63	5	0	5	4	4	1	4	4	12.8265496	0.3
64	4	1	4	5	3	1	3	4	14.5739562	1.1
65	4	1	4	4	3	1	3	3	14.5740745	2.8
66	4	1	4	3	3	1	3	2	14.5740559	−1.7
67	2	1	2	3	1	0	1	2	14.9117710	4.9
68	2	1	2	2	1	0	1	1	14.9124137	−5.4
69	2	1	2	1	1	0	1	0	14.9119254	−6.3
70	2	1	2	2	1	0	1	2	14.9129730	−5.6
71	2	1	2	1	1	0	1	1	14.9105253	−7.7
72	4	0	4	5	3	0	3	4	15.2151714	−0.2
73	4	0	4	4	3	0	3	3	15.2152771	−1.0

Appendix F

N,N-Diethylpropionamide

Table F.1: Nuclear coordinates (in Å) in the principal axis system of conformer **0PM** and **0MM** of N,N-Diethylpropionamide, calculated at the MP2/6-311++G(d,p) level of theory.

	0PM			0MM		
	a	*b*	*c*	*a*	*b*	*c*
N_1	−0.601698	0.092625	−0.020255	0.539924	0.065515	−0.424224
C_2	−0.979700	1.374295	0.561941	1.529102	−1.004541	−0.562399
C_3	−1.679601	−0.771747	−0.496407	0.994098	1.441333	−0.579485
C_4	0.680509	−0.388112	−0.084566	−0.761096	−0.308450	−0.203481
O_5	0.925465	−1.503702	−0.545176	−1.079348	−1.496797	−0.144172
C_6	1.789732	0.516793	0.445905	−1.795894	0.801079	−0.028938
C_7	3.170692	−0.008241	0.063761	−3.141709	0.242424	0.424127
H_8	3.948857	0.642815	0.472535	−3.870083	1.051802	0.528715
H_9	3.316876	−1.019859	0.445640	−3.519890	−0.484043	−0.296949
H_{10}	3.281526	−0.046953	−1.022322	−3.044232	−0.267718	1.384971
C_{11}	−2.146448	−1.750908	0.578945	1.783084	1.955518	0.624944
H_{12}	−2.495219	−1.216380	1.468328	2.687633	1.362159	0.782966
H_{13}	−2.970101	−2.367584	0.204884	2.083538	2.996298	0.464418
H_{14}	−1.320369	−2.407324	0.861673	1.173961	1.902309	1.532110
C_{15}	−1.159005	2.471696	−0.487875	1.910084	−1.647959	0.770323
H_{16}	−1.482500	3.405319	−0.015847	2.656603	−2.432493	0.607692
H_{17}	−0.218786	2.655125	−1.015327	2.330542	−0.909012	1.457673
H_{18}	−1.912218	2.181376	−1.225829	1.028176	−2.099070	1.228735
H_{19}	−1.917123	1.223506	1.110915	1.117289	−1.765901	−1.231873
H_{20}	−0.235089	1.672552	1.302411	2.409404	−0.565605	−1.044011
H_{21}	−2.503117	−0.125564	−0.818887	1.617112	1.492024	−1.481779
H_{22}	−1.313594	−1.317836	−1.368624	0.131062	2.082125	−0.761687
H_{23}	1.652651	1.536247	0.069522	−1.426930	1.536482	0.695193
H_{24}	1.696298	0.571626	1.538432	−1.909844	1.330600	−0.983359

Table F.2: Nuclear coordinates (in Å) in the principal axis system of conformer **MMP** of N,N-diethylpropionamide, calculated at the MP2/6-311++G(d,p) level of theory.

	MMP		
	a	*b*	*c*
N_1	0.515421	0.117366	−0.096042
C_2	0.625661	1.420615	0.548961
C_3	1.747336	−0.651656	−0.263361
C_4	−0.657385	−0.457808	−0.510383
O_5	−0.681627	−1.584248	−1.010968
C_6	−1.947931	0.313585	−0.284750
C_7	−2.570888	−0.071835	1.064534
H_8	−3.537862	0.420682	1.201578
H_9	−2.725169	−1.153363	1.106067
H_{10}	−1.922587	0.210883	1.900170
C_{11}	1.991759	−1.597112	0.910884
H_{12}	1.172953	−2.317157	0.978599
H_{13}	2.928950	−2.146107	0.773384
H_{14}	2.054606	−1.042246	1.852473
C_{15}	0.950340	2.541971	−0.437941
H_{16}	1.070590	3.494853	0.088115
H_{17}	1.878393	2.326188	−0.975017
H_{18}	0.148212	2.647789	−1.173758
H_{19}	−0.295723	1.641323	1.091036
H_{20}	1.415316	1.344704	1.305925
H_{21}	1.666317	−1.219004	−1.192949
H_{22}	2.571569	0.062073	−0.368447
H_{23}	−1.806611	1.395609	−0.352321
H_{24}	−2.616231	0.012660	−1.095164

Table F.3: Observed frequencies ν_{obs} in GHz of conformer **0PM** of N,N-diethylpropionamide. $\nu_c - \nu_o$ values in kHz are obtained after a fit with the program XIAM. J, K_a, and K_c are the symmetric top rotational quantum numbers, F is the total angular momentum in the coupled basis with $F = J + I$.

No.	J'	K_a'	K_c'	F'	J	K_a	K_c	F	ν_{obs}	$\nu_c - \nu_o$
1	4	2	3	5	3	2	2	4	8.0925041	−0.2
2	4	2	3	4	3	2	2	3	8.0928337	0.1
3	4	2	3	3	3	2	2	2	8.0924140	−5.7
4	4	2	3	4	3	2	2	4	8.0928337	0.1
5	4	2	3	3	3	2	2	3	8.0924140	−5.7
6	3	1	2	4	2	0	2	3	8.2172025	0.4
7	3	1	2	3	2	0	2	2	8.2162145	−0.1
8	3	1	2	2	2	0	2	1	8.2177252	−1.0
9	3	1	2	3	2	0	2	3	8.2170820	−0.7
10	3	1	2	2	2	0	2	2	8.2163749	−0.8
11	3	2	2	4	2	1	1	3	8.2687493	2.3
12	3	2	2	3	2	1	1	2	8.2691166	−0.8
13	3	2	2	2	2	1	1	1	8.2685406	−0.6
14	3	2	2	3	2	1	1	3	8.2687493	2.3
15	3	2	2	2	2	1	1	2	8.2691166	−0.8
16	4	3	2	5	3	3	1	4	8.3672316	4.0
17	4	3	2	4	3	3	1	3	8.3677363	1.5
18	4	3	2	3	3	3	1	2	8.3670184	3.4
19	4	3	2	4	3	3	1	4	8.3668513	2.2
20	4	3	2	3	3	3	1	3	8.3682122	1.6
21	4	3	1	5	3	3	0	4	8.5014748	−2.2
22	4	3	1	4	3	3	0	3	8.5018847	3.8
23	4	3	1	3	3	3	0	2	8.5012904	2.8
24	4	3	1	4	3	3	0	4	8.5009619	2.5
25	4	3	1	3	3	3	0	3	8.5025336	2.0
26	4	1	3	5	3	1	2	4	8.6363323	−0.8
27	4	1	3	4	3	1	2	3	8.6365771	−0.1
28	4	1	3	3	3	1	2	2	8.6362580	−1.2
29	3	2	1	4	2	1	1	3	8.7996672	1.6
30	3	2	1	3	2	1	1	2	8.7995263	−0.3
31	3	2	1	2	2	1	1	1	8.7996375	−0.6
32	3	2	1	3	2	1	1	3	8.7991567	0.5

No.	J'	K_a'	K_c'	F'	J	K_a	K_c	F	ν_{obs}	$\nu_c - \nu_o$
33	3	2	1	2	2	1	1	2	8.8002134	−0.9
34	4	2	2	5	3	2	1	4	8.9051378	−1.1
35	4	2	2	4	3	2	1	3	8.9052603	4.2
36	4	2	2	3	3	2	1	2	8.9050591	−2.4
37	4	2	2	4	3	2	1	4	8.9047463	−0.4
38	4	2	2	3	3	2	1	3	8.9057480	−1.2
39	5	0	5	6	4	1	4	5	8.9098123	0.2
40	5	0	5	5	4	1	4	4	8.9099253	−0.1
41	5	0	5	4	4	1	4	3	8.9098662	0.0
42	5	0	5	5	4	1	4	5	8.9113681	−0.3
43	5	0	5	4	4	1	4	4	8.9080515	−0.6
44	5	1	5	6	4	1	4	5	8.9426890	−0.2
45	5	1	5	5	4	1	4	4	8.9428184	0.2
46	5	1	5	4	4	1	4	3	8.9427392	−0.8
47	5	1	5	5	4	1	4	5	8.9442610	−0.2
48	5	1	5	4	4	1	4	4	8.9409252	−0.8
49	5	0	5	6	4	0	4	5	8.9996192	−0.1
50	5	0	5	5	4	0	4	4	8.9997777	0.1
51	5	0	5	4	4	0	4	3	8.9996605	−1.3
52	5	0	5	5	4	0	4	5	9.0011758	0.2
53	5	0	5	4	4	0	4	4	8.9979036	−0.7
54	5	1	5	6	4	0	4	5	9.0324980	1.6
55	5	1	5	5	4	0	4	4	9.0326706	0.2
56	5	1	5	4	4	0	4	3	9.0325353	−0.3
57	5	1	5	5	4	0	4	5	9.0340686	0.2
58	5	1	5	4	4	0	4	4	9.0307778	−0.3
59	5	1	4	6	4	2	3	5	9.3540265	0.5
60	5	1	4	5	4	2	3	4	9.3540990	3.0
61	5	1	4	4	4	2	3	3	9.3540265	−2.9
62	5	1	4	5	4	2	3	5	9.3544244	−0.9
63	5	1	4	4	4	2	3	4	9.3536157	0.3
64	3	2	2	4	2	1	2	3	9.4165324	−0.8
65	3	2	2	3	2	1	2	2	9.4155293	−0.2
66	3	2	2	2	2	1	2	1	9.4170893	−1.5
67	3	2	2	3	2	1	2	3	9.4165324	−0.8
68	3	2	2	2	2	1	2	2	9.4155293	−0.2

No.	J'	K_a'	K_c'	F'	J	K_a	K_c	F	ν_{obs}	$\nu_c - \nu_o$
69	8	2	7	9	8	1	8	9	9.4629929	−5.4
70	8	2	7	8	8	1	8	8	9.4622302	−3.8
71	8	2	7	7	8	1	8	7	9.4631010	6.4
72	4	2	3	5	3	1	2	4	9.7368992	3.4
73	4	2	3	4	3	1	2	3	9.7373456	1.2
74	4	2	3	3	3	1	2	2	9.7367697	0.4
75	4	2	3	3	3	1	2	3	9.7369290	−1.4
76	3	2	1	4	2	1	2	3	9.9474582	6.5
77	3	2	1	3	2	1	2	2	9.9459395	0.9
78	3	2	1	2	2	1	2	1	9.9481880	0.4
79	3	2	1	3	2	1	2	3	9.9469408	−1.5
80	3	2	1	2	2	1	2	2	9.9466275	1.1
81	6	2	4	7	5	3	2	6	9.9530908	1.8
82	6	2	4	6	5	3	2	5	9.9533576	1.4
83	6	2	4	5	5	3	2	4	9.9530299	0.2
84	5	2	4	6	4	2	3	5	9.9731574	−0.8
85	5	2	4	5	4	2	3	4	9.9733894	−0.4
86	5	2	4	4	4	2	3	3	9.9731292	0.6
87	5	2	4	5	4	2	3	5	9.9737182	−0.9
88	5	2	4	4	4	2	3	4	9.9727125	−2.1
89	3	2	1	4	2	0	2	3	10.3925092	−2.8
90	3	2	1	3	2	0	2	2	10.3911366	2.1
91	3	2	1	2	2	0	2	1	10.3931738	1.1
92	5	3	3	6	4	3	2	5	10.4519203	−1.6
93	5	3	3	5	4	3	2	4	10.4522015	0.2
94	5	3	3	4	4	3	2	3	10.4518421	−2.7
95	5	1	4	6	4	1	3	5	10.4545888	0.1
96	5	1	4	5	4	1	3	4	10.4548633	0.1
97	5	1	4	4	4	1	3	3	10.4545394	−0.1
98	5	1	4	5	4	1	3	5	10.4549871	−0.9
99	5	1	4	4	4	1	3	4	10.4543821	−0.5
100	3	3	1	4	2	2	0	3	10.5915938	1.7
101	3	3	1	3	2	2	0	2	10.5915732	−1.3
102	3	3	1	2	2	2	0	1	10.5914195	−0.2
103	3	3	1	3	2	2	0	3	10.5907044	−2.0
104	3	3	1	2	2	2	0	2	10.5927675	−2.7

No.	J'	K_a'	K_c'	F'	J	K_a	K_c	F	ν_{obs}	$\nu_c - \nu_o$
105	6	0	6	7	5	1	5	6	10.6118675	−0.3
106	6	0	6	6	5	1	5	5	10.6119629	0.5
107	6	0	6	5	5	1	5	4	10.6119069	0.3
108	6	0	6	6	5	1	5	6	10.6135342	−0.2
109	6	0	6	5	5	1	5	5	10.6100139	−0.4
110	3	3	0	4	2	2	0	3	10.6156644	−0.2
111	3	3	0	3	2	2	0	2	10.6156104	−0.8
112	3	3	0	2	2	2	0	1	10.6155023	−2.5
113	3	3	0	3	2	2	0	3	10.6147424	−0.7
114	3	3	0	2	2	2	0	2	10.6168542	−1.1
115	6	1	6	7	5	1	5	6	10.6230920	1.8
116	6	1	6	6	5	1	5	5	10.6231899	0.0
117	6	1	6	5	5	1	5	4	10.6231285	0.3
118	6	1	6	6	5	1	5	6	10.6247619	0.0
119	6	1	6	5	5	1	5	5	10.6212353	−0.6
120	6	0	6	7	5	0	5	6	10.6447465	1.7
121	6	0	6	6	5	0	5	5	10.6448553	0.1
122	6	0	6	5	5	0	5	4	10.6447797	−0.7
123	6	0	6	6	5	0	5	6	10.6464115	0.0
124	6	0	6	5	5	0	5	5	10.6429065	−0.7
125	6	1	6	7	5	0	5	6	10.6559675	0.2
126	6	1	6	6	5	0	5	5	10.6560829	0.2
127	6	1	6	5	5	0	5	4	10.6560013	−0.7
128	6	1	6	6	5	0	5	6	10.6576389	0.0
129	6	1	6	5	5	0	5	5	10.6541283	−0.5
130	3	3	1	4	2	2	1	3	10.7095785	−1.6
131	3	3	1	3	2	2	1	2	10.7093261	−1.7
132	3	3	1	2	2	2	1	1	10.7095420	3.7
133	3	3	1	3	2	2	1	3	10.7086930	−1.5
134	3	3	1	2	2	2	1	2	10.7105210	−2.4
135	3	3	0	4	2	2	1	3	10.7336529	0.2
136	3	3	0	3	2	2	1	2	10.7333626	−1.8
137	3	3	0	3	2	2	1	3	10.7327308	−0.4
138	3	3	0	2	2	2	1	2	10.7346064	−2.1
139	5	3	2	6	4	3	1	5	10.8518471	0.2
140	5	3	2	5	4	3	1	4	10.8519563	−2.7

No.	J'	K_a'	K_c'	F'	J	K_a	K_c	F	ν_{obs}	$\nu_c - \nu_o$
141	5	3	2	4	4	3	1	3	10.8517967	0.3
142	5	3	2	5	4	3	1	5	10.8514416	0.2
143	5	3	2	4	4	3	1	4	10.8524450	−2.1
144	4	2	2	5	3	1	2	4	11.0804491	0.2
145	4	2	2	4	3	1	2	3	11.0801759	−0.1
146	4	2	2	3	3	1	2	2	11.0805079	−0.1
147	4	2	2	4	3	1	2	4	11.0800525	−4.2
148	4	2	2	3	3	1	2	3	11.0806684	−0.7
149	5	2	4	6	4	1	3	5	11.0737236	2.7
150	5	2	4	5	4	1	3	4	11.0741582	1.2
151	5	2	4	4	4	1	3	3	11.0736393	0.6
152	5	2	4	5	4	1	3	5	11.0742797	−2.1
153	5	2	4	4	4	1	3	4	11.0734835	1.7
154	4	1	3	5	3	0	3	4	11.1265962	1.6
155	4	1	3	4	3	0	3	3	11.1255534	0.2
156	4	1	3	3	3	0	3	2	11.1269720	1.3
157	5	2	3	6	4	2	2	5	11.1757555	−0.8
158	5	2	3	5	4	2	2	4	11.1758621	−0.7
159	5	2	3	4	4	2	2	3	11.1757134	−0.2
160	5	2	3	5	4	2	2	5	11.1754703	−0.3
161	5	2	3	4	4	2	2	4	11.1762048	−1.9
162	6	1	5	6	5	2	4	5	11.4863953	−2.8
163	6	1	5	5	5	2	4	4	11.4862989	−1.5
164	6	1	5	6	5	2	4	6	11.4869582	−0.9
165	6	1	5	5	5	2	4	5	11.4856243	−0.9
166	6	2	5	7	5	2	4	6	11.7808420	0.4
167	6	2	5	6	5	2	4	5	11.7810304	0.1
168	6	2	5	5	5	2	4	4	11.7808272	−2.1
169	6	2	5	6	5	2	4	6	11.7815909	−0.3
170	6	2	5	5	5	2	4	5	11.7801529	−1.2
171	7	2	5	8	6	3	3	7	11.8550641	1.3
172	7	2	5	7	6	3	3	6	11.8555097	2.8
173	7	2	5	6	6	3	3	5	11.8549894	0.1
174	4	2	3	5	3	1	3	4	12.0081329	0.8
175	4	2	3	4	3	1	3	3	12.0071920	0.3
176	4	2	3	3	3	1	3	2	12.0084928	0.9

No.	J'	K_a'	K_c'	F'	J	K_a	K_c	F	ν_{obs}	$\nu_c - \nu_o$
177	4	2	3	3	3	1	3	3	12.0067765	−1.2
178	6	1	5	7	5	1	4	6	12.1054302	0.3
179	6	1	5	6	5	1	4	5	12.1056919	0.0
180	6	1	5	5	5	1	4	4	12.1054003	0.7
181	6	1	5	6	5	1	4	6	12.1060917	0.5
182	6	1	5	5	5	1	4	5	12.1049182	−0.7
183	7	0	7	8	6	1	6	7	12.2896323	0.5
184	7	0	7	7	6	1	6	6	12.2897088	0.4
185	7	0	7	6	6	1	6	5	12.2896622	0.3
186	7	0	7	7	6	1	6	7	12.2913802	0.1
187	7	0	7	6	6	1	6	6	12.2877069	−1.0
188	7	1	7	8	6	1	6	7	12.2932880	−0.1
189	7	1	7	7	6	1	6	6	12.2933672	0.9
190	7	1	7	6	6	1	6	5	12.2933176	−0.4
191	7	1	7	7	6	1	6	7	12.2950380	0.0
192	7	1	7	6	6	1	6	6	12.2913620	−2.0
193	7	0	7	8	6	0	6	7	12.3008543	0.0
194	7	0	7	7	6	0	6	6	12.3009346	−1.3
195	7	0	7	6	6	0	6	5	12.3008824	−1.1
196	7	0	7	7	6	0	6	7	12.3026042	1.6
197	7	0	7	6	6	0	6	6	12.2989351	−0.3
198	7	1	7	8	6	0	6	7	12.3045108	0.2
199	7	1	7	7	6	0	6	6	12.3045937	−0.1
200	7	1	7	6	6	0	6	5	12.3045409	1.3
201	7	1	7	7	6	0	6	7	12.3062606	0.2
202	7	1	7	6	6	0	6	6	12.3025905	−1.0
203	6	2	5	7	5	1	4	6	12.3999745	0.8
204	6	2	5	6	5	1	4	5	12.4003246	0.6
205	6	2	5	5	5	1	4	4	12.3999302	1.7
206	6	2	5	6	5	1	4	6	12.4007246	1.3
207	6	2	5	5	5	1	4	5	12.3994471	−0.8
208	4	3	2	5	3	2	1	4	12.4061387	−4.5
209	4	3	2	4	3	2	1	3	12.4062799	5.7
210	4	3	2	3	3	2	1	2	12.4060624	0.1
211	4	3	2	4	3	2	1	4	12.4057688	4.0
212	4	3	2	3	3	2	1	3	12.4067488	−1.2

No.	J'	K_a'	K_c'	F'	J	K_a	K_c	F	ν_{obs}	$\nu_c - \nu_o$
213	6	3	4	7	5	3	3	6	12.4828984	−1.7
214	6	3	4	6	5	3	3	5	12.4830963	0.0
215	6	3	4	5	5	3	3	4	12.4828630	−0.5
216	4	3	1	5	3	2	1	4	12.5644651	−0.1
217	4	3	1	4	3	2	1	3	12.5644548	−2.2
218	4	3	1	3	3	2	1	2	12.5644242	4.2
219	4	3	1	4	3	2	1	4	12.5639470	−0.5
220	4	3	1	3	3	2	1	3	12.5651069	−0.8
221	6	4	3	7	5	4	2	6	12.6428465	0.0
222	6	4	3	6	5	4	2	5	12.6430962	0.9
223	6	4	3	5	5	4	2	4	12.6427852	0.3
224	6	4	3	6	5	4	2	6	12.6425336	−0.8
225	6	4	3	5	5	4	2	5	12.6434596	−0.5
226	6	4	2	7	5	4	1	6	12.7700317	−0.2
227	6	4	2	6	5	4	1	5	12.7702192	−0.1
228	6	4	2	5	5	4	1	4	12.7699800	0.3
229	6	4	2	6	5	4	1	6	12.7696312	0.5
230	6	4	2	5	5	4	1	5	12.7706901	1.9
231	4	3	2	5	3	2	2	4	12.9370600	−1.8
232	4	3	2	4	3	2	2	3	12.9366823	−1.0
233	4	3	2	3	3	2	2	2	12.9371597	0.6
234	4	3	2	4	3	2	2	4	12.9366823	−1.0
235	4	3	2	3	3	2	2	3	12.9371597	0.6
236	4	3	1	5	3	2	2	4	13.0953847	1.0
237	4	3	1	4	3	2	2	3	13.0948642	−1.9
238	4	3	1	3	3	2	2	2	13.0955134	−3.5
239	4	3	1	4	3	2	2	4	13.0948642	−1.9
240	4	3	1	3	3	2	2	3	13.0955134	−3.5
241	7	2	5	8	6	3	4	7	13.2199372	−7.0
242	7	2	5	7	6	3	4	6	13.2199135	6.4
243	7	2	5	6	6	3	4	5	13.2199446	−7.3
244	6	2	4	7	5	2	3	6	13.2885059	0.0
245	6	2	4	6	5	2	3	5	13.2886535	0.2
246	6	2	4	5	5	2	3	4	13.2884722	1.2
247	4	2	2	5	3	1	3	4	13.3516873	2.0
248	4	2	2	4	3	1	3	3	13.3500247	1.4

No.	J'	K_a'	K_c'	F'	J	K_a	K_c	F	ν_{obs}	$\nu_c - \nu_o$
249	4	2	2	3	3	1	3	2	13.3522300	−0.5
250	4	2	2	4	3	1	3	4	13.3512964	3.4
251	4	2	2	3	3	1	3	3	13.3505131	−3.3
252	7	1	6	8	6	2	5	7	13.4041180	1.1
253	7	1	6	7	6	2	5	6	13.4042387	−0.8
254	7	1	6	6	6	2	5	5	13.4041180	0.3
255	7	1	6	7	6	2	5	7	13.4049884	−0.7
256	7	1	6	6	6	2	5	6	13.4032412	−0.3
257	7	2	6	7	6	2	5	6	13.5276740	0.1
258	7	2	6	6	6	2	5	5	13.5275096	1.3
259	5	2	3	6	4	1	3	5	13.6198721	0.0
260	5	2	3	5	4	1	3	4	13.6194607	−0.9
261	5	2	3	4	4	1	3	3	13.6199640	1.6
262	7	1	6	8	6	1	5	7	13.6986633	2.5
263	7	1	6	7	6	1	5	6	13.6988734	1.7
264	7	1	6	6	6	1	5	5	13.6986445	−2.1
265	7	2	6	8	6	1	5	7	13.8220589	2.1
266	7	2	6	7	6	1	5	6	13.8223072	1.2
267	7	2	6	6	6	1	5	5	13.8220358	−1.4
268	7	2	6	7	6	1	5	7	13.8229647	−2.6
269	7	2	6	6	6	1	5	6	13.8212642	0.0
270	5	3	3	6	4	2	2	5	13.9529299	3.7
271	5	3	3	5	4	2	2	4	13.9532192	−0.1
272	5	3	3	4	4	2	2	3	13.9528418	−3.8
273	8	0	8	9	7	1	7	8	13.9582257	−1.8
274	8	0	8	8	7	1	7	7	13.9582884	−1.0
275	8	0	8	7	7	1	7	6	13.9582576	5.9
276	8	0	8	8	7	1	7	8	13.9600352	−4.0
277	8	0	8	7	7	1	7	7	13.9562494	−0.1
278	8	1	8	9	7	1	7	8	13.9593803	0.6
279	8	1	8	8	7	1	7	7	13.9594420	0.0
280	8	1	8	7	7	1	7	6	13.9594087	4.8
281	8	1	8	8	7	1	7	8	13.9611903	−1.6
282	8	1	8	7	7	1	7	7	13.9574011	−0.5
283	8	0	8	9	7	0	7	8	13.9618842	0.4
284	8	0	8	8	7	0	7	7	13.9619473	0.1

No.	J'	K_a'	K_c'	F'	J	K_a	K_c	F	ν_{obs}	$\nu_c - \nu_o$
285	8	0	8	7	7	0	7	6	13.9619111	3.3
286	8	1	8	9	7	0	7	8	13.9630359	−0.1
287	8	1	8	8	7	0	7	7	13.9630995	−0.4
288	8	1	8	7	7	0	7	6	13.9630630	3.0
289	8	1	8	8	7	0	7	8	13.9648485	0.3
290	8	1	8	7	7	0	7	7	13.9610593	−0.2
291	5	1	4	6	4	0	4	5	14.2113632	−0.6
292	5	1	4	5	4	0	4	4	14.2103669	1.8
293	5	1	4	4	4	0	4	3	14.2116419	−0.1
294	7	3	5	8	6	3	4	7	14.4385422	−1.4
295	7	3	5	7	6	3	4	6	14.4387101	1.5
296	7	3	5	6	6	3	4	5	14.4385136	−8.6
297	4	4	1	5	3	3	0	4	14.4974182	3.3
298	4	4	1	4	3	3	0	3	14.4973386	3.2
299	4	4	1	4	3	3	0	4	14.4964164	2.5
300	4	4	1	3	3	3	0	3	14.4985899	−3.9
301	4	4	0	5	3	3	0	4	14.5014546	0.1
302	4	4	0	4	3	3	0	3	14.5013675	−2.8
303	4	4	0	3	3	3	0	2	14.5013937	3.1
304	4	4	0	4	3	3	0	4	14.5004481	−0.7
305	4	4	0	3	3	3	0	3	14.5026351	0.4
306	5	3	2	6	4	2	2	5	14.5111791	5.9
307	5	3	2	4	4	2	2	3	14.5111561	1.2
308	4	4	1	5	3	3	1	4	14.5214888	1.4
309	4	4	1	4	3	3	1	3	14.5213738	1.7
310	4	4	1	3	3	3	1	2	14.5214373	2.5
311	4	4	1	4	3	3	1	4	14.5204862	−0.3
312	4	4	1	3	3	3	1	3	14.5226230	−7.4
313	4	4	0	5	3	3	1	4	14.5255275	0.4
314	4	4	0	4	3	3	1	3	14.5254078	0.9
315	4	4	0	3	3	3	1	2	14.5254792	3.5
316	4	4	0	4	3	3	1	4	14.5245205	−0.8
317	4	4	0	3	3	3	1	3	14.5266717	0.4
318	5	2	4	6	4	1	4	5	14.7406880	−0.7
319	5	2	4	5	4	1	4	4	14.7398090	2.3
320	5	2	4	4	4	1	4	3	14.7409527	7.2

No.	J'	K_a'	K_c'	F'	J	K_a	K_c	F	ν_{obs}	$\nu_c - \nu_o$
321	7	5	3	8	6	5	2	7	14.7522721	−2.7
322	7	5	3	7	6	5	2	6	14.7525155	2.2
323	7	5	3	6	6	5	2	5	14.7522292	5.4
324	7	4	4	8	6	4	3	7	14.7799100	−2.3
325	7	4	4	7	6	4	3	6	14.7800762	0.1
326	7	4	4	6	6	4	3	5	14.7798809	−0.1
327	7	5	2	8	6	5	1	7	14.7829047	−5.1
328	7	5	2	7	6	5	1	6	14.7831313	−2.0
329	7	5	2	6	6	5	1	5	14.7828637	2.9
330	7	4	3	8	6	4	2	7	15.1402955	2.6
331	7	4	3	7	6	4	2	6	15.1403427	−1.4
332	7	4	3	6	6	4	2	5	15.1402724	−3.3
333	8	1	7	9	7	2	6	8	15.1849736	0.3
334	8	1	7	8	7	2	6	7	15.1850959	−0.3
335	7	2	5	8	6	2	4	7	15.1915094	1.0
336	7	2	5	7	6	2	4	6	15.1917066	−0.1
337	7	2	5	6	6	2	4	5	15.1914772	0.8
338	8	2	7	9	7	2	6	8	15.2324021	−0.1
339	8	2	7	8	7	2	6	7	15.2325386	−1.0
340	8	2	7	7	7	2	6	6	15.2324021	0.5
341	6	3	4	7	5	2	3	6	15.2600709	0.8
342	6	3	4	6	5	2	3	5	15.2604503	−2.6
343	6	3	4	5	5	2	3	4	15.2599943	−1.2
344	5	3	3	6	4	2	3	5	15.2964784	−1.0
345	5	3	3	5	4	2	3	4	15.2960503	−0.7
346	5	3	3	4	4	2	3	3	15.2965843	0.1
347	8	1	7	8	7	1	6	7	15.3085306	0.1
348	8	1	7	7	7	1	6	6	15.3083643	−0.7
349	8	2	7	9	7	1	6	8	15.3557974	−0.9
350	8	2	7	8	7	1	6	7	15.3559769	3.0
351	8	2	7	7	7	1	6	6	15.3557911	−1.0
352	9	0	9	10	8	1	8	9	15.6236533	−1.1
353	9	0	9	9	8	1	8	8	15.6236978	−7.1
354	9	1	9	10	8	1	8	9	15.6240094	0.9
355	9	1	9	9	8	1	8	8	15.6240591	0.0
356	9	0	9	10	8	0	8	9	15.6248061	−0.5

No.	J'	K_a'	K_c'	F'	J	K_a	K_c	F	ν_{obs}	$\nu_c - \nu_o$
357	9	0	9	9	8	0	8	8	15.6248559	−1.6
358	9	1	9	10	8	0	8	9	15.6251626	1.9
359	9	1	9	9	8	0	8	8	15.6252121	0.3
360	8	2	6	9	7	3	5	8	15.6629808	0.0
361	8	2	6	8	7	3	5	7	15.6630131	10.5
362	8	2	6	7	7	3	5	6	15.6629817	−1.1
363	7	3	4	8	6	3	3	7	15.6798354	3.5
364	7	3	4	7	6	3	3	6	15.6798654	−1.0
365	7	3	4	6	6	3	3	5	15.6798167	−0.7
366	5	3	2	6	4	2	3	5	15.8547259	−0.4
367	5	3	2	5	4	2	3	4	15.8539916	0.1
368	5	3	2	4	4	2	3	3	15.8548941	0.5

Table F.4: Observed frequencies ν_{obs} in GHz of conformer **0MM** of N,N-diethylpropionamide. $\nu_c - \nu_o$ values in kHz are obtained after a fit with the program XIAM. J, K_a, and K_c are the symmetric top rotational quantum numbers, F is the total angular momentum in the coupled basis with $F = J + I$.

No.	J'	K_a'	K_c'	F'	J	K_a	K_c	F	ν_{obs}	$\nu_c - \nu_o$
1	4	2	3	5	3	2	2	4	8.093905	2.2
2	4	2	3	4	3	2	2	3	8.094224	0.6
3	4	2	3	3	3	2	2	2	8.093816	−4.7
4	4	2	3	4	3	2	2	4	8.094224	0.6
5	4	2	3	3	3	2	2	3	8.093816	−4.7
6	3	1	2	4	2	0	2	3	8.154579	0.9
7	3	1	2	3	2	0	2	2	8.153159	0.7
8	3	1	2	2	2	0	2	1	8.155255	−0.8
9	4	1	3	5	3	1	2	4	8.615781	0.0
10	4	1	3	4	3	1	2	3	8.616040	0.0
11	4	1	3	3	3	1	2	2	8.615664	0.7
12	4	1	3	4	3	1	2	4	8.615495	−0.9
13	4	1	3	3	3	1	2	3	8.616397	−0.7
14	4	2	2	5	3	2	1	4	8.671209	−1.4
15	4	2	2	4	3	2	1	3	8.671179	4.2
16	4	2	2	3	3	2	1	2	8.671153	−2.5
17	4	2	2	4	3	2	1	4	8.670483	−0.9

No.	J'	K_a'	K_c'	F'	J	K_a	K_c	F	ν_{obs}	$\nu_c - \nu_o$
18	4	2	2	3	3	2	1	3	8.672089	0.0
19	3	2	2	4	2	1	1	3	8.782590	−1.2
20	3	2	2	3	2	1	1	2	8.783374	0.0
21	3	2	2	2	2	1	1	1	8.782156	0.1
22	3	2	2	3	2	1	1	3	8.782590	−1.2
23	3	2	2	2	2	1	1	2	8.783374	0.0
24	5	0	5	6	4	1	4	5	9.060880	0.5
25	5	0	5	5	4	1	4	4	9.060967	1.4
26	5	0	5	5	4	1	4	5	9.062817	−0.4
27	5	0	5	4	4	1	4	4	9.058633	0.0
28	3	2	1	4	2	1	1	3	9.126492	1.2
29	3	2	1	3	2	1	1	2	9.126583	0.4
30	3	2	1	2	2	1	1	1	9.126297	−1.6
31	5	1	5	6	4	1	4	5	9.151936	0.4
32	5	1	5	5	4	1	4	4	9.152104	−0.2
33	5	1	5	4	4	1	4	3	9.152001	0.6
34	6	2	4	7	5	3	3	6	9.192268	−1.6
35	6	2	4	6	5	3	3	5	9.191804	−0.9
36	6	2	4	5	5	3	3	4	9.192341	−1.0
37	5	0	5	6	4	0	4	5	9.258810	0.9
38	5	0	5	5	4	0	4	4	9.259083	−0.1
39	5	0	5	4	4	0	4	3	9.258841	−1.5
40	5	0	5	5	4	0	4	5	9.260747	0.3
41	5	0	5	4	4	0	4	4	9.256750	−0.6
42	5	1	5	6	4	0	4	5	9.349865	−0.3
43	5	1	5	5	4	0	4	4	9.350224	2.0
44	5	1	5	4	4	0	4	3	9.349885	3.0
45	5	1	5	5	4	0	4	5	9.351886	−0.2
46	5	1	5	4	4	0	4	4	9.347789	−0.9
47	5	2	4	6	4	2	3	5	10.027647	−0.6
48	5	2	4	5	4	2	3	4	10.027894	0.9
49	5	2	4	4	4	2	3	3	10.027618	3.9
50	5	2	4	5	4	2	3	5	10.028216	2.6
51	5	2	4	4	4	2	3	4	10.027210	−1.0
52	3	2	1	4	2	1	2	3	10.095481	1.8
53	3	2	1	3	2	1	2	2	10.093430	2.7

No.	J'	K_a'	K_c'	F'	J	K_a	K_c	F	ν_{obs}	$\nu_c - \nu_o$
54	3	2	1	2	2	1	2	1	10.096478	0.3
55	4	2	3	5	3	1	2	4	10.330752	2.5
56	4	2	3	4	3	1	2	3	10.331611	−2.7
57	4	2	3	3	3	1	2	2	10.330475	−1.5
58	5	3	3	6	4	3	2	5	10.349620	2.3
59	5	3	3	5	4	3	2	4	10.349845	−0.1
60	5	3	3	4	4	3	2	3	10.349551	2.0
61	5	3	2	6	4	3	1	5	10.548761	−0.4
62	5	3	2	5	4	3	1	4	10.548793	−1.6
63	5	3	2	4	4	3	1	3	10.548727	1.1
64	5	1	4	6	4	1	3	5	10.566827	1.0
65	5	1	4	5	4	1	3	4	10.567156	0.5
66	5	1	4	4	4	1	3	3	10.566743	−0.8
67	6	0	6	7	5	1	5	6	10.855399	0.3
68	6	0	6	6	5	1	5	5	10.855505	0.3
69	6	0	6	5	5	1	5	4	10.855451	−0.5
70	6	0	6	6	5	1	5	6	10.857526	0.5
71	6	0	6	5	5	1	5	5	10.853018	−0.5
72	6	1	6	7	5	1	5	6	10.894332	0.3
73	6	1	6	6	5	1	5	5	10.894472	1.0
74	6	1	6	5	5	1	5	4	10.894377	−1.0
75	6	1	6	6	5	1	5	6	10.896491	0.2
76	6	1	6	5	5	1	5	5	10.891945	−0.8
77	6	0	6	7	5	0	5	6	10.946455	0.2
78	6	0	6	6	5	0	5	5	10.946644	0.4
79	6	0	6	5	5	0	5	4	10.946489	−0.7
80	6	0	6	6	5	0	5	6	10.948580	−1.7
81	6	0	6	5	5	0	5	5	10.944158	0.5
82	5	2	3	5	4	2	2	4	10.948196	1.1
83	5	2	3	4	4	2	2	3	10.948159	0.5
84	6	1	6	7	5	0	5	6	10.985388	0.6
85	6	1	6	6	5	0	5	5	10.985609	−0.6
86	6	1	6	5	5	0	5	4	10.985418	0.1
87	6	1	6	6	5	0	5	6	10.987548	0.6
88	6	1	6	5	5	0	5	5	10.983085	−0.3
89	6	1	5	7	5	2	4	6	11.198645	0.6

No.	J'	K_a'	K_c'	F'	J	K_a	K_c	F	ν_{obs}	$\nu_c - \nu_o$
90	6	1	5	6	5	2	4	5	11.198499	−0.6
91	6	1	5	5	5	2	4	4	11.198688	−0.7
92	6	1	5	6	5	2	4	6	11.199064	−1.8
93	6	1	5	5	5	2	4	5	11.198005	−1.9
94	4	2	2	4	3	1	2	3	11.251776	1.3
95	4	2	2	3	3	1	2	2	11.251957	2.5
96	3	3	1	4	2	2	0	3	11.337608	−0.7
97	3	3	1	3	2	2	0	2	11.337650	−1.8
98	3	3	1	2	2	2	0	1	11.337411	−2.4
99	3	3	1	3	2	2	0	3	11.336774	−0.5
100	3	3	1	2	2	2	0	2	11.338774	−3.4
101	3	3	1	4	2	2	1	3	11.410769	−1.3
102	3	3	1	3	2	2	1	2	11.410517	2.4
103	3	3	0	4	2	2	1	3	11.421449	1.6
104	3	3	0	3	2	2	1	2	11.421157	−0.8
105	3	3	0	2	2	2	1	1	11.421423	−6.5
106	3	3	0	3	2	2	1	3	11.420580	0.3
107	3	3	0	2	2	2	1	2	11.422328	−0.8
108	5	2	4	6	4	1	3	5	11.742616	0.3
109	5	2	4	5	4	1	3	4	11.743467	−0.1
110	5	2	4	4	4	1	3	3	11.742428	0.3
111	6	2	5	7	5	2	4	6	11.909469	0.7
112	6	2	5	6	5	2	4	5	11.909686	−0.1
113	6	2	5	5	5	2	4	4	11.909449	−1.7
114	6	2	5	6	5	2	4	6	11.910253	0.1
115	6	2	5	5	5	2	4	5	11.908768	−1.1
116	7	2	5	8	6	3	4	7	12.013181	−2.2
117	7	2	5	7	6	3	4	6	12.012728	−0.9
118	7	2	5	6	6	3	4	5	12.013251	1.9
119	6	1	5	7	5	1	4	6	12.374435	0.5
120	6	1	5	6	5	1	4	5	12.374811	0.2
121	6	1	5	5	5	1	4	4	12.374372	0.2
122	6	4	3	7	5	4	2	6	12.462590	−0.9
123	6	4	3	6	5	4	2	5	12.462787	0.5
124	6	4	3	5	5	4	2	4	12.462540	1.7
125	6	4	2	7	5	4	1	6	12.505901	−2.4

No.	J'	K_a'	K_c'	F'	J	K_a	K_c	F	ν_{obs}	$\nu_c - \nu_o$
126	6	4	2	6	5	4	1	5	12.506050	−1.2
127	6	4	2	5	5	4	1	4	12.505857	−0.4
128	7	0	7	8	6	1	6	7	12.606703	0.4
129	7	0	7	7	6	1	6	6	12.606805	0.1
130	7	0	7	6	6	1	6	5	12.606741	−0.5
131	7	0	7	7	6	1	6	7	12.608965	0.2
132	7	0	7	6	6	1	6	6	12.604216	−1.0
133	7	1	7	8	6	1	6	7	12.622556	0.6
134	7	1	7	7	6	1	6	6	12.622670	0.7
135	7	1	7	6	6	1	6	5	12.622592	0.5
136	7	1	7	7	6	1	6	7	12.624828	−0.8
137	7	1	7	6	6	1	6	6	12.620066	−1.3
138	7	0	7	8	6	0	6	7	12.645636	0.8
139	7	0	7	7	6	0	6	6	12.645771	0.1
140	7	0	7	6	6	0	6	5	12.645669	0.0
141	7	0	7	7	6	0	6	7	12.647898	1.0
142	7	1	7	8	6	0	6	7	12.661488	0.3
143	7	1	7	7	6	0	6	6	12.661637	1.6
144	7	1	7	6	6	0	6	5	12.661519	0.4
145	7	1	7	7	6	0	6	7	12.663762	0.1
146	7	1	7	6	6	0	6	6	12.659033	0.2
147	6	3	3	7	5	3	2	6	12.860499	−0.9
148	6	3	3	6	5	3	2	5	12.860401	−1.2
149	6	3	3	6	5	3	2	6	12.859889	−0.7
150	6	2	5	7	5	1	4	6	13.085253	−4.9
151	6	2	5	6	5	1	4	5	13.085997	−0.3
152	6	2	5	5	5	1	4	4	13.085133	−0.9
153	6	2	4	7	5	2	3	6	13.146924	−2.9
154	6	2	4	6	5	2	3	5	13.147011	1.1
155	6	2	4	5	5	2	3	4	13.146888	0.5
156	6	2	4	6	5	2	3	6	13.146281	0.1
157	6	2	4	5	5	2	3	5	13.147764	−0.5
158	4	3	2	5	3	2	1	4	13.224451	4.4
159	4	3	2	4	3	2	1	3	13.224733	3.5
160	4	3	2	4	3	2	1	4	13.224038	−0.4
161	4	3	2	3	3	2	1	3	13.225241	−2.3

No.	J'	K_a'	K_c'	F'	J	K_a	K_c	F	ν_{obs}	$\nu_c - \nu_o$
162	7	1	6	7	6	2	5	6	13.358657	2.1
163	7	1	6	6	6	2	5	5	13.358687	6.4
164	7	1	6	7	6	2	5	7	13.359440	0.5
165	7	1	6	6	6	2	5	6	13.357762	−1.1
166	4	3	1	5	3	2	2	4	13.640752	−6.1
167	4	3	1	4	3	2	2	3	13.640213	0.5
168	4	3	1	3	3	2	2	2	13.640902	3.3
169	4	3	1	4	3	2	2	4	13.640213	0.5
170	4	3	1	3	3	2	2	3	13.640902	3.3
171	7	2	6	8	6	2	5	7	13.740472	1.8
172	7	2	6	7	6	2	5	6	13.740673	0.3
173	7	2	6	6	6	2	5	5	13.740460	−0.1
174	7	2	6	7	6	2	5	7	13.741459	1.3
175	7	1	6	8	6	1	5	7	14.069483	−0.5
176	7	1	6	7	6	1	5	6	14.069842	−0.2
177	7	1	6	6	6	1	5	5	14.069443	0.3
178	8	0	8	9	7	1	7	8	14.337088	0.3
179	8	0	8	8	7	1	7	7	14.337177	0.5
180	8	0	8	7	7	1	7	6	14.337119	0.9
181	8	0	8	8	7	1	7	8	14.339447	−3.3
182	8	0	8	7	7	1	7	7	14.334517	0.8
183	8	1	8	9	7	1	7	8	14.343323	0.4
184	8	1	8	8	7	1	7	7	14.343417	0.7
185	8	1	8	7	7	1	7	6	14.343353	0.3
186	8	0	8	9	7	0	7	8	14.352940	−0.4
187	8	0	8	8	7	0	7	7	14.353042	0.3
188	8	0	8	7	7	0	7	6	14.352969	−0.1
189	8	1	8	9	7	0	7	8	14.359175	−0.1
190	8	1	8	8	7	0	7	7	14.359282	0.5
191	8	1	8	7	7	0	7	6	14.359203	−0.6
192	8	1	8	8	7	0	7	8	14.361541	−1.4
193	8	1	8	7	7	0	7	7	14.356615	−0.9
194	7	3	5	8	6	3	4	7	14.419937	0.9
195	7	3	5	7	6	3	4	6	14.420086	0.3
196	7	3	5	6	6	3	4	5	14.419911	−3.6
197	7	2	6	8	6	1	5	7	14.451292	−1.5

No.	J'	K_a'	K_c'	F'	J	K_a	K_c	F	ν_{obs}	$\nu_c - \nu_o$
198	7	2	6	7	6	1	5	6	14.451862	1.9
199	7	2	6	6	6	1	5	5	14.451220	−2.2
200	7	4	4	8	6	4	3	7	14.579984	0.2
201	7	4	4	7	6	4	3	6	14.580099	−1.9
202	7	4	4	6	6	4	3	5	14.579961	2.8
203	5	3	3	6	4	2	2	5	14.902856	2.6
204	5	3	3	5	4	2	2	4	14.903399	−0.3
205	5	3	3	4	4	2	2	3	14.902704	0.7
206	7	3	4	8	6	3	3	7	15.225415	0.6
207	7	3	4	7	6	3	3	6	15.225308	0.1
208	7	3	4	6	6	3	3	5	15.225415	0.3
209	7	2	5	8	6	2	4	7	15.225925	0.3
210	7	2	5	7	6	2	4	6	15.226101	1.9
211	7	2	5	6	6	2	4	5	15.225885	1.6
212	8	1	7	9	7	2	6	8	15.341386	−0.6
213	8	1	7	8	7	2	6	7	15.341472	1.1
214	8	1	7	7	7	2	6	6	15.341394	−0.6
215	8	1	7	9	7	1	6	8	15.723197	0.7
216	8	1	7	8	7	1	6	7	15.723489	0.1
217	8	1	7	7	7	1	6	6	15.723172	−2.1
218	8	2	7	9	7	1	6	8	15.910027	−2.0
219	8	2	7	8	7	1	6	7	15.910424	0.1
220	8	2	7	7	7	1	6	6	15.909994	0.8

Appendix G

N,N-Dimethylpropionamide

Table G.1: Nuclear coordinates (in Å) in the principal axis system of conformer **I** of N,N-dimethylpropionamide, calculated at the MP2/6-311++G(d,p) level of theory.

	conformer I		
	a	*b*	*c*
N_1	1.077780	0.152523	−0.170171
C_2	−0.221508	−0.285094	−0.021081
O_3	−0.492409	−1.479348	0.075686
C_4	−1.310799	0.782894	−0.023679
H_5	−1.168833	1.432090	0.849407
H_6	−1.188207	1.419276	−0.907701
C_7	−2.704658	0.163731	−0.001507
H_8	−3.466168	0.948779	0.004289
H_9	−2.859495	−0.469918	−0.877111
H_{10}	−2.835125	−0.461573	0.883543
C_{11}	2.132097	−0.838737	0.001444
H_{12}	3.029142	−0.491022	−0.516904
H_{13}	2.369095	−0.996141	1.062430
H_{14}	1.804316	−1.786132	−0.423342
C_{15}	1.467316	1.528765	0.096760
H_{16}	2.415539	1.727374	−0.409728
H_{17}	0.726705	2.226502	−0.291545
H_{18}	1.604099	1.717085	1.171478

Table G.2: Observed frequencies ν_{obs} in GHz of N,N-dimethylpropionamide. $\nu_c - \nu_o$ values in kHz are obtained after a fit with the program XIAM. J, K_a, and K_c are the symmetric top rotational quantum numbers, F is the total angular momentum in the coupled basis with $F = J + I$.

No.	J'	K_a'	K_c'	F'	J	K_a	K_c	F	ν_{obs}	$\nu_c - \nu_o$
1	3	0	3	4	2	0	2	3	9.3499917	0.6
2	3	0	3	3	2	0	2	2	9.3502716	0.4
3	3	0	3	2	2	0	2	1	9.3500687	2.2
4	3	0	3	3	2	0	2	3	9.3511155	0.5
5	3	0	3	2	2	0	2	2	9.3487536	−0.3
6	3	2	2	4	2	2	1	3	9.5568108	2.1
7	3	2	2	3	2	2	1	2	9.5574825	−1.1
8	3	2	2	2	2	2	1	1	9.5564353	1.6
9	3	2	2	3	2	2	1	3	9.5568108	2.1
10	3	2	2	2	2	2	1	2	9.5574825	−1.1
11	3	2	1	4	2	2	0	3	9.7637699	4.2
12	3	2	1	3	2	2	0	2	9.7641832	−2.2
13	3	2	1	2	2	2	0	1	9.7634445	−0.8
14	2	2	1	3	2	1	2	3	9.9999929	−1.3
15	2	2	1	2	2	1	2	2	9.9978150	−1.1
16	2	2	1	1	2	1	2	1	10.0012037	−0.5
17	2	2	1	3	2	1	2	2	9.9984954	4.4
18	2	2	1	2	2	1	2	1	10.0001538	−0.6
19	2	2	1	1	2	1	2	2	9.9988679	1.9
20	2	2	1	2	2	1	2	3	9.9993215	2.2
21	5	1	4	6	4	2	3	5	9.7583047	−1.7
22	5	1	4	5	4	2	3	4	9.7576877	−0.3
23	5	1	4	4	4	2	3	3	9.7584566	6.7
24	3	1	2	4	2	1	1	3	10.2240045	−0.4
25	3	1	2	3	2	1	1	2	10.2242087	−0.6
26	3	1	2	2	2	1	1	1	10.2237650	1.8
27	3	1	2	3	2	1	1	3	10.2233814	0.4
28	3	1	2	2	2	1	1	2	10.2250529	1.3
29	4	0	4	5	3	1	3	4	10.3275074	−0.3
30	4	0	4	4	3	1	3	3	10.3271673	−1.0
31	4	0	4	3	3	1	3	2	10.3277604	−0.2
32	4	0	4	4	3	1	3	4	10.3289529	0.0

No.	J'	K_a'	K_c'	F'	J	K_a	K_c	F	ν_{obs}	$\nu_c - \nu_o$
33	4	0	4	3	3	1	3	3	10.3253494	−2.0
34	3	2	2	4	3	1	3	4	10.7334147	1.5
35	3	2	2	3	3	1	3	3	10.7316288	0.2
36	3	2	2	2	3	1	3	2	10.7340394	1.6
37	3	1	3	4	2	0	2	3	11.2730193	−3.0
38	3	1	3	3	2	0	2	2	11.2739646	1.5
39	3	1	3	2	2	0	2	1	11.2728691	2.6
40	3	1	3	3	2	0	2	3	11.2748096	2.7
41	3	1	3	2	2	0	2	2	11.2715499	−4.0
42	4	2	3	5	4	1	4	5	11.7236404	−0.3
43	4	2	3	4	4	1	4	4	11.7220012	0.4
44	4	2	3	3	4	1	4	3	11.7240650	2.6
45	4	2	3	5	4	1	4	4	11.7216741	1.6
46	4	2	3	4	4	1	4	5	11.7239652	−3.9
47	4	2	3	4	4	1	4	3	11.7244750	−0.2
48	4	2	3	3	4	1	4	4	11.7215855	−2.5
49	4	1	4	5	3	1	3	4	11.7110804	0.9
50	4	1	4	4	3	1	3	3	11.7112631	0.0
51	4	1	4	3	3	1	3	2	11.7111967	−1.2
52	4	1	4	4	3	1	3	4	11.7130482	0.5
53	4	1	4	3	3	1	3	3	11.7087914	2.7
54	4	0	4	5	3	0	3	4	12.2505390	0.1
55	4	0	4	4	3	0	3	3	12.2508606	0.4
56	4	0	4	3	3	0	3	2	12.2505614	0.8
57	4	0	4	4	3	0	3	4	12.2519843	0.2
58	4	0	4	3	3	0	3	3	12.2490439	0.6
59	4	2	3	5	3	2	2	4	12.7013060	−1.0
60	4	2	3	4	3	2	2	3	12.7016330	−2.3
61	4	2	3	3	3	2	2	2	12.7012195	−3.0
62	4	2	3	4	3	2	2	4	12.7016330	−2.3
63	4	2	3	3	3	2	2	3	12.7012195	−3.0
64	4	3	2	5	3	3	1	4	12.8377133	15.6
65	4	3	2	4	3	3	1	3	12.8382552	5.8
66	4	3	2	3	3	3	1	2	12.8374711	1.2
67	4	3	1	5	3	3	0	4	12.8600066	−16.1
68	4	3	1	4	3	3	0	3	12.8605192	−25.2

No.	J'	K_a'	K_c'	F'	J	K_a	K_c	F	ν_{obs}	$\nu_c - \nu_o$
69	4	3	1	3	3	3	0	2	12.8597728	−29.0
70	4	2	2	5	3	2	1	4	13.1931338	−4.9
71	4	2	2	4	3	2	1	3	13.1931583	−3.8
72	4	2	2	3	3	2	1	2	13.1930907	−2.6
73	4	2	2	4	3	2	1	4	13.1927337	−4.4
74	4	2	2	3	3	2	1	3	13.1936600	−5.7
75	4	1	3	5	3	1	2	4	13.5611682	0.5
76	4	1	3	4	3	1	2	3	13.5613271	0.6
77	4	1	3	3	3	1	2	2	13.5610697	0.7
78	4	1	3	4	3	1	2	4	13.5607032	0.6
79	4	1	3	3	3	1	2	3	13.5619089	−2.4
80	4	1	4	5	3	0	3	4	13.6341130	2.3
81	4	1	4	4	3	0	3	3	13.6349550	0.0
82	4	1	4	3	3	0	3	2	13.6339976	−0.4
83	4	1	4	4	3	0	3	4	13.6360802	1.3
84	4	1	4	3	3	0	3	3	13.6324803	−0.3
85	5	0	5	6	4	1	4	5	13.6449134	0.8
86	5	0	5	5	4	1	4	4	13.6447042	−0.2
87	5	0	5	4	4	1	4	3	13.6450606	0.4
88	5	0	5	5	4	1	4	5	13.6466724	−0.3
89	5	0	5	4	4	1	4	4	13.6425846	−1.2
90	6	1	5	7	5	2	4	6	13.9374522	1.3
91	6	1	5	6	5	2	4	5	13.9368309	1.6
92	6	1	5	5	5	2	4	4	13.9375735	−1.3
93	5	1	5	6	4	1	4	5	14.5627092	0.0
94	5	1	5	5	4	1	4	4	14.5628566	−1.3
95	5	1	5	4	4	1	4	3	14.5627839	−0.2
96	5	1	5	5	4	1	4	5	14.5648250	−1.2
97	5	1	5	4	4	1	4	4	14.5603081	−1.7
98	5	0	5	6	4	0	4	5	15.0284837	−0.7
99	5	0	5	5	4	0	4	4	15.0288004	1.2
100	5	0	5	4	4	0	4	3	15.0285021	4.5
101	5	0	5	5	4	0	4	5	15.0302445	0.0
102	3	3	0	4	3	2	1	4	15.2710895	23.2
103	3	3	0	3	3	2	1	3	15.2705741	18.8
104	3	3	0	2	3	2	1	2	15.2712661	21.1

No.	J'	K_a'	K_c'	F'	J	K_a	K_c	F	ν_{obs}	$\nu_c - \nu_o$
105	3	3	1	4	3	2	2	4	15.5271072	−1.7
106	3	3	1	3	3	2	2	3	15.5261903	7.1
107	3	3	1	2	3	2	2	2	15.5274293	−3.5
108	2	2	1	3	1	1	0	2	15.4345501	−0.8
109	2	2	1	2	1	1	0	1	15.4352779	−1.1
110	2	2	1	1	1	1	0	0	15.4328195	−1.9
111	2	2	1	2	1	1	0	2	15.4338734	−2.6
112	2	2	1	1	1	1	0	1	15.4363242	−4.6
113	4	3	2	5	4	2	3	5	15.6635022	2.6
114	4	3	2	4	4	2	3	4	15.6628008	3.5
115	4	3	2	3	4	2	3	3	15.6636787	−1.6
116	5	3	3	6	5	2	4	6	15.9261160	−2.2
117	5	3	3	5	5	2	4	5	15.9254725	−0.3
118	5	3	3	4	5	2	4	4	15.9262467	−3.0
119	5	2	4	6	4	2	3	5	15.8109365	−1.7
120	5	2	4	5	4	2	3	4	15.8111540	−1.0
121	5	2	4	4	4	2	3	3	15.8109114	−0.1
122	5	2	4	5	4	2	3	5	15.8114814	−2.0
123	5	2	4	4	4	2	3	4	15.8104971	−1.6
124	2	2	0	3	1	1	1	2	15.9558532	1.2
125	2	2	0	2	1	1	1	1	15.9542301	−5.1
126	2	2	0	1	1	1	1	0	15.9574800	−0.4
127	2	2	0	2	1	1	1	2	15.9550101	1.9
128	2	2	0	1	1	1	1	1	15.9555568	9.0

Appendix H

N,N-Diethylacetamide

Table H.1: Nuclear coordinates (in Å) in the principal axis system of conformer **I** and conformer **II** of N,N-diethylacetamide, calculated at the MP2/6-311++G(d,p) level of theory.

	conformer I			conformer II		
	a	*b*	*c*	*a*	*b*	*c*
N_1	−0.063128	−0.211629	−0.011628	0.123336	−0.062295	0.384239
C_2	0.270916	1.116616	−0.065970	−1.194024	−0.127239	0.009135
O_3	1.350529	1.490887	−0.524705	−1.884987	0.889123	−0.070619
C_4	−0.744877	2.108978	0.476472	−1.770154	−1.498649	−0.305249
H_5	−0.785395	2.059261	1.569411	−1.839930	−2.114556	0.596647
H_6	−0.412937	3.105081	0.185049	−2.772878	−1.342982	−0.702099
H_7	−1.751205	1.933332	0.087949	−1.168876	−2.037036	−1.043233
C_8	−1.298427	−0.732413	0.559820	0.994567	−1.216820	0.558328
H_9	−1.679791	−0.027995	1.301444	0.382814	−2.118651	0.593679
H_{10}	−1.049395	−1.650658	1.105278	1.482685	−1.129921	1.537704
C_{11}	−2.364623	−1.022977	−0.496993	2.052112	−1.345739	−0.538166
H_{12}	−3.260144	−1.447676	−0.031494	2.661998	−2.239818	−0.371543
H_{13}	−2.645989	−0.105028	−1.020508	1.577409	−1.423128	−1.520724
H_{14}	−1.992179	−1.736464	−1.237430	2.717686	−0.478516	−0.545368
C_{15}	0.910515	−1.182524	−0.506394	0.675732	1.264302	0.662260
H_{16}	0.356211	−2.066536	−0.839251	−0.039195	1.806353	1.288611
H_{17}	1.410015	−0.746661	−1.374345	1.592539	1.113370	1.242071
C_{18}	1.938495	−1.555507	0.559848	0.964076	2.074000	−0.601228
H_{19}	2.640070	−2.300996	0.171878	1.378941	3.051261	−0.332935
H_{20}	2.501601	−0.666938	0.853992	1.683179	1.558800	−1.243547
H_{21}	1.448393	−1.973929	1.444732	0.038846	2.231882	−1.158226

Table H.2: Energy values in hartree, rotational constants in GHz and their deviations to the experimental values dev_A, dev_B, dev_C of conformer **I** of N,N-diethylacetamide optimized at different level of theory.

	E	A	dev_A	B	dev_B	C	dev_C
HF							
6-31G(d,p)	-364.124226	2.089	0.040	1.944	0.021	1.160	0.022
6-31G(df,pd)	-364.133670	2.092	0.043	1.945	0.021	1.160	0.022
6-31G(3df,3pd)	-364.155715	2.087	0.038	1.951	0.014	1.161	0.023
6-31+G(d,p)	-364.130825	2.076	0.027	1.949	0.016	1.159	0.021
6-31+G(df,pd)	-364.140244	2.079	0.030	1.950	0.016	1.160	0.021
6-31+G(3df,3pd)	-364.161334	2.081	0.032	1.954	0.012	1.161	0.023
6-31++G(d,p)	-364.131112	2.075	0.026	1.949	0.016	1.159	0.021
6-31++G(df,pd)	-364.140486	2.078	0.030	1.950	0.016	1.160	0.021
6-31++G(3df,3pd)	-364.161453	2.080	0.032	1.954	0.012	1.161	0.023
6-311G(d,p)	-364.196101	2.087	0.038	1.945	0.020	1.159	0.021
6-311G(df,pd)	-364.209836	2.092	0.043	1.950	0.015	1.162	0.024
6-311G(3df,3pd)	-364.229363	2.092	0.043	1.955	0.010	1.163	0.025
6-311+G(d,p)	-364.200847	2.076	0.027	1.950	0.015	1.158	0.020
6-311+G(df,pd)	-364.214871	2.080	0.032	1.956	0.010	1.161	0.023
6-311+G(3df,3pd)	-364.232024	2.083	0.034	1.960	0.005	1.163	0.025
6-311++G(d,p)	-364.201051	2.076	0.028	1.950	0.015	1.158	0.020
6-311++G(df,pd)	-364.215099	2.081	0.032	1.955	0.010	1.161	0.023
6-311++G(3df,3pd)	-364.232081	2.083	0.034	1.960	0.005	1.163	0.025
MP2							
/6-31G(d,p)	-365.331234	2.092	0.043	1.933	0.032	1.160	0.022
6-31G(df,pd)	-365.490288	2.108	0.059	1.944	0.022	1.168	0.030
6-31G(3df,3pd)	-365.616616	2.106	0.057	1.954	0.011	1.173	0.035
6-31+G(d,p)	-365.350621	2.071	0.023	1.939	0.027	1.158	0.020
6-31+G(df,pd)	-365.507582	2.089	0.040	1.949	0.017	1.166	0.028
6-31+G(3df,3pd)	-365.626277	2.092	0.043	1.958	0.007	1.172	0.034
6-31++G(d,p)	-365.352408	2.070	0.021	1.940	0.026	1.158	0.020
6-31++G(df,pd)	-365.508853	2.087	0.039	1.950	0.015	1.166	0.028
6-31++G(3df,3pd)	-365.626768	2.091	0.042	1.959	0.007	1.172	0.033
6-311G(d,p)	-365.466228	2.088	0.040	1.932	0.033	1.161	0.023
6-311G(df,pd)	-365.616559	2.101	0.052	1.945	0.020	1.168	0.030
6-311G(3df,3pd)	-365.715812	2.109	0.061	1.949	0.016	1.171	0.033

	E	A	dev_A	B	dev_B	C	dev_C
6-311+G(d,p)	-365.477932	2.075	0.026	1.938	0.028	1.160	0.021
6-311+G(df,pd)	-365.627363	2.086	0.037	1.951	0.014	1.167	0.029
6-311+G(3df,3pd)	-365.720971	2.094	0.045	1.957	0.008	1.170	0.032
6-311++G(d,p)	-365.478889	2.072	0.024	1.939	0.026	1.159	0.021
6-311++G(df,pd)	-365.628261	2.085	0.036	1.952	0.014	1.167	0.029
cc-pVDZ	-365.407352	2.066	0.017	1.926	0.040	1.154	0.016
B3LYP							
6-31G(d,p)	-366.479707	2.041	0.007	1.929	0.036	1.143	0.005
6-31G(df,pd)	-366.489233	2.051	0.002	1.927	0.039	1.145	0.007
6-31G(3df,3pd)	-366.512136	2.044	0.005	1.939	0.027	1.147	0.009
6-31+G(d,p)	-366.493311	2.024	0.025	1.933	0.033	1.142	0.003
6-31+G(df,pd)	-366.501559	2.027	0.022	1.934	0.031	1.143	0.005
6-31+G(3df,3pd)	-366.520054	2.033	0.016	1.940	0.025	1.146	0.008
6-31++G(d,p)	-366.493516	2.024	0.025	1.933	0.033	1.142	0.003
6-31++G(df,pd)	-366.501726	2.027	0.022	1.934	0.031	1.143	0.005
6-31++G(3df,3pd)	-366.520183	2.033	0.016	1.940	0.025	1.146	0.008
6-311G(d,p)	-366.564854	2.041	0.008	1.932	0.034	1.144	0.006
6-311G(df,pd)	-366.578019	2.049	0.001	1.936	0.029	1.148	0.009
6-311G(3df,3pd)	-366.593978	2.051	0.002	1.942	0.024	1.149	0.011
6-311+G(d,p)	-366.570838	2.028	0.021	1.938	0.028	1.144	0.006
6-311+G(df,pd)	-366.584334	2.034	0.015	1.943	0.022	1.147	0.009
6-311+G(3df,3pd)	-366.597775	2.036	0.013	1.949	0.016	1.149	0.011
6-311++G(d,p)	-366.570972	2.028	0.021	1.938	0.028	1.144	0.006
6-311++G(df,pd)	-366.584504	2.034	0.014	1.943	0.022	1.147	0.009
6-311++G(3df,3pd)	-366.597835	2.036	0.013	1.949	0.016	1.149	0.011
cc-pVDZ	-366.504349	2.029	0.020	1.934	0.031	1.144	0.006
cc-pVTZ	-366.604896	2.037	0.012	1.947	0.019	1.149	0.011

Table H.3: Observed frequencies ν_{obs} in GHz of conformer **I** of N,N-diethylacetamide. $\nu_c - \nu_o$ values in kHz are obtained after a fit with the program XIAM. J, K_a, and K_c are the symmetric top rotational quantum numbers, F is the total angular momentum in the coupled basis with $F = J + I$.

No.	J'	K_a'	K_c'	F'	J	K_a	K_c	F	sym.	ν_{obs}	$\nu_c - \nu_o$
1	3	2	2	4	2	2	1	3	A	9.3106382	−2.0
2	3	2	2	3	2	2	1	2	A	9.3109829	−0.8

No.	J'	K_a'	K_c'	F'	J	K_a	K_c	F	sym.	ν_{obs}	$\nu_c - \nu_o$
3	3	2	2	2	2	2	1	1	A	9.3104487	−0.7
4	3	2	2	3	2	2	1	3	A	9.3106382	−2.0
5	3	2	2	2	2	2	1	2	A	9.3109829	−0.8
6	3	2	2	4	2	2	1	3	E	9.3106153	3.3
7	3	2	2	3	2	2	1	2	E	9.3109574	1.9
8	3	2	2	2	2	2	1	1	E	9.3104224	1.3
9	3	2	2	3	2	2	1	3	E	9.3106153	3.3
10	3	2	2	2	2	2	1	2	E	9.3109574	1.9
11	3	1	2	4	2	1	1	3	A	9.6071603	0.3
12	3	1	2	3	2	1	1	2	A	9.6077323	−1.1
13	3	1	2	2	2	1	1	1	A	9.6068248	−2.1
14	3	1	2	4	2	1	1	3	E	9.6071173	1.9
15	3	1	2	3	2	1	1	2	E	9.6076894	0.6
16	3	1	2	2	2	1	1	1	E	9.6067829	0.7
17	3	2	1	4	2	2	0	3	A	10.8252728	1.8
18	3	2	1	3	2	2	0	2	A	10.8253138	−2.5
19	3	2	1	2	2	2	0	1	A	10.8250569	−1.0
20	3	2	1	3	2	2	0	3	A	10.8243548	−1.9
21	3	2	1	2	2	2	0	2	A	10.8265490	−1.6
22	3	2	1	4	2	2	0	3	E	10.8252191	2.6
23	3	2	1	3	2	2	0	2	E	10.8252611	−0.7
24	3	2	1	2	2	2	0	1	E	10.8250026	−0.8
25	3	2	1	3	2	2	0	3	E	10.8243036	1.4
26	3	2	1	2	2	2	0	2	E	10.8264966	0.5
27	3	1	2	4	2	2	1	3	A	9.2486883	0.5
28	3	1	2	3	2	2	1	2	A	9.2489607	0.4
29	3	1	2	2	2	2	1	1	A	9.2485212	−0.6
30	3	1	2	4	2	2	1	3	E	9.2486613	3.1
31	3	1	2	3	2	2	1	2	E	9.2489326	1.9
32	3	1	2	2	2	2	1	1	E	9.2484931	0.9
33	3	2	2	4	2	1	1	3	A	9.6691126	0.2
34	3	2	2	3	2	1	1	2	A	9.6697553	−1.5
35	3	2	2	2	2	1	1	1	A	9.6687522	−2.2
36	3	2	2	3	2	1	1	3	A	9.6691126	0.2
37	3	2	2	2	2	1	1	2	A	9.6697553	−1.5
38	3	2	2	4	2	1	1	3	E	9.6690711	2.0

No.	J'	K_a'	K_c'	F'	J	K_a	K_c	F	sym.	ν_{obs}	$\nu_c - \nu_o$
39	3	2	2	3	2	1	1	2	E	9.6697149	1.4
40	3	2	2	2	2	1	1	1	E	9.6687124	1.3
41	3	2	2	3	2	1	1	3	E	9.6690711	2.0
42	3	2	2	2	2	1	1	2	E	9.6697149	1.4
43	3	3	1	4	2	2	0	3	A	11.5414118	−0.7
44	3	3	1	3	2	2	0	2	A	11.5417673	−0.9
45	3	3	1	2	2	2	0	1	A	11.5410902	−0.5
46	3	3	1	3	2	2	0	3	A	11.5408084	−0.2
47	3	3	1	2	2	2	0	2	A	11.5425820	−1.5
48	3	3	1	4	2	2	0	3	E	11.5413252	1.3
49	3	3	1	3	2	2	0	2	E	11.5416809	1.2
50	3	3	1	2	2	2	0	1	E	11.5410025	0.3
51	3	3	1	3	2	2	0	3	E	11.5407200	−0.1
52	3	3	1	2	2	2	0	2	E	11.5424949	0.0
53	3	3	0	4	2	2	1	3	A	12.7689540	0.4
54	3	3	0	3	2	2	1	2	A	12.7683448	1.2
55	3	3	0	2	2	2	1	1	A	12.7690974	0.9
56	3	3	0	3	2	2	1	3	A	12.7680003	0.2
57	3	3	0	2	2	2	1	2	A	12.7696307	−0.1
58	3	3	0	4	2	2	1	3	E	12.7688860	0.8
59	3	3	0	3	2	2	1	2	E	12.7682758	0.6
60	3	3	0	2	2	2	1	1	E	12.7690299	1.8
61	3	3	0	3	2	2	1	3	E	12.7679317	0.0
62	3	3	0	2	2	2	1	2	E	12.7695622	−0.2
63	3	3	0	4	2	1	1	3	A	13.1274251	−0.7
64	3	3	0	3	2	1	1	2	A	13.1271160	−0.7
65	3	3	0	3	2	1	1	3	A	13.1264715	−0.8
66	3	3	0	2	2	1	1	2	A	13.1284029	−1.0
67	3	3	0	4	2	1	1	3	E	13.1273429	0.5
68	3	3	0	3	2	1	1	2	E	13.1270326	−0.7
69	3	3	0	3	2	1	1	3	E	13.1263889	0.0
70	3	3	0	2	2	1	1	2	E	13.1283203	−0.2
71	3	3	1	4	2	1	2	3	A	14.9505804	−3.1
72	3	3	1	3	2	1	2	2	A	14.9489918	0.1
73	3	3	1	2	2	1	2	1	A	14.9513435	−0.1
74	3	3	1	2	2	1	2	2	A	14.9498077	0.8

No.	J'	K_a'	K_c'	F'	J	K_a	K_c	F	sym.	ν_{obs}	$\nu_c - \nu_o$
75	3	3	1	4	2	1	2	3	E	14.9504423	1.7
76	3	3	1	3	2	1	2	2	E	14.9488497	0.9
77	3	3	1	2	2	1	2	1	E	14.9512017	0.9
78	3	3	1	2	2	1	2	2	E	14.9496646	0.5
79	3	3	1	4	2	0	2	3	A	14.9631504	−1.1
80	3	3	1	3	2	0	2	2	A	14.9615873	−0.8
81	3	3	1	2	2	0	2	1	A	14.9638928	−3.2
82	3	3	1	3	2	0	2	3	A	14.9625477	0.0
83	3	3	1	2	2	0	2	2	A	14.9624049	1.6
84	3	3	1	4	2	0	2	3	E	14.9630327	−0.4
85	3	3	1	3	2	0	2	2	E	14.9614703	0.7
86	3	3	1	2	2	0	2	1	E	14.9637782	0.6
87	3	3	1	3	2	0	2	3	E	14.9624296	0.3
88	3	3	1	2	2	0	2	2	E	14.9622835	−1.4
89	3	2	1	4	2	1	1	3	A	11.8662221	0.5
90	3	2	1	3	2	1	1	2	A	11.8659518	0.1
91	3	2	1	3	2	1	1	3	A	11.8653075	0.2
92	3	2	1	2	2	1	1	2	A	11.8671859	−0.1
93	3	2	1	4	2	1	1	3	E	11.8661547	0.7
94	3	2	1	3	2	1	1	2	E	11.8658844	0.3
95	3	2	1	3	2	1	1	3	E	11.8652398	0.1
96	3	2	1	2	2	1	1	2	E	11.8671185	0.1
97	3	1	2	4	2	0	2	3	A	11.9879466	−1.9
98	3	1	2	3	2	0	2	2	A	11.9869171	−0.7
99	3	1	2	2	2	0	2	1	A	11.9885069	0.5
100	3	1	2	4	2	0	2	3	E	11.9878873	0.2
101	3	1	2	3	2	0	2	2	E	11.9868569	0.5
102	3	1	2	2	2	0	2	1	E	11.9884464	1.3
103	3	2	2	4	2	1	2	3	A	12.0373340	1.2
104	3	2	2	3	2	1	2	2	A	12.0363453	0.4
105	3	2	2	2	2	1	2	1	A	12.0378823	0.7
106	3	2	2	3	2	1	2	3	A	12.0373340	1.2
107	3	2	2	2	2	1	2	2	A	12.0363453	0.4
108	3	2	2	4	2	1	2	3	E	12.0372479	−0.4
109	3	2	2	3	2	1	2	2	E	12.0362611	0.7
110	3	2	2	2	2	1	2	1	E	12.0377968	−0.3

No.	J'	K_a'	K_c'	F'	J	K_a	K_c	F	sym.	ν_{obs}	$\nu_c - \nu_o$
111	3	2	2	3	2	1	2	3	E	12.0372479	−0.4
112	3	2	2	2	2	1	2	2	E	12.0362611	0.7
113	3	3	0	4	2	2	0	3	A	12.0864749	−0.3
114	3	3	0	3	2	2	0	2	A	12.0864810	−0.3
115	3	3	0	2	2	2	0	1	A	12.0862753	−0.5
116	3	3	0	3	2	2	0	3	A	12.0855212	−0.5
117	3	3	0	2	2	2	0	2	A	12.0877680	−0.5
118	3	3	0	4	2	2	0	3	E	12.0864053	0.4
119	3	3	0	3	2	2	0	2	E	12.0864120	1.0
120	3	3	0	2	2	2	0	1	E	12.0862056	0.1
121	3	3	0	3	2	2	0	3	E	12.0854519	0.5
122	3	3	0	2	2	2	0	2	E	12.0876988	0.6
123	3	3	1	4	2	2	1	3	A	12.2238909	0.0
124	3	3	1	3	2	2	1	2	A	12.2236310	0.5
125	3	3	1	3	2	2	1	3	A	12.2232867	−0.3
126	3	3	1	2	2	2	1	2	A	12.2244448	−0.9
127	3	3	1	4	2	2	1	3	E	12.2238052	0.9
128	3	3	1	3	2	2	1	2	E	12.2235452	1.3
129	3	3	1	2	2	2	1	1	E	12.2238258	1.0
130	3	3	1	3	2	2	1	3	E	12.2232013	0.9
131	3	3	1	2	2	2	1	2	E	12.2243599	0.8
132	3	2	1	4	2	0	2	3	A	14.2470085	−1.5
133	3	2	1	3	2	0	2	2	A	14.2451365	0.4
134	3	2	1	2	2	0	2	1	A	14.2478623	−0.9
135	3	2	1	3	2	0	2	3	A	14.2460961	0.4
136	3	2	1	2	2	0	2	2	A	14.2463677	−2.8
137	3	2	1	4	2	0	2	3	E	14.2469236	−2.1
138	3	2	1	3	2	0	2	2	E	14.2450504	−1.4
139	3	2	1	2	2	0	2	1	E	14.2477774	−1.5
140	3	2	1	3	2	0	2	3	E	14.2460090	−2.4
141	3	2	1	2	2	0	2	2	E	14.2462838	−2.3
142	3	2	1	4	2	1	2	3	A	14.2344425	0.5
143	3	2	1	3	2	1	2	2	A	14.2325367	−3.1
144	3	2	1	2	2	1	2	1	A	14.2353082	−2.6
145	3	2	1	4	2	1	2	3	E	14.2343293	−3.9
146	3	2	1	3	2	1	2	2	E	14.2324293	−1.7

No.	J'	K_a'	K_c'	F'	J	K_a	K_c	F	sym.	ν_{obs}	$\nu_c - \nu_o$
147	3	2	1	2	2	1	2	1	E	14.2352016	−0.4
148	4	3	2	4	3	3	1	3	A	13.1462401	−1.3
149	4	3	2	3	3	3	1	2	A	13.1459429	−1.3
150	4	3	2	4	3	3	1	4	A	13.1456360	−1.5
151	4	3	2	3	3	3	1	3	A	13.1467594	0.0
152	4	3	2	5	3	3	1	4	E	13.1460090	2.7
153	4	3	2	4	3	3	1	3	E	13.1461986	0.5
154	4	3	2	3	3	3	1	2	E	13.1459020	1.1
155	4	3	2	4	3	3	1	4	E	13.1455969	2.7
156	4	3	2	3	3	3	1	3	E	13.1467195	3.4
157	4	2	2	5	3	2	1	4	A	13.6821477	0.0
158	4	2	2	4	3	2	1	3	A	13.6825285	0.4
159	4	2	2	3	3	2	1	2	A	13.6819635	−1.5
160	4	2	2	4	3	2	1	4	A	13.6816136	−0.1
161	4	2	2	3	3	2	1	3	A	13.6831977	−1.7
162	4	2	2	5	3	2	1	4	E	13.6820804	1.1
163	4	2	2	4	3	2	1	3	E	13.6824599	0.3
164	4	2	2	3	3	2	1	2	E	13.6818958	−0.8
165	4	2	2	4	3	2	1	4	E	13.6815463	1.0
166	4	2	2	3	3	2	1	3	E	13.6831313	0.4
167	4	3	1	3	3	3	0	2	A	14.5769013	−0.7
168	4	3	1	4	3	3	0	4	A	14.5759503	0.4
169	4	3	1	3	3	3	0	3	A	14.5781886	−0.6
170	4	3	1	5	3	3	0	4	E	14.5769013	2.8
171	4	3	1	4	3	3	0	4	E	14.5758762	0.5
172	4	3	1	3	3	3	0	3	E	14.5781164	1.4
173	4	3	2	5	3	2	1	4	A	13.8621904	−0.7
174	4	3	2	4	3	2	1	3	A	13.8626931	−0.2
175	4	3	2	3	3	2	1	2	A	13.8619784	1.4
176	4	3	2	4	3	2	1	4	A	13.8617780	−1.0
177	4	3	2	3	3	2	1	3	A	13.8632110	−0.3
178	4	3	2	5	3	2	1	4	E	13.8621137	0.0
179	4	3	2	4	3	2	1	3	E	13.8626163	0.4
180	4	3	2	3	3	2	1	2	E	13.8619003	0.7
181	4	3	2	4	3	2	1	4	E	13.8617019	0.3
182	4	3	2	3	3	2	1	3	E	13.8631346	0.7

No.	J'	K_a'	K_c'	F'	J	K_a	K_c	F	sym.	ν_{obs}	$\nu_c - \nu_o$
183	4	2	3	5	3	2	2	4	A	11.7738235	−0.2
184	4	2	3	4	3	2	2	3	A	11.7741690	−0.8
185	4	2	3	3	3	2	2	2	A	11.7737337	−1.0
186	4	2	3	4	3	2	2	4	A	11.7741690	−0.8
187	4	2	3	3	3	2	2	3	A	11.7737337	−1.0
188	4	2	3	5	3	2	2	4	E	11.7738441	1.1
189	4	2	3	4	3	2	2	3	E	11.7741904	1.4
190	4	2	3	3	3	2	2	2	E	11.7737552	1.2
191	4	2	3	4	3	2	2	4	E	11.7741904	1.4
192	4	2	3	3	3	2	2	3	E	11.7737552	1.2
193	4	1	3	5	3	1	2	4	A	11.8299855	0.1
194	4	1	3	4	3	1	2	3	A	11.8303956	−0.2
195	4	1	3	3	3	1	2	2	A	11.8298705	−2.8
196	4	1	3	5	3	1	2	4	E	11.8298872	2.2
197	4	1	3	4	3	1	2	3	E	11.8302961	0.6
198	4	1	3	3	3	1	2	2	E	11.8297718	−1.1
199	4	1	3	5	3	2	2	4	E	11.7679307	−0.5
200	4	1	3	4	3	2	2	3	E	11.7682709	0.2
201	4	1	3	3	3	2	2	2	E	11.7678438	−0.2
202	4	1	3	4	3	2	2	4	E	11.7682709	0.2
203	4	1	3	3	3	2	2	3	E	11.7678438	−0.2
204	4	1	3	5	3	2	2	4	A	11.7680333	0.3
205	4	1	3	4	3	2	2	3	A	11.7683717	−0.6
206	4	1	3	3	3	2	2	2	A	11.7679480	2.3
207	4	1	3	4	3	2	2	4	A	11.7683717	−0.6
208	4	1	3	3	3	2	2	3	A	11.7679480	2.3
209	4	2	3	5	3	1	2	4	A	11.8357755	−0.6
210	4	2	3	4	3	1	2	3	A	11.8361924	−0.9
211	4	2	3	3	3	1	2	2	A	11.8356612	−1.1
212	4	2	3	5	3	1	2	4	E	11.8357990	2.3
213	4	2	3	4	3	1	2	3	E	11.8362154	1.6
214	4	2	3	3	3	1	2	2	E	11.8356845	1.6
215	4	0	4	5	3	0	3	4	A	10.1045801	−1.7
216	4	0	4	4	3	0	3	3	A	10.1047697	−1.3
217	4	0	4	3	3	0	3	2	A	10.1046485	−2.6
218	4	0	4	4	3	0	3	4	A	10.1060398	−1.7

No.	J'	K_a'	K_c'	F'	J	K_a	K_c	F	sym.	ν_{obs}	$\nu_c - \nu_o$
219	4	0	4	3	3	0	3	3	A	10.1029342	−1.6
220	4	0	4	5	3	0	3	4	E	10.1041017	0.3
221	4	0	4	4	3	0	3	3	E	10.1042885	−1.8
222	4	0	4	3	3	0	3	2	E	10.1041725	1.7
223	4	0	4	4	3	0	3	4	E	10.1055610	−0.2
224	4	0	4	3	3	0	3	3	E	10.1024538	−1.3
225	4	1	4	5	3	1	3	4	A	10.1037943	−0.8
226	4	1	4	4	3	1	3	3	A	10.1039827	−0.1
227	4	1	4	3	3	1	3	2	A	10.1038643	−0.6
228	4	1	4	4	3	1	3	4	A	10.1052539	−1.0
229	4	1	4	3	3	1	3	3	A	10.1021456	−1.9
230	4	1	4	5	3	1	3	4	E	10.1042406	0.5
231	4	1	4	4	3	1	3	3	E	10.1044297	1.6
232	4	1	4	3	3	1	3	2	E	10.1043114	1.5
233	4	1	4	4	3	1	3	4	E	10.1057024	2.5
234	4	1	4	3	3	1	3	3	E	10.1025954	2.5
235	4	0	4	5	3	1	3	4	A	10.1037483	−1.0
236	4	0	4	4	3	1	3	3	A	10.1039370	0.0
237	4	0	4	3	3	1	3	2	A	10.1038182	−1.0
238	4	0	4	4	3	1	3	4	A	10.1052074	−1.7
239	4	0	4	3	3	1	3	3	A	10.1021000	−1.8
240	4	1	4	5	3	0	3	4	A	10.1046280	0.5
241	4	1	4	4	3	0	3	3	A	10.1048151	−1.7
242	4	1	4	3	3	0	3	2	A	10.1046961	−0.7
243	4	1	4	4	3	0	3	4	A	10.1060868	−0.5
244	4	1	4	3	3	0	3	3	A	10.1029827	1.2
245	5	2	4	6	4	2	3	5	A	14.1110109	−0.9
246	5	2	4	5	4	2	3	4	A	14.1112852	−0.6
247	5	2	4	4	4	2	3	3	A	14.1109735	−1.0
248	5	2	4	6	4	2	3	5	E	14.1115221	−3.7
249	5	2	4	5	4	2	3	4	E	14.1118001	0.5
250	5	1	4	6	4	2	3	5	A	14.1106012	−0.9
251	5	1	4	5	4	2	3	4	A	14.1108752	−0.4
252	5	1	4	4	4	2	3	3	A	14.1105655	0.6
253	5	1	4	6	4	2	3	5	E	14.1098817	−1.2
254	5	1	4	5	4	2	3	4	E	14.1101580	1.4

No.	J'	K_a'	K_c'	F'	J	K_a	K_c	F	sym.	ν_{obs}	$\nu_c - \nu_o$
255	5	1	4	6	4	1	3	5	A	14.1163920	−0.8
256	5	1	4	5	4	1	3	4	A	14.1166727	−0.4
257	5	1	4	4	4	1	3	3	A	14.1163541	0.2
258	5	1	4	5	4	1	3	5	A	14.1170121	−0.4
259	5	1	4	4	4	1	3	4	A	14.1159269	−0.3
260	5	2	4	6	4	1	3	5	A	14.1168019	−0.7
261	5	2	4	5	4	1	3	4	A	14.1170830	−0.3
262	5	2	4	4	4	1	3	3	A	14.1167627	−0.8
263	5	2	4	5	4	1	3	5	A	14.1174214	−1.2
264	5	1	5	6	4	1	4	5	E	12.4185701	2.0
265	5	1	5	5	4	1	4	4	E	12.4186993	1.0
266	5	1	5	4	4	1	4	3	E	12.4186206	1.1
267	5	1	5	5	4	1	4	5	E	12.4201602	2.1
268	5	1	5	4	4	1	4	4	E	12.4167857	1.3
269	5	0	5	6	4	0	4	5	E	12.4181711	1.2
270	5	0	5	5	4	0	4	4	E	12.4182993	−0.8
271	5	0	5	4	4	0	4	3	E	12.4182217	0.3
272	5	0	5	5	4	0	4	5	E	12.4197603	0.4
273	5	0	5	4	4	0	4	4	E	12.4163870	0.8
274	6	0	6	7	5	0	5	6	A	14.7326251	−1.8
275	6	0	6	6	5	0	5	5	A	14.7327205	−1.9
276	6	0	6	5	5	0	5	4	A	14.7326646	−1.6
277	6	0	6	7	5	0	5	6	E	14.7324078	2.1
278	6	0	6	6	5	0	5	5	E	14.7325031	1.9
279	6	0	6	5	5	0	5	4	E	14.7324467	1.6
280	6	1	6	7	5	1	5	6	A	14.7326251	0.4
281	6	1	6	6	5	1	5	5	A	14.7327205	0.3
282	6	1	6	5	5	1	5	4	A	14.7326637	−0.4
283	6	1	6	7	5	1	5	6	E	14.7328055	1.1
284	6	1	6	6	5	1	5	5	E	14.7328991	−0.7
285	6	1	6	5	5	1	5	4	E	14.7328426	−1.1
286	6	1	5	7	6	0	6	7	A	9.3099815	1.0
287	6	1	5	6	6	0	6	6	A	9.3091253	0.4
288	6	1	5	5	6	0	6	5	A	9.3101248	−0.2
289	6	1	5	7	6	0	6	7	E	9.3100713	1.8
290	6	1	5	6	6	0	6	6	E	9.3092154	1.5

No.	J'	K_a'	K_c'	F'	J	K_a	K_c	F	sym.	ν_{obs}	$\nu_c - \nu_o$
291	6	1	5	5	6	0	6	5	E	9.3102157	1.8
292	6	2	5	7	6	1	6	7	E	9.3096651	−0.2
293	6	2	5	6	6	1	6	6	E	9.3088095	−0.2
294	6	2	5	5	6	1	6	5	E	9.3098096	−0.2
295	7	2	6	8	7	1	7	8	A	11.0041917	3.6
296	7	2	6	7	7	1	7	7	A	11.0034267	2.9
297	7	2	6	6	7	1	7	6	A	11.0043010	2.7
298	7	2	6	8	7	1	7	8	E	11.0038397	3.4
299	7	2	6	7	7	1	7	7	E	11.0030707	−1.3
300	7	2	6	6	7	1	7	6	E	11.0039448	−1.7
301	7	3	5	8	7	2	6	8	A	9.3002891	2.3
302	7	3	5	7	7	2	6	7	A	9.2996391	1.8
303	7	3	5	6	7	2	6	6	A	9.3003811	0.6
304	7	3	5	8	7	2	6	8	E	9.2998916	2.8
305	7	3	5	7	7	2	6	7	E	9.2992381	−1.0
306	7	3	5	6	7	2	6	6	E	9.2999816	−0.9
307	8	2	7	9	8	1	8	9	A	12.6982096	0.1
308	8	2	7	8	8	1	8	8	A	12.6975200	0.6
309	8	2	7	7	8	1	8	7	A	12.6982970	0.5
310	8	2	7	9	8	1	8	9	E	12.6978354	0.5
311	8	2	7	8	8	1	8	8	E	12.6971442	−0.5
312	8	2	7	7	8	1	8	7	E	12.6979231	1.3
313	8	2	6	9	8	1	7	9	A	10.9954636	0.4
314	8	2	6	8	8	1	7	8	A	10.9948616	−1.5
315	8	2	6	7	8	1	7	7	A	10.9955420	3.2
316	8	2	6	9	8	1	7	9	E	10.9955189	−4.1
317	8	2	6	8	8	1	7	8	E	10.9949202	−2.6
318	8	2	6	7	8	1	7	7	E	10.9955962	−2.3
319	8	2	6	9	8	2	7	9	A	10.9954636	0.4
320	8	2	6	8	8	2	7	8	A	10.9948616	−1.4
321	8	2	6	7	8	2	7	7	A	10.9955420	3.3
322	8	3	6	9	8	2	7	9	A	10.9954711	−1.6
323	8	3	6	8	8	2	7	8	A	10.9948694	−3.2
324	8	3	6	7	8	2	7	7	A	10.9955471	−1.2
325	8	3	6	9	8	2	7	9	E	10.9951186	1.0
326	8	3	6	8	8	2	7	8	E	10.9945179	0.4

No.	J'	K_a'	K_c'	F'	J	K_a	K_c	F	sym.	ν_{obs}	$\nu_c - \nu_o$
327	8	3	6	7	8	2	7	7	E	10.9951947	1.5
328	9	3	7	10	9	2	8	10	A	12.6901411	0.8
329	9	3	7	9	9	2	8	9	A	12.6895849	1.0
330	9	3	7	8	9	2	8	8	A	12.6902019	−0.5
331	9	3	7	10	9	2	8	10	E	12.6897658	−0.4
332	9	3	7	9	9	2	8	9	E	12.6892094	−0.4
333	9	3	7	8	9	2	8	8	E	12.6898293	0.9
334	9	1	8	10	9	0	9	10	A	14.3921224	0.9
335	9	1	8	9	9	0	9	9	A	14.3914935	0.9
336	9	1	8	8	9	0	9	8	A	14.3921932	1.4
337	9	1	8	10	9	0	9	10	E	14.3921293	−2.6
338	9	1	8	9	9	0	9	9	E	14.3915030	0.0
339	9	1	8	8	9	0	9	8	E	14.3922006	−1.6
340	9	2	8	10	9	1	9	10	A	14.3921224	0.9
341	9	2	8	9	9	1	9	9	A	14.3914935	0.9
342	9	2	8	8	9	1	9	8	A	14.3921932	1.4
343	9	2	8	10	9	1	9	10	E	14.3917196	−3.6
344	9	2	8	9	9	1	9	9	E	14.3910912	−3.0
345	9	2	8	8	9	1	9	8	E	14.3917912	−2.2

Table H.4: Observed frequencies ν_{obs} in GHz of conformer **II** of N,N-diethylacetamide. $\nu_c - \nu_o$ values in kHz are obtained after a fit with the program XIAM. J, K_a, and K_c are the symmetric top rotational quantum numbers, F is the total angular momentum in the coupled basis with $F = J + I$.

No.	J'	K_a'	K_c'	F'	J	K_a	K_c	F	sym.	ν_{obs}	$\nu_c - \nu_o$
1	2	2	0	3	1	1	1	2	A	9.0242566	4.6
2	2	2	0	2	1	1	1	1	A	9.0223687	−0.4
3	2	2	0	1	1	1	1	0	A	9.0259710	−0.6
4	2	2	0	2	1	1	1	2	A	9.0230857	3.5
5	2	2	0	1	1	1	1	1	A	9.0241906	1.8
6	2	2	0	3	1	1	1	2	E	9.0242275	−3.9
7	2	2	0	2	1	1	1	1	E	9.0223479	−0.6
8	2	2	0	1	1	1	1	0	E	9.0259500	−1.0
9	2	2	0	2	1	1	1	2	E	9.0230593	−2.3
10	2	2	0	1	1	1	1	1	E	9.0241678	−0.4

No.	J'	K_a'	K_c'	F'	J	K_a	K_c	F	sym.	ν_{obs}	$\nu_c - \nu_o$
11	2	2	0	3	1	0	1	2	A	9.2717902	−1.7
12	2	2	0	2	1	0	1	1	A	9.2701720	−0.7
13	2	2	0	1	1	0	1	0	A	9.2731186	2.7
14	2	2	0	2	1	0	1	2	A	9.2706209	−1.2
15	2	2	0	1	1	0	1	1	A	9.2719933	0.9
16	2	2	0	3	1	0	1	2	E	9.2717758	1.1
17	2	2	0	2	1	0	1	1	E	9.2701555	−0.1
18	2	2	0	1	1	0	1	0	E	9.2730986	−0.1
19	2	2	0	2	1	0	1	2	E	9.2706032	−1.8
20	2	2	0	1	1	0	1	1	E	9.2719752	0.0
21	3	1	2	4	2	2	1	3	A	9.1288700	−1.6
22	3	1	2	3	2	2	1	2	A	9.1291799	−0.6
23	3	1	2	2	2	2	1	1	A	9.1286627	−1.7
24	3	1	2	3	2	2	1	3	A	9.1286973	−1.7
25	3	1	2	2	2	2	1	2	A	9.1294129	−0.5
26	3	1	2	4	2	2	1	3	E	9.1288479	1.9
27	3	1	2	3	2	2	1	2	E	9.1291554	0.5
28	3	1	2	2	2	2	1	1	E	9.1286399	1.0
29	3	1	2	2	2	2	1	2	E	9.1293891	1.2
30	3	2	2	4	2	2	1	3	A	9.3767323	−0.3
31	3	2	2	3	2	2	1	2	A	9.3772156	1.5
32	3	2	2	2	2	2	1	1	A	9.3764659	0.8
33	3	2	2	3	2	2	1	3	A	9.3767323	−0.3
34	3	2	2	2	2	2	1	2	A	9.3772156	1.5
35	3	2	2	4	2	2	1	3	E	9.3767146	0.0
36	3	2	2	3	2	2	1	2	E	9.3771953	−0.8
37	3	2	2	2	2	2	1	1	E	9.3764449	−2.2
38	3	2	2	3	2	2	1	3	E	9.3767146	0.0
39	3	2	2	2	2	2	1	2	E	9.3771953	−0.8
40	3	1	2	4	2	1	1	3	A	9.8715565	2.9
41	3	1	2	3	2	1	1	2	A	9.8721451	0.0
42	3	1	2	2	2	1	1	1	A	9.8711899	0.4
43	3	1	2	2	2	1	1	2	A	9.8723782	0.2
44	3	1	2	4	2	1	1	3	E	9.8715377	−0.3
45	3	1	2	3	2	1	1	2	E	9.8721294	−0.1
46	3	1	2	2	2	1	1	1	E	9.8711730	−0.9

No.	J'	K_a'	K_c'	F'	J	K_a	K_c	F	sym.	ν_{obs}	$\nu_c - \nu_o$
47	3	1	2	3	2	1	1	3	E	9.8713631	−2.4
48	3	1	2	2	2	1	1	2	E	9.8723609	−1.6
49	3	2	2	4	2	1	1	3	E	10.1194079	1.3
50	3	2	2	3	2	1	1	2	E	10.1201710	0.3
51	3	2	2	2	2	1	1	1	E	10.1189812	−0.9
52	3	2	2	3	2	1	1	3	E	10.1194079	1.3
53	3	2	2	2	2	1	1	2	E	10.1201710	0.3
54	3	2	1	4	2	2	0	3	A	10.7210967	1.4
55	3	2	1	3	2	2	0	2	A	10.7211810	0.6
56	3	2	1	2	2	2	0	1	A	10.7208276	2.6
57	3	2	1	3	2	2	0	3	A	10.7200099	−0.7
58	3	2	1	2	2	2	0	2	A	10.7226448	0.1
59	3	2	1	4	2	2	0	3	E	10.7210618	−1.2
60	3	2	1	3	2	2	0	2	E	10.7211453	−2.8
61	3	2	1	2	2	2	0	1	E	10.7207899	−2.8
62	3	2	1	3	2	2	0	3	E	10.7199809	2.5
63	3	2	1	2	2	2	0	2	E	10.7226167	4.3
64	3	2	1	4	2	1	1	3	A	12.0103901	−1.9
65	3	2	1	3	2	1	1	2	A	12.0100699	−1.5
66	3	2	1	3	2	1	1	3	A	12.0093048	−2.6
67	3	2	1	2	2	1	1	2	A	12.0115330	−2.7
68	3	2	1	4	2	1	1	3	E	12.0103643	1.4
69	3	2	1	3	2	1	1	2	E	12.0100435	1.2
70	3	2	1	2	2	1	1	1	E	12.0103189	0.8
71	3	2	1	3	2	1	1	3	E	12.0092789	0.6
72	3	2	1	2	2	1	1	2	E	12.0115083	1.7
73	3	1	2	4	2	0	2	3	A	12.1494772	−1.4
74	3	1	2	3	2	0	2	2	A	12.1481345	−1.7
75	3	1	2	2	2	0	2	1	A	12.1501867	−2.1
76	3	1	2	3	2	0	2	3	A	12.1493047	−1.3
77	3	1	2	2	2	0	2	2	A	12.1483671	−2.1
78	3	1	2	4	2	0	2	3	E	12.1494486	1.1
79	3	1	2	3	2	0	2	2	E	12.1481058	0.7
80	3	1	2	2	2	0	2	1	E	12.1501581	0.3
81	3	1	2	3	2	0	2	3	E	12.1492760	1.1
82	3	1	2	2	2	0	2	2	E	12.1483396	1.5

No.	J'	K_a'	K_c'	F'	J	K_a	K_c	F	sym.	ν_{obs}	$\nu_c - \nu_o$
83	3	3	1	4	2	2	0	3	E	12.1993745	1.9
84	3	3	1	3	2	2	0	2	E	12.1997429	1.7
85	3	3	1	2	2	2	0	1	E	12.1990042	1.2
86	3	3	1	3	2	2	0	3	E	12.1985734	1.9
87	3	3	1	2	2	2	0	2	E	12.2008228	0.1
88	3	3	0	4	2	2	0	3	A	12.5402024	0.9
89	3	3	0	3	2	2	0	2	A	12.5402500	−2.1
90	3	3	0	2	2	2	0	1	A	12.5399425	−0.8
91	3	3	0	3	2	2	0	3	A	12.5390815	−0.8
92	3	3	0	2	2	2	0	2	A	12.5417636	0.7
93	3	3	0	4	2	2	0	3	E	12.5401839	1.4
94	3	3	0	3	2	2	0	2	E	12.5402306	−2.5
95	3	3	0	2	2	2	0	1	E	12.5399234	−0.9
96	3	3	0	3	2	2	0	3	E	12.5390620	−1.3
97	3	3	0	2	2	2	0	2	E	12.5417432	−0.7
98	3	3	1	4	2	2	1	3	A	12.7459988	−1.8
99	3	3	1	3	2	2	1	2	A	12.7456830	2.0
100	3	3	1	2	2	2	1	1	A	12.7460119	−1.6
101	3	3	1	3	2	2	1	3	A	12.7451986	−0.9
102	3	3	1	2	2	2	1	2	A	12.7467623	−0.2
103	3	3	1	4	2	2	1	3	E	12.7459809	0.5
104	3	3	1	3	2	2	1	2	E	12.7456616	0.8
105	3	3	1	3	2	2	1	3	E	12.7451797	0.4
106	3	3	1	2	2	2	1	2	E	12.7467418	−0.5
107	3	3	0	4	2	2	1	3	A	13.0868149	−1.2
108	3	3	0	3	2	2	1	2	A	13.0861778	−0.7
109	3	3	0	2	2	2	1	1	A	13.0869390	−1.4
110	3	3	0	3	2	2	1	3	A	13.0856962	−0.8
111	3	3	0	2	2	2	1	2	A	13.0876905	1.1
112	3	3	0	4	2	2	1	3	E	13.0867920	1.7
113	3	3	0	3	2	2	1	2	E	13.0861524	−0.3
114	3	3	0	2	2	2	1	1	E	13.0869125	−2.0
115	3	3	0	3	2	2	1	3	E	13.0856717	0.5
116	3	3	0	2	2	2	1	2	E	13.0876617	−1.8
117	3	3	0	4	2	1	1	3	A	13.8294950	−3.2
118	3	3	0	3	2	1	1	2	A	13.8291433	0.2

No.	J'	K_a'	K_c'	F'	J	K_a	K_c	F	sym.	ν_{obs}	$\nu_c - \nu_o$
119	3	3	0	3	2	1	1	3	A	13.8283809	1.8
120	3	3	0	2	2	1	1	2	A	13.8306541	0.2
121	3	3	0	4	2	1	1	3	E	13.8294829	0.5
122	3	3	0	3	2	1	1	2	E	13.8291275	0.2
123	3	3	0	3	2	1	1	3	E	13.8283637	0.5
124	3	3	0	2	2	1	1	2	E	13.8306393	1.2
125	3	2	1	4	2	1	2	3	A	14.2359938	−0.5
126	3	2	1	3	2	1	2	2	A	14.2336647	0.6
127	3	2	1	2	2	1	2	1	A	14.2370657	−0.2
128	3	2	1	4	2	1	2	3	E	14.2359488	1.2
129	3	2	1	3	2	1	2	2	E	14.2336204	3.0
130	3	2	1	2	2	1	2	1	E	14.2370208	1.6
131	4	0	4	5	3	1	3	4	A	10.3888551	−0.8
132	4	0	4	4	3	1	3	3	A	10.3890914	−0.3
133	4	0	4	4	3	1	3	4	A	10.3906855	0.4
134	4	0	4	3	3	1	3	3	A	10.3867919	−0.1
135	4	0	4	5	3	1	3	4	E	10.3887996	−0.4
136	4	0	4	4	3	1	3	3	E	10.3890358	−0.1
137	4	0	4	4	3	1	3	4	E	10.3906296	0.3
138	4	0	4	3	3	1	3	3	E	10.3867363	0.1
139	4	1	4	5	3	1	3	4	A	10.3896551	1.7
140	4	1	4	4	3	1	3	3	A	10.3898916	1.5
141	4	1	4	3	3	1	3	2	A	10.3897405	0.1
142	4	1	4	4	3	1	3	4	A	10.3914847	1.2
143	4	1	4	3	3	1	3	3	A	10.3875904	1.1
144	4	1	4	5	3	1	3	4	E	10.3896914	−0.1
145	4	1	4	4	3	1	3	3	E	10.3899277	−0.5
146	4	1	4	4	3	1	3	4	E	10.3915210	−0.7
147	4	0	4	5	3	0	3	4	A	10.3959618	0.4
148	4	0	4	4	3	0	3	3	A	10.3962079	1.2
149	4	0	4	3	3	0	3	2	A	10.3960446	−0.9
150	4	0	4	4	3	0	3	4	A	10.3977893	−1.4
151	4	0	4	5	3	0	3	4	E	10.3959135	1.3
152	4	0	4	4	3	0	3	3	E	10.3961556	−2.0
153	4	0	4	4	3	0	3	4	E	10.3977413	−0.2
154	4	1	3	5	3	2	2	4	A	11.9668637	2.6

No.	J'	K_a'	K_c'	F'	J	K_a	K_c	F	sym.	ν_{obs}	$\nu_c - \nu_o$
155	4	1	3	4	3	2	2	3	A	11.9672392	2.2
156	4	1	3	3	3	2	2	2	A	11.9667645	0.1
157	4	1	3	4	3	2	2	4	A	11.9672392	2.2
158	4	1	3	3	3	2	2	3	A	11.9667645	0.1
159	4	1	3	5	3	2	2	4	E	11.9668409	−0.5
160	4	1	3	4	3	2	2	3	E	11.9672170	−0.3
161	4	1	3	3	3	2	2	2	E	11.9667439	−0.8
162	4	1	3	4	3	2	2	4	E	11.9672170	−0.3
163	4	1	3	3	3	2	2	3	E	11.9667439	−0.8
164	4	2	3	5	3	2	2	4	A	12.0152841	2.4
165	4	2	3	4	3	2	2	3	A	12.0156981	1.8
166	4	2	3	3	3	2	2	2	A	12.0151767	1.6
167	4	2	3	4	3	2	2	4	A	12.0156981	1.8
168	4	2	3	3	3	2	2	3	A	12.0151767	1.6
169	4	2	3	5	3	2	2	4	E	12.0152638	−1.6
170	4	2	3	4	3	2	2	3	E	12.0156778	−2.1
171	4	2	3	3	3	2	2	2	E	12.0151564	−2.4
172	4	2	3	4	3	2	2	4	E	12.0156778	−2.1
173	4	2	3	3	3	2	2	3	E	12.0151564	−2.4
174	4	1	3	5	3	1	2	4	A	12.2147237	1.6
175	4	1	3	4	3	1	2	3	A	12.2152717	1.1
176	4	1	3	3	3	1	2	2	A	12.2145657	0.6
177	4	1	3	4	3	1	2	4	A	12.2150979	−0.1
178	4	1	3	3	3	1	2	3	A	12.2148004	2.3
179	4	1	3	5	3	1	2	4	E	12.2147084	−1.6
180	4	1	3	4	3	1	2	3	E	12.2152570	−1.4
181	4	1	3	3	3	1	2	2	E	12.2145514	−1.5
182	4	1	3	4	3	1	2	4	E	12.2150843	−1.6
183	4	1	3	3	3	1	2	3	E	12.2147838	−2.1
184	4	3	2	5	3	3	1	4	A	13.1315854	−0.1
185	4	3	2	4	3	3	1	3	A	13.1318775	0.0
186	4	3	2	3	3	3	1	2	A	13.1314353	−0.8
187	4	3	2	4	3	3	1	4	A	13.1310761	−0.3
188	4	3	2	3	3	3	1	3	A	13.1325166	−0.9
189	4	3	2	5	3	3	1	4	E	13.1315565	1.5
190	4	3	2	4	3	3	1	3	E	13.1318462	−0.7

No.	J'	K_a'	K_c'	F'	J	K_a	K_c	F	sym.	ν_{obs}	$\nu_c - \nu_o$
191	4	3	2	3	3	3	1	2	E	13.1314066	1.1
192	4	3	2	4	3	3	1	4	E	13.1310471	1.3
193	4	3	2	3	3	3	1	3	E	13.1324864	−0.6
194	4	2	2	5	3	2	1	4	A	13.9385377	−1.7
195	4	2	2	4	3	2	1	3	A	13.9388614	−1.3
196	4	2	2	3	3	2	1	2	A	13.9383565	0.9
197	4	2	2	4	3	2	1	4	A	13.9377776	−0.4
198	4	2	2	3	3	2	1	3	A	13.9398178	−2.0
199	4	2	2	5	3	2	1	4	E	13.9385101	0.5
200	4	2	2	4	3	2	1	3	E	13.9388338	1.0
201	4	2	2	3	3	2	1	2	E	13.9383270	1.3
202	4	2	2	4	3	2	1	4	E	13.9377481	−0.1
203	4	2	2	3	3	2	1	3	E	13.9397897	−0.3
204	4	3	2	5	3	2	1	4	E	14.6098655	1.0
205	4	3	2	4	3	2	1	3	E	14.6104429	2.9
206	4	3	2	3	3	2	1	2	E	14.6096131	−2.7
207	4	3	2	3	3	2	1	3	E	14.6110822	2.1
208	5	1	4	6	4	2	3	5	A	14.4683143	0.4
209	5	1	4	5	4	2	3	4	A	14.4686512	1.6
210	5	1	4	4	4	2	3	3	A	14.4682703	2.6
211	5	1	4	5	4	2	3	5	A	14.4690641	−0.1
212	5	1	4	4	4	2	3	4	A	14.4677493	2.8
213	5	1	4	6	4	2	3	5	E	14.4682905	−1.6
214	5	1	4	5	4	2	3	4	E	14.4686282	0.3
215	5	1	4	4	4	2	3	3	E	14.4682457	−0.2
216	5	1	4	5	4	2	3	5	E	14.4690430	0.6
217	5	1	4	4	4	2	3	4	E	14.4677242	−0.5
218	5	2	4	6	4	2	3	5	A	14.4753682	1.3
219	5	2	4	5	4	2	3	4	A	14.4757103	2.1
220	5	2	4	4	4	2	3	3	A	14.4753216	2.1
221	5	2	4	5	4	2	3	5	A	14.4761262	3.5
222	5	2	4	4	4	2	3	4	A	14.4748015	3.2
223	5	2	4	6	4	2	3	5	E	14.4753543	−2.4
224	5	2	4	5	4	2	3	4	E	14.4756965	−1.4
225	5	2	4	4	4	2	3	3	E	14.4753081	−1.2
226	5	2	4	5	4	2	3	5	E	14.4761109	−1.6

No.	J'	K_a'	K_c'	F'	J	K_a	K_c	F	sym.	ν_{obs}	$\nu_c - \nu_o$
227	5	2	4	4	4	2	3	4	E	14.4747859	−2.2
228	5	1	4	6	4	1	3	5	A	14.5167363	1.7
229	5	1	4	5	4	1	3	4	A	14.5171102	1.2
230	5	1	4	4	4	1	3	3	A	14.5166802	1.8
231	5	1	4	5	4	1	3	5	A	14.5174841	−0.8
232	5	1	4	4	4	1	3	4	A	14.5162073	1.5
233	5	1	4	6	4	1	3	5	E	14.5167154	−0.7
234	5	1	4	5	4	1	3	4	E	14.5170900	−0.5
235	5	1	4	4	4	1	3	3	E	14.5166592	−0.7
236	5	1	4	5	4	1	3	5	E	14.5174634	−3.0
237	5	1	4	4	4	1	3	4	E	14.5161833	−4.1
238	5	2	4	6	4	1	3	5	A	14.5237877	0.1
239	5	2	4	5	4	1	3	4	A	14.5241677	0.2
240	5	2	4	4	4	1	3	3	A	14.5237304	0.1
241	5	2	4	5	4	1	3	5	A	14.5245418	−1.6
242	5	2	4	4	4	1	3	4	A	14.5232583	0.6
243	5	2	4	6	4	1	3	5	E	14.5237801	−0.5
244	5	2	4	5	4	1	3	4	E	14.5241602	−0.4
245	5	2	4	4	4	1	3	3	E	14.5237227	−0.6
246	5	2	4	5	4	1	3	5	E	14.5245322	−4.3
247	5	2	4	4	4	1	3	4	E	14.5232503	−0.5

Appendix I

N-Methyldiacetamide

Table I.1: Coefficients of the symmetry-adapted two-dimensional Fourier expansion of the potential energy surface calculated at the MP2/6-311++G(d,p) level of theory obtained by varying φ_1 and φ_2.

N°	Fourier term	Coefficient/E_h	Coefficient/cm^{-1}
1	1	−400.1663393	
2	$\cos(1{\cdot}\varphi_1)$	0.0010506	230.580
3	$\sin(1{\cdot}\varphi_1)$	0.0002354	51.664
4	$\cos(1{\cdot}\varphi_2)$	0.0016004	351.247
5	$\sin(1{\cdot}\varphi_2)$	−0.0002656	−58.292
6	$\cos(2{\cdot}\varphi_1)$	−0.0078561	−1724.215
8	$\cos(2{\cdot}\varphi_2)$	−0.0077670	−1704.659
9	$\sin(2{\cdot}\varphi_2)$	−0.0000548	−12.027
10	$\cos(3{\cdot}\varphi_1)$	0.0014236	312.444
11	$\sin(3{\cdot}\varphi_1)$	−0.0001907	−41.854
12	$\cos(3{\cdot}\varphi_2)$	0.0005802	127.339
13	$\sin(3{\cdot}\varphi_2)$	0.0002058	45.168
14	$\cos(4{\cdot}\varphi_1)$	0.0007584	166.450
15	$\sin(4{\cdot}\varphi_1)$	−0.0000561	−12.313
16	$\cos(4{\cdot}\varphi_2)$	0.0006027	132.277
17	$\sin(4{\cdot}\varphi_2)$	0.0000517	11.347
18	$\cos(5{\cdot}\varphi_1)$	−0.0002820	−61.892
19	$\sin(5{\cdot}\varphi_1)$	0.0001316	28.883
20	$\cos(5{\cdot}\varphi_2)$	0.0000481	10.557
21	$\sin(5{\cdot}\varphi_2)$	−0.0001354	−29.717
22	$\cos(6{\cdot}\varphi_1)$	0.0001240	27.215

N°	Fourier term	Coefficient/E_h	Coefficient/cm^{-1}
23	$\sin(6\cdot\varphi_1)$	0.0000535	11.742
24	$\cos(6\cdot\varphi_2)$	0.0001070	23.484
26	$\cos(1\cdot\varphi_1)\ \cos(1\cdot\varphi_2)$	0.0053408	1172.170
27	$\sin(1\cdot\varphi_1)\sin(1\cdot\varphi_2)$	−0.0016163	−354.737
30	$\cos(2\cdot\varphi_1)\ \cos(1\cdot\varphi_2)$	0.0006022	132.168
31	$\sin(2\cdot\varphi_1)\ \sin(1\cdot\varphi_2)$	0.0003366	73.875
32	$\cos(2\cdot\varphi_1)\ \sin(1\cdot\varphi_2)$	0.0004129	90.621
33	$\sin(2\cdot\varphi_1)\ \cos(1\cdot\varphi_2)$	−0.0001290	−28.312
34	$\cos(3\cdot\varphi_1)\ \cos(1\cdot\varphi_2)$	−0.0005821	−127.756
35	$\sin(3\cdot\varphi_1)\ \sin(1\cdot\varphi_2)$	−0.0004209	−92.377
36	$\cos(3\cdot\varphi_1)\ \sin(1\cdot\varphi_2)$	0.0001019	22.364
38	$\cos(4\cdot\varphi_1)\ \cos(1\cdot\varphi_2)$	−0.0001455	−31.934
39	$\sin(4\cdot\varphi_1)\ \sin(1\cdot\varphi_2)$	0.0004126	90.555
40	$\cos(4\cdot\varphi_1)\ \sin(1\cdot\varphi_2)$	−0.0003316	−72.778
41	$\sin(4\cdot\varphi_1)\ \cos(1\cdot\varphi_2)$	0.0001417	31.100
42	$\cos(5\cdot\varphi_1)\ \cos(1\cdot\varphi_2)$	0.0001618	35.511
43	$\sin(5\cdot\varphi_1)\ \sin(1\cdot\varphi_2)$	−0.0002860	−62.770
44	$\cos(5\cdot\varphi_1)\ \sin(1\cdot\varphi_2)$	−0.0000816	−17.909
47	$\sin(6\cdot\varphi_1)\ \sin(1\cdot\varphi_2)$	−0.0002559	−56.164
48	$\cos(6\cdot\varphi_1)\ \sin(1\cdot\varphi_2)$	0.0001310	28.751
49	$\sin(6\cdot\varphi_1)\ \cos(1\cdot\varphi_2)$	−0.0001142	−25.064
50	$\cos(1\cdot\varphi_1)\ \cos(2\cdot\varphi_2)$	0.0016241	356.449
51	$\sin(1\cdot\varphi_1)\ \sin(2\cdot\varphi_2)$	0.0019524	428.502
52	$\cos(1\cdot\varphi_1)\ \sin(2\cdot\varphi_2)$	0.0001106	24.274
53	$\sin(1\cdot\varphi_1)\ \cos(2\cdot\varphi_2)$	−0.0004576	−100.432
54	$\cos(2\cdot\varphi_1)\ \cos(2\cdot\varphi_2)$	0.0039480	866.486
55	$\sin(2\cdot\varphi_1)\ \sin(2\cdot\varphi_2)$	−0.0012740	−279.611
58	$\cos(3\cdot\varphi_1)\ \cos(2\cdot\varphi_2)$	−0.0015682	−344.180
59	$\sin(3\cdot\varphi_1)\ \sin(2\cdot\varphi_2)$	−0.0007999	−175.558
60	$\cos(3\cdot\varphi_1)\ \sin(2\cdot\varphi_2)$	−0.0002223	−48.789
61	$\sin(3\cdot\varphi_1)\ \cos(2\cdot\varphi_2)$	0.0003598	78.967
62	$\cos(4\cdot\varphi_1)\ \cos(2\cdot\varphi_2)$	−0.0002574	−56.493
64	$\cos(4\cdot\varphi_1)\ \sin(2\cdot\varphi_2)$	0.0000734	16.109
66	$\cos(5\cdot\varphi_1)\ \cos(2\cdot\varphi_2)$	0.0002592	56.888
67	$\sin(5\cdot\varphi_1)\ \sin(2\cdot\varphi_2)$	0.0005654	124.091
68	$\cos(5\cdot\varphi_1)\ \sin(2\cdot\varphi_2)$	0.0002045	44.883

N°	Fourier term	Coefficient/E_h	Coefficient/cm^{-1}
69	$\sin(5{\cdot}\varphi_1)\ \cos(2{\cdot}\varphi_2)$	−0.0002021	−44.356
70	$\cos(6{\cdot}\varphi_1)\ \cos(2{\cdot}\varphi_2)$	−0.0003391	−74.424
72	$\cos(6{\cdot}\varphi_1)\ \sin(2{\cdot}\varphi_2)$	−0.0000725	−15.912
74	$\cos(1{\cdot}\varphi_1)\ \cos(3{\cdot}\varphi_2)$	−0.0004878	−107.060
75	$\sin(1{\cdot}\varphi_1)\ \sin(3{\cdot}\varphi_2)$	−0.0001108	−24.318
77	$\sin(1{\cdot}\varphi_1)\ \cos(3{\cdot}\varphi_2)$	−0.0000857	−18.809
79	$\sin(2{\cdot}\varphi_1)\ \sin(3{\cdot}\varphi_2)$	0.0005507	120.865
80	$\cos(2{\cdot}\varphi_1)\ \sin(3{\cdot}\varphi_2)$	−0.0003286	−72.119
81	$\sin(2{\cdot}\varphi_1)\ \cos(3{\cdot}\varphi_2)$	0.0002438	53.508
83	$\sin(3{\cdot}\varphi_1)\ \sin(3{\cdot}\varphi_2)$	0.0001925	42.249
86	$\cos(4{\cdot}\varphi_1)\ \cos(3{\cdot}\varphi_2)$	−0.0003362	−73.787
87	$\sin(4{\cdot}\varphi_1)\ \sin(3{\cdot}\varphi_2)$	−0.0005436	−119.306
88	$\cos(4{\cdot}\varphi_1)\ \sin(3{\cdot}\varphi_2)$	0.0002651	58.183
89	$\sin(4{\cdot}\varphi_1)\ \cos(3{\cdot}\varphi_2)$	−0.0002934	−64.394
90	$\cos(5{\cdot}\varphi_1)\ \cos(3{\cdot}\varphi_2)$	0.0001947	42.732
91	$\sin(5{\cdot}\varphi_1)\ \sin(3{\cdot}\varphi_2)$	0.0002962	65.008
93	$\sin(5{\cdot}\varphi_1)\ \cos(3{\cdot}\varphi_2)$	0.0001089	23.901
94	$\cos(6{\cdot}\varphi_1)\ \cos(3{\cdot}\varphi_2)$	0.0001644	36.082
95	$\sin(6{\cdot}\varphi_1)\ \sin(3{\cdot}\varphi_2)$	0.0001290	28.312
96	$\cos(6{\cdot}\varphi_1)\ \sin(3{\cdot}\varphi_2)$	−0.0001123	−24.647
97	$\sin(6{\cdot}\varphi_1)\ \cos(3{\cdot}\varphi_2)$	0.0001769	38.825
98	$\cos(1{\cdot}\varphi_1)\ \cos(4{\cdot}\varphi_2)$	−0.0008152	−178.916
99	$\sin(1{\cdot}\varphi_1)\ \sin(4{\cdot}\varphi_2)$	−0.0008719	−191.360
100	$\cos(1{\cdot}\varphi_1)\ \sin(4{\cdot}\varphi_2)$	−0.0001461	−32.065
101	$\sin(1{\cdot}\varphi_1)\ \cos(4{\cdot}\varphi_2)$	0.0003183	69.859
103	$\sin(2{\cdot}\varphi_1)\ \sin(4{\cdot}\varphi_2)$	0.0000941	20.653
106	$\cos(3{\cdot}\varphi_1)\ \cos(4{\cdot}\varphi_2)$	0.0006483	142.285
107	$\sin(3{\cdot}\varphi_1)\ \sin(4{\cdot}\varphi_2)$	0.0005535	121.479
108	$\cos(3{\cdot}\varphi_1)\ \sin(4{\cdot}\varphi_2)$	0.0003358	73.700
109	$\sin(3{\cdot}\varphi_1)\ \cos(4{\cdot}\varphi_2)$	−0.0002246	−49.294
111	$\sin(4{\cdot}\varphi_1)\ \sin(4{\cdot}\varphi_2)$	−0.0005544	−121.677
112	$\cos(4{\cdot}\varphi_1)\ \sin(4{\cdot}\varphi_2)$	−0.0001012	−22.211
114	$\cos(5{\cdot}\varphi_1)\ \cos(4{\cdot}\varphi_2)$	−0.0001503	−32.987
115	$\sin(5{\cdot}\varphi_1)\ \sin(4{\cdot}\varphi_2)$	−0.0002174	−47.714
116	$\cos(5{\cdot}\varphi_1)\ \sin(4{\cdot}\varphi_2)$	−0.0002260	−49.601
117	$\sin(5{\cdot}\varphi_1)\ \cos(4{\cdot}\varphi_2)$	0.0001225	26.886

N°	Fourier term	Coefficient/E_h	Coefficient/cm^{-1}
118	$\cos(6\cdot\varphi_1)\ \cos(4\cdot\varphi_2)$	0.0003677	80.701
119	$\sin(6\cdot\varphi_1)\ \sin(4\cdot\varphi_2)$	0.0000850	18.655
120	$\cos(6\cdot\varphi_1)\ \sin(4\cdot\varphi_2)$	0.0000835	18.326
121	$\sin(6\cdot\varphi_1)\ \cos(4\cdot\varphi_2)$	−0.0000734	−16.109
123	$\sin(1\cdot\varphi_1)\ \sin(5\cdot\varphi_2)$	−0.0003926	−86.166
126	$\cos(2\cdot\varphi_1)\ \cos(5\cdot\varphi_2)$	−0.0003534	−77.562
128	$\cos(2\cdot\varphi_1)\ \sin(5\cdot\varphi_2)$	0.0001516	33.272
129	$\sin(2\cdot\varphi_1)\ \cos(5\cdot\varphi_2)$	−0.0002334	−51.225
130	$\cos(3\cdot\varphi_1)\ \cos(5\cdot\varphi_2)$	0.0003742	82.127
131	$\sin(3\cdot\varphi_1)\ \sin(5\cdot\varphi_2)$	0.0003179	69.771
133	$\sin(3\cdot\varphi_1)\ \cos(5\cdot\varphi_2)$	0.0000856	18.787
134	$\cos(4\cdot\varphi_1)\ \cos(5\cdot\varphi_2)$	0.0001148	25.196
135	$\sin(4\cdot\varphi_1)\ \sin(5\cdot\varphi_2)$	0.0002041	44.795
136	$\cos(4\cdot\varphi_1)\ \sin(5\cdot\varphi_2)$	−0.0001235	−27.105
137	$\sin(4\cdot\varphi_1)\ \cos(5\cdot\varphi_2)$	0.0002231	48.965
138	$\cos(5\cdot\varphi_1)\ \cos(5\cdot\varphi_2)$	−0.0003436	−75.411
139	$\sin(5\cdot\varphi_1)\ \sin(5\cdot\varphi_2)$	−0.0004348	−95.428
140	$\cos(5\cdot\varphi_1)\ \sin(5\cdot\varphi_2)$	0.0001003	22.013
141	$\sin(5\cdot\varphi_1)\ \cos(5\cdot\varphi_2)$	−0.0001317	−28.905
142	$\cos(6\cdot\varphi_1)\ \cos(5\cdot\varphi_2)$	0.0001410	30.946
145	$\sin(6\cdot\varphi_1)\ \cos(5\cdot\varphi_2)$	−0.0001172	−25.722
146	$\cos(1\cdot\varphi_1)\ \cos(6\cdot\varphi_2)$	0.0001715	37.640
148	$\cos(1\cdot\varphi_1)\ \sin(6\cdot\varphi_2)$	0.0001367	30.002
149	$\sin(1\cdot\varphi_1)\ \cos(6\cdot\varphi_2)$	−0.0000850	−18.655
150	$\cos(2\cdot\varphi_1)\ \cos(6\cdot\varphi_2)$	−0.0003489	−76.575
151	$\sin(2\cdot\varphi_1)\ \sin(6\cdot\varphi_2)$	−0.0001200	−26.337
153	$\sin(2\cdot\varphi_1)\ \cos(6\cdot\varphi_2)$	0.0000715	15.692
156	$\cos(3\cdot\varphi_1)\ \sin(6\cdot\varphi_2)$	−0.0001934	−42.446
158	$\cos(4\cdot\varphi_1)\ \cos(6\cdot\varphi_2)$	0.0003242	71.154
159	$\sin(4\cdot\varphi_1)\ \sin(6\cdot\varphi_2)$	0.0001672	36.696
160	$\cos(4\cdot\varphi_1)\ \sin(6\cdot\varphi_2)$	0.0001311	28.773
161	$\sin(4\cdot\varphi_1)\ \cos(6\cdot\varphi_2)$	−0.0000859	−18.853
163	$\sin(5\cdot\varphi_1)\ \sin(6\cdot\varphi_2)$	−0.0003203	−70.298
164	$\cos(5\cdot\varphi_1)\ \sin(6\cdot\varphi_2)$	0.0001088	23.879
166	$\cos(6\cdot\varphi_1)\ \cos(6\cdot\varphi_2)$	−0.0001351	−29.651

Table I.2: Nuclear coordinates (in Å) in the principal axis system of conformer **I** of N-methyldiacetamide, calculated at the MP2/6-311++G(d,p) level of theory.

Conformer **I**			
	a	*b*	*c*
N_1	−0.033152	0.451070	0.098459
C_2	−1.186347	−0.341337	−0.034837
O_3	−1.147000	−1.545890	−0.223436
C_4	−2.509155	0.392544	0.075475
H_5	−2.596408	1.180239	−0.677210
H_6	−3.298595	−0.342720	−0.075445
H_7	−2.624177	0.850466	1.062023
C_8	1.288488	−0.067476	0.008073
O_9	2.210408	0.701506	−0.206913
C_{10}	1.516778	−1.539157	0.245283
H_{11}	0.929229	−1.911634	1.084546
H_{12}	1.220654	−2.114727	−0.632999
H_{13}	2.584384	−1.663501	0.430058
C_{14}	−0.133925	1.915020	0.052750
H_{15}	0.790911	2.328096	0.449873
H_{16}	−0.258920	2.276323	−0.972731
H_{17}	−0.969010	2.249499	0.665189

Table I.3: Nuclear coordinates (in Å) in the principal axis system of conformer **II** and **III** of N-methyldiacetamide, calculated at the MP2/6-311++G(d,p) level of theory.

	Conformer II			Conformer III		
	a	*b*	*c*	*a*	*b*	*c*
N_1	−0.014706	−0.461793	−0.100771	0.015351	0.429728	−0.105385
C_2	1.268551	0.114035	0.009399	−1.233485	−0.250255	−0.095877
O_3	2.208781	−0.573427	0.373363	−1.344496	−1.400349	−0.462370
C_4	1.489632	1.542589	−0.448908	−2.427406	0.557041	0.386980
H_5	1.349714	2.246731	0.373555	−2.822464	1.180553	−0.421217
H_6	2.531152	1.601304	−0.767080	−3.200187	−0.156394	0.673124
H_7	0.837833	1.824632	−1.275461	−2.182394	1.200900	1.234805
C_8	−1.266414	0.174869	0.002938	1.216702	−0.298964	0.080943
O_9	−2.286831	−0.479983	−0.142643	1.232817	−1.469054	0.403076
C_{10}	−1.340424	1.640316	0.381809	2.496086	0.490653	−0.135334
H_{11}	−0.662322	1.888962	1.199261	2.544624	0.893760	−1.151027
H_{12}	−1.116838	2.285197	−0.469692	2.580043	1.323761	0.568006
H_{13}	−2.368536	1.824080	0.693071	3.327831	−0.194830	0.022731
C_{14}	−0.060145	−1.932129	−0.091747	0.045847	1.893963	−0.087449
H_{15}	−0.220878	−2.309082	0.921862	0.194495	2.296029	0.921516
H_{16}	−0.882969	−2.252833	−0.727073	0.843717	2.257887	−0.734480
H_{17}	0.889960	−2.306988	−0.465550	−0.890337	2.280686	−0.485416

Table I.4: Observed frequencies ν_{obs} in GHz of conformer I of N-methyldiacetamide. $\nu_c - \nu_o$ values in kHz are obtained after a fit with the program XIAM. J, K_a, and K_c are the symmetric top rotational quantum numbers, F is the total angular momentum in the coupled basis with $F = J + I$.

No.	J'	K_a'	K_c'	F'	J	K_a	K_c	F	sym.	ν_{obs}	$\nu_c - \nu_o$
1	3	0	3	4	2	0	2	3	0 0	8.285906	−1.9
2	3	0	3	3	2	0	2	2	0 0	8.286297	−4.6
3	3	0	3	2	2	0	2	1	0 0	8.285941	−6.1
4	3	0	3	3	2	0	2	3	0 0	8.287159	−4.9
5	3	0	3	2	2	0	2	2	0 0	8.284601	−4.6
6	3	0	3	4	2	0	2	3	0 1	8.285906	1.9
7	3	0	3	3	2	0	2	2	0 1	8.286297	−0.8
8	3	0	3	2	2	0	2	1	0 1	8.285941	−2.4
9	3	0	3	3	2	0	2	3	0 1	8.287159	−1.2
10	3	0	3	2	2	0	2	2	0 1	8.284601	−0.8

No.	J'	K_a'	K_c'	F'	J	K_a	K_c	F	sym.	ν_{obs}	$\nu_c - \nu_o$
11	3	0	3	4	2	0	2	3	1 0	8.282974	−1.2
12	3	0	3	3	2	0	2	2	1 0	8.283371	−0.2
13	3	0	3	2	2	0	2	1	1 0	8.283007	−1.9
14	3	0	3	3	2	0	2	3	1 0	8.284211	−1.8
15	3	0	3	2	2	0	2	2	1 0	8.281699	−0.8
16	3	0	3	4	2	0	2	3	1 1	8.282974	2.1
17	3	0	3	3	2	0	2	2	1 1	8.283371	3.0
18	3	0	3	2	2	0	2	1	1 1	8.283007	1.4
19	3	0	3	3	2	0	2	3	1 1	8.284211	1.4
20	3	0	3	2	2	0	2	2	1 1	8.281699	2.5
21	3	0	3	4	2	0	2	3	-1 1	8.282974	3.0
22	3	0	3	3	2	0	2	2	-1 1	8.283371	3.9
23	3	0	3	2	2	0	2	1	-1 1	8.283007	2.2
24	3	0	3	3	2	0	2	3	-1 1	8.284211	2.3
25	3	0	3	2	2	0	2	2	-1 1	8.281699	3.4
26	3	2	2	4	2	2	1	3	0 0	8.896625	4.6
27	3	2	2	3	2	2	1	2	0 0	8.897182	3.7
28	3	2	2	2	2	2	1	1	0 0	8.896313	2.9
29	3	2	2	3	2	2	1	3	0 0	8.896625	4.6
30	3	2	2	2	2	2	1	2	0 0	8.897182	3.7
31	3	2	2	4	2	2	1	3	0 1	8.896625	5.1
32	3	2	2	3	2	2	1	2	0 1	8.897182	4.2
33	3	2	2	2	2	2	1	1	0 1	8.896313	3.4
34	3	2	2	3	2	2	1	3	0 1	8.896625	5.1
35	3	2	2	2	2	2	1	2	0 1	8.897182	4.2
36	3	2	2	4	2	2	1	3	1 0	8.886505	4.1
37	3	2	2	3	2	2	1	2	1 0	8.887064	0.2
38	3	2	2	2	2	2	1	1	1 0	8.886194	4.8
39	3	2	2	3	2	2	1	3	1 0	8.886505	2.3
40	3	2	2	2	2	2	1	2	1 0	8.887064	2.7
41	3	2	1	4	2	2	0	3	0 0	9.507445	5.9
42	3	2	1	3	2	2	0	2	0 0	9.507630	5.5
43	3	2	1	2	2	2	0	1	0 0	9.507202	5.0
44	3	2	1	3	2	2	0	3	0 0	9.506767	4.7
45	3	2	1	2	2	2	0	2	0 0	9.508543	3.9
46	3	2	1	4	2	2	0	3	0 1	9.507431	−5.8

No.	J'	K_a'	K_c'	F'	J	K_a	K_c	F	sym.	ν_{obs}	$\nu_c - \nu_o$
47	3	2	1	3	2	2	0	2	0 1	9.507619	−3.1
48	3	2	1	2	2	2	0	1	0 1	9.507187	−7.3
49	3	2	1	3	2	2	0	3	0 1	9.506753	−6.0
50	3	2	1	2	2	2	0	2	0 1	9.508530	−6.5
51	3	1	2	4	2	1	1	3	0 0	9.706847	−0.2
52	3	1	2	3	2	1	1	2	0 0	9.707094	0.2
53	3	1	2	2	2	1	1	1	0 0	9.706629	3.2
54	3	1	2	3	2	1	1	3	0 0	9.706438	−0.4
55	3	1	2	2	2	1	1	2	0 0	9.707646	0.9
56	3	1	2	4	2	1	1	3	1 0	9.670602	1.1
57	3	1	2	3	2	1	1	2	1 0	9.670840	−1.2
58	3	1	2	2	2	1	1	1	1 0	9.670385	−1.3
59	3	1	2	3	2	1	1	3	1 0	9.670208	−0.2
60	3	1	2	2	2	1	1	2	1 0	9.671371	−0.5
61	3	1	2	4	2	1	1	3	1 1	9.670574	2.2
62	3	1	2	3	2	1	1	2	1 1	9.670817	3.6
63	3	1	2	2	2	1	1	1	1 1	9.670361	2.9
64	3	1	2	3	2	1	1	3	1 1	9.670182	2.1
65	3	1	2	2	2	1	1	2	1 1	9.671345	2.4
66	3	1	2	4	2	1	1	3	-1 1	9.670621	0.9
67	3	1	2	3	2	1	1	2	-1 1	9.670863	1.1
68	3	1	2	2	2	1	1	1	-1 1	9.670406	0.3
69	3	1	2	3	2	1	1	3	-1 1	9.670228	0.1
70	3	1	2	2	2	1	1	2	-1 1	9.671391	0.0
71	4	1	4	5	3	1	3	4	0 0	10.346729	−2.5
72	4	1	4	4	3	1	3	3	0 0	10.346925	−2.8
73	4	1	4	3	3	1	3	2	0 0	10.346816	−3.4
74	4	1	4	4	3	1	3	4	0 0	10.348413	−3.2
75	4	1	4	3	3	1	3	3	0 0	10.344808	−2.7
76	4	1	4	5	3	1	3	4	0 1	10.346729	−0.4
77	4	1	4	4	3	1	3	3	0 1	10.346925	−0.6
78	4	1	4	3	3	1	3	2	0 1	10.346816	−1.2
79	4	1	4	4	3	1	3	4	0 1	10.348413	−1.1
80	4	1	4	3	3	1	3	3	0 1	10.344808	−0.5
81	4	1	4	5	3	1	3	4	1 0	10.340101	−1.8
82	4	1	4	4	3	1	3	3	1 0	10.340297	−1.5

No.	J'	K_a'	K_c'	F'	J	K_a	K_c	F	sym.	ν_{obs}	$\nu_c - \nu_o$
83	4	1	4	3	3	1	3	2	1 0	10.340190	−0.4
84	4	1	4	4	3	1	3	4	1 0	10.341781	−2.2
85	4	1	4	3	3	1	3	3	1 0	10.338184	−2.2
86	4	1	4	5	3	1	3	4	1 1	10.340101	2.5
87	4	1	4	4	3	1	3	3	1 1	10.340297	2.8
88	4	1	4	3	3	1	3	2	1 1	10.340190	3.9
89	4	1	4	4	3	1	3	4	1 1	10.341781	2.1
90	4	1	4	3	3	1	3	3	1 1	10.338184	2.0
91	4	1	4	5	3	1	3	4	-1 1	10.340101	−1.8
92	4	1	4	4	3	1	3	3	-1 1	10.340297	−1.5
93	4	1	4	3	3	1	3	2	-1 1	10.340190	−0.4
94	4	1	4	4	3	1	3	4	-1 1	10.341781	−2.2
95	4	1	4	3	3	1	3	3	-1 1	10.338184	−2.2
96	4	0	4	5	3	0	3	4	0 0	10.613956	−0.4
97	4	0	4	4	3	0	3	3	0 0	10.614274	−4.4
98	4	0	4	3	3	0	3	3	0 0	10.612293	−1.9
99	4	0	4	5	3	0	3	4	0 1	10.613954	1.4
100	4	0	4	4	3	0	3	3	0 1	10.614273	−1.0
101	4	0	4	3	3	0	3	2	0 1	10.613982	−3.8
102	4	0	4	4	3	0	3	4	0 1	10.615530	0.2
103	4	0	4	3	3	0	3	3	0 1	10.612289	−1.0
104	4	0	4	5	3	0	3	4	1 0	10.616328	2.6
105	4	0	4	4	3	0	3	3	1 0	10.616657	2.8
106	4	0	4	3	3	0	3	2	1 0	10.616357	1.3
107	4	0	4	4	3	0	3	4	1 0	10.617894	1.9
108	4	0	4	3	3	0	3	3	1 0	10.614687	2.5
109	4	0	4	5	3	0	3	4	1 1	10.616328	2.7
110	4	0	4	4	3	0	3	3	1 1	10.616657	2.9
111	4	0	4	3	3	0	3	2	1 1	10.616357	1.4
112	4	0	4	4	3	0	3	4	1 1	10.617894	2.0
113	4	0	4	3	3	0	3	3	1 1	10.614687	2.6
114	4	0	4	5	3	0	3	4	-1 1	10.616317	0.5
115	4	0	4	4	3	0	3	3	-1 1	10.616646	1.1
116	4	0	4	4	3	0	3	4	-1 1	10.617883	0.3
117	4	2	3	5	3	2	2	4	0 0	11.727511	−0.8
118	4	2	3	4	3	2	2	3	0 0	11.727825	−0.9

No.	J'	K_a'	K_c'	F'	J	K_a	K_c	F	sym.	ν_{obs}	$\nu_c - \nu_o$
119	4	2	3	3	3	2	2	2	0 0	11.727429	−1.5
120	4	2	3	4	3	2	2	4	0 0	11.727825	−0.9
121	4	2	3	3	3	2	2	3	0 0	11.727429	−1.5
122	4	2	3	5	3	2	2	4	0 1	11.727511	2.5
123	4	2	3	4	3	2	2	3	0 1	11.727825	2.3
124	4	2	3	3	3	2	2	2	0 1	11.727429	1.7
125	4	2	3	4	3	2	2	4	0 1	11.727825	2.3
126	4	2	3	3	3	2	2	3	0 1	11.727429	1.7
127	4	3	2	5	3	3	1	4	0 0	12.130420	−4.9
128	4	3	2	4	3	3	1	3	0 0	12.130828	−7.5
129	4	3	2	3	3	3	1	2	0 0	12.130235	−8.4
130	4	3	2	5	3	3	1	4	0 1	12.130449	2.5
131	4	3	2	4	3	3	1	3	0 1	12.130856	−1.4
132	4	3	2	3	3	3	1	2	0 1	12.130263	−3.4
133	4	1	3	5	3	1	2	4	0 0	12.669265	1.4
134	4	1	3	4	3	1	2	3	0 0	12.669541	1.2
135	4	1	3	3	3	1	2	2	0 0	12.669156	1.0
136	4	1	3	3	3	1	2	3	0 0	12.669707	0.7
137	4	1	3	5	3	1	2	4	0 1	12.669258	0.8
138	4	1	3	4	3	1	2	3	0 1	12.669534	0.7
139	4	1	3	3	3	1	2	2	0 1	12.669148	0.4
140	4	1	3	3	3	1	2	3	0 1	12.669700	0.5
141	4	1	3	5	3	1	2	4	1 0	12.627712	−1.2
142	4	1	3	4	3	1	2	3	1 0	12.627971	−1.8
143	4	1	3	3	3	1	2	2	1 0	12.627607	−2.7
144	4	1	3	4	3	1	2	4	1 0	12.627580	−0.1
145	4	1	3	3	3	1	2	3	1 0	12.628139	−1.1
146	4	1	3	5	3	1	2	4	1 1	12.627680	0.4
147	4	1	3	4	3	1	2	3	1 1	12.627940	1.2
148	4	1	3	3	3	1	2	2	1 1	12.627580	3.8
149	4	1	3	3	3	1	2	3	1 1	12.628102	−3.7
150	4	1	3	5	3	1	2	4	-1 1	12.627732	−1.6
151	4	1	3	4	3	1	2	3	-1 1	12.627991	−2.2
152	4	1	3	3	3	1	2	2	-1 1	12.627629	−2.0
153	4	1	3	3	3	1	2	3	-1 1	12.628161	0.0
154	5	1	5	6	4	1	4	5	0 0	12.764508	−4.0

No.	J'	K_a'	K_c'	F'	J	K_a	K_c	F	sym.	ν_{obs}	$\nu_c - \nu_o$
155	5	1	5	5	4	1	4	4	0 0	12.764667	−1.0
156	5	1	5	4	4	1	4	3	0 0	12.764568	−2.5
157	5	1	5	5	4	1	4	5	0 0	12.766349	−2.9
158	5	1	5	4	4	1	4	4	0 0	12.762450	−2.8
159	5	1	5	6	4	1	4	5	0 1	12.764508	−1.2
160	5	1	5	5	4	1	4	4	0 1	12.764667	1.7
161	5	1	5	4	4	1	4	3	0 1	12.764568	0.3
162	5	1	5	5	4	1	4	5	0 1	12.766349	−0.2
163	5	1	5	4	4	1	4	4	0 1	12.762450	−0.1
164	5	1	5	6	4	1	4	5	1 0	12.759650	−1.1
165	5	1	5	5	4	1	4	4	1 0	12.759804	−3.3
166	5	1	5	4	4	1	4	3	1 0	12.759707	−2.2
167	5	1	5	5	4	1	4	5	1 0	12.761485	−2.3
168	5	1	5	4	4	1	4	4	1 0	12.757594	−2.9
169	5	1	5	6	4	1	4	5	1 1	12.759650	2.7
170	5	1	5	5	4	1	4	4	1 1	12.759804	0.4
171	5	1	5	4	4	1	4	3	1 1	12.759707	1.6
172	5	1	5	5	4	1	4	5	1 1	12.761485	1.4
173	5	1	5	4	4	1	4	4	1 1	12.757594	0.9
174	5	1	5	6	4	1	4	5	-1 1	12.759650	0.6
175	5	1	5	5	4	1	4	4	-1 1	12.759804	−1.6
176	5	1	5	4	4	1	4	3	-1 1	12.759707	−0.4
177	5	1	5	5	4	1	4	5	-1 1	12.761485	−0.6
178	5	1	5	4	4	1	4	4	-1 1	12.757594	−1.2
179	5	0	5	6	4	0	4	5	0 0	12.895985	1.3
180	5	0	5	5	4	0	4	4	0 0	12.896204	−1.3
181	5	0	5	5	4	0	4	5	0 0	12.897782	−1.2
182	5	0	5	4	4	0	4	4	0 0	12.894038	−1.7
183	5	0	5	6	4	0	4	5	0 1	12.895981	1.4
184	5	0	5	5	4	0	4	4	0 1	12.896201	0.3
185	5	0	5	4	4	0	4	3	0 1	12.896017	−1.7
186	5	0	5	5	4	0	4	5	0 1	12.897777	−1.6
187	5	0	5	4	4	0	4	4	0 1	12.894035	0.1
188	5	0	5	6	4	0	4	5	1 0	12.897214	1.2
189	5	0	5	5	4	0	4	4	1 0	12.897439	0.1
190	5	0	5	4	4	0	4	3	1 0	12.897251	0.6

No.	J'	K_a'	K_c'	F'	J	K_a	K_c	F	sym.	ν_{obs}	$\nu_c - \nu_o$
191	5	0	5	5	4	0	4	5	1 0	12.899005	−0.7
192	5	0	5	4	4	0	4	4	1 0	12.895280	−0.8
193	5	0	5	6	4	0	4	5	1 1	12.897214	2.4
194	5	0	5	5	4	0	4	4	1 1	12.897439	1.4
195	5	0	5	4	4	0	4	3	1 1	12.897251	1.9
196	5	0	5	5	4	0	4	5	1 1	12.899005	0.5
197	5	0	5	4	4	0	4	4	1 1	12.895280	0.4
198	5	0	5	6	4	0	4	5	-1 1	12.897205	0.6
199	5	0	5	5	4	0	4	4	-1 1	12.897430	−0.8
200	5	0	5	4	4	0	4	3	-1 1	12.897241	−1.5
201	5	0	5	5	4	0	4	5	-1 1	12.898997	−1.1
202	5	0	5	4	4	0	4	4	-1 1	12.895271	−1.4
203	4	2	2	5	3	2	1	4	0 0	12.971408	−0.2
204	4	2	2	4	3	2	1	3	0 0	12.971422	3.0
205	4	2	2	3	3	2	1	2	0 0	12.971344	1.8
206	4	2	2	4	3	2	1	4	0 0	12.970741	−0.9
207	4	2	2	3	3	2	1	3	0 0	12.972259	1.5
208	4	2	2	5	3	2	1	4	0 1	12.971404	−2.1
209	4	2	2	4	3	2	1	3	0 1	12.971415	−1.8
210	4	2	2	3	3	2	1	2	0 1	12.971338	−2.2
211	4	2	2	4	3	2	1	4	0 1	12.970738	−1.4
212	4	2	2	3	3	2	1	3	0 1	12.972251	−4.3
213	4	2	2	5	3	2	1	4	1 0	12.957141	54.0*
214	4	2	2	4	3	2	1	3	1 0	12.957165	58.3*
215	4	2	2	3	3	2	1	2	1 0	12.957073	54.0*
216	4	2	2	4	3	2	1	4	1 0	12.956487	55.2*
217	4	2	2	3	3	2	1	3	1 0	12.957984	53.8*
218	4	2	2	5	3	2	1	4	1 1	12.957128	54.0*
219	4	2	2	4	3	2	1	3	1 1	12.957152	57.7*
220	4	2	2	3	3	2	1	2	1 1	12.957060	54.0*
221	4	2	2	4	3	2	1	4	1 1	12.956471	52.2*
222	4	2	2	3	3	2	1	3	1 1	12.957971	53.5*
223	4	2	2	4	3	2	1	3	-1 1	12.957177	61.6*
224	4	2	2	3	3	2	1	2	-1 1	12.957085	57.6*
225	4	2	2	4	3	2	1	4	-1 1	12.956501	61.3*
226	4	2	2	3	3	2	1	3	-1 1	12.957996	57.0*

No.	J'	K_a'	K_c'	F'	J	K_a	K_c	F	sym.	ν_{obs}	$\nu_c - \nu_o$
227	5	2	4	6	4	2	3	5	0 0	14.452372	1.6
228	5	2	4	5	4	2	3	4	0 0	14.452615	2.0
229	5	2	4	4	4	2	3	3	0 0	14.452341	2.6
230	5	2	4	6	4	2	3	5	0 1	14.452368	2.1
231	5	2	4	5	4	2	3	4	0 1	14.452611	2.2
232	5	2	4	4	4	2	3	3	0 1	14.452336	2.6
233	5	2	4	5	4	2	3	5	0 1	14.452925	1.8
234	5	2	4	4	4	2	3	4	0 1	14.451938	0.4
235	5	2	4	6	4	2	3	5	1 0	14.434194	0.0
236	5	2	4	5	4	2	3	4	1 0	14.434435	0.1
237	5	2	4	4	4	2	3	3	1 0	14.434162	0.2
238	5	2	4	5	4	2	3	5	1 0	14.434750	−0.5
239	6	1	6	7	5	1	5	6	0 0	15.142378	0.7
240	6	1	6	6	5	1	5	5	0 0	15.142502	0.1
241	6	1	6	5	5	1	5	4	0 0	15.142419	−1.2
242	6	1	6	6	5	1	5	6	0 0	15.144340	−1.1
243	6	1	6	5	5	1	5	5	0 0	15.140205	−0.5
244	6	1	6	7	5	1	5	6	0 1	15.142378	3.9
245	6	1	6	6	5	1	5	5	0 1	15.142502	3.3
246	6	1	6	5	5	1	5	4	0 1	15.142419	2.0
247	6	1	6	6	5	1	5	6	0 1	15.144340	2.0
248	6	1	6	5	5	1	5	5	0 1	15.140205	2.6
249	6	1	6	7	5	1	5	6	1 0	15.138696	−2.5
250	6	1	6	6	5	1	5	5	1 0	15.138822	−1.6
251	6	1	6	5	5	1	5	4	1 0	15.138738	−3.5
252	6	1	6	6	5	1	5	6	1 0	15.140658	−2.2
253	6	1	6	5	5	1	5	5	1 0	15.136529	−2.1
254	6	1	6	7	5	1	5	6	1 1	15.138696	0.9
255	6	1	6	6	5	1	5	5	1 1	15.138822	1.8
256	6	1	6	5	5	1	5	4	1 1	15.138738	−0.1
257	6	1	6	6	5	1	5	6	1 1	15.140658	1.3
258	6	1	6	5	5	1	5	5	1 1	15.136529	1.3
259	6	1	6	7	5	1	5	6	-1 1	15.138696	0.3
260	6	1	6	6	5	1	5	5	-1 1	15.138822	1.2
261	6	1	6	5	5	1	5	4	-1 1	15.138738	−0.7
262	6	1	6	6	5	1	5	6	-1 1	15.140658	0.7

No.	J'	K_a'	K_c'	F'	J	K_a	K_c	F	sym.	ν_{obs}	$\nu_c - \nu_o$
263	6	1	6	5	5	1	5	5	-1 1	15.136529	0.8
264	5	3	3	6	4	3	2	5	0 0	15.167303	0.4
265	5	3	3	5	4	3	2	4	0 0	15.167534	1.2
266	5	3	3	4	4	3	2	3	0 0	15.167235	0.3
267	5	3	3	6	4	3	2	5	0 1	15.167303	0.8
268	5	3	3	5	4	3	2	4	0 1	15.167534	1.6
269	5	3	3	4	4	3	2	3	0 1	15.167235	0.7
270	6	0	6	7	5	0	5	6	0 0	15.197887	1.1
271	6	0	6	6	5	0	5	5	0 0	15.198038	1.4
272	6	0	6	6	5	0	5	6	0 0	15.199836	0.0
273	6	0	6	5	5	0	5	5	0 0	15.195758	1.1
274	6	0	6	7	5	0	5	6	0 1	15.197882	0.5
275	6	0	6	6	5	0	5	5	0 1	15.198035	2.1
276	6	0	6	5	5	0	5	4	0 1	15.197918	−1.1
277	6	0	6	6	5	0	5	6	0 1	15.199832	0.2
278	6	0	6	5	5	0	5	5	0 1	15.195755	2.1
279	6	0	6	7	5	0	5	6	1 0	15.197233	−0.2
280	6	0	6	6	5	0	5	5	1 0	15.197386	−0.3
281	6	0	6	5	5	0	5	4	1 0	15.197269	−0.8
282	6	0	6	6	5	0	5	6	1 0	15.199179	−0.7
283	6	0	6	5	5	0	5	5	1 0	15.195110	−1.7
284	6	0	6	7	5	0	5	6	1 1	15.197233	2.3
285	6	0	6	6	5	0	5	5	1 1	15.197386	2.2
286	6	0	6	5	5	0	5	4	1 1	15.197269	1.7
287	6	0	6	6	5	0	5	6	1 1	15.199179	1.8
288	6	0	6	5	5	0	5	5	1 1	15.195110	0.8
289	6	0	6	6	5	0	5	5	-1 1	15.197381	−0.3
290	6	0	6	5	5	0	5	4	-1 1	15.197264	−0.2
291	6	0	6	6	5	0	5	6	-1 1	15.199172	−2.1
292	5	1	4	6	4	1	3	5	0 0	15.349524	1.2
293	5	1	4	5	4	1	3	4	0 0	15.349865	1.5
294	5	1	4	4	4	1	3	3	0 0	15.349445	−1.1
295	5	1	4	6	4	1	3	5	0 1	15.349510	−2.2
296	5	1	4	5	4	1	3	4	0 1	15.349851	−1.7
297	5	1	4	4	4	1	3	3	0 1	15.349433	−3.3
298	4	2	3	5	4	1	4	5	0 0	8.365720	−6.7

No.	J'	K_a'	K_c'	F'	J	K_a	K_c	F	sym.	ν_{obs}	$\nu_c - \nu_o$
299	4	2	3	4	4	1	4	4	0 0	8.364352	−4.7
300	4	2	3	5	4	1	4	5	1 0	8.362018	−4.0
301	4	2	3	4	4	1	4	4	1 0	8.360652	−5.1
302	4	2	3	3	4	1	4	3	1 0	8.362369	−4.4
303	4	1	3	4	3	2	2	3	0 0	9.396258	1.6
304	4	1	3	4	3	2	2	4	0 0	9.396258	1.6
305	5	2	3	6	4	3	2	5	0 0	9.512228	1.4
306	5	2	3	4	4	3	2	3	0 0	9.512248	−0.9
307	5	2	3	5	4	3	2	4	0 1	9.512062	−0.2
308	4	0	4	5	3	1	3	4	0 0	10.126355	−0.3
309	4	0	4	4	3	1	3	3	0 0	10.126446	0.3
310	4	0	4	3	3	1	3	2	0 0	10.126469	−0.6
311	4	0	4	4	3	1	3	4	0 0	10.127932	−1.0
312	4	0	4	3	3	1	3	3	0 0	10.124462	0.0
313	4	0	4	5	3	1	3	4	0 1	10.126355	−1.0
314	4	0	4	4	3	1	3	3	0 1	10.126446	−0.6
315	4	0	4	3	3	1	3	2	0 1	10.126471	−0.4
316	4	0	4	4	3	1	3	4	0 1	10.127932	−2.4
317	4	0	4	3	3	1	3	3	0 1	10.124462	−1.2
318	4	0	4	5	3	1	3	4	1 0	10.108478	−1.1
319	4	0	4	4	3	1	3	3	1 0	10.108561	−0.3
320	4	0	4	3	3	1	3	2	1 0	10.108594	−2.0
321	4	0	4	4	3	1	3	4	1 0	10.110044	−1.5
322	4	0	4	3	3	1	3	3	1 0	10.106590	−1.8
323	4	0	4	5	3	1	3	4	1 1	10.108468	−2.6
324	4	0	4	4	3	1	3	3	1 1	10.108551	−1.7
325	4	0	4	3	3	1	3	2	1 1	10.108585	−2.7
326	4	0	4	4	3	1	3	4	1 1	10.110035	−2.7
327	4	0	4	3	3	1	3	3	1 1	10.106580	−2.5
328	4	0	4	5	3	1	3	4	-1 1	10.108490	0.1
329	4	0	4	4	3	1	3	3	-1 1	10.108573	0.5
330	4	0	4	3	3	1	3	2	-1 1	10.108607	0.2
331	4	0	4	4	3	1	3	4	-1 1	10.110057	−0.3
332	4	0	4	3	3	1	3	3	-1 1	10.106602	−0.6
333	2	2	1	2	1	1	0	2	0 0	10.637320	−0.3
334	2	2	1	2	1	1	0	1	0 0	10.638451	−1.6

No.	J'	K_a'	K_c'	F'	J	K_a	K_c	F	sym.	ν_{obs}	$\nu_c - \nu_o$
335	2	2	1	2	1	1	0	2	0 1	10.637289	1.6
336	2	2	1	3	1	1	0	2	0 1	10.637847	1.7
337	2	2	1	2	1	1	0	1	0 1	10.638426	6.7
338	2	2	1	3	1	1	0	2	-1 1	10.625624	2.6
339	2	2	1	2	1	1	0	1	-1 1	10.626184	2.9
340	2	2	1	1	1	1	0	0	-1 1	10.624255	1.5
341	2	2	1	2	1	1	0	2	-1 1	10.625064	3.0
342	2	2	1	1	1	1	0	1	-1 1	10.627054	1.8
343	6	3	4	7	6	2	5	7	0 0	10.648120	0.7
344	6	3	4	6	6	2	5	6	0 0	10.647353	−1.7
345	6	3	4	5	6	2	5	5	0 0	10.648246	−2.7
346	6	3	4	7	6	2	5	7	0 1	10.648077	2.8
347	6	3	4	6	6	2	5	6	0 1	10.647312	3.2
348	6	3	4	5	6	2	5	5	0 1	10.648204	1.3
349	6	3	4	7	6	2	5	6	1 0	10.648754	2.3
350	6	3	4	6	6	2	5	6	-1 1	10.648721	1.0
351	4	1	4	5	3	0	3	4	0 0	10.834334	1.0
352	4	1	4	4	3	0	3	3	0 0	10.834762	0.9
353	4	1	4	5	3	0	3	4	0 1	10.834324	−1.0
354	4	1	4	4	3	0	3	3	0 1	10.834756	3.0
355	4	1	4	3	3	0	3	2	0 1	10.834334	2.4
356	4	1	4	4	3	0	3	4	0 1	10.836012	2.7
357	4	1	4	3	3	0	3	3	0 1	10.832638	1.7
358	4	1	4	5	3	0	3	4	1 0	10.847952	2.2
359	4	1	4	4	3	0	3	3	1 0	10.848393	1.5
360	4	1	4	3	3	0	3	2	1 0	10.847953	2.9
361	4	1	4	4	3	0	3	4	1 0	10.849631	1.2
362	4	1	4	3	3	0	3	3	1 0	10.846282	2.6
363	4	1	4	5	3	0	3	4	1 1	10.847953	0.2
364	4	1	4	4	3	0	3	3	1 1	10.848394	−1.6
365	4	1	4	3	3	0	3	2	1 1	10.847953	−1.0
366	4	1	4	4	3	0	3	4	1 1	10.849631	−2.7
367	4	1	4	3	3	0	3	3	1 1	10.846282	−1.4
368	4	1	4	5	3	0	3	4	-1 1	10.847930	0.9
369	4	1	4	4	3	0	3	3	-1 1	10.848371	−0.4
370	4	1	4	3	3	0	3	2	-1 1	10.847930	−0.3

No.	J'	K_a'	K_c'	F'	J	K_a	K_c	F	sym.	ν_{obs}	$\nu_c - \nu_o$
371	4	1	4	4	3	0	3	4	-1 1	10.849611	1.3
372	4	1	4	3	3	0	3	3	-1 1	10.846258	−1.1
373	2	2	0	3	1	1	1	2	0 0	11.431943	1.1
374	2	2	0	2	1	1	1	1	0 0	11.430465	−2.6
375	2	2	0	2	1	1	1	2	0 0	11.431075	−4.1
376	2	2	0	3	1	1	1	2	0 1	11.431913	0.1
377	2	2	0	2	1	1	1	1	0 1	11.430446	7.0
378	2	2	0	2	1	1	1	2	0 1	11.431048	−2.6
379	2	2	0	2	1	1	1	1	1 0	11.438625	−150.9*
380	2	2	0	2	1	1	1	2	1 0	11.439238	−149.9*
381	2	2	0	1	1	1	1	1	1 0	11.439962	−151.4*
382	2	2	0	3	1	1	1	2	1 1	11.440228	−150.3*
383	2	2	0	2	1	1	1	1	1 1	11.438758	−150.5*
384	2	2	0	2	1	1	1	2	1 1	11.439372	−146.9*
385	2	2	0	3	1	1	1	2	-1 1	11.439915	−142.7*
386	2	2	0	2	1	1	1	1	-1 1	11.438437	−149.9*
387	2	2	0	2	1	1	1	2	-1 1	11.439054	−144.3*
388	2	2	0	1	1	1	1	1	-1 1	11.439779	−145.6*
389	4	4	1	5	4	3	2	5	0 0	11.481670	−1.1
390	4	4	1	4	4	3	2	4	0 0	11.481162	0.2
391	4	4	1	3	4	3	2	3	0 0	11.481801	−1.0
392	4	4	1	5	4	3	2	5	0 1	11.481280	0.0
393	4	4	1	4	4	3	2	4	0 1	11.480772	0.7
394	4	4	1	3	4	3	2	3	0 1	11.481413	1.8
395	4	4	1	5	4	3	2	4	0 1	11.481675	−2.3
396	5	0	5	6	4	1	4	5	0 0	12.675606	−1.1
397	5	0	5	5	4	1	4	4	0 0	12.675721	−1.4
398	5	0	5	4	4	1	4	3	0 0	12.675673	−1.3
399	5	0	5	5	4	1	4	5	0 0	12.677405	−2.2
400	5	0	5	4	4	1	4	4	0 0	12.673555	−1.8
401	5	0	5	6	4	1	4	5	0 1	12.675606	0.0
402	5	0	5	5	4	1	4	4	0 1	12.675721	−0.2
403	5	0	5	4	4	1	4	3	0 1	12.675673	−0.1
404	5	0	5	5	4	1	4	5	0 1	12.677405	−1.0
405	5	0	5	4	4	1	4	4	0 1	12.673555	−0.7
406	5	0	5	6	4	1	4	5	1 0	12.665589	0.7

No.	J'	K_a'	K_c'	F'	J	K_a	K_c	F	sym.	ν_{obs}	$\nu_c - \nu_o$
407	5	0	5	5	4	1	4	4	1 0	12.665702	0.6
408	5	0	5	4	4	1	4	3	1 0	12.665656	0.8
409	5	0	5	5	4	1	4	5	1 0	12.667383	1.6
410	5	0	5	4	4	1	4	4	1 0	12.663544	1.0
411	5	0	5	6	4	1	4	5	1 1	12.665583	0.0
412	5	0	5	5	4	1	4	4	1 1	12.665695	−0.3
413	5	0	5	4	4	1	4	3	1 1	12.665650	−0.3
414	5	0	5	6	4	1	4	5	-1 1	12.665592	0.6
415	5	0	5	5	4	1	4	4	-1 1	12.665705	0.5
416	5	0	5	4	4	1	4	3	-1 1	12.665659	0.7
417	5	0	5	5	4	1	4	5	-1 1	12.667383	−1.6
418	5	0	5	4	4	1	4	4	-1 1	12.663544	−2.1
419	3	2	2	4	2	1	1	3	0 0	12.979721	−0.5
420	3	2	2	3	2	1	1	2	0 0	12.980378	1.0
421	3	2	2	2	2	1	1	1	0 0	12.979359	1.9
422	3	2	2	3	2	1	1	3	0 0	12.979721	−0.5
423	3	2	2	2	2	1	1	2	0 0	12.980378	1.0
424	3	2	2	2	2	1	1	1	0 1	12.979329	2.4
425	3	2	2	3	2	1	1	2	0 1	12.980348	1.8
426	3	2	2	2	2	1	1	2	0 1	12.980348	1.8
427	3	2	2	4	2	1	1	3	1 0	12.967362	0.6
428	3	2	2	3	2	1	1	2	1 0	12.967996	−0.4
429	3	2	2	2	2	1	1	1	1 0	12.967008	−0.4
430	3	2	2	3	2	1	1	3	1 0	12.967362	−1.2
431	3	2	2	2	2	1	1	2	1 0	12.967996	2.1
432	3	2	2	4	2	1	1	3	1 1	12.967286	0.1
433	3	2	2	3	2	1	1	2	1 1	12.967920	−1.2
434	3	2	2	2	2	1	1	1	1 1	12.966932	−1.5
435	3	2	2	3	2	1	1	3	1 1	12.967286	−1.8
436	3	2	2	2	2	1	1	2	1 1	12.967920	1.3
437	3	2	2	4	2	1	1	3	-1 1	12.967373	0.0
438	3	2	2	3	2	1	1	2	-1 1	12.968008	−0.7
439	3	2	2	2	2	1	1	1	-1 1	12.967019	−1.4
440	3	2	2	3	2	1	1	3	-1 1	12.967373	−1.8
441	3	2	2	2	2	1	1	2	-1 1	12.968008	1.8
442	5	1	5	6	4	0	4	5	0 0	12.984890	1.6

No.	J'	K_a'	K_c'	F'	J	K_a	K_c	F	sym.	ν_{obs}	$\nu_c - \nu_o$
443	5	1	5	5	4	0	4	4	0 0	12.985152	1.3
444	5	1	5	4	4	0	4	3	0 0	12.984920	0.3
445	5	1	5	5	4	0	4	5	0 0	12.986728	−0.3
446	5	1	5	4	4	0	4	4	0 0	12.982935	−0.6
447	5	1	5	6	4	0	4	5	0 1	12.984881	−1.3
448	5	1	5	5	4	0	4	4	0 1	12.985143	−1.1
449	5	1	5	4	4	0	4	3	0 1	12.984911	−2.9
450	5	1	5	5	4	0	4	5	0 1	12.986721	−1.4
451	5	1	5	4	4	0	4	4	0 1	12.982928	−1.5
452	5	1	5	6	4	0	4	5	1 0	12.991275	−0.5
453	5	1	5	5	4	0	4	4	1 0	12.991544	−0.7
454	5	1	5	4	4	0	4	3	1 0	12.991302	−2.0
455	5	1	5	5	4	0	4	5	1 0	12.993110	−1.4
456	5	1	5	4	4	0	4	4	1 0	12.989332	−1.9
457	5	1	5	6	4	0	4	5	1 1	12.991275	−0.9
458	5	1	5	5	4	0	4	4	1 1	12.991544	−1.0
459	5	1	5	4	4	0	4	3	1 1	12.991302	−2.3
460	5	1	5	5	4	0	4	5	1 1	12.993110	−1.7
461	5	1	5	4	4	0	4	4	1 1	12.989332	−2.2
462	5	1	5	6	4	0	4	5	-1 1	12.991259	−3.8
463	5	1	5	5	4	0	4	4	-1 1	12.991529	−2.9
464	5	1	5	5	4	0	4	5	-1 1	12.993095	−3.5
465	5	1	5	4	4	0	4	4	-1 1	12.989317	−4.1
466	4	2	3	5	3	1	2	4	0 0	15.000385	−1.2
467	4	2	3	4	3	1	2	3	0 0	15.001108	−1.7
468	4	2	3	4	3	1	2	3	0 1	15.001078	−0.8
469	4	2	3	3	3	1	2	2	0 1	15.000131	−0.5
470	6	0	6	7	5	1	5	6	0 0	15.108981	0.3
471	6	0	6	6	5	1	5	5	0 0	15.109092	0.0
472	6	0	6	5	5	1	5	4	0 0	15.109026	−0.8
473	6	0	6	6	5	1	5	6	0 0	15.110931	−0.9
474	6	0	6	5	5	1	5	5	0 0	15.106811	−0.7
475	6	0	6	7	5	1	5	6	0 1	15.108981	2.8
476	6	0	6	6	5	1	5	5	0 1	15.109092	2.6
477	6	0	6	5	5	1	5	4	0 1	15.109026	1.8
478	6	0	6	6	5	1	5	6	0 1	15.110931	1.7

No.	J'	K_a'	K_c'	F'	J	K_a	K_c	F	sym.	ν_{obs}	$\nu_c - \nu_o$
479	6	0	6	5	5	1	5	5	0 1	15.106811	1.9
480	6	0	6	7	5	1	5	6	1 0	15.103172	1.1
481	6	0	6	6	5	1	5	5	1 0	15.103282	0.8
482	6	0	6	5	5	1	5	4	1 0	15.103216	0.2
483	6	0	6	6	5	1	5	6	1 0	15.105117	0.2
484	6	0	6	5	5	1	5	5	1 0	15.101005	−0.4
485	6	0	6	7	5	1	5	6	-1 1	15.103172	2.1
486	6	0	6	6	5	1	5	5	-1 1	15.103282	1.8
487	6	0	6	5	5	1	5	4	-1 1	15.103216	1.1
488	6	0	6	6	5	1	5	6	-1 1	15.105117	1.1
489	6	0	6	5	5	1	5	5	-1 1	15.101005	0.6
490	6	1	6	6	5	0	5	6	0 0	15.233247	0.6
491	6	1	6	5	5	0	5	5	0 0	15.229152	1.3
492	6	1	6	5	5	0	5	4	0 1	15.231313	1.1
493	6	1	6	7	5	0	5	6	0 1	15.231276	−0.6
494	6	1	6	7	5	0	5	6	1 0	15.232760	−1.0
495	6	1	6	5	5	0	5	4	1 0	15.232793	−2.6
496	6	1	6	6	5	0	5	6	1 0	15.234722	−1.4
497	6	1	6	7	5	0	5	6	1 1	15.232760	0.8
498	6	1	6	5	5	0	5	4	1 1	15.232793	−0.7
499	6	1	6	6	5	0	5	6	1 1	15.234722	0.5
500	6	1	6	7	5	0	5	6	-1 1	15.232750	−3.1
501	6	1	6	6	5	0	5	5	-1 1	15.232925	3.0
502	6	1	6	5	5	0	5	5	-1 1	15.230631	1.7

* not included in the fit

Table I.5: Rotational constants A, B, C of N-methyldiacetamide in MHz calculated at different levels of theory and their deviations to the experimental values dev_A, dev_B, dev_C.

	A	dev_A	B	dev_B	C	dev_C
MP2						
6-31++G(df,pd)	3151.550	3.900	1800.108	−8.826	1182.005	−11.077
6-31++G(d,p)	3131.025	24.425	1788.983	2.299	1173.375	−2.447
6-31+G(df,pd)	3152.300	3.150	1800.288	−9.005	1180.657	−9.729
6-31+G(d,p)	3131.772	23.678	1789.301	1.982	1171.831	−0.902
6-311++G(df,pd)	3155.964	−0.514	1800.302	−9.020	1187.769	−16.840
6-311++G(d,p)	3136.298	19.152	1790.334	0.948	1179.313	−8.385
6-311++g(d,p)	3136.298	19.152	1790.334	0.948	1179.313	−8.385
6-311+G(df,pd)	3156.125	−0.675	1800.399	−9.116	1187.359	−16.431
6-311+G(d,p)	3136.281	19.169	1790.351	0.931	1179.129	−8.201
6-311G(df,pd)	3168.445	−12.995	1803.611	−12.329	1178.778	−7.850
6-311G(d,p)	3147.229	8.221	1792.860	−1.577	1171.369	−0.441
6-31G(3df,2pd)	3169.463	−14.013	1808.851	−17.569	1177.059	−6.131
6-31G(3df,3pd)	3170.619	−15.169	1808.393	−17.111	1176.627	−5.699
6-31G(df,pd)	3166.587	−11.137	1804.176	−12.893	1175.852	−4.924
6-31G(d,p)	3144.592	10.858	1792.542	−1.260	1167.667	3.261
B3LYP						
6-31++G(df,pd)	3143.900	11.550	1779.846	11.436	1161.014	9.914
6-31++G(d,p)	3139.557	15.893	1778.405	12.878	1159.954	10.974
6-31+G(df,pd)	3143.919	11.531	1779.781	11.501	1161.003	9.925
6-31+G(d,p)	3139.609	15.841	1778.365	12.917	1159.928	11.000
6-311++G(df,pd)	3159.059	−3.609	1786.078	5.204	1165.849	5.079
6-311++G(d,p)	3150.050	5.400	1782.408	8.875	1163.025	7.904
6-311+G(df,pd)	3158.993	−3.543	1785.990	5.292	1165.906	5.022
6-311+G(d,p)	3150.011	5.439	1782.344	8.938	1163.074	7.854
6-311G(df,pd)	3160.858	−5.408	1787.987	3.295	1166.675	4.253
6-311G(d,p)	3151.753	3.697	1784.147	7.135	1163.861	7.067
6-31G(3df,2pd)	3158.203	−2.753	1787.452	3.830	1166.047	4.881
6-31G(3df,3pd)	3157.986	−2.536	1787.075	4.207	1165.889	5.039
6-31G(df,pd)	3148.566	6.884	1784.501	6.781	1163.524	7.404
6-31G(d,p)	3143.531	11.919	1782.811	8.471	1162.216	8.712
cc-pVTZ	3164.832	−9.382	1789.493	1.790	1167.780	3.148

	A	dev_A	B	dev_B	C	dev_C
HF						
6-31++G(df,pd)	3199.109	−43.659	1814.077	−22.795	1189.026	−18.098
6-31++G(d,p)	3195.069	−39.619	1813.608	−22.325	1187.397	−16.469
6-31+G(df,pd)	3199.018	−43.568	1814.087	−22.805	1189.059	−18.130
6-31+G(d,p)	3194.933	−39.483	1813.659	−22.376	1187.442	−16.514
6-311++G(df,pd)	3206.944	−51.494	1815.899	−24.617	1194.346	−23.417
6-311++G(d,p)	3199.968	−44.518	1813.305	−22.023	1191.931	−21.003
6-311+G(df,pd)	3206.595	−51.145	1815.752	−24.469	1194.782	−23.853
6-311+G(d,p)	3199.809	−44.359	1813.188	−21.906	1192.154	−21.226
6-311G(df,pd)	3210.277	−54.827	1817.875	−26.592	1192.516	−21.588
6-311G(d,p)	3203.315	−47.865	1814.996	−23.714	1190.222	−19.294
6-31G(3df,2pd)	3207.834	−52.384	1819.368	−28.086	1189.488	−18.560
6-31G(3df,3pd)	3207.869	−52.419	1819.501	−28.219	1189.137	−18.209
6-31G(df,pd)	3203.892	−48.442	1816.201	−24.919	1188.369	−17.441
6-31G(d,p)	3199.073	−43.623	1815.380	−24.098	1186.789	−15.861
cc-pVTZ	3212.427	−56.977	1820.339	−29.056	1193.479	−22.551
experimental	**3155.450**		**1791.282**		**1170.928**	

Bibliography

[1] A. v. Hofmann, *Ber. Dtsch. Chem. Ges.*, 1881, **14**, 2725–2736.

[2] S. Nishimura, et al., *Handbook of heterogeneous catalytic hydrogenation for organic synthesis*, Wiley New York etc, 2001.

[3] A. Kryvda, V. Gerasimov, S. Dyubko, E. Alekseev, R. Motiyenko, *J. Mol. Spectrosc.*, 2009, **254**, 28–32.

[4] Y. Kawashima, T. Usami, R. D. Suenram, G. Y. Golubiatnikov, E. Hirota, *J. Mol. Spectrosc.*, 2010, **263**, 11–20.

[5] K. Ohba, T. Usami, Y. Kawashima, E. Hirota, *J. Mol. Struct.*, 2005, **744–747**, 815–819.

[6] Y. Kawashima, T. Usami, N. Ohashi, R. D. Suenram, J. T. Hougen, E. Hirota, *Acc. Chem. Res.*, 2006, **39**, 216–220.

[7] W. Gordy, R. L. Cook, *Microwave molecular spectra*, *Vol. XVIII*, Wiley, New York, 1984.

[8] R. Kilb, C. C. Lin, E. B. Wilson Jr, *J. Chem. Phys.*, 1957, **26**, 1695–1703.

[9] B. Van Eijck, J. Van Opheusden, M. Van Schaik, E. Van Zoeren, *J. Mol. Spectrosc.*, 1981, **86**, 465–479.

[10] J. Sheridan, W. Bossert, A. Bauder, *J. Mol. Spectrosc.*, 1980, **80**, 1–11.

[11] D. Jelisavac, D. C. Gómez, H. V. L. Nguyen, L. Sutikdja, W. Stahl, I. Kleiner, *J. Mol. Spectrosc.*, 2009, **257**, 111–115.

[12] T. Attig, L. Sutikdja, R. Kannengießer, I. Kleiner, W. Stahl, *J. Mol. Spectrosc.*, 2013, **284–285**, 8–15.

[13] K. Eibl, R. Kannengießer, W. Stahl, H. V. L. Nguyen, I. Kleiner, *Mol. Phys., accepted for publication*, 2016.

[14] K. Eibl, *private communication about the barrier to internal rotation of 4-hexyn-3-ol*, 2016.

[15] V. Ilyushin, R. Rizzato, L. Evangelisti, G. Feng, A. Maris, S. Melandri, W. Caminati, *Journal of Molecular Spectroscopy*, 2011, **267**, 186–190.

[16] M. J. Tubergen, R. L. Kuczkowski, *J. Am. Chem. Soc.*, 1993, **115**, 9263–9266.

[17] L. B. Favero, B. M. Giuliano, S. Melandri, A. Maris, W. Caminati, *Chem. Eur. J.*, 2007, **13**, 5833–5837.

[18] B. M. Giuliano, W. Caminati, *Angew. Chem. Int. Ed.*, 2005, **44**, 603–606.

[19] P. Herbine, T. R. Dyke, *J. Chem. Phys.*, 1985, **83**, 3768–3774.

[20] F. J. Lovas, R. D. Suenram, G. T. Fraser, C. W. Gillies, J. Zozom, *J. Chem. Phys.*, 1988, **88**, 722–729.

[21] R. J. Lavrich, , M. J. Tubergen, *J. Am. Chem. Soc.*, 2000, **122**, 2938–2943.

[22] V. Vaquero, M. E. Sanz, I. Peña, S. Mata, C. Cabezas, J. C. López, J. L. Alonso, *J. Phys. Chem. A*, 2014, **118**, 2584–2590.

[23] Q. Gou, G. Feng, L. Evangelisti, M. Vallejo-López, L. Spada, A. Lesarri, E. J. Cocinero, W. Caminati, *Chem. Eur. J.*, 2014, **20**, 1980–1984.

[24] Z. Kisiel, *PROSPE – Programs for ROtational SPEctroscopy*, 2016. `http://info.ifpan.edu.pl/~kisiel/prospe.htm#introduction`.

[25] H. Hartwig, H. Dreizler, *Z. Naturforsch. A*, 1996, **51**, 923–932.

[26] J. T. Hougen, I. Kleiner, M. Godefroid, *J. Mol. Spectrosc.*, 1994, **163**, 559–586.

[27] I. Kleiner, J. T. Hougen, et al., *J. Chem. Phys.*, 2003, **119**, 5505–5509.

[28] M. Tudorie, I. Kleiner, J. Hougen, S. Melandri, L. Sutikdja, W. Stahl, *J. Mol. Spectrosc.*, 2011, **269**, 211–225.

[29] V. V. Ilyushin, Z. Kisiel, L. Pszczólkowski, H. Mäder, J. T. Hougen, *J. Mol. Spectrosc.*, 2010, **259**, 26–38.

[30] P. Groner, *J. Chem. Phys.*, 1997, **107**, 4483–4498.

[31] P. Groner, *J. Mol. Spectrosc.*, 2012, **278**, 52–67.

[32] C. T. Townes, B. P. Dailey, *J. Chem. Phys.*, 1949, **17**, 782–796.

[33] Z. Kisiel, B. Pietrewicz, L. Pszczółkowski, *Acta. Phys. Pol. A*, 2002, **101**, 231–242.

[34] J. Raymonda, W. Klemperer, *J. Chem. Phys.*, 1971, **55**, 232–233.

[35] C. Gottlieb, S. Brunken, M. McCarthy, P. Thaddeus, *J. Chem. Phys.*, 2007, **126**, 191101.

[36] W. C. Bowman, E. Herbst, F. C. De Lucia, *J. Chem. Phys.*, 1982, **77**, 4261–4262.

[37] W. C. Bailey, *Calculation of Nuclear Quadrupole Coupling Constants in Gaseous State Molecules*, 2016. `http://nqcc.wcbailey.net/Publ_N.html`.

[38] H. M. Pickett, *J. Mol. Spectrosc.*, 1991, **148**, 371–377.

[39] H. S. Müller, B. J. Drouin, J. C. Pearson, *A & A*, 2009, **506**, 1487–1499.

[40] G. Cazzoli, L. Dore, C. Puzzarini, *A & A*, 2009, **507**, 1707–1710.

[41] J. Demaison, L. Margules, J. E. Boggs, *Chem. Phys.*, 2000, **260**, 65–81.

[42] H. Dreizler, *Mikrowellenspektroskopische Bestimmung von Rotationsbarrieren freier Moleküle*, Springer Berlin Heidelberg, Berlin, Heidelberg, 1968, pp. 59–155.

[43] B. Kirtman, *J. Chem. Phys.*, 1962, **37**, 2516–2539.

[44] R. Lees, J. Baker, *J. Chem. Phys.*, 1968, **48**, 5299–5318.

[45] E. Herbst, J. Messer, F. C. De Lucia, P. Helminger, *J. Mol. Spectrosc.*, 1984, **108**, 42–57.

[46] C. C. Lin, J. D. Swalen, *Rev. Mod. Phys.*, 1959, **31**, 841–892.

[47] R. Kannengießer, W. Stahl, H. V. L. Nguyen, I. Kleiner, *J. Phys. Chem. A*, 2016, **120**, 3992–3997.

[48] M. Kitano, K. Kuchitsu, *Bull. Chem. Soc. Jpn.*, 1973, **46**, 3048–3051.

[49] J.-U. Grabow, W. Stahl, H. Dreizler, *Rev. Sci. Instrum.*, 1996, **67**, 4072–4084.

[50] I. Merke, H. Dreizler, *Z. Naturforsch. A*, 1994, **49**, 490–496.

[51] J.-U. Grabow, W. Stahl, *Z. Naturforsch. A*, 1990, **45**, 1043–1044.

[52] American-Chemical-Society, *Scifinder - CAS Solution*, 2016. `https://scifinder.cas.org/`.

[53] M. J. Frisch, G. W. Trucks, H. B. Schlegel, G. E. Scuseria, M. A. Robb, J. R. Cheeseman, G. Scalmani, V. Barone, B. Mennucci, G. A. Petersson, H. Nakatsuji, M. Caricato, X. Li, H. P. Hratchian, A. F. Izmaylov, J. Bloino, G. Zheng, J. L. Sonnenberg, M. Hada, M. Ehara, K. Toyota, R. Fukuda, J. Hasegawa, M. Ishida, T. Nakajima, Y. Honda, O. Kitao, H. Nakai, T. Vreven, J. A. Montgomery, Jr., J. E. Peralta, F. Ogliaro, M. Bearpark, J. J. Heyd, E. Brothers, K. N. Kudin, V. N. Staroverov, R. Kobayashi, J. Normand, K. Raghavachari, A. Rendell, J. C. Burant, S. S. Iyengar, J. Tomasi, M. Cossi, N. Rega, J. M. Millam, M. Klene, J. E. Knox, J. B. Cross, V. Bakken, C. Adamo, J. Jaramillo, R. Gomperts, R. E. Stratmann, O. Yazyev, A. J. Austin, R. Cammi, C. Pomelli, J. W. Ochterski, R. L. Martin, K. Morokuma, V. G. Zakrzewski, G. A. Voth, P. Salvador, J. J. Dannenberg, S. Dapprich, A. D. Daniels, O. Farkas, J. B. Foresman, J. V. Ortiz, J. Cioslowski, D. J. Fox, Gaussian 09 Revision E.01, Gaussian Inc. Wallingford CT 2009.

[54] W. C. Bailey, *Chem. Phys.*, 2000, **252**, 57–66.

[55] H. V. L. Nguyen, R. Kannengießer, W. Stahl, *Phys. Chem. Chem. Phys.*, 2012, **14**, 11753–11758.

[56] H. V. L. Nguyen, W. Stahl, *J. Chem. Phys.*, 2011, **135**, 024310.

[57] H. Heineking, H. Dreizler, *Z. Naturforsch. A*, 1993, **48**, 570–576.

[58] Q. Lou, R. K. Bohn, *abstract TK11, OSU International Symposium on Molecular Spectroscopy*, 1995.

[59] S. Blanco, J. C. López, A. Lesarri, W. Caminati, J. L. Alonso, *Mol. Phys.*, 2005, **103**, 1473–1479.

[60] J.-R. A. Moreno, T. R. Huet, D. Petitprez, *J. Mol. Struct.*, 2006, **780-781**, 234.

[61] H. Møllendal, S. Samdal, *J. Phys. Chem. A*, 2012, **116**, 12073–12081.

[62] W. E. Steinmetz, *J. Am. Chem. Soc.*, 1973, **95**, 2777–2782.

[63] N. S. True, *J. Mol. Struct.*, 1984, **112**, 333–336.

[64] M. Kitano, T. Fukuyama, K. Kuchitsu, *Bull. Chem. Soc. Jpn.*, 1973, **46**, 384–387.

[65] N. Ohashi, J. T. Hougen, R. Suenram, F. J. Lovas, Y. Kawashima, M. Fujitake, J. Pyka, *J. Mol. Spectrosc.*, 2004, **227**, 28–42.

[66] H. Møllendal, S. Samdal, *J. Phys. Chem. A*, 2006, **110**, 2139–2146.

[67] N. Heineking, H. Dreizler, *Z. Naturforsch. A*, 1993, **48**, 787–792.

[68] H. V. L. Nguyen, I. Kleiner, S. T. Shipman, Y. Mae, K. Hirose, S. Hatanaka, K. Kobayashi, *J. Mol. Spectrosc.*, 2014, **299**, 17–21.

[69] T. Attig, R. Kannengießer, I. Kleiner, W. Stahl, *J. Mol. Spectrosc.*, 2014, **298**, 47–53.

[70] H. V. L. Nguyen, A. Jabri, V. Van, W. Stahl, *J. Phys. Chem. A*, 2014, **118**, 12130–12136.

[71] H. V. L. Nguyen, W. Stahl, *J. Mol. Spectrosc.*, 2010, **264**, 120–124.

[72] H. Dreizler, *Z. Naturforsch. A*, 1961, **16**, 1354–1367.

[73] V. Van, C. Dindic, H. V. L. Nguyen, W. Stahl, *ChemPhysChem*, 2015, **16**, 291–294.

[74] H. V. L. Nguyen, H. Mouhib, S. Klahm, W. Stahl, I. Kleiner, *Phys. Chem. Chem. Phys.*, 2013, **15**, 10012–10018.

[75] Y. Zhao, W. Stahl, H. V. L. Nguyen, *Chem. Phys. Lett.*, 2012, **545**, 9–13.

[76] H. V. L. Nguyen, H. Mouhib, W. Stahl, I. Kleiner, *Mol. Phys.*, 2010, **108**, 763–770.

[77] H. V. L. Nguyen, V. Van, W. Stahl, I. Kleiner, *J. Chem. Phys.*, 2014, **140**, 214303.

[78] E. Fliege, H. Dreizler, J. Demaison, D. Boucher, J. Burie, A. Dubrulle, *J. Chem. Phys.*, 1983, **78**, 3541–3544.

[79] Y. Zhao, J. Jin, W. Stahl, I. Kleiner, *J. Mol. Spectrosc.*, 2012, **281**, 4–8.

[80] L. Sutikdja, D. Jelisavac, W. Stahl, I. Kleiner, *Mol. Phys.*, 2012, **110**, 2883–2893.

[81] T. Attig, R. Kannengießer, I. Kleiner, W. Stahl, *J. Mol. Spectrosc.*, 2013, **290**, 24–30.

[82] Y. Zhao, H. Mouhib, G. Li, I. Kleiner, W. Stahl, *J. Mol. Spectrosc.*, 2016, **322**, 38–42.

[83] R. Lavrich, A. H. Walker, D. Plusquellic, I. Kleiner, R. Suenram, J. Hougen, G. Fraser, *J. Chem. Phys.*, 2003, **119**, 5497–5504.

[84] D. F. Plusquellic, I. Kleiner, J. Demaison, R. D. Suenram, R. J. Lavrich, F. J. Lovas, G. T. Fraser, V. V. Ilyushin, *J. Chem. Phys.*, 2006, **125**, 104312.

[85] A. Jabri, V. Van, H. V. L. Nguyen, W. Stahl, I. Kleiner, *ChemPhysChem*, 2016, **17**, 2660–2665.

[86] V. Van, W. Stahl, H. V. L. Nguyen, *Phys. Chem. Chem. Phys.*, 2015, **17**, 32111–32114.

[87] M. Akashi, E. Yashima, T. Yamashita, N. Miyauchi, S. Sugita, K. Marumo, *J. Polym. Sci., Part A: Polym. Chem.*, 1990, **28**, 3487–3497.

[88] M. Fujitake, Y. Kubota, N. Ohashi, *J. Mol. Spectrosc.*, 2006, **236**, 97–109.

[89] K.-M. Marstokk, H. Møllendal, S. Samdal, *J. Mol. Struct.*, 1996, **376**, 11–24.

[90] H. V. L. Nguyen, W. Stahl, *ChemPhysChem*, 2011, **12**, 1900–1905.

[91] Y. Zhao, H. V. L. Nguyen, W. Stahl, J. T. Hougen, *J. Mol. Spectrosc.*, 2015, **318**, 91–100.

[92] R. Kannengießer, M. J. Lach, W. Stahl, H. V. L. Nguyen, *ChemPhysChem*, 2015, **16**, 1906–1911.

[93] W. H. Kirchhoff, D. R. Johnson, *J. Mol. Spectrosc.*, 1973, **45**, 159–165.

[94] A. Mescheryakov, E. Alekseev, V. Ilyushin, R. Motiyenko, L. Margulès, F. Lovas in *69th International Symposium on Molecular Spectroscopy*.

[95] Y. Kawashima, R. D. Suenram, E. Hirota, *J. Mol. Spectrosc.*, 2003, **219**, 105–118.

[96] P. Novak, A. Kišić, T. Hrenar, T. Jednačak, S. Miljanić, G. Verbanec, *J. Pharm. Biomed. Anal.*, 2011, **54**, 660–666.

[97] A. Hofmann, *LSD-mein Sorgenkind: die Entdeckung einer" Wunderdroge"*, Klett-Cotta, 2010.

[98] H. Aissaoui, R. Koberstein, C. Zumbrunn, J. Gatfield, C. Brisbare-Roch, F. Jenck, A. Treiber, C. Boss, *Bioorg. Med. Chem. Lett.*, 2008, **18**, 5729–5733.

[99] D. Consalvo, W. Stahl, *J. Mol. Struct.*, 1998, **447**, 119–126.

[100] O. Indris, W. Stahl, U. Kretschmer, *J. Mol. Spectrosc.*, 1998, **190**, 372–378.

[101] G. Feng, Q. Gou, L. Evangelisti, W. Caminati, *Angew. Chem. Int. Ed.*, 2014, **53**, 530–534.

[102] M. J. Tubergen, A. R. Conrad, R. E. Chavez, I. Hwang, R. D. Suenram, J. J. Pajski, B. H. Pate, *J. Mol. Spectrosc.*, 2008, **251**, 330–338.

[103] C. Cabezas, I. Peña, A. M. Daly, J. L. Alonso, *Chem. Commun.*, 2013, **49**, 10826–10828.

[104] H. V. L. Nguyen, W. Stahl, I. Kleiner, *Mol. Phys.*, 2012, **110**, 2035–2042.

[105] K. Schmidt, J. Moskowitz, *J. Chem. Phys.*, 1990, **93**, 4172–4178.

[106] J. Toulouse, C. J. Umrigar, *J. Chem. Phys.*, 2007, **126**, 084102.

[107] J. B. Anderson, *J. Chem. Phys.*, 1976, **65**, 4121–4127.

[108] S. Manten, A. Lüchow, *J. Chem. Phys.*, 2001, **115**, 5362–5366.

[109] W. Klopper, T. Helgaker, *Theor. Chem. Acc.*, 1998, **99**, 265–271.

[110] S. Klahm, A. Lüchow, *Chem. Phys. Lett.*, 2014, **600**, 7–9.

[111] T. J. Lee, P. R. Taylor, *Int. J. Quantum Chem.*, 1989, **36**, 199–207.

[112] E. Hirota, Y. Kawashima, T. Usami, K. Seto, *J. Mol. Spectrosc.*, 2010, **260**, 30–35.

[113] V. V. Ilyushin, E. Alekseev, S. Dyubko, I. Kleiner, J. Hougen, *J. Mol. Spectrosc.*, 2004, **227**, 115–139.

[114] J. Swalen, C. Costain, *J. Chem. Phys.*, 1959, **31**, 1562–1574.

[115] R. Peter, H. Dreizler, *Z. Naturforsch. A*, 1965, **20**, 301–312.